



The University of
Nottingham

UNITED KINGDOM • CHINA • MALAYSIA

Design and Evaluation of a Human Microglia Model:
Drug Delivery and the Inhibitory Impact of PPAR β
Agonist on Inflammation

Submitted By

Rawan Aloufi (BSc, MSc)

Supervised by

Dr. Andrew Bennett

Dr. Stephen Alexander

Thesis submitted to the University of Nottingham

for the degree of Doctor of Philosophy

April 2024

Contents

Abstract -----	i
Acknowledgements -----	iv
Declaration -----	v
Dedication -----	vi
List of Figures -----	vii
List of Tables -----	x
Chapter 1 General Introduction -----	1
<i>1.1 Neuroinflammation and its role in neurodegenerative disorders</i> -----	2
<i>1.2 Microglia: The resident immune cells of the CNS</i> -----	3
1.2.1 Origin, distribution, and microglial functions-----	3
1.2.2 Microglia activation-----	5
1.2.3 Morphological and functional changes in activated microglia-----	7
1.2.4 Phagocytosis and cell proliferation-----	7
1.2.5 Antigen presentation-----	8
1.2.6 Cytokine production-----	9
<i>1.3 Astrocyte: Multifunctional glial cells in the CNS</i> -----	10
<i>1.4 Age-related alterations in the role and phenotype of cortical and spinal cord microglia and astrocytes</i> -----	12
1.4.1 Developmental roles of microglia and astrocytes-----	12
1.4.2 Age-dependent alterations in microglial and astrocytic phenotypes and functions-----	12
1.4.3 Impact of aging on neuroinflammatory responses-----	13
<i>1.5 Microglia Models for Studying Neuroinflammation and Neurodegenerative Diseases</i> -----	14
<i>1.6 Peroxisome Proliferator-Activated Receptors (PPARs) in neuroinflammation</i> -----	17
1.6.1 Overview of PPARs and their functions-----	17
1.6.2 PPAR expression in the CNS and glial cells-----	19
1.6.3 Anti-inflammatory and neuroprotective effects of PPAR agonists-----	20
PPAR γ agonists-----	20
1.6.4 Post-translational modifications (SUMOylation) regulating PPAR activity.-----	22
<i>1.7 Fatty Acid-Binding Proteins (FABPs) in the CNS</i> -----	23

1.7.1 Overview of FABPs and their functions	23
1.7.2 FABP expression in the CNS and glial cells	24
1.7.3. Potential roles of FABPs in neuroinflammation and neurodegeneration	25
1.8 <i>Role of ABC Transporters and the Blood-Brain Barrier in CNS Drug Pharmacokinetics</i>	27
1.9 <i>Hypothesis and Aims</i>	29
Chapter 2 Materials and Methods	31
2.1 <i>Reagents</i>	32
2.2 <i>Animal Primary Cell Culture</i>	32
2.2.1 Neonatal Microglia	33
2.2.2 Adult Microglia	36
2.2.3 Neonatal Astrocytes	37
2.2.4 An Alternative Rapid Method to Isolate Neonatal Astrocytes	38
2.3 <i>Culture of Immortalised Cell Lines</i>	39
2.3.1 Cell Lines	39
2.3.2 Culture and Maintenance of Induced Human Pluripotent Stem Cells (hiPSCs)	40
2.3.3 Differentiation of iPSCs into Microglia-like Cells (iPS-microglia)	42
2.3.4 Generation of Induced Microglia-Like Cells (iMG Cells) From Monocytes	46
2.3.5 Generation of Induced Dopaminergic Neurons (iDANs)	48
2.4 <i>Cell Counting</i>	49
2.5 <i>Coating Cell Culture Flasks and Plates</i>	49
2.6 <i>Cell Treatment and Microglia Condition Media (MCM)</i>	50
2.7 <i>Phagocytosis Assay</i>	50
2.8 <i>Immunocytochemistry</i>	51
2.9 <i>In-vitro SUMOylation Assay</i>	53
2.10 <i>Functional Transport Assay</i>	55
2.11 <i>Molecular Biology</i>	56
2.11.1 RNA Extraction and cDNA Synthesis	56
2.11.2 TaqMan qPCR	56
2.11.3 Multi Cytokine Arrays	59
2.11.4 RNAseq Analysis	60
2.11.5 Western Blotting	61
2.11.6 Plasmid DNA purification using Mini-prep.	63
2.11.7 Lentivirus Production	64

2.12 Statistical Analysis-----	65
Chapter 3 Investigation of Age-related Changes in Rat Spinal and Cortical Microglia and Microglia-Astrocyte Crosstalk-----	66
3.1 Introduction-----	67
3.2 Aims-----	68
3.3 Results-----	69
3.3.1 Purity of Adult and Neonatal Primary Microglia Culture-----	69
3.3.2 Morphological Differences between Adult and Neonatal Microglia-----	72
3.3.3 Assessment of Maintenance of Microglial Developmental Stage in Post-Isolation Culture -----	74
3.3.4 Evaluating Phagocytic Efficacy of Microglia Across Developmental Stages-----	76
3.3.5 Assessment of the Purity of Primary Astrocyte Culture -----	78
3.3.6 Analysis of PPAR and FABP Gene Expression in Microglia from Different Developmental Stages and Tissue Locations -----	80
3.3.7 Astrocyte Expression of PPARs and FABPs-----	82
3.3.8 Effects of Stimulating Microglia and Astrocytes with ATP and LPS-----	83
3.4 Discussion -----	90
3.4.1 PPAR and FABP Expression in the Microglia and Astrocyte Cells -----	91
3.4.2 Comparative Analysis of the Responses in Neonatal Versus Adult, and Spinal Cord Versus Cortical Microglia to ATP and LPS Exposure-----	92
Chapter 4 Overcoming iPSCs Challenges with PBMCs: Establishing a Functional In Vitro Human Microglia Model for Neuroinflammation Studies-----	95
4.1 Introduction-----	96
4.2 Aims-----	98
4.3 Results: Development of a Human Microglia Derived Induced Pluripotent Stem Cells (iPSCs) -----	99
4.3.1 Assessment of iPSC Quality and Morphology-----	99
4.3.2 Assessment of Various Basement Membranes for iPSC Culture-----	100
4.3.3 Investigation of Different Methods for Splitting iPSCs -----	101
4.3.4 Assessment of Pluripotency of iPSCs -----	102
4.3.5 Routine Monitoring of iPSC Cultures -----	105
4.3.6 Generation of iPSC-Derived Dopaminergic Neurons -----	106
4.3.7 Differentiation of Human iPSC-Derived Microglia -----	109

4.4 Generation of Human-Derived Microglia Using Peripheral Blood Mononuclear Cells (PBMCs)-----	119
4.4.1 Functional Assessment and Validation of Human Monocyte-Derived Microglia-	121
4.4.2 Stimulation of Microglia: An Investigation of the Effects of PAMPs and DAMPs Upon Microglial Phenotype and gene expression -----	130
4.5 Summary and Discussion-----	135
Chapter 5 The Impact of PPARβ Agonists on Inflammation-----	140
5.1 Introduction-----	141
5.2 Aims-----	143
5.3 Results: Investigating The Role of PPAR β in Animal-Based Neuroinflammatory Models -----	144
5.3.1 Impact of LPS And ATP on PPAR β Expression in Adult and Neonatal Rat Microglia -----	144
5.3.2 Investigation of PPAR β Activation in Adult and Neonatal Rat Microglia and its Effect on Inflammatory Cytokine Gene Expression. -----	145
5.3.3 Investigating the Role of PPAR β in Adult Spinal Primary Rat Microglia-----	149
5.3.4 Investigating the Role of PPAR β using Microglial Conditioned Media (MCM) on Cortical Astrocyte Activation as a Model of Glial Cell Neuroinflammation-----	150
5.4 Investigating The role of PPAR β in a Human-Based Neuroinflammatory Model-----	152
5.4.1 Assessing Activation of PPAR β in Macrophages in Response to Low-Grade Inflammation Induced by DAMPs (ATP) and PAMPs (LPS) -----	152
5.4.2 Investigating the effect of inflammatory stimuli upon PPAR β expression in Monocyte-Derived Microglia-----	154
5.4.3 Examination of the Effects of GW0742 on mRNA Levels of PDK4 and ANGPTL4-	155
5.4.4 Evaluation of the Impact of GW0742 on mRNA Levels of Inflammatory Cytokines in ATP-Stimulated Monocyte-Derived Microglia (iMG)-----	156
5.4.5 Assessment of the Impact of GW0742 on mRNA Levels of Inflammatory Cytokines in LPS-Stimulated Monocyte-Derived Microglia (iMG)-----	158
5.4.6 Cytokine Profiling of Monocyte-Derived Microglia: Effects of DAMP and PAMP Stimulation and Effects of PPAR β Agonist (GW0742) -----	159
5.4.7 Transcriptomic Profiling of microglia activated with ATP and effects of treatment with PPAR β Agonist (GW0742)-----	162
5.4.8 Identification of Genes Significantly Modulated by GW0742 and ATP Treatment in iMG Cells.-----	163
5.4.9 Investigation of GW0742-Mediated Anti-Inflammatory Effects -----	173

5.4.10 Investigating SUMOylation of PPAR β in response to ligand treatment as a potential mechanism involved in inhibition of inflammatory gene expression. -----	175
5.5 Discussion -----	180
Chapter 6 Assessment of the Role of ABCG2/BCRP in PPARβ Drug Delivery to the Central Nervous System -----	190
6.1 Introduction-----	191
6.2 Aim -----	193
6.3 Results-----	193
6.3.1 Impact of PPAR β Agonists on Mitoxantrone Accumulation in BCRP-Overexpressing Cells -----	194
6.4 Discussion -----	197
Chapter 7 General Discussion and Future Directions -----	200
7.1 Summary of Findings -----	201
7.2 Discussion -----	202
7.3 Limitations and Future Work-----	206
Appendices -----	208
References -----	218

Abstract

Neuroinflammation is a hallmark of various neurodegenerative disorders, including Alzheimer's disease, Parkinson's disease, and multiple sclerosis. Microglia and astrocytes, the primary immune cells of the central nervous system (CNS), play a crucial role in the initiation and progression of neuroinflammation. Peroxisome proliferator-activated receptors (PPARs) and fatty acid-binding proteins (FABPs), which are thought to deliver ligands to PPARs, have emerged as important regulators of glial cell functions and neuroinflammation, making them attractive therapeutic targets for neurodegenerative diseases. However, the specific roles of PPARs in microglia and astrocytes, as well as the impact of age and inflammatory stimuli on their expression and function, remain largely unexplored.

Treatment of neuroinflammatory conditions, such as Alzheimer's disease and Parkinson's disease, has been hampered by a lack of translational models and effective drug targets, as well as limited access of drugs through the blood-brain barrier. This thesis aims to elucidate the expression patterns and functions of PPARs and FABPs in microglia and astrocytes and to investigate the therapeutic potential of targeting PPARs for the treatment of neuroinflammatory and neurodegenerative disorders. This research is focused particularly on the role of PPAR β , the most abundant PPAR isoform in the CNS, and its role in modulating glial cell activation and neuroinflammation.

To address these objectives, this study employed a combination of ex vivo and in vitro approaches, including primary rat microglia and astrocyte cultures and human monocyte-derived microglia (iMG) cell models. TaqMan quantitative PCR (qPCR) was employed to characterize the expression of PPARs and FABPs in microglia and astrocytes under basal conditions and in response to inflammatory stimuli, such as lipopolysaccharide (LPS) and adenosine triphosphate (ATP). The findings revealed that PPAR α , PPAR β , and PPAR γ were expressed in both neonatal and adult microglia in the rat brain and spinal cord. Notably, neonatal microglia expressed

higher levels of FABP5, FABP7, PPAR α , and PPAR β compared to adult microglia in cortical and spinal cord cultures. Additionally, age-related and region-specific differences in microglia were observed in response to LPS and ATP, highlighting the importance of considering developmental stage and CNS region when studying microglial function.

To further investigate the role of PPAR β in regulating microglial activation and neuroinflammation, human iMG cells were developed which closely resemble primary human microglia in terms of morphology, gene expression, and functional properties. This study validated the iMG model by demonstrating the expression of key microglial markers, such as TMEM119, P2RY12, and HEXB, and their responsiveness to inflammatory stimuli. Using RNA sequencing (RNA-seq) analysis, iMG cells exhibit a transcriptional profile distinct from peripheral monocytes and macrophages and more closely resembling that of primary human microglia.

Treatment with the PPAR β agonist GW0742 exerted potent anti-inflammatory effects in iMG cells, reducing the production of pro-inflammatory cytokines, such as TNF- α and IL-1 β , in response to LPS and ATP stimulation. RNA-seq analysis revealed that PPAR β activation in ATP-stimulated iMG cells resulted in the upregulation of genes involved in neuroprotection, such as ATG3, RB1CC1, and BNIP3L, while downregulating inflammation-related pathways. Moreover, this study demonstrated that the anti-inflammatory effects of GW0742 were mediated through the modulation of microglia metabolism, autophagy, and the inhibition of NF- κ B signalling. Additionally, the role of SUMOylation in regulating PPAR β activity was investigated, as PPAR β was found to be minimally SUMOylated compared to the Liver X receptor – a nuclear receptor which has been shown to be a target of SUMOylation, and this modification was reduced in the presence of the PPAR β agonist GW0742, suggesting that ligand-induced SUMOylation is not a major mechanism in terms of the anti-inflammatory actions of PPAR β . This study also assessed whether PPAR ligands function as substrates for the ABCG2 efflux transporter, which could hinder their passage through the blood-brain barrier,

affecting their ability to reach therapeutic levels within the CNS. By employing a cell line overexpressing ABCG2, the potential of PPAR ligands to interact with this transporter and be effluxed was evaluated, with data indicating that none of the PPAR ligands tested were ligands for ABCG2.

In conclusion, this thesis provides valuable insights into the role of PPARs in regulating microglial and astrocytic functions and highlights the therapeutic potential of targeting PPAR β for the treatment of neuroinflammatory and neurodegenerative diseases. The findings, obtained through Taq-Man qPCR, RNA-seq analysis, and functional assays, contribute to a better understanding of the molecular mechanisms underlying glial cell activation and neuroinflammation. The validation of the iMG model and the demonstration of the anti-inflammatory effects of PPAR β activation in these cells provide a promising platform for future drug discovery and translational research. Further studies should focus on elucidating the complex interactions between PPARs, FABPs, and other signalling pathways in the CNS, as well as translating these findings into clinical applications for the treatment of age-related neurodegenerative disorders.

Keywords: Peroxisome proliferator-activated receptors (PPARs), fatty acid-binding proteins (FABPs), microglia, astrocytes, neuroinflammation, neurodegenerative diseases, PPAR β , GW0742, monocyte-derived microglia, RNA sequencing, SUMOylation, NF- κ B signaling, pro-inflammatory cytokines, neuroprotection.

Acknowledgements

First and foremost, I want to extend my profound gratitude to Almighty Allah for providing me with guidance and strength throughout this journey. I am immensely thankful to my parents, Mom and Dad. You have been my unwavering pillar of support with your prayers and encouraging calls.

My heartfelt appreciation goes to my supervisors, Dr Andrew Bennett and Dr Stephen Alexander, for their continuous support, invaluable advice, and every "well done." Their readiness to assist and provide guidance has been the cornerstone of my success.

I am indebted to Taif University and the Saudi Cultural Bureau for their generous funding, which made this research possible. Working in the lab has been a joy, and I am grateful to the FRAME lab team, particularly Monika Owen and Nicola de Vivo, for their guidance and expertise. Special thanks to Rawan Edan for her steadfast support from my first day as a PhD student to the last. Masi Almalki, I am truly grateful for your kind assistance. Nash, thanks for being a great friend. Appreciation is extended to David Watson, Claire Spicer, Stephen Woodhams, Ian Kerr, and Gareth Hathway for their training and valuable support.

To my beloved husband, Mohanad, your unwavering support, and love have been my rock; this journey would have been far more challenging without it. To my sons, Khalid, and Zeyad, you are my heroes; your understanding and strength have been a source of pride and joy to me. To my brothers and sisters, your support has been immeasurable. Moud, thank you for all your constant support throughout my journey. My cousin Mariam, I was incredibly fortunate to have you with me in Nottingham. Thank you Reem, Wafa, Arwa, and Nada for always lending a helping hand when I needed it. Afaf, thank you for making writing up time enjoyable. To all my friends in Nottingham, who made it feel like a second home—you know who you are—I thank you from the bottom of my heart.

Declaration

The studies presented in this dissertation represent original work carried out by the author, Rawan Aloufi, a Ph.D. student, at the University of Nottingham between February 2019 and April 2024 under the supervision of Associate Professor Andrew J Bennett and Associate Professor Stephen P Alexander. The thesis has not been submitted for any other degree or qualification.

Dedication

I dedicate this thesis to my parents, my husband, and the light of my life, my children, Khalid and Zeyad.

List of Figures

Figure 1.1.: Overview of Microglial Functions.....	3
Figure 1. 2: Microglial Activation	5
Figure 1. 3: Structure of PPAR β and its selective agonist GW0742.....	17
Figure 1. 4: Modulating Neuroinflammation with PPAR β Agonist GW0742: Proposed hypothesis.....	29
Figure 2. 1 Timeline for induced microglia cell using iPSCs.....	42
Figure 2. 2 Differentiation of human monocyte to microglia-like cells.....	46
Figure 2. 3 Morphology Changes in HEK293FT Cells During the Virus Production Stage.....	65
Figure 3. 1: Determination of adult cortical microglia culture purity.	70
Figure 3. 2: Determination of adult spinal microglia culture purity.....	71
Figure 3. 3: The morphological characterization of isolated cortical neonatal and adult microglia.	73
Figure 3. 4: The relative expression of biomarkers for adult and neonatal microglia	75
Figure 3. 5: Microglia phagocytic activity	77
Figure 3. 6: Isolation of astrocyte culture purity.	79
Figure 3. 7: Differential gene Expression in Adult and Neonatal Microglia.	81
Figure 3. 8 : PPAR α , β , γ , FABP5, FABP7 and FABP8 (pmp2) gene expression in astrocytes .	82
Figure 3. 9: Effects of 100 ng/mL LPS 1-6 h on inflammatory markers	85
Figure 3. 10: Effects of 100 μ M ATP 3 h on Inflammatory Markers	87
Figure 3. 11 Effects of 100 μ M ATP 1-3 h on Inflammatory Markers.....	88
Figure 4. 1: Morphological Characteristics of iPSCs Grown in TeSR™-E8 Medium.....	99
Figure 4. 2 Morphology of iPSCs Cultured on TESR-E8 media.....	100
Figure 4. 3: Morphology of iPSCs cultures that have undergone passaging with ReLeSR. ..	101
Figure 4. 4 Schematic Representation of iPSC Reprogramming and subsequent Trilineage Differentiation	102
Figure 4. 5 Expression of Pluripotency Markers in iPSCs.	103
Figure 4. 6 Verification of Human Induced Pluripotent Stem Cell Pluripotency.	104
Figure 4. 7 Identification of iPSCs Abnormality.....	105
Figure 4. 8: Assessment of Optimal Viral Concentrations for Effective Transduction.	107
Figure 4. 9: Generation of Dopaminergic Neurones via ASCL1, LMX1B, and NURR1 Transduction.	108

Figure 4. 10: Timeline for Induced Microglia Cell Differentiation Using iPSCs	110
Figure 4. 11: Expression of Key Markers in Hematopoietic Cells Derived from iPSCs Using Stem Cell Kit.....	113
Figure 4. 12: Different Methods to Differentiate iPSCs Toward HPCs	114
Figure 4. 13: Expression of Key Markers in Hematopoietic Cells Derived from iPSCs Using Cytokine Cocktail Method	115
Figure 4. 14: Assessment of Microglial Markers in iPSC-Derived Human Microglia	118
Figure 4. 15: Morphology of Primary Human Macrophage and Microglia-like Cells.....	120
Figure 4. 16: Monocyte-derived Macrophage (iMAC) and monocyte-derived microglia (iMG) Cells express Surface Markers.	122
Figure 4. 17: Monocyte-Derived Macrophage (iMAC) and Monocyte-Derived Microglia (iMG) Cells Express Surface Markers: mRNA Expression of microglia-specific markers and myeloid markers.....	123
Figure 4. 18: Phagocytic Capability of iMAC and iMG Cells.	125
Figure 4. 19: PCA of Monocytes, iMACs, and iMG: Cell-type-specific segregation between monocytes, iMAC, and iMG samples.	126
Figure 4. 20: The unique and differential gene expression among iMG, iMacs, and monocyte cell types was analysed through various methods.	129
Figure 4. 21: The Optimal Concentration and Timing for Macrophage Stimulation.....	131
Figure 4. 22: Investigation of effects of LPS and ATP on Microglia	134
Figure 5. 1: Impact of ATP and LPS on PPAR β Expression in Neonatal vs Adult Cortical Microgli.....	144
Figure 5. 2: Impact of GW0742 on IL-1 β and IL-10 in Neonatal and Adult Microglia	146
Figure 5. 3: Impact of 50 nM GW0742 Pre-treatment on IL-1 β , iNOS, and IL-10 Expression in Neonatal and Adult Cortical Microglia Following LPS Stimulation	148
Figure 5. 4: Impact of 50 nM GW0742 Pre-treatment on IL-1 β and iNOS Expression in Adult Spinal Microglia Following LPS Stimulation	149
Figure 5. 5: Impact of Microglial Conditioned Media on Pro-inflammatory Marker Expression in Cortical and Spinal Astrocytes	151
Figure 5. 6: GW0742 Pre-treatment Effects on Inflammatory and Anti-inflammatory Marker Levels in LPS-Stimulated Monocyte-Derived Macrophages	152
Figure 5. 7: Modulating Effects of GW0742 Pre-treatment on IL-1 β and IL-10 Levels in ATP-Stimulated Macrophages	153
Figure 5. 8: The effects of ATP (10-100 μ M, 2 hours) and LPS (5 and 10 ng/mL, 2 hours) on PPAR β Gene Expression in Monocyte-Derived Microglia (iMG).....	154

Figure 5. 9: Rapid Upregulation of PDK4 and ANGPTL4 in iMG Cells Following GW0742	
Treatment	156
Figure 5. 10: Modulating Effects of 50 nM GW0742 Pre-treatment on Inflammatory Markers	
Levels in ATP-Stimulated iMG	157
Figure 5. 11: GW0742 Pre-treatment Effects on Inflammatory and Anti-inflammatory	
Marker Levels in LPS-Stimulated Monocyte-Derived Microglia	158
Figure 5. 12: Cytokine Expression in iMG Under Various Stimuli.	161
Figure 5. 13: PCA Plot Showing Extent of Clustering of Treatments Along the First Two	
Principal Components.	163
Figure 5. 14: Volcano Plot Analysis of iMG Cell Response to Treatments.....	164
Figure 5. 15: Heatmap of Key Gene Expression from RNA-Seq Data.	174
Figure 5. 16: LXRβ Response to Synthetic and Natural Agonists	177
Figure 5. 17: SUMOylation Analysis in HeLa Cells.	178
Figure 5. 18: Influence of GW0742 on PPARβ SUMOylation	179
Figure 5. 19: The stages of the autophagic process and the role of specific genes	
upregulated by GW0742.	182
Figure 5. 20: The Effect of PPARβ Activation on Inflammatory Response.	183
Figure 5. 21: Increased transcription of the ABCA1 gene.	184
Figure 5. 22: Proposed Mechanism of PPARβ Agonists in Inhibiting Neuroinflammation. .	189
Figure 6.1: Assay Validation: BCRP/ABCG2-overexpressing HEK293T cells.	194
Figure 6.2: Lack of Impact by PPARβ Agonists GW0742 and GW01516 on Mitoxantrone	
Accumulation	195
Figure 6.3: Evaluation of PPARα and PPARγ Agonists WY14643 and Rosiglitazone on	
Mitoxantrone Fluorescence.....	196

List of Tables

Table 1. 1: Comparison of microglia models for studying neuroinflammation and neurodegenerative diseases.....	16
Table 2. 1 Bioreagents and Inhibitors Used.....	32
Table 2. 2 Immunopanning Buffers Composition	36
Table 2. 3 Cell Lines Used	39
Table 2. 4 Different Methods to Differentiate iPSCs Towards HPCs	44
Table 2. 5 Immunocytochemistry Buffers	52
Table 2. 6 Primary Antibodies Used for Immunocytochemistry	52
Table 2. 7 Secondary Antibodies Used for Immunocytochemistry	52
Table 2. 8 The condition of Transfection.....	53
Table 2. 9 Pull-Down Buffer Composition	54
Table 2. 10 Primers and Probes Sequences for Real-Time qPCR, Rat Gene	57
Table 2. 11 Primers and probes sequences for real-time qPCR, Human gene	58
Table 2. 12 Western Blot Buffer Recipe	62
Table 2. 13 Primary Antibodies for Western Blot.....	62
Table 2. 14 Table 2.14 Secondary Antibodies for Western Blotting	62
Table 2. 15 Plasmids Used	63
Table 4. 1: Differentiation of iPSCs Using the STEMdiff Hematopoietic Kit.	111
Table 4. 2: Morphological Changes During Attempted iPSC-Derived Microglia Differentiation.	117

Presentations

Poster Presentation

Aloufi, R., Bennett, A., and Alexander, S., 2020. Fatty acid and lipid signalling in glial cells. University of Nottingham School of Life Sciences PGR Conference, 20-24 July 2020.

Aloufi, R., Bennett, A., and Alexander, S., 2021a. Fatty acid and lipid signalling in glial cells. Virtual Glia Trainee Symposium, 12-13 March 2021.

Aloufi, R., Bennett, A., and Alexander, S., 2021b. Fatty acid and lipid signalling in glial cells. XV European Meeting on Glial Cells in Health and Disease, GLIA 2021 Online, 5-9 July 2021.

Aloufi, R., Bennett, A., and Alexander, S., 2022a. Targeting fatty acid signaling pathways to regulate inflammatory responses in macrophages *in vitro*. Pharmacology 2022, Liverpool, UK, 13-14 September 2022.

Aloufi, R., Bennett, A., and Alexander, S., 2023. Targeting fatty acid signalling pathways to regulate inflammatory responses in Microglia *in vitro*. XVI European Meeting on Glial Cells in Health and Disease, GLIA 2023, Berlin, Germany, 8-11 July.

Aloufi, R., Almalki, M., Alexander, S. and Bennett, A. (2024) Developing Alternative Human-Based Model of Microglia for Neuroinflammation Drug Discovery. NAMs Network Launch Event. London, 30 April.

Aloufi, R., Bennett, A. and Alexander, S. (2024) Investigating the Anti-Inflammatory and Neuroprotective Effects of PPAR β Agonists in a Human Monocyte-Derived Microglia Model. EMBO Workshop on Microglia in health and disease. Genoa, Italy, 21-24 May.

Oral presentation:

Aloufi, R., Bennett, A., and Alexander, S., 2021c. Fatty acid and lipid signalling in glial cells. University of Nottingham School of Life Sciences PGR Conference, 12-16 July 2021.

List of Abbreviations

AA	Arachidonic Acid
AD	Alzheimer's Disease
APC	Antigen Presentation Cell
APOE	Apolipoprotein E
ASTN2	Astrotactin 2
ATG3	Autophagy related 3
ATP	Adenosine Triphosphate
BBB	Blood-Brain Barrier
BDNF	Brain-Derived Neurotrophic Factor
BNIP3L	BCL2 interacting protein 3 like C1q
C1q	Complement component 1q
CCR2	C-C chemokine receptor type 2
CD	Cluster of differentiation
CNS	Central Nervous System
COX-2	Cyclooxygenase-2
CSF1	Colony-Stimulating Factor 1
CXCL1	C-X-C Motif Chemokine Ligand 1
CXCL2	C-X-C motif chemokine ligand 2
DAMP	Damage-Associated Molecular Patterns
DHA	Docosahexaenoic Acid
DRD2	Dopamine Receptor D2
EAE	Experimental Autoimmune Encephalomyelitis
ERK	Extracellular signal-regulated kinase
FABP	Fatty Acid-Binding Protein
FABP3	Fatty acid-binding protein 3, heart
FABP5	Fatty acid-binding protein 5, epidermal
FABP7	Fatty acid-binding protein 7, brain
FABP8	Fatty acid-binding protein 8, myelin
FAT	Fatty acid translocase
GABA	Gamma-Aminobutyric Acid
GABRE	GABA Receptor Subunit
GDNF	Glial Cell Line-Derived Neurotrophic Factor
GM-CSF	Granulocyte-Macrophage Colony-Stimulating Factor
GPR34	G protein-coupled receptor 34
GRIN1	NMDA Receptor Subunit
HD	Huntington's Disease
HMGB1	High Mobility Group Box 1
ICAM-1	Intercellular adhesion molecule 1
IFN- γ	Interferon-gamma
IGF1	Insulin-Like Growth Factor 1
IL-	Interleukin
IL-1 β	Interleukin-1 β

IMG	Monocyte-Derived Microglia
iNOS	Inducible Nitric Oxide
IPSC	Induced Pluripotent Stem Cell
JNK	c-Jun N-terminal kinase
LBP	LPS Binding Protein
LDLR	Low-Density Lipoprotein Receptor
LPS	Lipopolysaccharide
LXR	Liver X Receptor
MAPK	Mitogen-activated protein kinase
MCP-1	Monocyte Chemoattractant Protein-1
MD-2	Myeloid Differentiation
MHC	Major Histocompatibility Complex
MIP-1 α	Macrophage Inflammatory Protein-1 α
MPTP	1-Methyl-4-Phenyl-1, 2, 3, 6-Tetrahydropyridine
MS	Multiple Sclerosis
MUFA	Monounsaturated Fatty Acid
NF- κ B	Nuclear Factor Kappa B
NLRP	NOD-Like Receptor Protein
P2RY12	Purinergic receptor P2Y12
P2X4R	P2X purinoceptor 4
P2X7	Purinergic Receptors
P2X7R	P2X purinoceptor 7
PAMP	Pathogen-Associated Molecular Patterns
Panx-1	Pannexin-1
PD	Parkinson's Disease
PIAS1	Protein inhibitor of activated STAT 1
PMP2	Peripheral myelin protein 2
PNS	Peripheral Nervous System
PPAR	Peroxisome Proliferator-Activated Receptor
PPAR β	Peroxisome Proliferator-Activated Receptor Beta
PPRE	Peroxisome Proliferator Response Element
PRR	Pattern Recognition Receptor
PUFA	Polyunsaturated Fatty Acid
RAGE	Advanced Glycation End Products
RB1CC1	RB1 inducible coiled-coil
RXR	Retinoid X Receptor
SEN2	SUMO-Specific Protease-2
SEPRING1	Septin ring finger protein 1 SIRT1
SLC30A2	Solute carrier family 30 member 2
SUMO	Small Ubiquitin-Like Modifier
SYT	Synaptotagmin
TGF β	Transforming Growth Factor-B
TLRs	Toll-Like Receptors
TMEM119	Transmembrane protein 119
TNF- α	Tumor Necrosis Factor- α
TREM2	Triggering receptor expressed on myeloid cells

TSP	Thrombospondin
Ubc9	Ubiquitin-conjugating enzyme 9
VCAM-1	Vascular cell adhesion molecule 1
ASCL1	Achaete-Scute family BHLH transcription factor 1
DAPI	4',6-diamidino-2-phenylindole
FBS	Fetal bovine serum
GAPDH	Glyceraldehyde-3-phosphate dehydrogenase
IKK	Inhibitory kappa B kinase
Nurr1	Nuclear related receptor 1 (NR4A2)
RIBA	Radioimmunoprecipitation assay
RT-qPCR	Real-time quantitative PCR
STAT	Signal transducer and activator of transcription
MyD88	myeloid differentiation primary response 88

Chapter 1 General Introduction

1.1 Neuroinflammation and its role in neurodegenerative disorders

Neuroinflammation has emerged as a crucial factor in the development and progression of various neurodegenerative disorders, such as Alzheimer's disease, Parkinson's disease, and multiple sclerosis. Numerous studies, both in animal models and human patients, have provided compelling evidence linking neuroinflammation to the chronic neuronal loss and functional impairments observed in these conditions (de Wit et al., 2019, Schain and Kreisl, 2017, Chen et al., 2016). The inflammatory response within the central nervous system (CNS) is primarily mediated by the activation of glial cells, specifically microglia and astrocytes, which are the main cellular components of the neuroimmune system (Schain and Kreisl, 2017).

Under normal physiological conditions, glial cells play a vital role in maintaining brain homeostasis by secreting a balanced array of pro- and anti-inflammatory cytokines in response to various stimuli (Chen et al., 2016). However, in the context of neurodegenerative diseases, the persistent activation of glial cells and the chronic production of inflammatory mediators can lead to neurotoxicity and neuronal damage (Glass et al., 2010). This sustained inflammatory state results in a progressive loss of neuronal cells, ultimately affecting critical functions regulated by the CNS, such as cognition, memory, mobility, and learning (Ransohoff, 2016, de Wit et al., 2019). Despite the growing recognition of the significance of neuroinflammation in neurodegenerative disorders, the molecular mechanisms governing the interaction between glial cells and neurons in these conditions remain largely elusive (de Wit et al., 2019).

Microglia and astrocytes are the primary cellular mediators of neuroinflammation and play a critical role in maintaining CNS homeostasis. As the resident immune cells of the CNS, microglia constantly monitor their microenvironment and respond to a wide range of stimuli, including pathogens, tissue damage, and cellular debris (Davalos et al., 2005, Hanisch and Kettenmann, 2007). Activated microglia secrete a plethora of pro-inflammatory cytokines, such as interleukin-1 β (IL-1 β), tumor

necrosis factor- α (TNF- α), and IL-6, as well as reactive oxygen and nitrogen species, which can contribute to neuronal damage and dysfunction (Glass et al., 2010; Saijo and Glass, 2011).

1.2 Microglia: The resident immune cells of the CNS

1.2.1 Origin, distribution, and microglial functions

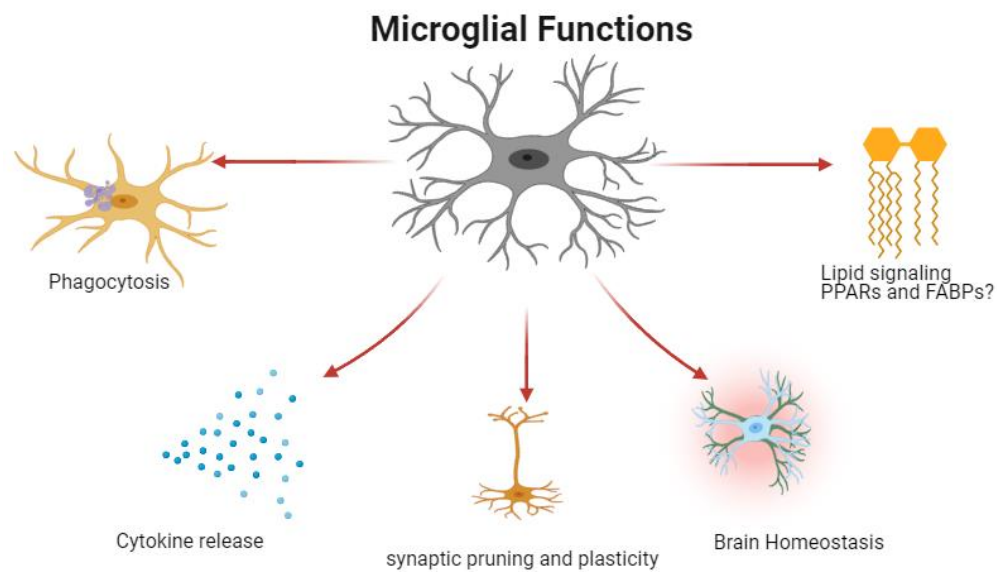


Figure 1.1.: Overview of Microglial Functions. Central to the diagram is a microglial cell, depicted with its various roles in brain physiology. Phagocytosis is shown to the left, where a microglial cell is engulfing particles, denoting its role in cellular debris clearance. Cytokine release is illustrated by a cluster of blue dots, representing the cell's participation in immune signalling. Synaptic pruning is featured to suggest microglia's involvement in neural connectivity and plasticity. On the right, the graphic indicates microglia can influence lipid metabolism pathways, which are crucial for brain homeostasis. The PPARs, particularly PPAR β , that the project focuses on play a role in regulating genes involved in inflammation and metabolism. Created Using Biorender.

Microglia, the specialized macrophage-like cells of the central nervous system (CNS), constitute approximately 10-15% of the total cells in the brain (Kielian, 2004, Spittau, 2017, Glass et al., 2010, Schain and Kreisl, 2017, Clarke et al., 2018). As the primary resident immune cells in the CNS, microglia play a crucial role in maintaining brain homeostasis, defending against pathogens, and regulating inflammatory processes (Glass et al., 2010, Kielian, 2004). Microglia are derived from primitive yolk sac macrophages that migrate into the CNS during early embryonic development (Ginhoux et al., 2010). They are distributed throughout the brain and spinal cord, with regional differences in density and morphology (Savchenko et al., 2000).

In the healthy CNS (Figure 1.1), microglia constantly survey their microenvironment, extending and retracting their processes to monitor synaptic function and neuronal activity (Sellgren et al., 2019, Wake et al., 2009). This dynamic surveillance allows microglia to detect and respond to various stimuli, including pathogens, tissue damage, and cellular debris (Davalos et al., 2005, Hanisch and Kettenmann, 2007). In addition to their immune functions, microglia also contribute to CNS development, synaptic plasticity, and neuronal survival by releasing neurotrophic factors such as brain-derived neurotrophic factor (BDNF), insulin-like growth factor 1 (IGF1), and transforming growth factor- β (TGF β) (Butovsky et al., 2006, Nakajima et al., 2001).

1.2.2 Microglia activation

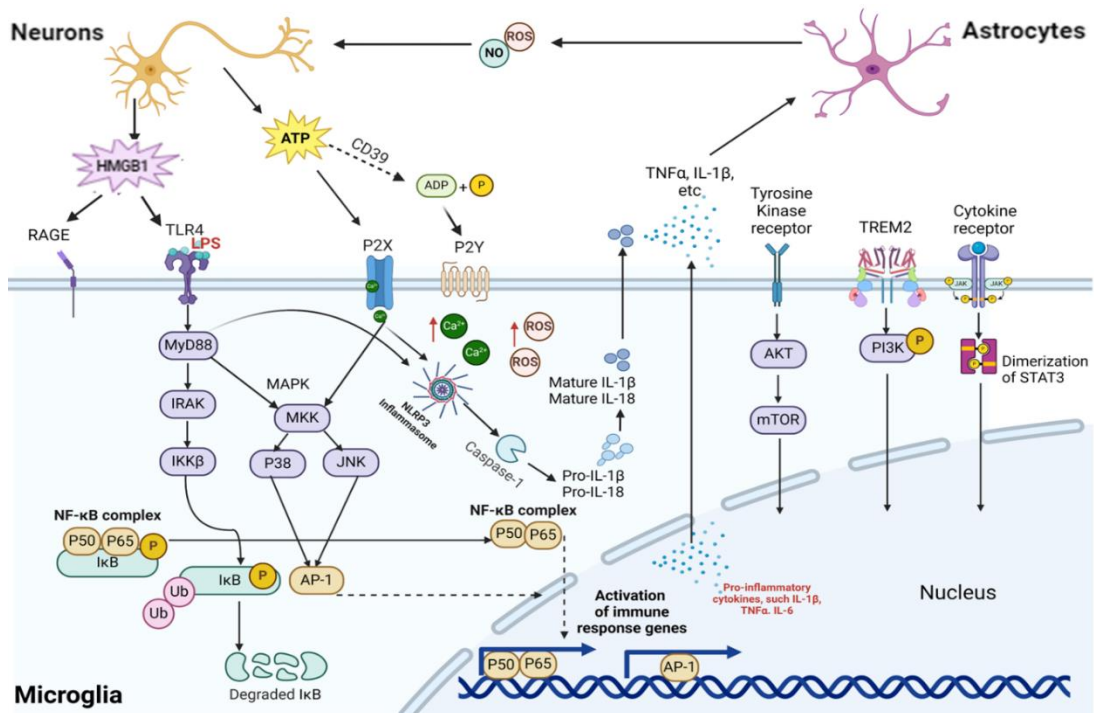


Figure 1.2: Microglial Activation: A Molecular Cascade Leading to Inflammatory Cytokine Production. Neurons release ATP and HMGB3, activating microglia through P2X/P2Y receptors and RAGE/TLR4, respectively. Activated microglia produce ROS, NO, and pro-inflammatory cytokines (e.g., TNF α , IL-1 β), which affect both neurons and astrocytes. In microglia, LPS activates TLR4, triggering the MyD88-dependent pathway leading to NF- κ B activation. ATP stimulates P2X/P2Y receptors, increasing intracellular Ca²⁺ and activating the NLRP3 inflammasome. MAPK pathways (p38, JNK) are also activated, leading to AP-1 transcription factor activation. Astrocytes respond to microglial-derived cytokines through cytokine receptors, activating JAK-STAT and NF- κ B pathways. TREM2 signalling through PI3K/AKT/mTOR is also shown. Both microglia and astrocytes produce ROS and NO, contributing to neuronal stress. Activation of these pathways leads to the transcription of pro-inflammatory genes, perpetuating the inflammatory response.

Microglia can be activated by a wide range of pro-inflammatory stimuli (Figure 1.2), often classified as pathogen-associated molecular patterns (PAMPs) and damage-associated molecular patterns (DAMPs) (Davalos et al., 2005, Kigerl et al., 2014). PAMPs include lipopolysaccharide (LPS) from gram-negative bacteria, viral RNA, and fungal β -glucans, which bind to pattern recognition receptors (PRRs) such as Toll-like receptors (TLRs) expressed on microglia (Balistreri et al., 2009, Kigerl et al.,

2014), for example, recognizes LPS and triggers the activation of NF- κ B signalling, leading to the production of pro-inflammatory cytokines, chemokines, and growth factors (Balistreri et al., 2009, Kigerl et al., 2014).

DAMPs are endogenous molecules released from damaged or dying cells, including ATP, high mobility group box 1 (HMGB1), heat shock proteins, and S100 proteins (Kigerl et al., 2014, Venegas and Heneka, 2017). These molecules bind to receptors on microglia, such as purinergic receptors (e.g., P2X7), receptors for advanced glycation end products (RAGE), and TLRs, triggering microglial activation and inflammatory responses (Inoue, 2002, Bianchi, 2007).

Multiple signalling pathways are implicated in microglial activation. The PAMP pathway, initiated by LPS, involves LPS binding protein (LBP) transferring LPS to CD14, followed by engagement of MD-2 and TLR4 (Fenton and Golenbock, 1998, Akira et al., 2006). This activates the MyD88-dependent pathway, leading to NF- κ B activation and cytokine production (Barger et al., 2007, Chhor et al., 2013). Another TLR4 signalling route, the TRIF-dependent pathway, activates IRF3 and late-phase NF- κ B, inducing type I interferons (Kawai and Akira, 2010).

In the DAMP pathway, ATP activates purinergic receptors, including P2X (ligand-gated ion channels) and P2Y (G protein-coupled receptors) families (Inoue, 2002, Koizumi et al., 2013, Di Virgilio et al., 2020). High ATP concentrations activate the NLRP3 inflammasome, leading to IL-1 β release (Minkiewicz et al., 2013). Lower ATP concentrations trigger a cascade through P2X4R, ultimately activating P2X7R and stimulating inflammasome activation (Bernier, 2012).

Other important signalling pathways in microglial activation include the MAPK cascades (p38, JNK, and ERK), which regulate various cellular responses, including cytokine production and apoptosis (Kaminska et al., 2009). The PI3K/AKT pathway, activated by growth factors and cytokines, modulates microglial survival and phagocytosis (Ulland et al., 2017). Additionally, the JAK-STAT pathway, triggered by

cytokines like IFN- γ and IL-6, plays a crucial role in microglial polarization and inflammatory gene expression (O'Shea and Plenge, 2012).

Inflammasomes, including NLRP3, NLRC4, and AIM2, are cytosolic protein complexes activated by various PAMPs and DAMPs. They play a crucial role in processing and releasing inflammatory cytokines like IL-1 β and IL-18. Inflammasome activation leads to caspase-1 activation, which then processes these pro-inflammatory cytokines for release (Gross et al., 2011, Guo et al., 2015).

1.2.3 Morphological and functional changes in activated microglia

Upon activation, microglia undergo distinct morphological and functional changes, transitioning from a ramified, resting state to an amoeboid, phagocytic phenotype (Stence et al., 2001, Gyoneva et al., 2014). Activated microglia exhibit increased expression of surface markers, such as CD11b, CD68, and major histocompatibility complex (MHC) class II (Hendrickx et al., 2017, Melief et al., 2012). They also upregulate the production of pro-inflammatory cytokines, including interleukin-1 β (IL-1 β), tumour necrosis factor- α (TNF- α), and IL-6, as well as reactive oxygen and nitrogen species (Burguillos et al., 2011, Glass et al., 2010, Kigerl et al., 2014)

The activation of microglia is a dynamic process, and the specific phenotype adopted by microglia depends on the nature, intensity, and duration of the activating stimulus (Hanisch and Kettenmann, 2007). While acute microglial activation is essential for host defence and tissue repair, chronic or excessive activation can lead to neurotoxicity and contribute to the pathogenesis of various neurodegenerative disorders.

1.2.4 Phagocytosis and cell proliferation

One of the primary functions of microglia is phagocytosis, which involves the engulfment and removal of pathogens, cellular debris, and apoptotic cells (Schafer and Stevens, 2015). Microglia express a variety of receptors that mediate

phagocytosis, such as complement receptors, scavenger receptors, and phosphatidylserine receptors (Fu et al., 2014). In the developing CNS, microglia play a crucial role in synaptic pruning, removing excess or weak synapses through complement-dependent phagocytosis (Schafer et al., 2012, Stevens et al., 2007). This process is essential for the refinement of neural circuits and the establishment of proper synaptic connectivity.

In addition to phagocytosis, microglia can also undergo proliferation in response to injury or pathological conditions (Gomez-Nicola and Perry, 2015). Microglial proliferation is regulated by various factors, including colony-stimulating factor 1 (CSF1) and its receptor CSF1R (Elmore et al., 2014). Increased microglial proliferation has been observed in several neurodegenerative diseases, such as Alzheimer's disease and Parkinson's disease, and is thought to contribute to the chronic inflammatory state associated with these disorders (Elmore et al., 2014, Gómez-Nicola et al., 2013).

1.2.5 Antigen presentation

Microglia also function as antigen-presenting cells (APCs) in the CNS, playing a role in the initiation and regulation of adaptive immune responses (Aloisi, 2001). While resting microglia express low levels of MHC class I and II molecules, activated microglia upregulate the expression of these molecules, as well as co-stimulatory molecules such as CD40, CD80, and CD86 (Aloisi, 2001). This enables microglia to present antigens to T cells and modulate their activation and differentiation.

The efficiency of microglia as APCs varies depending on the developmental stage and the specific CNS region (Aloisi, 2001). Neonatal microglia appear to be more effective APCs than adult microglia, and microglia isolated from the spinal cord exhibit a more activated phenotype compared to those from the brain (Aloisi et al., 2000). However, under pathological conditions, adult microglia can become potent APCs, effectively stimulating T cell responses (Aloisi, 2001).

1.2.6 Cytokine production

Microglia are a major source of cytokines in the CNS, producing both pro-inflammatory and anti-inflammatory mediators in response to various stimuli (Hanisch, 2002). Pro-inflammatory cytokines secreted by microglia include IL-1 β , TNF- α , IL-6, and IL-12, which are involved in the amplification of inflammatory responses and the activation of other glial cells and immune cells (Hanisch, 2002, Lee et al., 2002). These cytokines can also have direct effects on neurons, modulating their survival, synaptic function, and plasticity (Pickering et al., 2005, Viviani et al., 2003).

In addition to pro-inflammatory cytokines, microglia also produce anti-inflammatory cytokines, such as IL-10 and TGF- β , which play a crucial role in resolving inflammation and promoting tissue repair (Lee et al., 2002). The balance between pro-inflammatory and anti-inflammatory cytokines is tightly regulated, and dysregulation of this balance is implicated in the pathogenesis of various neurodegenerative and neuroinflammatory disorders (Heneka et al., 2015, Glass et al., 2010).

Microglia also secrete chemokines, such as monocyte chemoattractant protein-1 (MCP-1) and macrophage inflammatory protein-1 α (MIP-1 α), which are involved in the recruitment of peripheral immune cells to the CNS during injury or infection (Hanisch, 2002). The production of chemokines by microglia is regulated by various factors, including cytokines, neurotransmitters, and neurohormones (Lee et al., 2002).

In conclusion, microglia are highly versatile and dynamic cells that play a central role in maintaining CNS homeostasis, defending against pathogens, and regulating neuroinflammation. Their functions extend beyond traditional immune roles, as they also participate in CNS development, synaptic plasticity, and neuronal survival. Understanding the complex biology of microglia and their responses to various

stimuli is crucial for developing targeted therapies for neurodegenerative and neuroinflammatory disorders.

It is essential to understand how these cytokines, which are produced by microglia, influence the function of astrocytes. This is because astrocytes play a vital role in maintaining neuronal balance and are also heavily involved in the brain's immune response.

1.3 Astrocyte: Multifunctional glial cells in the CNS

Astrocytes are a major type of glial cell in the central nervous system (CNS), accounting for approximately 30% of all CNS cells (Matias et al., 2019). These cells are highly heterogeneous in terms of their morphology and function, and they play essential roles in various aspects of CNS physiology and pathology (Matias et al., 2019, Liddelov and Barres, 2017).

One of the primary functions of astrocytes is to provide structural and metabolic support to neurons. Astrocytes are involved in the formation and maintenance of the blood-brain barrier (BBB) and in neurotransmitter uptake and recycling, particularly for glutamate, regulating extracellular levels to prevent excitotoxicity (Liddelov et al., 2017, Matias et al., 2019, Rothstein et al., 1996). Astrocytes also play a role in synaptic development, maturation, and plasticity through the secretion of factors like thrombospondins and glypicans, as well as modulating synaptic transmission via gliotransmitters (Christopherson et al., 2005, Allen et al., 2012, Panatier et al., 2006, Henneberger et al., 2010).

Furthermore, astrocytes are critical for CNS energy metabolism, providing neurons with metabolic substrates like lactate and mobilising glycogen reserves during metabolic stress (Pellerin and Magistretti, 1994, Bélanger et al., 2011, Brown and Ransom, 2007).

In response to various CNS insults, such as trauma, ischemia, or neuroinflammation, astrocytes undergo a process called reactive astrogliosis (Zamanian et al., 2012, Liddelov and Barres, 2017). Depending on the insult, reactive astrocytes can exert

neuroprotective effects by secreting neurotrophic factors or neurotoxic effects by releasing pro-inflammatory cytokines, contributing to neuroinflammation and neuronal damage (Liddelw and Barres, 2017, Matias et al., 2019, Dougherty et al., 2000, Liddelw et al., 2017, Clarke et al., 2018).

The crosstalk between astrocytes and microglia plays a crucial role in the regulation of neuroinflammation (Jha et al., 2019). This bidirectional communication involves a complex interplay of signalling molecules and can either amplify or resolve inflammatory responses:

1. Microglia to Astrocyte Signalling:

- Activated microglia release cytokines such as IL-1 α , TNF- α , and C1q, which can induce a neurotoxic "A1" phenotype in astrocytes (Liddelw et al., 2017).
- Microglial-derived ATP activates astrocytic P2Y receptors, leading to calcium wave propagation and further astrocyte activation (Pascual et al., 2012).

2. Astrocyte to Microglia Signalling:

- Astrocytic ATP activates microglial P2X7 receptors, promoting microglial activation and proliferation (Davalos et al., 2005).
- Astrocyte-derived TGF- β can suppress microglial activation and promote a neuroprotective phenotype (Norden et al., 2014).

3. Amplification of Inflammatory Responses:

- Microglial-derived IL-1 β induces astrocytes to release CSF1, which in turn promotes microglial proliferation and activation (Choi et al., 2014).
- Astrocyte-derived S100 β activates microglia through RAGE receptors, leading to increased production of pro-inflammatory cytokines (Bianchi et al., 2010).

4. Resolution of Inflammation:

- Astrocyte-derived IL-10 can dampen microglial pro-inflammatory responses (Norden et al., 2014).

This complex interplay between astrocytes and microglia can either exacerbate neuroinflammation, potentially contributing to neuronal dysfunction and degeneration or promote tissue repair and neuroprotection, depending on the nature and context of the activation signals (Matejuk and Ransohoff, 2020).

1.4 Age-related alterations in the role and phenotype of cortical and spinal cord microglia and astrocytes

1.4.1 Developmental roles of microglia and astrocytes

Microglia and astrocytes play crucial roles in the development and maturation of the central nervous system (CNS). During early development, microglia are involved in synaptic pruning, neuronal survival, and the refinement of neural circuits (Schafer et al., 2012, Paolicelli et al., 2011). Microglia actively engulf and eliminate weak or unnecessary synapses, a process that is essential for the proper formation and functioning of neural networks (Schafer et al., 2012). Additionally, microglia secrete various neurotrophic factors, such as brain-derived neurotrophic factor (BDNF) and insulin-like growth factor 1 (IGF-1), which support neuronal survival and differentiation (Ueno et al., 2013).

1.4.2 Age-dependent alterations in microglial and astrocytic phenotypes and functions

As the brain ages, microglia and astrocytes undergo significant changes in their phenotypes and functions. Microglia in the aging brain exhibit a more pro-inflammatory profile, characterized by increased expression of pro-inflammatory cytokines such as interleukin-1 β (IL-1 β), tumour necrosis factor- α (TNF- α), and interleukin-6 (IL-6) (Sierra et al., 2007). This age-related shift towards a pro-inflammatory state is often referred to as "microglial priming" (Perry and Holmes, 2014). Primed microglia have a lower threshold for activation and produce an

exaggerated inflammatory response when challenged with immune stimuli (Norden and Godbout, 2013).

In addition to the increased pro-inflammatory profile, aged microglia also display reduced phagocytic capacity and decreased motility (Damani et al., 2011, Hefendehl et al., 2014). These functional impairments may contribute to the accumulation of protein aggregates and debris in the aging brain, leading to a decline in neural tissue homeostasis (Mosher and Wyss-Coray, 2014). Microglia in the aging brain exhibit significant changes in their dynamic behavior and response to injury. In vivo imaging studies in mice have shown that aged microglia display reduced process motility and delayed migration to sites of injury compared to young microglia (Damani et al., 2011, Hefendehl et al., 2014). Specifically, Damani et al. (2011) found that the average velocity of aged microglial processes towards laser-induced injury in the retina was 36% slower than that of young microglia. Similarly, Hefendehl et al. (2014) observed a 50% slower response of aged microglia to laser-induced injury in the brain compared to young microglia. This impaired ability of aged microglia to respond to injury may contribute to the increased susceptibility of the aging brain to neurodegenerative disorders (Caldeira et al., 2014).

1.4.3 Impact of aging on neuroinflammatory responses

The age-related changes in microglial and astrocytic phenotypes have significant implications for neuroinflammatory responses in the aging brain. The increased pro-inflammatory profile of aged microglia and their heightened reactivity to immune stimuli can lead to exaggerated and prolonged neuroinflammatory responses (Norden and Godbout, 2013).

In the context of neurodegenerative diseases, age-related alterations in microglial functions may exacerbate the progression of pathology. For instance, in Alzheimer's disease, the reduced phagocytic capacity of aged microglia may contribute to the accumulation of amyloid- β (A β) plaques, while the increased pro-inflammatory profile may lead to chronic neuroinflammation and neuronal damage (Mosher and

Wyss-Coray, 2014, Hickman et al., 2008). Similarly, in Parkinson's disease, the age-related changes in microglial and astrocytic functions may contribute to the accumulation of α -synuclein aggregates and the degeneration of dopaminergic neurons (Collier et al., 2017).

The impact of ageing on neuroinflammatory responses is further complicated by the crosstalk between microglia and astrocytes. As discussed in the previous section, activated microglia can induce A1 astrocyte reactivity, which in turn can exacerbate neuroinflammation and neurodegeneration (Liddel et al., 2017). These astrocytes are induced by microglial-derived IL-1 α , TNF, and C1q, and are characterized by upregulation of genes destructive to synapses. A1 astrocytes lose many normal astrocytic functions that support neuronal health and instead secrete neurotoxic factors. They have been observed in various neurodegenerative diseases, suggesting their potential role in disease progression. However, it's important to note that astrocyte reactivity likely exists on a spectrum rather than in discrete states, and the A1/A2 classification is a simplified model of a more complex reality (Escartin et al., 2021). In the ageing brain, the increased pro-inflammatory profile of microglia and the altered reactivity of astrocytes may create a feed-forward loop that amplifies and sustains neuroinflammatory responses, contributing to the development and progression of age-related neurodegenerative disorders.

1.5 Microglia Models for Studying Neuroinflammation and Neurodegenerative Diseases

Dysregulated microglial activation has been implicated in various neurodegenerative diseases, making the development of accurate and reliable microglia models a key priority for research in this field. Several microglia models have been established, each with their own advantages and limitations (Table 1. 1).

Primary microglia cultures derived from rodent brain tissue have been widely used to study microglial function and activation. These cultures provide a relatively pure population of microglia and closely resemble their in vivo counterparts (Tamashiro

et al., 2012). However, the yield of microglia from primary cultures is relatively low, and the cells may exhibit altered phenotypes due to the isolation process and in vitro culture conditions (Caldeira et al., 2014).

Immortalized microglia cell lines, such as BV2 and HAPI cells, offer the advantage of a virtually unlimited supply of cells with consistent properties (Nagai et al., 2005, Janabi et al., 1995, Stansley et al., 2012). These cell lines have been used extensively to investigate microglial responses to various stimuli and to screen potential therapeutic compounds. However, immortalized cell lines do not fully recapitulate the phenotypes and responses of primary microglia, and their relevance to in vivo conditions has been questioned (Butovsky et al., 2014).

To overcome the limitations of rodent-derived microglia models and to better represent human biology, several human microglia models have been developed. Human microglia can be isolated from postmortem brain tissue or surgically resected brain tissue from patients with epilepsy or brain tumors (Mizee et al., 2017). These primary human microglia provide valuable insights into human-specific microglial properties and responses. However, the availability of human brain tissue is limited, and the microglia isolated may be affected by the disease state or postmortem interval.

Induced pluripotent stem cell (iPSC)-derived microglia have emerged as a promising alternative to primary human microglia. iPSCs can be generated from patient-specific somatic cells and differentiated into microglia-like cells using defined protocols (Abud et al., 2017, Muffat et al., 2016). This approach allows for the generation of large numbers of microglia with consistent properties and enables the study of microglia from patients with specific genetic backgrounds or disease conditions. However, iPSC-derived microglia may not fully recapitulate the phenotypes and responses of adult human microglia, and the differentiation protocols can be time-consuming and costly.

More recently, microglia-like cells have been generated from human peripheral blood monocytes using a simplified protocol (Ohgidani et al., 2014, Banerjee et al.,

2021, Ryan et al., 2017). These monocyte-derived microglia (iMG) exhibit similar morphological and functional properties to primary human microglia and can be used to study microglial responses to various stimuli and to screen potential therapeutic compounds. The IMG model offers the advantage of using readily accessible peripheral blood monocytes and a relatively short differentiation protocol. However, the extent to which iMG recapitulates the phenotypes and responses of human brain-resident microglia remains to be fully established.

Table 1. 1: Comparison of microglia models for studying neuroinflammation and neurodegenerative diseases.

Model	Advantages	Limitations	References
Primary rodent microglia	Relatively pure population, closely resemble in vivo microglia	Low yield, altered phenotypes due to isolation and culture conditions	(Tamashiro et al., 2012, Caldeira et al., 2014)
Immortalized cell lines	Virtually unlimited supply, consistent properties, suitable for high-throughput screening	May not fully recapitulate primary microglia, relevance to in vivo conditions questioned	(Stansley et al., 2012, Butovsky et al., 2014)
Primary human microglia	Represent human-specific properties and responses	Limited availability, affected by disease state or postmortem interval	(Mizee et al., 2017)
iPSC-derived microglia	Patient-specific, large numbers, consistent properties, suitable for studying genetic backgrounds	May not fully recapitulate adult human microglia, time-consuming and costly differentiation protocols	(Abud et al., 2017, Muffat et al., 2016)
Monocyte-derived microglia	Readily accessible, similar morphological and functional properties to primary human microglia, suitable for screening compounds	Extent of recapitulation of human brain-resident microglia phenotypes and responses remains to be established	(Ohgidani et al., 2014, Banerjee et al., 2021, Ryan et al., 2017).

Various microglia models have been developed to study neuroinflammation and neurodegenerative diseases, each with its own strengths and weaknesses. The choice of model depends on the specific research question, the desired level of

throughput, and the availability of resources. Combining insights from multiple models and validating key findings across different platforms will be essential for advancing the understanding of microglial biology and for developing effective therapies targeting microglial dysfunction in neurological disorders.

1.6 Peroxisome Proliferator-Activated Receptors (PPARs) in neuroinflammation

1.6.1 Overview of PPARs and their functions

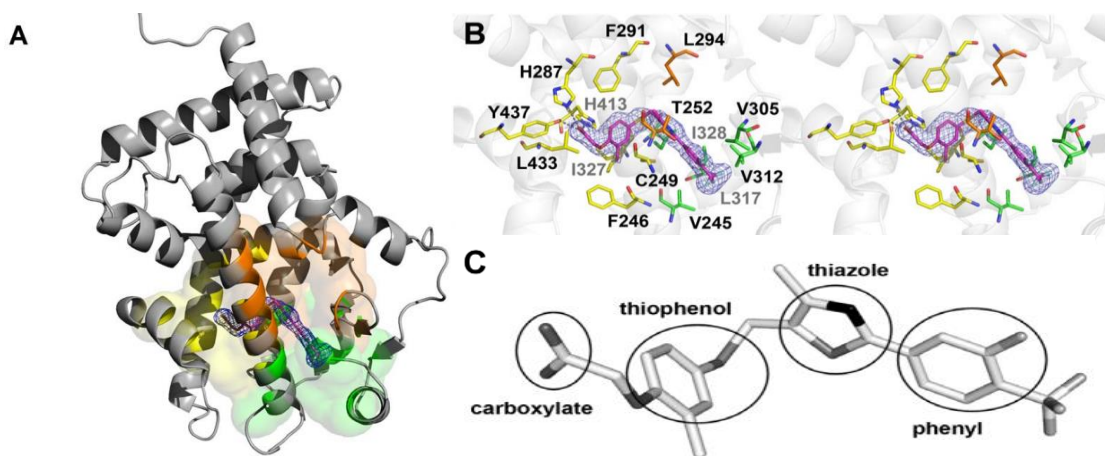


Figure 1. 3: Structure of PPAR β and its selective agonist GW0742. (A) The overall structure of PPAR β (grey cartoon) with bound GW0742 agonist (magenta sticks). (B) Detailed view of the binding pocket, showing key amino acid residues interacting with GW0742. Hydrogen bonds are shown as dashed lines. Nitrogen, oxygen, sulphur and fluorine atoms are blue, red, yellow and light blue, respectively. (C) The three-dimensional structure of GW0742 highlights its key functional groups. Carbon, fluoride, sulphur, oxygen, and nitrogen atoms are coloured white, light grey, grey, dark grey and black, respectively. Figures adapted from (Batista et al., 2012).

Peroxisome proliferator-activated receptors (PPARs) are a family of ligand-activated transcription factors that belong to the nuclear receptor superfamily. There are three PPAR isotypes: PPAR α (NR1C1), PPAR β (NR1C2), and PPAR γ (NR1C3), each

with distinct tissue distribution and functions (Berger and Moller, 2002, Michalik and Wahli, 2006). PPARs form heterodimers with retinoid X receptors (RXRs) and bind to specific DNA sequences called PPAR response elements (PPREs) in the promoter regions of target genes, regulating their transcription (Coll et al., 2009, de Lange et al., 2008).

PPARs play essential roles in various biological processes, including lipid and glucose metabolism, energy homeostasis, inflammation, and cell differentiation (Berger and Moller, 2002). A diversity of synthetic and natural ligands bind and activate these nuclear receptors. Monounsaturated (MUFAs) and polyunsaturated (PUFAs) fatty acids appear to be the preferred endogenous ligands for PPARs, as validated by means of several ligand-binding assays. Rosiglitazone is a synthetic PPAR γ agonist with EC₅₀ values of 0.08-0.2 μ M, while GW0742, GW501516, and L1165041 are synthetic PPAR β ligands with EC₅₀ values of 1.0, 1.1, and 50 nM, respectively (Bernardo and Minghetti, 2006, Coll et al., 2009). Each PPAR regulates a different gene expression profile; even though their distributions are overlapping, they appear to have specificity of a ligand for each PPAR. The structure of the ligand-binding pocket varies noticeably amongst the PPARs, as shown through X-ray crystal-structure investigation (Xu et al., 2001, Zoete et al., 2007). By contrast, natural fatty acids can bind all three PPAR isoforms. Conformational changes occur during ligand binding, allowing interaction with specific coactivator proteins that permit transcription of specific target genes (Xu et al., 1999, Forman et al., 1997). Therefore, it is possible that different fatty acids cause different conformational changes in different PPAR isoforms. The crystal structure of PPAR β (Figure 1. 3). provides crucial insights into how this nuclear receptor interacts with its agonists. Panel A shows the overall structure, with the ligand binding domain forming a large pocket that accommodates the GW0742 agonist. Panel B reveals the specific molecular interactions between PPAR β and GW0742, highlighting key amino acid residues involved in ligand binding. These include H287, T252, H413, and Y437, which form hydrogen bonds with the agonist. These one-letter codes represent

histidine (H), threonine (T), and tyrosine (Y), respectively. The structure demonstrates how synthetic agonists like GW0742 can precisely fit into the binding pocket, leading to conformational changes that activate PPAR β .

1.6.2 PPAR expression in the CNS and glial cells

All three PPAR isotypes are expressed in the central nervous system (CNS), with distinct distribution patterns across different cell types and brain regions (Warden et al., 2016). PPAR α is found in neurons, astrocytes, and microglia, with notable expression in the hippocampus and cortex (Moreno et al., 2004). PPAR β (also known as PPAR δ) is the most widely expressed isotype in the CNS, present in neurons, astrocytes, microglia, and oligodendrocytes (Heneka and Landreth, 2007). PPAR γ is expressed in microglia, astrocytes, and neurons, with higher levels observed in the hippocampus and cortex (Sarruf et al., 2009). This distribution pattern suggests diverse roles for PPARs in CNS function and homeostasis (Iglesias et al., 2017).

In microglia, PPAR α and PPAR γ have been shown to modulate inflammatory responses and promote an anti-inflammatory phenotype (Xu et al., 2005, Aronowski and Zhao, 2011). PPAR β expression in microglia has been studied less, but emerging evidence suggests that it may also play a role in regulating microglial activation and neuroinflammation (Schnegg and Robbins, 2011).

Astrocytes express all three PPAR isotypes, and PPAR activation has been implicated in regulating astrocyte reactivity and neuroinflammation (Iglesias et al., 2017). For example, PPAR γ agonists have been shown to reduce astrocyte activation and promote an anti-inflammatory phenotype in various models of CNS injury and disease (Xu et al., 2006, Storer et al., 2005).

1.6.3 Anti-inflammatory and neuroprotective effects of PPAR agonists

PPAR γ agonists

PPAR γ agonists, such as rosiglitazone and pioglitazone, have demonstrated anti-inflammatory and neuroprotective effects in various models of CNS disorders, including Alzheimer's disease, Parkinson's disease, multiple sclerosis, and ischemic stroke (Heneka et al., 2005, Combs et al., 2000, Drew et al., 2008). These effects were mediated, at least in part, by the inhibition of pro-inflammatory gene expression and the promotion of an anti-inflammatory microglial phenotype (Bernardo and Minghetti, 2008). For example, Pioglitazone treatment reduced excessive microglial and astrocyte activation, which is often associated with chronic neuroinflammation in Alzheimer's disease. Interestingly, this reduction in glial activation was accompanied by a decrease in β -amyloid accumulation (Heneka et al., 2005). While this might seem counterintuitive, as microglia are typically involved in β -amyloid clearance, chronic overactivation of microglia can lead to a dysfunctional state where they become less effective at clearing β -amyloid and may even contribute to its accumulation (Hickman et al., 2008). Pioglitazone's effect likely involves modulating the inflammatory state of microglia, potentially shifting them towards a more efficient phagocytic phenotype, and reducing the production of pro-inflammatory factors that can exacerbate β -amyloid deposition (Mandrekar-Colucci et al., 2012).

PPAR α agonists

PPAR α agonists, such as fenofibrate and gemfibrozil, have also shown anti-inflammatory and neuroprotective properties in various CNS disorder models (Deplanque et al., 2003, Guo et al., 2010). In a mouse model of multiple sclerosis, fenofibrate treatment reduced clinical symptoms, decreased microglial activation, and inhibited pro-inflammatory cytokine production (Lovett-Racke et al., 2004). Similarly, in a rat model of ischemic stroke, fenofibrate pre-treatment reduced infarct volume and improved neurological outcomes, accompanied by a decrease in

microglial activation and pro-inflammatory gene expression (Deplanque et al., 2003).

PPAR β agonists

PPAR β is also known as PPAR δ , but, for the purpose of this thesis, the term PPAR β will be used. While less studied compared to PPAR γ and PPAR α agonists, PPAR β agonists have also demonstrated anti-inflammatory and neuroprotective effects in CNS disorder models (Schneeg and Robbins, 2011). Several studies have demonstrated the anti-inflammatory and neuroprotective effects of PPAR β agonists in various animal models of CNS disorders. For instance, in a mouse model of Alzheimer's disease, treatment with the PPAR β agonist GW0742 reduced neuroinflammation, decreased β -amyloid accumulation, and improved cognitive function (Malm et al., 2015). Similarly, in a rat model of spinal cord injury, GW0742 treatment reduced microglial activation, pro-inflammatory cytokine expression, and neuronal apoptosis, leading to improved functional recovery (Paterniti et al., 2010). These findings highlight the therapeutic potential of targeting PPAR β for the treatment of neuroinflammatory and neurodegenerative diseases.

The mechanisms underlying the anti-inflammatory effects of PPAR β agonists involve the modulation of various signalling pathways and transcriptional regulators. PPAR β has been reported to interact with and sequester pro-inflammatory transcription factors, such as NF- κ B and AP-1, thereby inhibiting the expression of pro-inflammatory genes (Schneeg and Robbins, 2011). Additionally, PPAR β activation has been reported to promote the expression of anti-inflammatory genes, such as IL-10 and TGF- β , through direct binding to PPAR response elements (PPREs) in their promoter regions (Schneeg and Robbins, 2011).

Studies have also implicated PPAR β in the regulation of lipid metabolism and energy homeostasis in the CNS. Hall et al. (2008) reported that the brain fatty acid composition was altered in female PPAR β -null mice, with reduced levels of phosphatidylinositol compared to control mice. This alteration in phospholipid

composition could lead to impaired peroxisomal acyl-CoA utilization in the brain, potentially affecting myelination and contributing to demyelination in PPAR β -deficient mice (Hall et al., 2008). These findings suggest a critical role for PPAR β in maintaining brain lipid homeostasis and myelin integrity.

In addition to its roles in neuroinflammation and lipid metabolism, PPAR β has been implicated in the regulation of neuronal survival and differentiation. In a mouse model of Parkinson's disease, treatment with the PPAR β agonist GW501516 protected dopaminergic neurons from MPTP-induced toxicity and improved motor function (Iwashita et al., 2007). Furthermore, PPAR β activation has been shown to promote the differentiation of neural stem cells into mature neurons, suggesting a potential role in neurogenesis and brain repair (Bernal et al., 2015).

The neuroprotective effects of PPAR β agonists have also been demonstrated in models of ischemic stroke and traumatic brain injury. In a rat model of middle cerebral artery occlusion, treatment with the PPAR β agonist GW0742 reduced infarct size, improved neurological function, and attenuated neuroinflammation (Chehaibi et al., 2017).

While most studies on PPAR β in the CNS have been conducted using animal models, recent research has begun to investigate its role in human brain cells. In primary human astrocytes, activation of PPAR β with GW0742 inhibited the expression of pro-inflammatory cytokines and chemokines induced by TNF- α and IL-1 β (Schneeg et al., 2012).

1.6.4 Post-translational modifications (SUMOylation) regulating PPAR activity.

Post-translational modifications, such as SUMOylation, have been shown to regulate PPAR activity and function (Diezko and Suske, 2013). SUMOylation involves the covalent attachment of small ubiquitin-like modifier (SUMO) proteins to lysine residues of target proteins, modulating their stability, subcellular localization, and transcriptional activity (Flotho and Melchior, 2013). All three PPAR isotypes have been reported to undergo SUMOylation, which can either enhance or repress their

transcriptional activity depending on the cellular context and the specific target genes (Diezko and Suske, 2013). For example, SUMOylation of PPAR γ has been shown to promote its transcriptional repression of pro-inflammatory genes in macrophages (Pascual et al., 2005). In contrast, SUMOylation of PPAR α has been reported to enhance its transcriptional activity on target genes involved in lipid metabolism (Pourcet et al., 2010). The role of SUMOylation in regulating PPAR β activity is less well understood. The only reported post-translational modification of PPAR β involves its SUMOylation at K104, as identified by Koo et al., 2015, who suggest that it may also play a role in modulating its anti-inflammatory and metabolic functions (Koo et al., 2015).

1.7 Fatty Acid-Binding Proteins (FABPs) in the CNS

1.7.1 Overview of FABPs and their functions

Fatty acid-binding proteins (FABPs) are a family of small, highly conserved cytoplasmic proteins that play crucial roles in the intracellular transport and metabolism of long-chain fatty acids (Furuhashi and Hotamisligil, 2008). FABPs are expressed in various tissues and cell types, and they are named according to the tissues in which they were first identified or are most abundantly expressed (Smathers and Petersen, 2011). These proteins have a molecular weight of approximately 15 kDa and share a common three-dimensional structure, consisting of a β -barrel formed by ten antiparallel β -strands and a helix-turn-helix motif that caps the barrel (Storch and Corsico, 2008).

FABPs bind to a wide range of hydrophobic ligands, including saturated and unsaturated long-chain fatty acids, eicosanoids, and other lipids, with high affinity (Furuhashi and Hotamisligil, 2008). By binding to these ligands, FABPs facilitate their transport through the aqueous cytosol and deliver them to specific organelles, such as the mitochondria, peroxisomes, endoplasmic reticulum, and nucleus (Furuhashi and Hotamisligil, 2008, Smathers and Petersen, 2011). In the nucleus, FABPs can interact with transcription factors, such as peroxisome proliferator-activated

receptors (PPARs) and retinoid X receptors (RXRs), thereby modulating gene expression related to lipid metabolism, inflammation, and cell differentiation (Tan et al., 2002, Liu et al., 2010).

In addition to their role in lipid transport and metabolism, FABPs have been implicated in various cellular processes, including cell growth, differentiation, and signaling (Furuhashi and Hotamisligil, 2008). Moreover, altered FABP expression and function have been associated with several pathological conditions, such as obesity, diabetes, atherosclerosis, and cancer (Furuhashi and Hotamisligil, 2008, Smathers and Petersen, 2011).

1.7.2 FABP expression in the CNS and glial cells

The central nervous system (CNS) is rich in long-chain polyunsaturated fatty acids (PUFAs), such as docosahexaenoic acid (DHA) and arachidonic acid (AA), which play essential roles in maintaining the structure and function of neural membranes, regulating signal transduction, and modulating gene expression (Bazinet and Layé, 2014). Given the hydrophobic nature of these fatty acids, their intracellular transport and metabolism require the assistance of FABPs (Liu et al., 2010).

Among the ten FABP isoforms, five are expressed in the CNS: FABP3 (heart FABP), FABP5 (epidermal FABP), FABP7 (brain FABP), FABP8 (myelin FABP), and FABP12 (retinal FABP) (Liu et al., 2010, Matsumata et al., 2012). These FABPs exhibit distinct spatial and temporal expression patterns in the developing and adult CNS, suggesting their involvement in various aspects of brain development and function (Liu et al., 2010).

FABP5 is the most widely expressed FABP isoform in the CNS, with high levels of expression in the cortex and neural stem cells during mid-term embryonic development (Liu et al., 2010). As development progresses, FABP5 expression decreases, and it is only weakly expressed in the adult brain (Liu et al., 2010). FABP5 has a high affinity for retinoic acid and has been implicated in neuronal

differentiation and survival through the activation of PPAR β signalling (Falomir Lockhart et al., 2019, Yu et al., 2012).

FABP7 is expressed at high levels in the embryonic and neonatal brain, particularly in neural stem cells and radial glia, but its expression declines in the adult brain (Matsumata et al., 2012). The high expression of FABP7 during early development is thought to be related to the increased demand for PUFAs during neural stem cell proliferation and differentiation (Liu et al., 2010). In the adult brain, FABP7 expression is restricted to astrocytes and neural stem cells in the subventricular zone and the dentate gyrus of the hippocampus (Matsumata et al., 2012).

FABP3 is expressed in neurons throughout the brain, with particularly high levels in the cortex, hippocampus, and cerebellum (Owada et al., 1996). FABP3 has been implicated in the regulation of neurite outgrowth and synapse formation (Yamamoto et al., 2009).

FABP8, also known as myelin FABP or PMP2, is predominantly expressed in the peripheral nervous system (PNS), specifically in myelin sheaths and Schwann cells (Zenker et al., 2014). FABP8 expression is highest during the early postnatal phase, coinciding with the period of active myelination, suggesting its involvement in fatty acid metabolism and myelin formation (Zenker et al., 2014, Falomir Lockhart et al., 2019).

In contrast to the well-characterized expression and functions of FABPs in neurons and oligodendrocytes, their roles in microglia and astrocytes are less well understood. However, recent studies have begun to shed light on the potential involvement of FABPs in glial cell function and neuroinflammation (Boneva et al., 2011, Kagawa et al., 2015).

1.7.3. Potential roles of FABPs in neuroinflammation and neurodegeneration

Growing evidence suggests that FABPs may play important roles in modulating neuroinflammation and the pathogenesis of neurodegenerative diseases (Pan et al., 2015). FABPs have been shown to interact with PPARs, which are key regulators of

inflammation and lipid metabolism in the central nervous system CNS (Falomir Lockhart et al., 2019). For instance, FABP5 and FABP7 have been identified as ligand-dependent activators of PPAR β and PPAR γ , respectively (Tan et al., 2002, Yu et al., 2012).

In microglia, the main immune cells of the CNS, FABP5 expression has been reported to be upregulated in response to inflammatory stimuli, such as lipopolysaccharide (LPS) (Boneva et al., 2011). Elevated FABP5 levels in microglia have been associated with increased production of pro-inflammatory cytokines, suggesting a potential role for FABP5 in promoting microglial activation and neuroinflammation (Boneva et al., 2011).

Similarly, FABP7 has been implicated in astrocyte reactivity and neuroinflammation. In a mouse model of spinal cord injury, FABP7 expression was found to be upregulated in reactive astrocytes, and FABP7 deficiency attenuated astrogliosis and inflammation (Kagawa et al., 2015). These findings suggest that FABP7 may contribute to the inflammatory response of astrocytes in the context of CNS injury and disease.

On the other hand, FABPs are crucial for the proper functioning of PPARs, which generally exert anti-inflammatory effects (Tan et al., 2002) FABPs act as intracellular lipid chaperones, facilitating the transport of fatty acids and other lipid ligands to PPARs in the nucleus (Furuhashi and Hotamisligil, 2008). This FABP-mediated activation of PPARs can lead to the suppression of inflammatory responses (Korbecki et al., 2019).

Understanding this intricate relationship is crucial for developing targeted therapies for neurodegenerative diseases. Modulating specific FABP-PPAR interactions could potentially offer a way to fine-tune inflammatory responses in the CNS.

In addition to their potential roles in neuroinflammation, FABPs have been linked to the pathogenesis of neurodegenerative diseases, such as Alzheimer's disease (AD)

and Parkinson's disease (PD). These findings suggest that FABPs may be involved in the pathological processes underlying these neurodegenerative disorders.

In conclusion, FABPs are a family of lipid-binding proteins that play essential roles in the transport and metabolism of fatty acids in the CNS. The distinct expression patterns of FABP isoforms in neurons, glia, and neural stem cells suggest their involvement in various aspects of brain development and function. Emerging evidence indicates that FABPs, particularly FABP5 and FABP7, may modulate neuroinflammation through their interactions with PPARs and their effects on glial cell activation. Moreover, FABPs have been implicated in the pathogenesis of neurodegenerative diseases such as AD and PD.

1.8 Role of ABC Transporters and the Blood-Brain Barrier in CNS Drug Pharmacokinetics

The blood-brain barrier (BBB) is a crucial interface between the central nervous system (CNS) and the peripheral circulation, playing a vital role in maintaining brain homeostasis and regulating the entry of substances into the brain. The BBB is composed of specialized endothelial cells connected by tight junctions, along with pericytes and astrocyte end-feet, forming a highly selective barrier (Abbott et al., 2006).

A key component of the BBB's selectivity is the expression of ATP-binding cassette (ABC) transporters, which are integral membrane proteins that actively efflux a wide range of substrates out of cells. In the context of CNS drug delivery, three ABC transporters are particularly important:

1. P-glycoprotein (P-gp, ABCB1): P-gp is the most studied ABC transporter at the BBB. It has a broad substrate specificity and can efflux many drugs, including anticancer agents, antibiotics, and antidepressants (Schinkel, 1999).
2. Breast Cancer Resistance Protein (BCRP, ABCG2): BCRP works in concert with P-gp to limit the brain penetration of many drugs. It has been shown to transport various anticancer drugs, antibiotics, and antivirals (Kodaira et al., 2010).

3. Multidrug Resistance-associated Proteins (MRPs, ABCC family): Several MRPs, particularly MRP1 and MRP4, are expressed at the BBB and contribute to the efflux of organic anions and drug conjugates (Dallas et al., 2006).

These ABC transporters significantly influence the pharmacokinetics of CNS-targeted drugs in several ways:

1. Reduced Brain Penetration: By actively pumping drugs out of the brain capillary endothelial cells back into the bloodstream, ABC transporters can dramatically reduce the amount of drug reaching the brain parenchyma. This can result in subtherapeutic drug concentrations in the CNS, even when peripheral drug levels are adequate (Löscher and Potschka, 2005).

2. Altered Drug Distribution: ABC transporters can affect the regional distribution of drugs within the brain, as their expression levels may vary across different brain regions (Syvänen et al., 2009).

3. Drug-Drug Interactions: Many drugs can inhibit or induce ABC transporters, potentially leading to clinically significant drug-drug interactions that affect CNS drug concentrations (König et al., 2013).

4. Inter-individual Variability: Genetic polymorphisms in ABC transporter genes can lead to variations in transporter expression or function, contributing to inter-individual differences in drug response (Hoffmeyer et al., 2000).

Understanding the role of ABC transporters at the BBB is crucial for CNS drug development. Strategies to overcome ABC transporter-mediated efflux include designing drugs that are poor substrates for these transporters, using transporter inhibitors, and developing novel drug delivery systems that can bypass the BBB (Pardridge, 2012). In the context of PPAR β agonists and their potential use in treating neuroinflammatory conditions, it is important to consider their interactions with ABC transporters. The ability of these compounds to cross the BBB and achieve therapeutic concentrations in the brain will be a critical factor in their efficacy as CNS-targeted drugs.

1.9 Hypothesis and Aims

BioRender Roles of PPAR β/δ in Neuroinflammation

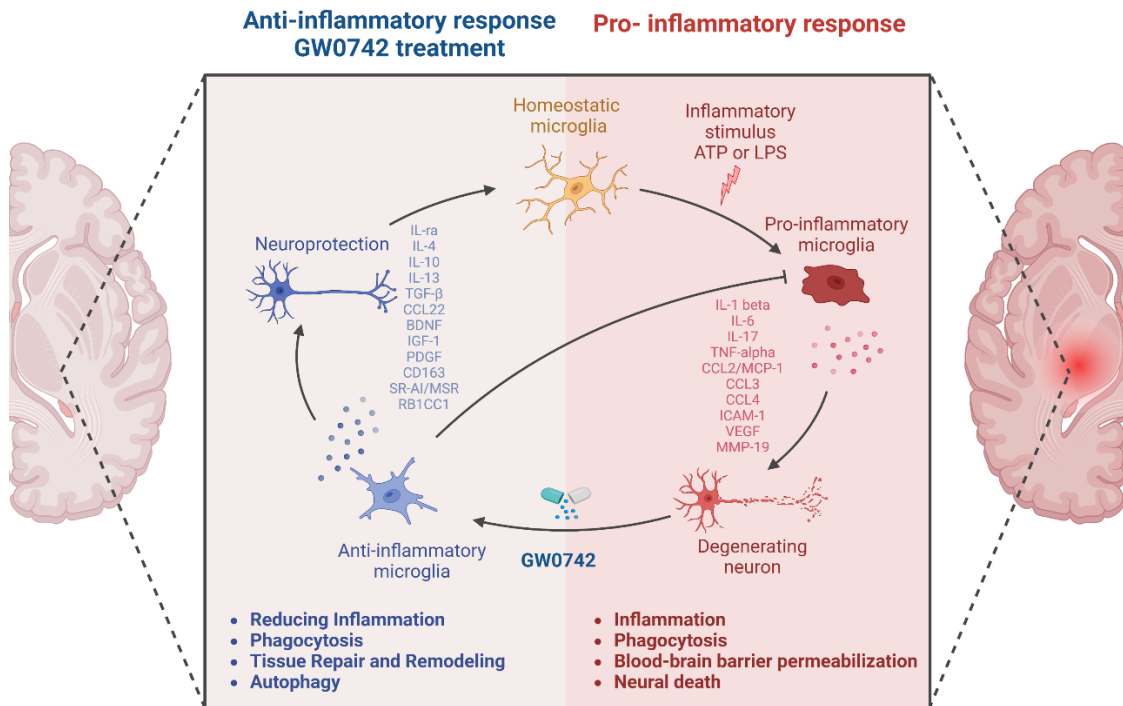


Figure 1. 4: Modulating Neuroinflammation with PPAR β Agonist GW0742: Proposed hypothesis. Balancing Pro-Inflammatory and Neuroprotective Responses. Created with BioRender.

The main objective of this thesis is to fill the knowledge gaps regarding the expression and function of PPAR β in glial cells, specifically microglia. Additionally, it aims to investigate the therapeutic potential of targeting PPAR β in the context of neuroinflammatory and neurodegenerative diseases.

1. Investigating the expression and function of PPARs and FABPs in microglia and astrocytes.

To characterize the expression patterns and functions of different PPAR isoforms and brain expressed FABPs in microglia and astrocytes (Warden et al., 2016a, Fidaleo et al., 2014, Boneva et al., 2011, Kagawa et al., 2015).

2. Examining the effects of age and inflammatory stimuli on PPAR and FABP expression in glial cells.

To investigate how age and inflammatory stimuli influence the expression and function of PPARs and FABPs in microglia and astrocytes.

3. Evaluating the anti-inflammatory and neuroprotective effects of PPAR β agonist.

To investigate the anti-inflammatory and neuroprotective effects of PPAR β agonists on microglia and astrocytes. Additionally, the potential interactions between PPAR β agonists, FABPs, and other signaling pathways will be explored to better understand their therapeutic potential in CNS disorders.

4. Utilizing human microglia-like cell models to study PPAR β agonist-effects upon inflammation.

To investigate the effects of PPAR agonists, particularly PPAR β agonists, on human microglial functions (Ohgidani et al., 2014).

5. Evaluate the interaction of PPAR ligands with the ABCG2 (BCRP) efflux transporter and its potential implications for CNS drug delivery.

By addressing these aims, this thesis hopes to provide new insights into the roles of PPAR β in regulating glial cell functions, the impact of age and inflammatory stimuli on their expression and function, and the therapeutic potential of PPAR β agonists in neuroinflammatory and neurodegenerative diseases. Ultimately, the findings from this study may contribute to the development of novel therapeutic strategies targeting glial cells and PPAR signalling pathways for age-related CNS disorders.

Chapter 2 Materials and Methods

2.1 Reagents

All chemicals were purchased from Sigma unless specified otherwise. All ligands/reagents were dissolved in DMSO unless stated otherwise and diluted in a cell culture medium to achieve a final DMSO concentration of 0.05% or less. The table below summarises the reagents, drugs, and inhibitors utilised.

Table 2.1 Bioreagents and Inhibitors Used

Name	Source
LPS from <i>Escherichia Coli</i> (strain O111: B4	Sigma-Aldrich, St Louis, MO, USA
Adenosine Triphosphate, ATP	Sigma-Aldrich, St Louis, MO, USA #A26209
Bovine serum Albumin, BSA	Sigma-Aldrich, St Louis, MO, USA #A8806
X-tremeGENE HP DNA Transfection	Roche
Complete EDTA-Free Protease Inhibitor Cocktail Tablets	Roche
Ni-NTA Agarose Beads	QIAGEN #30210
Nitrocellulose Membrane; 0.45 µm pore size	Amersham Protran
GW0742, PPAR β Agonist	Sigma-Aldrich, St Louis, MO, USA
GW 501516, PPAR β Agonist	Sigma-Aldrich, St Louis, MO, USA
Pioglitazone, PPAR γ Agonist	Sigma-Aldrich, St Louis, MO, USA
Rosiglitazone, PPAR γ Agonist	Sigma-Aldrich, St Louis, MO, USA
Gemfibrozil, PPAR α Agonist	Sigma-Aldrich, St Louis, MO, USA
WY-14,643, PPAR α Agonist	Sigma-Aldrich, St Louis, MO, USA
Aspirin	Sigma-Aldrich, St Louis, MO, USA
Mitoxantrone	Sigma-Aldrich, St Louis, MO, USA
Y-27632, Rho Kinase Inhibitor	Sigma-Aldrich, St Louis, MO, USA

2.2 Animal Primary Cell Culture

Adult male Sprague-Dawley rats (P40) were utilised for microglia isolation, whereas male and female neonatal (P0-2) rats were employed for the isolation of both astrocytes and microglia. All procedures were conducted in accordance with the guidelines of the Animals (Scientific Procedures) Act 1986 (ASPA). Adult rats were subjected to regulated procedures (licence PP3DA999F). Neonatal rats were utilised under the auspices of the Animal Welfare and Ethical Review Body (AWERB) non-ASPA 000217.

2.2.1 Neonatal Microglia

2.2.1.1 Isolation of Microglia

Rat litters, typically consisting of 10-14 pups, were collected at postnatal days 0-2 (P0-2) and euthanized by cervical dislocation and decapitation, then rinsed with 70% ethanol and sterile 1x phosphate-buffered saline (PBS). The brain and spinal cord were collected in ice-cold L-15 Leibovitz media with L-glutamine (HyClone) containing 1% (v/v) penicillin/streptomycin (P/S) and 0.1% bovine serum albumin (BSA). The meninges were gently removed from both the brain and spinal cord, discarded, and then the remaining tissue was transferred to 50 mL Falcon tubes using a serological pipette and centrifuged for 5 min at 2,500 x g at 4°C. The supernatant layers were discarded, and the pellets were resuspended in 5 mL fresh L-15 media, gently triturated using a serological pipette, and then the suspension was filtered through a 100 µm cell strainer to remove tissue debris. The cells were centrifuged for 5 min at 2,500 x g at 4°C, then the supernatant layer was discarded, and the cells were resuspended in 10 mL of culture media (DMEM, high glucose, no glutamine, no calcium, Gibco, Thermo Fisher Scientific) supplemented with 1% penicillin/streptomycin and 10% fetal bovine serum (FBS) for cortical cells and 5 mL for spinal cord cells. Cells were cultured in T-75 culture flasks and incubated at 37°C in a humidified atmosphere containing 5% CO₂. The medium was changed on the 5th day and subsequently every 3 days thereafter. Upon confluence, flasks were agitated on an orbital shaker at 120 rpm for 2 h at 37°C to detach the microglial cells. Media containing floating microglia were collected and centrifuged at 2,500 x g for 5 min at 4°C. The cells were subsequently resuspended in a seeding media (DMEM, high glucose, no glutamine, no calcium, supplemented with 1% penicillin/streptomycin and heat-inactivated horse foetal serum). The cells were seeded on plates pre-coated with poly-D-lysine at a density of approximately 100,000 cells/mL in a 12-well plate (Tamashiro et al., 2012).

2.2.1.2 Isolation of Microglia by Immunopanning

The immunopanning technique was employed in this study primarily to optimise the microglia culture and to facilitate microglia culture in serum-free media. Immunopanning is a method that allows for the selective isolation of microglial cells from a mixed cell population based on specific surface antigens. This technique was chosen due to its potential to yield highly pure microglial cultures, which is crucial for subsequent analyses that require minimal contamination from other cell types.

Despite its advantages, the immunopanning method resulted in a lower yield of microglia than anticipated. Consequently, the use of this technique was limited to a specific set of experiments within this study. The only successful application of the immunopanning method was in the investigation of morphological differences between adult and neonatal microglia.

Cells were isolated in a manner essentially as described previously. Rat litters, typically consisting of 10-14 pups, were collected at postnatal days 0-2 (P0-2) and euthanized by cervical dislocation and decapitation, then rinsed with 70% ethanol and sterile 1x phosphate-buffered saline (PBS). The brain and spinal cord were collected in ice-cold dissociation buffer. The meninges were gently removed from both the brain and spinal cord and discarded; then the remaining tissue was transferred to a Petri dish containing dissociation buffer and cut into 1 mm³ pieces. A glass tissue grinder was utilised to dissociate the tissue, which was then transferred to 50 mL Falcon tubes using a serological pipette, followed by the addition of cold myelin separation buffer and centrifugation for 15 min at 500 x g at 4°C with slow braking. The supernatant was removed using a pipette. The cell pellets were resuspended in 1 mL of panning buffer, then further diluted in 12 mL of panning buffer. The suspension was filtered through a 70 µm cell strainer to remove tissue debris. The cell suspension was added to the OX42-coated panning dish after three washes with Dulbecco's Phosphate-Buffered Saline supplemented with calcium and magnesium ions (DPBS++) (Gibco). To allow the cells to adhere, they were incubated at room temperature for 20 min on a flat surface. Removal of

non-adherent cells was achieved by rinsing the dish three times with PBS; then, to facilitate the detachment of microglial cells, the last wash was replaced with 15 mL of TrypLE Express Enzyme (Gibco) and incubated for 10 min at room temperature. The TrypLE was removed, and the dish was gently washed twice with 15 mL of PBS. A final wash was performed with 12 mL of ice-cold microglia growth medium (MGM). Cells were dislodged from the dish by vigorous pipetting with a 10 mL pipette. Cell suspensions were collected in a 15 mL conical tube and centrifuged for 15 min at 500 x g and 4°C, with slow braking. The cells were resuspended in MGM and seeded on pre-coated plates at a density of approximately 50,000 cells/mL in a 24-well plate. Every two days, 50% of the medium was replaced with fresh MGM media. The cells were maintained for 8 days until they reached confluence and were ready for use.

Panning Dish:

In the subsequent step, 25 mL of 50 mM Tris, pH 9.5, was added to a 15-cm untreated plastic Petri dish, followed by the addition of 6 µg/mL goat anti-mouse IgG (H+L chains). The dish was then incubated at 37°C for 3 hours. The dishes were subsequently washed three times with panning buffer, and a final wash was performed with panning buffer supplemented with 1 µg/mL anti-OX42 antibody. The dish was incubated at room temperature on a flat surface overnight.

Table 2. 2 Immunopanning Buffers Composition

Dissociation Buffer	200 µl of 4 mg/mL DNase I stock (Sigma) in 50 mL DPBS ⁺⁺
MGM	49 mL DMEM/F-12 (phenol red free, Gibco), 500 µL 100× pen-strep/glutamine, 500 µL TNS stock, 50 µL COG stock and 50 µL TCH stock.
TNS Stock	50 mg/mL <i>N</i> -acetyl cysteine (Sigma), 10 mg/mL sodium selenite (Sigma) and 100 mg/mL apo-transferrin in DMEM/F-12 (phenol red free, Gibco)
COG Stock	Oleic acid (Cayman Chemicals), 1 mg/mL and gondoic acid (Cayman Chemicals) and 1.67 mg/mL cholesterol (from ovine wool, Avanti Polar Lipids) in ethanol.
TCH Stock	12.5 µg/mL CSF-1 (Peprotech) to 12.5 µg/mL, human TGF-β2 (Peprotech), and 10 mg/mL heparan sulfate (Galen Laboratory) in PBS
Myelin Separation Buffer	90 mL Percoll PLUS (GE Healthcare), 10 mL 10× PBS, 90 µL 1 M CaCl ₂ and 50 µL 1 M MgCl ₂
Panning Buffer	Milk peptone solids (Sigma) dissolved to 2 mg/mL in DPBS ⁺⁺

2.2.2 Adult Microglia

For each experiment, four male rats were deeply anaesthetised with pentobarbital. Transcardiac perfusion was performed using heparin (2 U/mL) (UK, Wockhardt) in PBS at approximately 80 mmHg hydrostatic pressure. This procedure was essential for the removal of blood cells and for preventing contamination by monocytes from the brain and spinal cord. After about 5 minutes of perfusion or once the rat's liver appeared pale, the spinal cord and brain were removed using aseptic techniques, and the meninges were carefully excised. The brain and spinal cord were sectioned into 0.5 mm thick slices with a sterile scalpel, and the tissues were placed into 10 mL of Hibernate media (Gibco) supplemented with 130 U of papain (USA, Worthington). The tissues were incubated at 37°C with moderate rotation for 15 minutes. Following this, gentle trituration was applied before the tissues were returned to the incubator for an additional 15 minutes. Tissue dissociation was halted by adding an equal volume of DMEM, GlutaMAX™, high-glucose media (Gibco, Thermo Fisher Scientific), supplemented with 1% penicillin/streptomycin

and 10% heat-inactivated FBS. The cell suspension was filtered through a 100 μm cell strainer followed by a 70 μm cell strainer. The cells were then centrifuged at 397 x g for 5 minutes at room temperature. After discarding the supernatant layer, the cells were resuspended in DMEM, GlutaMAX™, high-glucose media. The cells were cultured in T-75 culture flasks pre-coated with poly-D-lysine. Following 24 hours of incubation at 37°C in a CO2 incubator, the flasks were tapped and washed twice with DMEM, GlutaMAX™, to remove non-adherent cells, then incubated with 15 mL of fresh media. The cells were maintained in the same media for 7 days until they reached confluence and were prepared for use. The cells were seeded on plates pre-coated with poly-D-lysine at a density of approximately 100,000 cells/mL in a 12-well plate (Yip et al., 2009, Rustenhoven et al., 2016).

2.2.3 Neonatal Astrocytes

Rat litters, typically consisting of 10-14 pups, were collected at postnatal days 0-2 (P0-2) and euthanized by cervical dislocation and decapitation. Bodies and heads were rinsed with 70% ethanol then with sterile 1x phosphate-buffered saline (PBS). The brain and spinal cord were collected and transferred to universal tubes containing ice-cold 5 mL of glial media (DMEM high glucose, Sigma, Life Science with L-glutamine and sodium pyruvate, supplemented with 1% P/S, L-proline, and 10% FBS). The media were discarded, and a vial of papain was reconstituted with 5 mL of media. Tissues were dissociated with papain, gently triturated with a serological pipette, then incubated for 40 min at 37°C. 500 μL of DNase solution was added to the tissues followed by centrifugation at 212 x g for 6 min. Supernatant layers were aspirated, and fresh media with 500 μL of DNase were added; then, the tissues were gently triturated with a pipette. The tissues were spun at 182 x g for 3 min, supernatant layers were transferred to a 25 mL universal tube, and the remaining cell pellets were resuspended in 10 mL of glial media and spun again at 182 x g for 3 min. Supernatant layers were combined with the previously collected supernatant. The cell pellets were then resuspended again in 10 mL of glial media and spun at 182 x g for 3 min. Supernatants were also

combined with the previously collected supernatant and spun at 212 x g for 6 min; then, the supernatant layers were removed, and the cells resuspended in 10 mL of glial media. The cell suspension was filtered through a 100 µm cell strainer, supplemented with fresh glial media, and transferred to T-75 culture flasks. The cells were incubated at 37°C and, to remove microglia, after 24 hours, flasks were shaken overnight at 120 rpm. The media were changed every 4 days until the cells reached confluence, around 19 days.

2.2.4 An Alternative Rapid Method to Isolate Neonatal Astrocytes

After the isolation of microglia cells using the shaking method described above, warm DMEM was immediately added to the flasks. The flasks were then shaken on an orbital shaker at 120 rpm overnight at 37°C to detach oligodendrocyte cells. The culture media were replaced with 5 mL of warm PBS to wash the cells twice, removing all traces of serum to ensure the enzyme's effectiveness. PBS was removed, and 5 mL of trypsin was added. The flasks were placed in the incubator for 5-10 min, then gently shaken to detach the cells from the bottom. The effectiveness of trypsinization is crucial for lifting the astrocyte monolayer; the time required for the removal of cells depends on their density, serum concentration, and temperature. To inactivate the trypsin, 5 mL of DMEM containing 10% FBS was added to each flask. The supernatant layer was collected and spun at 168 x g for 10 min. The cells were subsequently resuspended in glial seeding media (DMEM high glucose, Sigma Life Science, with L-glutamine and sodium pyruvate supplemented with 1% P/S, L-proline, and 10% FBS) (Mecha et al., 2011).

2.3 Culture of Immortalised Cell Lines

2.3.1 Cell Lines

The Human Embryonic Kidney (HEK) 293FT cell line and the HeLa Human cervical cancer cell line were obtained from the American Type Culture Collection (ATCC). The HEK293T-SNAP-ABCG2 cell line was kindly provided by Dr Ian Kerr, University of Nottingham.

All cells were tested for Mycoplasma contamination (MycoAlert, Lonza) following thawing and prior to cryopreservation. EMEM (M4526) or DMEM (D5671), Sigma-Aldrich, St. Louis, MO, USA, were supplemented with 10% FBS and 2 mM L-glutamine. Table 2. 3 outlines the cell lines and their respective uses in these studies.

Table 2. 3 Cell Lines Used

Cell Line	Purpose
(HEK) 293FT	Lentivirus Production
HeLa	Investigating SUMOylation of PPAR β
HEK293S-SNAP-ABCG2	Functional Transport Assay

The cells were incubated at 37°C in a humidified atmosphere containing 5% CO₂. The medium was changed every 2-3 days, and cells were passaged upon reaching approximately 80% confluency. Experiments were conducted using cells that had been passaged up to 20 times. To subculture the cells, the medium was aspirated from the flask, and the cells were washed twice with 1x phosphate-buffered saline (PBS) (BR0014G; Oxoid, Cheshire, UK). An appropriate volume of trypsin-ethylene-diamine-tetraacetic acid (EDTA) solution (T3924; Sigma-Aldrich, St. Louis, MO, USA) was added (2 mL for T75 flasks and 1 mL for T25 flasks). The cells were incubated at 37°C until complete detachment was observed (5-7 min). To inactivate the trypsin, serum-containing culture medium (at least double the volume of the trypsin) was added. In a sterile tube, cells were collected by gentle pipetting. Cell suspensions

were centrifuged at 125 g for 5 min. The supernatant layer was discarded, and the cell pellet was resuspended in fresh culture medium. An aliquot of the cell suspension was transferred to a new flask containing fresh media. The sub-cultivation ratios for HEK293FT, HeLa, and HEK293T-SNAP-ABCG2 cells were 1:10, 1:10, and 1:5, respectively.

2.3.2 Culture and Maintenance of Induced Human Pluripotent Stem Cells (hiPSCs)

Two feeder-free lines of human iPSCs were utilised in studies: LoPCK hiPSCs, kindly provided by Dr Nick Hannan, University of Nottingham (generated from human skin fibroblasts), and the Healthy Control Human iPSC Line, Female, SCTi003-A (Stem Cell Technologies), derived from peripheral blood mononuclear cells (PBMCs).

hiPSCs were cultured under feeder-free conditions in T25 flasks coated with a thin layer of Cultrex™ Stem Cell Qualified RGF BME (80 µg/mL; Bio-Techne) and nourished with TeSR™-E8™ media (Stem Cell Technologies). The medium was changed daily, and cells were passaged using ReLeSR (05872, Stem Cell Technologies) every 3-5 days (or at 70% confluency). For passaging, cells were washed once with PBS, and ReLeSR was added for 30 seconds; the dissociation reagent was then removed by aspiration, and cells were incubated at 37°C for 3 minutes. Fresh TeSR™-E8™ medium was gently added to detach the colonies by lightly tapping the flasks for 60 seconds. The newly coated flask was seeded at a 1:10 to 1:50 ratio depending on cell confluency. The flasks were agitated in several quick, short, back-and-forth, and side-to-side motions to ensure an even distribution of cell aggregates, then placed in the incubator for 24 hours without disruption.

2.3.2.1 Cell Freezing

The mixture of detached cell aggregates was transferred to a 20 mL Universal tube and centrifuged for 5 minutes at 300 rpm. The supernatant layer was aspirated, and the cell pellet was gently resuspended in CryoStor using 5 mL serological pipettes to minimise the breakup of cell aggregates (CS10 07930, Stem Cell Technologies). The cell aggregates were cryopreserved following a standard slow rate-controlled cooling protocol, reducing temperatures at approximately -1°C per minute, followed by long-term storage in liquid nitrogen.

2.3.2.2 STEMdiff™ Trilineage Differentiation Kit and hPSC Genetic Analysis Kit

To functionally validate the ability of iPSCs to differentiate towards ectoderm, mesoderm, and endoderm, the STEMdiff™ Trilineage Differentiation Kit (05230, Stem Cell Technologies) was utilised in accordance with the manufacturer's instructions. For the detection of the most recurrent karyotyping abnormalities reported in human iPSCs, the hPSC Genetic Analysis Kit (07550, Stem Cell Technologies) was employed as per the manufacturer's guidelines. Genomic DNA purification was carried out using the Genomic DNA Purification Kit (Thermo Scientific GeneJET).

2.3.3 Differentiation of iPSCs into Microglia-like Cells (iPS-microglia)

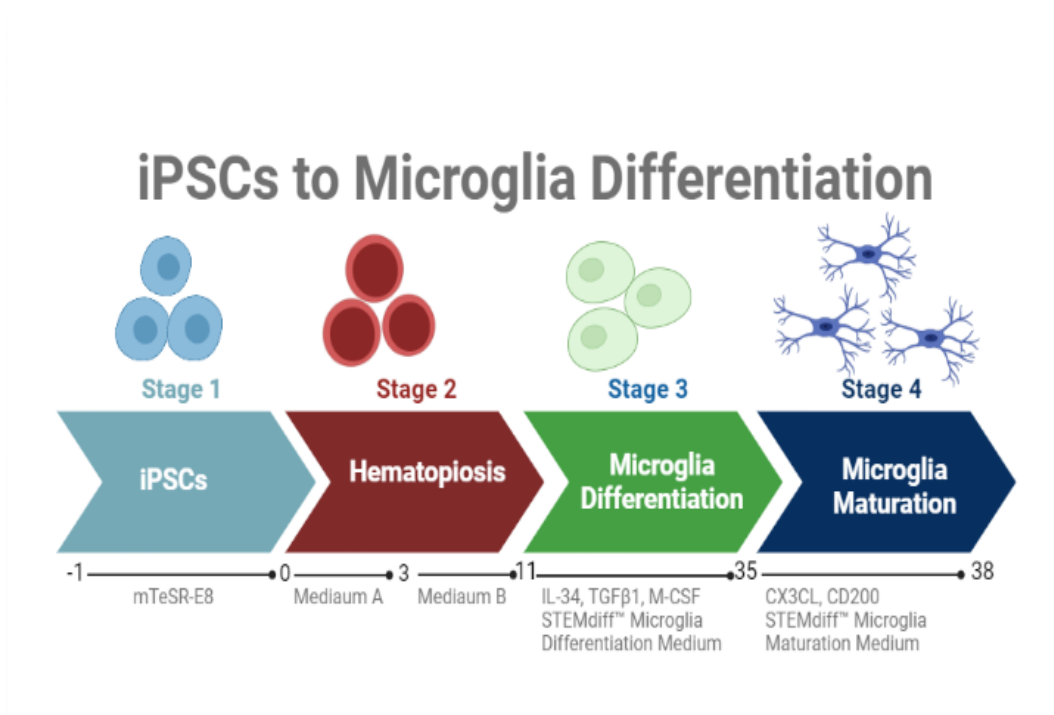


Figure 2. 1 Timeline for induced microglia cell using iPSCs. Differentiation from iPSCs was initiated through the mesoderm lineage (days 0–3), leading subsequently to hematopoiesis (days 3–11). Thereafter, floating haematopoietic progenitor cells (HPCs) were transferred to a new medium for a period of 27 days to induce microglial differentiation. Additional neuronal and astrocytic ligands were introduced during the final three days of differentiation to enhance the brain-like characteristics of the microglia. This figure was generated using BioRender.com.

2.3.3.1 Differentiation of Human iPSCs into Hematopoietic Progenitor Cells (HPCs)

Differentiation of iPSCs to CD43⁺ primitive hematopoietic progenitor cells (HPCs) was achieved utilising the STEMdiff™ Hematopoietic Kit (STEMCELL Technologies). Feeder-free iPSCs grown in TeSR-E8 media were passaged with ReLeaSR, and small aggregates of approximately 100 cells each were plated at densities of 10–20 aggregates per cm² onto Cultrex pre-coated 6-well plates. Cells were plated at 2–3 different densities on day 0. Wells with optimal density were selected, as higher densities impair mesoderm differentiation, while lower densities decrease yield. On day 1, TeSR-E8 medium was replaced with Medium A after achieving two 100-cell colonies per cm² (Basal medium plus Supplement A at a 1:200 dilution, 2 mL per well of a 6-well plate). On day 2, 50% of Medium A was replaced, 1 mL per well of a 6-well plate. On day 3, all media were carefully removed by tilting the plate and aspirating from one edge, then 2 mL of Medium B (1:200) was added to each well (Basal medium plus Supplement B). On days 5, 7, and 9, 1 mL of Medium B was added to each well without removing the existing media. Non-adherent cells were carefully collected on day 12 to maintain purity without washing the well, and the cells were centrifuged at 300g for 5 minutes. Different methods were employed to achieve the best population of hematopoietic progenitor cells (see Table 2. 4) (Heo et al., 2018, Niwa et al., 2011, Douvaras et al., 2017, Fattorelli et al., 2021). Real-time qPCR measurement of gene expression confirmed these non-adherent cells represent highly pure populations of CD43⁺ or CD34⁺ hematopoietic progenitor cells.

Table 2. 4 Different Methods to Differentiate iPSCs Towards HPCs

Stemline II Hematopoietic Stem Cell Expansion Medium (Sigma #S0192), BMP4 (R&D #314-BP-01), FLT3 (R&D #308-FK), G-CSF (R&D #214-CS), VEGF (R&D #293-VE), Tpo (R&D #288-TPN), and SCF (R&D #255-SC) are detailed with culture numbers, seeding, media, and durations for various methods.

Culture No:	Seeding	Media				Duration
V1	2D culture 1-10 Aggregates seeded per well	Day 0-4 Stemline II SFM + ITS BMP4 (20ng/mL)	Day 4-6 Stemline II SFM + ITS VEGF (40ng/mL) SCF (50ng/mL)	Day 6- 17 Stemline II SFM + ITS SCF (50ng/mL) TPO (10ng/mL) IL-3 (50ng/mL) G-CSF (50ng/mL) FLT3 (50ng/mL)		17 days
V2	2D 1-5 aggregates seeded per well	Day 0-4 Stemline II SFM + ITS BMP4 (80ng/mL)	Day 4-6 Stemline II SFM + ITS VEGF (80ng/mL) SCF (100ng/mL)	Day 6- 14 Stemline II SFM + ITS SCF (50ng/mL) TPO (5ng/mL) IL-3 (50ng/mL) G-CSF (50ng/mL) FLT3 (50ng/mL)	Day 14-25 Stemline II SFM + ITS G-CSF (50ng/mL) FLT3 (50ng/mL)	25-40 days
	3D culture EB's were formed in ultra-low U bottom 96 well plates in TeSR-E8, before seeding in 6 well plates					
V3	2D 1-5 Aggregates seeded per well	Day 0-4 Stemline II SFM BMP4 (50ng/mL) VEGF (50ng/mL) SCF (50ng/mL)	Day 4-11 Stemline II SFM SCF (50ng/mL) M-CSF (50ng/mL) IL3 (50ng/mL) FLT3 (50ng/mL) TPO (5ng/mL)	Day 11-18 Stemline II SFM FLT3 (50ng/mL) GM-CSF (25ng/mL) M-CSF (50ng/mL)		18 days
	3D culture EB's were formed in ultra-low U bottom 96 well plates in TeSR-E8 + BVS from day 1-4, before seeding in 6 well plates on day 4	Day 0-4 TeSR-E8 + BVS BMP4 (50ng/mL) VEGF (50ng/mL) SCF (20ng/mL)	Day 4-11 Stemline II SFM + SMIFT SCF (50ng/mL) M-CSF (50ng/mL) IL3 (50ng/mL) FLT3 (50ng/mL) TPO (5ng/mL)	Day 11-18 Stemline II SFM + FMG FLT3 (50ng/mL) M-CSF (50ng/mL) GM-CSF (25ng/mL)		
Stem Cell Kit	2D culture 5-20 aggregates	Day 0-3 Media A	Day 3-12 Media B			12 days

2.3.3.2 Differentiation of HPCs to iPS-Microglia

On day 0 of iPS-microglia differentiation, HPCs were plated at a density of 10,000 cells per cm² onto Cultrex-coated plates. Cells were seeded into iPS-microglia medium (DMEM/F12, 2X insulin-transferrin-selenite, 2X B27, 0.5X N2, 1X GlutaMAX, 1X non-essential amino acids, 400 µM monothioglycerol, 5 µg/mL insulin). Prior to use, the microglial medium was supplemented with 100 ng/mL IL-34, 50 ng/mL TGFβ1, and 25 ng/mL M-CSF, taken from single-use frozen aliquots.

On days 2, 4, 6, 8, and 10, 500 µL of fresh media plus a freshly thawed tri-cytokine cocktail were added to the cells' conditioned media without removal, since these cells secrete paracrine cytokine signals essential for their proper differentiation. On day 12, 3 mL of media from each well were collected, leaving 500 µL of conditioned medium on the plate. The non-adherent cells in the collected medium were centrifuged at 300g for 5 minutes. The collected medium was discarded, and non-adherent cells were resuspended in 500 µL of fresh media containing a tri-cytokine cocktail per well of a 12-well plate and added to the same well containing 500 µL of conditioned medium. Cells were continuously supplemented with 500 µL of fresh media on days 14, 16, 18, 20, 22, and 24. On day 25, cells were centrifuged, leaving 500 µL of conditioned medium per well, as on day 12.

On day 25, cells were resuspended in microglia medium supplemented with 100 ng/mL IL-34, 50 ng/mL TGFβ1, 25 ng/mL M-CSF, 100 ng/mL CD200, and 100 ng/mL CX3CL1 to further mature the microglia and ensure homeostasis. On day 27, the cells were fed with microglia medium containing the five-cytokine cocktail (500 µL per well). On day 28, the cells were collected for RNA extraction or for functional assays (McQuade et al., 2018).

2.3.3.3 Differentiation of HPCs to iPS-Microglia Using the STEMdiff™ Microglia Differentiation Kit

The STEMdiff™ Microglia Differentiation Kit (Catalogue #100-0019) and the STEMdiff™ Microglia Maturation Kit (Catalogue #100-0020) from Stem Cell Technologies were employed to differentiate and mature microglia derived from human pluripotent stem cells (hPSCs), utilising the STEMdiff™ Hematopoietic Kit (Catalogue #05310) in accordance with the manufacturer's protocol.

2.3.4 Generation of Induced Microglia-Like Cells (iMG Cells) From Monocytes

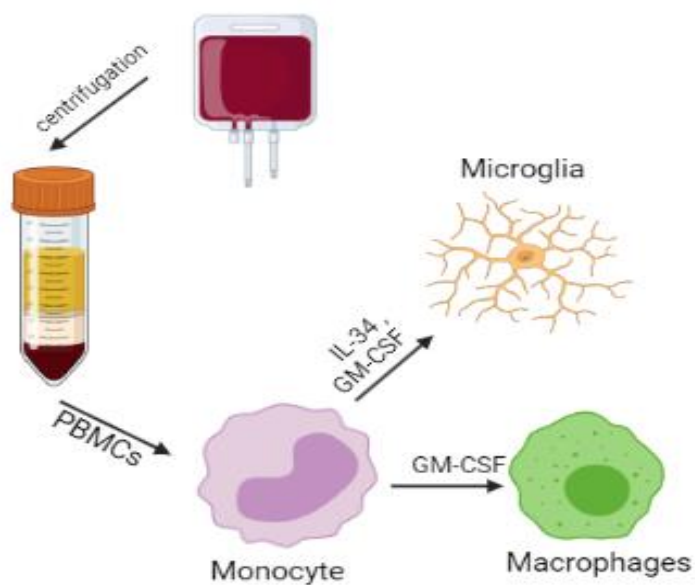


Figure 2. 2 Differentiation of human monocyte to microglia like cells. Human peripheral blood monocytes were isolated from blood and stimulated with IL-34 and GM-CSF for microglia-like cells and GM-CSF only for macrophages.

2.3.4.1 Human Peripheral Blood Mononuclear Cell (PBMCs) Isolation

In this study, buffy coat samples were procured from the National Health Service (NHS) Blood and Transplant service. Human peripheral blood mononuclear cells (PBMCs) were isolated by density gradient centrifugation. 5 mL of buffy coat was carefully overlaid on 5 mL Histopaque-1077 in a 15 mL conical centrifuge tube. Subsequently, the samples were centrifuged at 400x g for 30 minutes at room temperature, employing slow brakes and accelerations to prevent clumping and ensure efficient recovery. After centrifugation, the upper layer was collected for autologous serum preparation; PBMCs from the Histopaque-1077 interface were transferred into a new tube using a sterile Pasteur pipette. Cells underwent three wash cycles in cell culture media, with pipetting used for mixing. They were centrifuged at 300x g for 10 minutes, discarding the supernatant layer each time. A final spin at 200x g for 10 minutes was performed to remove platelets. The number of PBMCs was determined using a hemocytometer, with cells being utilised either immediately or after being frozen.

2.3.4.2 Isolation of Monocytes

Monocytes were isolated either through plastic adherence or utilising CD14 MicroBeads UltraPure, an LS Column, and a MiniMACS™ Separator (Miltenyi Biotec, #130-118-906). For the CD14+ microbeads method, the cell pellet was resuspended in 80 µL of buffer (PBS, pH 7.2, 0.5% bovine serum albumin (BSA), and 2 mM EDTA) per 10^7 total cells. To this, 20 µL of CD14 MicroBeads were added per 10^7 total cells, the cell suspension was thoroughly mixed and incubated for 15 minutes at 2-8 °C. The cells were then washed by adding 2 mL of buffer per 10^7 cells and centrifuged at 300x g for 10 minutes. The supernatant layer was completely discarded. Cell pellets were resuspended in up to 10^8 cells in 500 µL of buffer. Magnetic separation was conducted using LS Columns. The LS column was positioned in the magnetic field of the MACS Separator and pre-washed with 3 mL buffer. A Pre-Separation Filter was moistened by introducing 500 µL of buffer into the reservoir. Cells were

passed through a pre-separation filter (30 μm , Miltenyi Biotec) to eliminate cell clumps. The cell suspension was applied to the column, followed by the addition of 3 mL of buffer three times to the column. The flow-through, containing unlabelled cells, was discarded. The column was removed from the separator and positioned in a collection tube; 5 mL of buffer was added to the column, and magnetically separated cells were eluted by firmly pressing the plunger into the column.

Cells were resuspended in complete media (RPMI-1640, 10% FBS, 1% (v/v) penicillin/streptomycin) and seeded at the required density on plates pre-coated with Cultrex. They were allowed to adhere in a 5% CO₂ incubator at 37°C for 2 hours or overnight. PBMCs from frozen samples were thawed and washed with complete media before use.

Nonadherent cells were carefully removed. For microglia induction, the adherent monocytes were cultured in serum-free media (RPMI-1640 GlutaMAX supplemented with 10 ng/mL GM-CSF, 100 ng/mL IL-34, and 1% penicillin/streptomycin) for 10–14 days. Induced macrophages (iMacs) were also generated from monocytes, cultured in RPMI-1640 GlutaMAX media containing 10% FBS, 10 ng/mL GM-CSF, and 1% penicillin/streptomycin for 7 days. IL-34 and GM-CSF, purchased from R&D Systems, during differentiation, media were refreshed every 3-4 days.

2.3.5 Generation of Induced Dopaminergic Neurons (iDANs)

iPSCs were harvested by incubation with Accutase Cell Detachment Solution to generate single-cell suspensions. The suspension was quenched with DMEM in a volumetric ratio of 1:3 (Accutase:DMEM). The cells were then centrifuged at room temperature at 800x g for 5 minutes. The pellets were resuspended in mTeSR plus media containing a Rho kinase inhibitor (10 μM) and seeded at high density in a 12-well plate, 500k-750k cells per well, with 10 μM Rho kinase inhibitor. Appropriate viruses, pUBIQ-rTTa and tetO-ALN, were added at the proper concentration. The

hiPSCs were plated on a Matrigel-coated plate and incubated overnight at 37°C with the virus. The following day, Day 1, the media was aspirated and switched to Induction Media [DMEM/F12, 25 µg/mL insulin, 50 µg/mL transferrin, 30 nM sodium selenite, 20 nM progesterone, 100 nM putrescine, and the addition of doxycycline (1 µg/mL)]. Media were refreshed daily due to the presence of many dead cells. On Day 5, to inhibit the proliferation of non-neuronal cells, the media was supplemented with 2.0 µM arabinosylcytosine ("Ara-C"). After 7 days of differentiation, 50X B27 was added and maintained for the next 7-18 days, with the medium being changed every 2-3 days. Half media changes were performed every other day until the desired time point (Theka et al., 2013, Powell et al., 2021).

2.4 Cell Counting

A hemocytometer was used to determine the number of cells.

2.5 Coating Cell Culture Flasks and Plates

Culture flasks or plates were coated with Stem Cell Qualified Reduced Growth Factor Basement Membrane Extract (RGF BME) to facilitate the attachment and growth of cells. BME (8-12 mg/mL) was thawed on ice, mixed gently by pipetting up and down, and Cultrex™ Stem Cell Qualified Reduced Growth Factor (R&D #3434-005-02) was diluted 1:100 in a cold serum-free medium to achieve the desired concentration. A sufficient amount of the solution was added to cover the entire growth surface area. The coated culture ware was incubated for 1 hour at room temperature, then sealed with Parafilm® and stored for up to two weeks in a refrigerator at 2-8 °C. Before use, the coated flasks or plates were brought to room temperature for one hour and washed once with PBS.

2.6 Cell Treatment and Microglia Condition Media (MCM)

Cells were seeded on 12-well plates pre-coated with poly-D-lysine. Rat microglia or astrocytes were seeded in either serum-rich or serum-free medium using advanced DMEM/F-12 [Gibco supplied with G-5 (Gibco), L-glutamine, and 1% penicillin/streptomycin] media. The cells were incubated overnight at 37°C to allow them to adhere. To induce inflammation, adult and neonatal rat microglia were incubated with 100 ng/mL LPS for 6 hours or 100 µM ATP for 3 and 6 hours. PPAR agonists were added to the medium 1 hour before stimulation. After incubating adult and neonatal microglia for either 3 or 6 hours, the media were removed, and the cells were washed with PBS. Fresh media, either serum-rich or serum-free, were added to the cells, then incubated for 24 hours. M10 were collected, and then the cells were lysed using 300 µL of Tri Reagent and stored at -80°C for further assay.

Human induced macrophages and microglia were treated on 12-well plates pre-coated with Cultrex using the same induction media. To trigger inflammation, the cells were incubated with 5-100 ng/mL LPS or 10-100 µM ATP at different time points.

2.7 Phagocytosis Assay

The phagocytosis assay was conducted principally as described by (Lian et al., 2016). Green, fluorescent latex beads (Sigma-Aldrich, #L1030) were pre-opsinised in FBS for 1 hour at 37°C at a ratio of beads to FBS of 1:5 to coat them with proteins that enhance their uptake by immune cells. Subsequently, they were diluted in microglia media (MGM) to achieve a final concentration of 0.01% (v/v) beads and 0.05% (v/v) FBS in MGM. The media in cultures were replaced with MGM containing the beads and incubated at 37°C for either 1 hour or 24 hours, followed by washing the cultures five times with ice-cold PBS. The cells were then fixed using 4% paraformaldehyde (PFA) for 15 minutes. To permeabilise the cells, Triton X-100 0.1% was added, followed by rinsing with PBS. To block non-specific binding, BSA at

0.5% was used for 1 hour at room temperature. Cells were incubated with a goat primary antibody anti-Iba-1 (Novus Biotechnologies) overnight at 4°C at a dilution of 1:1000 in 0.5% BSA in PBS. After being rinsed three times with PBS, cells were incubated for 45 minutes with a donkey anti-goat secondary antibody (1:500) at room temperature. This was followed by rinsing with PBS, and DAPI (Sigma #32670) was used to stain cell nuclei for 2 minutes, followed by a final rinse with PBS. Images were captured using 10x or 20x magnification with a widefield inverted fluorescence microscope.

2.8 Immunocytochemistry

Cells were rinsed twice with PBS to eliminate any debris and dead cells. Cells were then fixed using 4% paraformaldehyde (PFA) for 10 minutes, followed by three washes with PBS. Post-fixation, samples were treated with a permeabilization buffer (Triton X-100) for 10 minutes at room temperature on a shaker to permeabilize the cells (Table 2. 5). Following this, the cells were washed three times with PBS for 5 minutes each. A blocking buffer was then applied to prevent non-specific binding for 1 hour at room temperature. Overnight, cells were incubated with the primary antibody diluted in blocking buffer with gentle agitation at 4°C (Table 2. 5), (Table 2. 6).

After washing three times with PBS, cells were incubated with the secondary antibody for 45 minutes at room temperature in the dark (Table 2. 7). This was followed by a final series of PBS washes, and then cells were stained with 4',6-diamidino-2-phenylindole (DAPI, Sigma #32670) at a concentration of 1 µg/mL (1:1000) for 2 minutes, followed by a final wash with PBS. Images were captured at 10x or 20x magnification using an epifluorescence microscope.

Table 2. 5 Immunocytochemistry Buffers

Buffer	Composition
Permeabilization buffer for glial cells	0.3% w/v Triton™ X-100 in PBS
Blocking buffer for glial cells	0.5% w/v BSA in PBS
Permeabilization and Blocking buffer for iPSCs	0.3% w/v Triton™ X-100, 1% BSA, 10% Horse serum in PBS

Table 2. 6 Primary Antibodies Used for Immunocytochemistry

Antibody	Dilution	Source
Polyclonal Goat Human SOX17 Antibody	10 µg/mL	R&D systems AF1924
Polyclonal Goat Human Otx2 Antibody	10 µg/mL	R&D systems AF1979
Polyclonal Goat Human/Mouse Brachyury Antibody	10 µg/mL	R&D systems AF2085
TMEM119 Rabbit Polyclonal Antibody	1:500	Proteintech 2758-5-AP
P2RY12 Rabbit Polyclonal Antibody	1:200	Sigma HPA014518
MOUSE ANTI-NEURONAL NUCLEI (NeuN) Monoclonal Antibody	1:100	Millipore MAB377
Polyclonal Rabbit Anti-Glial Fibrillary Acidic Protein	1:500	Dako Z0334
AIF-1/Iba1 Antibody	1:500	Novusbio NB100-1028

Table 2. 7 Secondary Antibodies Used for Immunocytochemistry

Antibody	Dilution	Source
Donkey anti-Rabbit IgG (H+L) Highly Cross-Adsorbed Secondary Antibody, Alexa Fluor 647	1:500	Invitrogen A-31573
Donkey anti-Goat IgG (H+L) Cross-Adsorbed Secondary Antibody, Alexa Fluor 594	1:500	Invitrogen A-11058
Donkey anti-Mouse IgG (H+L) Highly Cross-Adsorbed Secondary Antibody, Alexa Fluor 488	1:500	Invitrogen A-21202

2.9 In-vitro SUMOylation Assay

The in-vitro SUMOylation assay was performed essentially as per the method described by (Pourcet et al., 2013). HeLa cells were seeded at a density of 3×10^6 in 10 cm Petri dishes and transfected with 9 μg of the appropriate plasmids for 48 hours, as detailed in (Table 2. 8).

Table 2. 8 The condition of Transfection

Gene	Amount	Vector	Source
6xHis-SUMO3GG or 6xHis-SUMO2GG	2.5 μg	pSG5 pSG5	Frame lab (Razan, 2018)
HA-PPAR β Or (FLAG-LXR β positive control)	2.5 μg	PPAR β , 2x HA pAdTrack-CMV LXR β , p3xFLAG- CMV-7.1	(Addgene #16529) Frame lab (Razan, 2018)
HA-Ubc-9	2 μg	pcDNA3.1(+) zeo	Frame lab (Razan, 2018)
PIAS1, PIASy or HDAC4	2 μg	PIAS1 and PIASy pcDNA3.1(+) zeo HDAC4, Flag pcDNA3.1(+)	Frame lab (Razan, 2018) (Addgene #13821)
Transfection mix:			
Serum free medium	900 μl		
X-tremeGENE	18 μl		
The mix was combined with plasmids and incubated for 30 min at RT. Afterward, 900 μl of the mixture was added to each cell culture dish.			

After the medium was refreshed 24 hours post-transfection, the cells were treated with either a LXR β or PPAR β agonist and incubated for 1, 8, and 24 hours. Following this, the cells underwent three washes with ice-cold PBS and were then harvested in 2 mL of PBS using a scraper. They were centrifuged at 800x g for 5 minutes at 4°C to pellet the cells. The whole protein extract was divided, with 200 μL (10%) allocated as input and prepared in RIPA buffer (Table 2. 9). The remaining 1800 μL (90%) of the cell lysate was used for protein isolation with nickel (Ni-NTA) beads, followed by lysis using denaturing lysis buffer (Table 2. 9) and sonication. After a 30-minute incubation at 4°C on a roller, the lysates were centrifuged at 20,000 g for 15

minutes at 4°C to separate the supernatant layer. The 10% input was stored at -80°C for further protein content analysis and determination using the Pierce™ BCA Protein Assay Kit.

The Ni-NTA beads were washed twice with denaturing lysis buffer, then resuspended in the same volume of buffer to create a 50% slurry. The 90% cell lysate was incubated with 70 µL of the 50% v/v Ni-NTA matrix slurry overnight at 4°C on a roller. After three washes, 1 mL of washing buffer I was added, the mixture was vortexed and centrifuged at 5,000 g for 2 minutes at 4°C. The supernatant was discarded, and this process was repeated with washing buffer II and III. His-tagged proteins were eluted from the beads by adding 60 µL of 500 mM imidazole and vortexing for 30 seconds. The supernatant layers were collected by centrifugation at 20,000 g for one minute at 4°C, and 30 µL of Laemmli 3× buffer (187.5 mM Tris-HCl, pH 6.8; 6% SDS; 30% Glycerol; 6% β-mercaptoethanol; 0.3% w/v Bromophenol blue) was added. The mixture was vortexed for 30 seconds and centrifuged at 5,000 g for 2 minutes at 4°C. SDS-PAGE was employed to resolve purified and unpurified proteins, followed by immunoblotting with appropriate antibodies, Anti-HA for PPARβ, or Anti-flag for LXRβ.

Table 2. 9 Pull-Down Buffer Composition

Buffer	Composition
RIPA Buffer	10 mM Tris-HCl, 150 mM NaCl, 0.5% Na Deoxycholate, 1 mM EDTA, 1% Triton X-100, 0.1% SDS and 1x EDTA-free protease inhibitor
Lysis Buffer	6 M guanidine-HCl, 10 mM Tris-HCl (pH 8.0), 100 mM NaH ₂ PO ₄ , 10 mM imidazole and 1x EDTA-free protease inhibitor adjusted to pH 8
Wash Buffer I	6 M Guanidine-HCl; 1 mM Tris-HCl, pH 8.0; 100 mM NaH ₂ PO ₄ ; 10 mM imidazole; 300 mM NaCl; 0.5% Triton X-100; 1x protease inhibitor cocktail complete EDTA-free
Wash Buffer II	8 M urea, 10 mM Tris-HCl, pH 8.0; 100 mM NaH ₂ PO ₄ ; 20 mM imidazole; 300 mM NaCl; 0.5% Triton X-100; 1x protease inhibitor cocktail complete EDTA-free
Wash Buffer III	Ice cold PBS

2.10 Functional Transport Assay

ABCG2-expressing cell lines were employed to evaluate the capability of PPAR β ligands to be transported across the blood-brain barrier, utilising mitoxantrone transport inhibition as a model. Black-sided/clear-bottom 96-well plates (Costar) were treated for one hour with 10 μ g/mL poly-D-lysine, followed by aspiration and washing with HPLC water. HEK293S SNAP-ABCG2 cells were seeded in DMEM (10% FBS, penicillin/streptomycin, and L-glutamine solution) with geneticin (G418 [61-234-RG; Corning, Corning, NY, USA]) for selection, at a density of 40,000 cells per well. The cells were incubated overnight at 37°C with 5% CO₂, ensuring >90% confluence before initiating the assays. Media were removed from each well by aspiration. Each well received 200 μ L of the designated solution (vehicle control: DMSO; No inhibitor control: Mitoxantrone (MX); Positive control inhibitor: Ko143+ MX; PPAR ligand (GW0742, GW501516, WY 14643, or Rosiglitazone) + MX).

Following the initial addition of treatment, cells were incubated for 1 hour at 37°C. Each well was washed once with ice-cold PBS, then treated with 100 μ L of 4% paraformaldehyde for 10 minutes (in a fume hood). Afterward, the wells were washed again with ice-cold PBS, and 200 μ L of ice-cold PBS was added to each well. Fluorescence was measured using a fluorescence microplate reader at the appropriate excitation and emission wavelengths (λ_{ec} 607 nm, λ_{em} 684 nm for mitoxantrone). The values for the vehicle control DMSO were subtracted from the substrate data.

2.11 Molecular Biology

2.11.1 RNA Extraction and cDNA Synthesis

Total RNA from cells was extracted using Tri Reagent® following the manufacturer's instructions. RNA purity and concentration were assessed spectrophotometrically at absorbance ratios of 260 nm and 280 nm. cDNA was synthesised from 100-500 ng of RNA samples using the AffinityScript Multiple Temperature cDNA Synthesis Kit (Agilent Technologies), adhering to the manufacturer's guidelines.

2.11.2 TaqMan qPCR

Quantification of gene expression via real-time qPCR was performed using the AriaMx real-time PCR system from Agilent. Gene expression levels were normalised to GAPDH. Primer and probe sequences were designed using Primer Express Software Version 3.0 (Applied Biosystems Inc., Foster City, CA, USA). Primers for rat and human genes were listed in Table 2.10 and Table 2.11 respectively. Primers and probes were procured from Eurofins Scientific (Luxembourg). Sterile DNase RNase free water was utilised as per the manufacturer's instructions to reconstitute the primers, creating a 100 µM stock concentration. This stock was further diluted to a working concentration of 10 µM before use.

Table 2. 10 Primers and Probes Sequences for Real-Time qPCR, Rat Gene

Genes	Rat Primers/probes	Sequences 5' to 3'
GAPDH	Forward primer	TCTGCTCCTCCCTGTTCTAGAGA
	Reverse primer	CGACCTTCACCATCTTGTCTATGA
	TaqMan probe	ATCTTCTTGTGCAGTGCCAGCCTCG
PPARα	Forward primer	TGGAGTCCACGCATGTGAAG
	Reverse primer	TGTTCCGGTTCTTTTTCTGAATCT
	TaqMan probe	CTTCTTTCGGCGAACTATTCGGCTAAAGC
PPARβ	Forward primer	GAGCATCCTCACTGGCA AGTC
	Reverse primer	TGCCACAGCGTCTCAATGTC
	TaqMan probe	AGCCATAACGCACCCTTCATCATCCA
PPARγ	Forward primer	TGCCAAAAATATCCCTGGTTTC
	Reverse primer	TGAATCCTTGTCCCTCTGATATGA
	TaqMan probe	AGATCATCTACACCATGCTGGCCTCCC
FABP5	Forward primer	TGAGGACTACATGAAGG AACTAGGAGTAG
	Reverse primer	TTTTGACGGTGAGGTTGTTGTT
	TaqMan probe	CCAAACCAGACTGCATCATTACCCTCGA
FABP7	Forward primer	CTCTGGGCGTGGGCTTT
	Reverse primer	CAAACCTTTCTCCCAGCTGGAA
	TaqMan probe	TGGTGATCCGGACACAATGCACATTC
FABP8	Forward primer	GGGAAAATGGTAGTGGAATGTATAATG
	Reverse primer	CAACGATTTTCTCAGACCTTCTCA
	TaqMan probe	TGAAGGCTCTAGGCCTGG
IL-1β	Forward primer	CACCTCTCAAGCAGAGCACAG
	Reverse primer	GGGTGTCCCACCATTGCTGTTTCCTAGG
	TaqMan probe	TGTCCCACCATTGCTGTTTCCTAGG

Table 2. 11 Primers and probes sequences for real-time qPCR, Human gene

Genes	Rat Primers/probes	Sequences 5' to 3'
PPARβ	Forward primer	CATCCTCACCGGCAAAG C
	Reverse primer	CCTTCTCTGCCTGCCACA AT
	TaqMan probe	ACACGGCGCCCTTTGTG ATCCA
PPARγ	Forward primer	GTGGAGACCGCCCAGGTT
	Reverse primer	ACTCAGGGTGGTTCAGCTTCA
	TaqMan probe	ACAACCTGCTACAAGCCCTGGAGCTCC
FABP5	Forward primer	GGTGCATTGGTTCAGCATCA
	Reverse primer	ACACTCCACCACTAATTTCCCATCT
	TaqMan probe MGB	AGGAAAGCACAATAAC
FABP7	Forward primer	TGGTGGAGGCTTTCTGTG
	Reverse primer	TTCCACCTGCCTAGTG
	TaqMan probe	TGGTGGAGGCTTTCTGTG
FABP8	Forward primer	GGCCAGGAATTTGAAGAAACC
	Reverse primer	CCATCTCTGCACTTGATTCAGT
	TaqMan probe	GACCAAGAGCATCGTAACCCTGCAGA
IL-1β	Forward primer	CCCTAAACAGATGAAGTGCTCCTT
	Reverse primer	GGTGGTCGGAGATTCGTAGCT
	TaqMan probe	CGCCCACTGCTCCTGTGACAGC
IL-6	Forward primer	ACCTCTTCAGAACGAATTGACAAAC
	Reverse primer	TGTTACTCTTGTTACATGTCTCCTTTCTC
	TaqMan probe	TACATCCTCGACGGCATCTCAGCCC
TNF-α	Forward primer	CCCAGGGACCTCTCTAATCA
	Reverse primer	GGTTTGCTACAACATGGGCTACA
	TaqMan probe	CTCTGGCCCAGGCAGTCAGATCATCT
IL-10	Forward primer	TTGCTGGAGGACTTTAAGGGTTAC
	Reverse primer	GTCTGGGTCTTGGTTCTCAGCTT
	TaqMan probe	TTGCCAAGCCTTGCTGAGATGATCCA
GAPDH	Forward primer	CAA CAG CCT CAA GAT CAT CAG C
	Reverse primer	TGG CAT GGA CTG TGG TCA TGA G
	TaqMan probe	CCT GGC CAA GGT CAT CCA TGA CAA C
IL-4	Forward primer	GCCTCCAAGAACAACAAGTGA
	Reverse primer	GCTGCTTGTGCTGTGGAA
	TaqMan probe	CTGGGACTGTGCTCCGGCAGTTCTA
ANGPTL4	Forward primer	ACCTGGAGAAGCAGCAC
	Reverse primer	ATGGTCTAGGTGCTTGTG
	TaqMan probe	CGAATTCAGCATCTGCAAAGCCAGT
PDK4	Forward primer	TCACATCGTGTATGTTCTTCTCA
	Reverse primer	CCCGCATTGCATTCTTAAATAGT
	TaqMan probe MGB	CTCCATCATATGCTCTTT
CyclophilinA	Forward primer	CAAATGCTGGACCCAACACA
	Reverse primer	TGCCATCCAACCACTCAGTCT
	TaqMan probe	TGGTTCCAGTTTTTTCATCTGCACTGC
DNMT3B	Forward primer	CATGAAGGTTGGCGACAAGA
	Reverse primer	ATGCTATCACGGCCTGTTC

	TaqMan probe	TCTGCTGCTCACAGGGCCCGATA
TDGF1	Forward primer	CTGTTTTGGCAATGACTCTGAATT
	Reverse primer	CATGATCCAAATCACACTGTAAGAGA
	TaqMan probe	ATGCTAACGCCTCTTTTCCCCCTAATTGTT
CD43	Forward primer	TCAAAGATGTACACCCTTCAA
	Reverse primer	TGTTGGCTCAGGTAAAGG
	TaqMan probe	CCCTACCTCCCTCAACTTCCATCAA
CD45	Forward primer	GACTCTTTGGATAATGCTAGTG
	Reverse primer	ATGTCTGCGTGTCAATT
	TaqMan probe	ACAGGTGTTTCATCAGTACAGACGC
CD34	Forward primer	AAGCACC AATCTGACCTGA
	Reverse primer	CAGTGCAATCAGGGTCTT
	TaqMan probe	GCTGGGGATCCTAGATTTCACTGAGCAA
TMEM119	Forward primer	ATGGGATAGTGGACTTCTTCC
	Reverse primer	AAGGACGATGGGTAATAGGC
	TaqMan probe	TCTGCTGATGTTTCATCGTCTGTGC
ARG1	Forward primer	ATTGGCAAGGTGATGGA
	Reverse primer	GTAGCTGGTGTGAAAGATG
	TaqMan probe	AACACTCAGCTATCTACTAGGAAGAAAG
P2Y12	Forward primer	TGCACCAGAGACTACAA
	Reverse primer	AGATCAGAAATGACTGTGTTT
	TaqMan probe	CCACTGCTCTACTACTGTCCTGTTT
SPI1	Forward primer	CCAAACGCACGAGTATTACC
	Reverse primer	TGAAGTTGTTCTCGGCGA
	TaqMan probe	CCATAGCGACCATTACTGGGACTT
TREM2	Forward primer	ATGTGGAGCACAGCATCT
	Reverse primer	TGGCTGCTAGAATCTTGATGA
	TaqMan probe	AGGAGCCTCTTGAAGGAGAAATCC
HEXB	Forward primer	CTTGATTTTGGCGGTA CT CAGA
	Reverse primer	GAACTCCAGAGTCTCTCACCAACA
	TaqMan probe	ACTCCAAGATTATGGCCTCGGGCAA
Past1	Forward primer	CCAGGCAGGTGGTCAACTTT
	Reverse primer	CACTAATGCCAACTCCTTTGTAGTCT
	TaqMan probe	CCAAGCTGCCGCACTCAGTGTGT

2.11.3 Multi Cytokine Arrays

Microglia were cultured in a 12-well plate pre-coated with Cultrex, utilising the same induction media. 24 hours post-plating, the supernatants were collected and centrifuged at 10,000 g for 1 minute. The resultant supernatants were then stored at -80°C for subsequent analysis. Protein concentrations within these supernatants were quantified using the Proteome Profiler Human Cytokine Array Kit (R&D Systems, catalog number ARY005B), in accordance with the manufacturer's

instructions. For analysis, 1 mL of the microglia supernatant was employed. The membranes were visualised on a Li-Cor Odyssey imaging system, ensuring consistent exposure times across experiments. Signal strengths for each protein were determined in duplicate, with total pixel intensity calculated using Fiji software.

2.11.4 RNAseq Analysis

RNA Quality Control:

RNA quality was assessed using the Agilent TapeStation 4200, coupled with ScreenTape Assays to ensure the samples' suitability for both differential cell type and PPAR β agonist investigations. These evaluations were carried out by Dr. Graeme Fox at Deep-SEQ. For these studies, cDNA synthesis was undertaken using the QuantSeq 3' mRNA-Seq Library Prep Kit (Lexogen; 015.96), incorporating 100 ng and 50 ng of total RNA for the differential cell type and PPAR β agonist experiments, respectively. Indexed libraries were prepared employing the Lexogen i7 6nt Index Set, adjusting the PCR cycles according to the experiment (15 cycles for the differential cell type study and 17 cycles for the PPAR β agonist investigation).

Library Quantification and Quality Check:

Library quantification and fragment-length distribution analysis were performed using the Qubit Fluorometer (with the dsDNA HS Kit) and the Agilent TapeStation 4200 (with the High Sensitivity D1000 ScreenTape Assay), respectively. The KAPA Library Quantification Kit (Roche) was used for pooled library quantification.

Sequencing:

Libraries were sequenced on the Illumina NextSeq 500 platform, generating approximately 5 million 75 bp single-end reads per sample. Sequencing data underwent quality control, trimming, and alignment using the Lexogen QuantSeq workflow, a pipeline developed specifically for data generated from the QuantSeq

3' mRNA-Seq library prep kits for Illumina, with Cutadapt for adapter removal (Martin, 2011) and the STAR aligner for genome mapping (Dobin et al., 2013). The trimmed reads were aligned to the human reference genome (Homo sapiens GRCh38_emsembl_release_107_ERCC_SIRV) using the STAR aligner. Alignments were classified and counted with 'FeatureCounts' (Liao et al., 2014), and differential expression analysis was performed using the 'R' package 'DESeq2' (Love et al., 2014), which included PCA for replicate clustering and treatment separation. Enrichment analysis was conducted using DAVID (Martin, 2011, Liao et al., 2014). Each contrast was assessed for significantly differentially expressed genes (adjusted p -value <0.1) (Love et al., 2014, Core, 2019), and log₂ fold changes were adjusted using the 'apeglm' method. The enrichment pathways analysis of RNA-Seq data was performed using Visualization and Integrated Discovery (DAVID), available at: <https://david.ncifcrf.gov/>.

2.11.5 Western Blotting

For Western blot analysis, after the careful removal of culture media, cells were gently washed three times with ice-cold 1x PBS, then harvested by scraping in PBS. Pellets were collected via centrifugation for 5 minutes at 4°C at 800 g. Whole-cell extracts were lysed with RIPA buffer, sonicated, and incubated at 4°C for 30 minutes on a roller. The lysate was then centrifuged for 15 minutes at 4°C at 20,000 g to pellet the debris. The supernatant layer was collected for further analysis. Protein content was determined using the Pierce™ BCA Protein Assay Kit (Thermo Fisher Scientific, 23227).

To denature the proteins, 6x Laemmli buffer was added to achieve a final concentration of 1x, and the mixture was heated to 95°C for 5 minutes. Denatured protein samples were separated on a 10% polyacrylamide gel submerged in running buffer for 15 minutes at 100 V through the stacking gel, followed by 45 minutes at 200 V. Proteins were then transferred to a nitrocellulose membrane at 200 milliamperes (mA) for 90 minutes, or at 300 mA for 120 minutes for two gels. Post-

transfer, the membrane was stained with diluted Ponceau S solution (P7170, Sigma-Aldrich, St. Louis, MO, USA) to visualise protein bands. The membrane was destained with deionized water and washed in Tris-buffered saline with 0.1% Tween 20 (TBST) on an orbital shaker. Blocking was performed with 5% milk in TBST for one hour at room temperature before overnight incubation at 4°C with the appropriate primary antibody (Table 2. 13).

The next day, the membrane was washed three times with TBST for 10 minutes each to remove excess primary antibody, followed by incubation with IRDye secondary antibodies (LI-COR) for 1 hour at room temperature on a roller (Table 2. 14). After three final washes with TBST for five minutes each, Odyssey imaging was used to visualise the bands.

Table 2. 12 Western Blot Buffer Recipe

Buffer	Composition
RIPA buffer	150 mM NaCl, 25 mM Tris (pH 7.6), 1 % Triton X-100, 1% sodium deoxycholate, 0.1 % SDS, 1 x complete protease inhibitor
Running buffer	0.1% SDS, 25 mM Tris, 190 mM glycine
Transfer buffer	25 mM Tris, 190 mM glycine and 20% methanol
TBST	20 mM Tris, 150 mM NaCl, 0.1% Tween 20 (pH 7.6)

Table 2. 13 Primary Antibodies for Western Blot

Antibody	Dilution	Blocking buffer in TBST	Expected Band Size	Source
Mouse Anti human β -Actin	1: 5,000	5% Milk	42 kDa	Sigma A5441
Mouse Anti human HA-TAG	1:1,000	5% Milk		Cell signaling 2367
Anti human Mouse Flag-Tag	1:1,000	5% Milk		Cell signaling 8146
Anti PPAR β	1: 1,000	5% milk	50kDa	Persus Proteomics

Table 2. 14 Table 2.14 Secondary Antibodies for Western Blotting

Secondary Antibodies	Dilution	Source
IRDye 680LT, 800CW 0.5 mg	1:10,000	Licor

2.11.6 Plasmid DNA purification using Mini-prep.

Plasmid DNA purification was performed following a process that began with bacteria transformation using NEB® 10-beta Competent *E. coli* (High Efficiency), adhering strictly to the manufacturer's instructions. A single colony was carefully selected and inoculated into 5 mL of LB medium supplemented with ampicillin at a concentration of 50 µg/mL. This bacterial culture was then incubated on a horizontal shaker set to 250 rpm at 37 °C for 8 hours. Subsequently, 400 µL of this bacterial culture was transferred into 200 mL of LB medium, also containing ampicillin at 50 µg/mL, and incubated overnight at 37 °C on a horizontal shaker at 250 rpm. The plasmid DNA was then extracted from the microbial culture using the NucleoBond Xtra Midi kit (740410.50; Macherey-Nagel GmbH & Co. KG, Düren, Germany), following the protocol provided by the manufacturer. After the purification process, the plasmid samples were sent for Sanger sequencing to Source BioScience, located in Nottingham, UK, to confirm the sequence integrity and verify the successful cloning of the desired inserts.

Table 2. 15 Plasmids Used

Plasmid	Source
pINDUCER20-GFP	Frame Lab (Wichitra,2021)
pINDUCER20-empty	Addgene (44012)
psPAX2	Addgene (12260)
pMD2.G	Addgene (12259)
tetO-ALN	Addgene (43918)
FUM-M2rtTa	Addgene (20342)
pAdTrack-PPARdelta	Addgene (16529)
6xHis-SUMO2GG	Frame Lab
6xHis-SUMO3GG	
FLAG-LXRβ	
HA-Ubc-9	
PIAS1	
PIASγ	
HDAC4	

2.11.7 Lentivirus Production

HEK 293FT cells were seeded at a density of 1.4×10^6 cells per 10 cm dish in EMEM, supplemented with 10% FBS and 0.292 g/L L-glutamine (2 mM), and incubated overnight at 37°C in a 5% CO₂ incubator to achieve 80% confluency in preparation for transfection.

On the day following cell seeding, transfection preparations commenced with 2 µg of a lentiviral transfer plasmid, either FUM-M2rtTa (20342, Addgene), tetO-ALN (43918, Addgene), or pINDUCER20-GFP for positive control and optimization purposes. Additionally, 2 µg of the packaging plasmid psPAX2 (12260; Addgene) and 2 µg of the envelope plasmid pMD2.G (12259; Addgene) were combined in 600 µL of Opti-MEM™ I media (11058021; Thermo Fisher Scientific). To this solution, 18 µL of X-tremeGENE HP DNA Transfection Reagent (06366236001; Roche) was added, maintaining a 3:1 ratio of transfection reagent to plasmid DNA. The mixture was thoroughly mixed by pipetting and allowed to incubate at room temperature for 30 minutes to form the transfection complex.

The medium in the HEK 293FT cells was then replaced with 7 mL of fresh Opti-MEM™ I media, and the transfection complex was added dropwise to the cells, ensuring even distribution by gently swirling the plate. The cells were then incubated at 37°C in a 5% CO₂ atmosphere for 24 hours

Following this period, the Opti-MEM™ I media was substituted with 12 mL of fresh, complete EMEM medium, and the cells were incubated for a further 48 hours. Post-incubation, the supernatant, now containing lentivirus, was collected, passed through a 0.45 µm syringe filter to remove cell debris, and stored at 4°C for up to 14 days. See Figure 2. 3 shows the morphology of HEK293FT cells during viral production.

To concentrate the virus, the filtered lentiviral supernatant was layered over a 10% sucrose cushion in an ultracentrifuge tube and spun at 100,000 g (28,000 rpm) at 4°C for 2 hours using a SW 41 Ti rotor. The supernatant was discarded, and the tube

inverted on absorbent paper to remove residual liquid. The viral pellet was resuspended in 300 μL of PBS, stored overnight at 4°C, then mixed with an equal volume of 50% glycerol for long-term storage at -80°C in screw-cap tubes. This procedure ensures a high concentration of virus for subsequent experimental use.

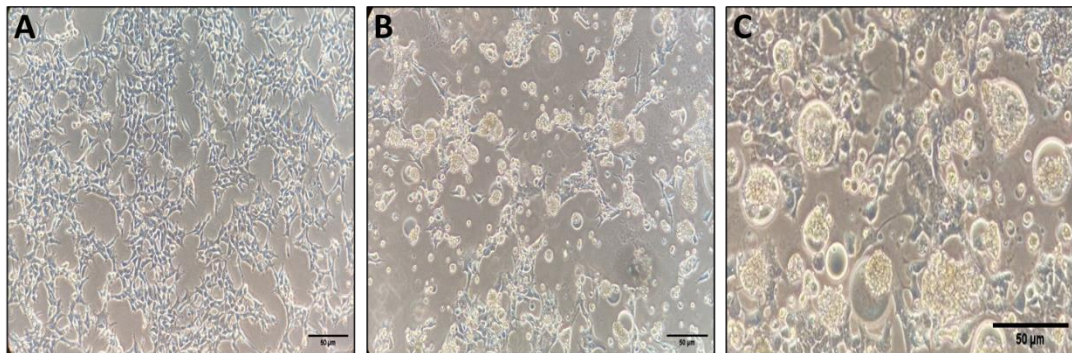


Figure 2. 3 Morphology Changes in HEK293FT Cells During the Virus Production Stage. **A:** HEK293FT cell morphology before transfection. **B:** After 48 hrs of transfection, many cells died. The infected cells exhibited cytopathic effects of viral infection, such as rounding and syncytial formation (fusion with surrounding cells). **C:** There are signs of nuclear or cytoplasmic inclusion bodies, as well as cellular swelling. The images were captured using an inverted light microscope. The scale bar is representative of 50 μm .

2.12 Statistical Analysis

For statistical analysis, Graph Pad Prism software (version 10.0) was used. The specific tests used are indicated in the corresponding figure legends. A p-value less than 0.05 was considered statistically significant. The Grubbs test was used to identify and remove significant outliers from the data. All figures were created using the Prism software. The results presented in the text and figures represent the mean values with the standard error of the mean (SEM) calculated from the independent samples specified in each figure legend.

Chapter 3 Investigation of Age-related Changes in Rat Spinal and Cortical Microglia and Microglia-Astrocyte Crosstalk

3.1 Introduction

Microglial activation and the subsequent release of cytokines and chemokines are crucial steps in response to brain injury or infection. The developmental stage of microglia can significantly affect responses to stimuli and the ability to modify neuronal health (Ye and Johnson, 2002). This investigation examined the responses of adult and neonatal rat microglia to inflammatory stimuli such as ATP and LPS. The expression of PPARs and FABPs (5, 7, and 8), which are integral in lipid metabolism and inflammation regulation within the CNS, was analysed. The aim of this study was to elucidate the differential reactions of microglia across developmental stages to these external inflammatory signals. Glial cells, including microglia and astrocytes, undergo significant changes throughout an individual's life. In the neonatal stage, microglia play a crucial role in shaping the nervous system. They are involved in the formation and upkeep of synapses, as well as overall neural development. Over time, these cells assume several key responsibilities, such as phagocytosis of dead cells, control of neurogenesis, synapse pruning and plasticity, and myelin formation (Hammond et al., 2019, Stevens et al., 2007).

Emerging evidence suggests that microglia from neonatal and aged populations may exert differential influences on astrocytes. Specifically, it has been proposed that aged microglia, when stimulated with damage-associated molecular patterns (DAMPs) or pathogen-associated molecular patterns (PAMPs), can induce a neurotoxic phenotype in astrocytes (Rozovsky et al., 1998, Matias et al., 2019, Clarke et al., 2018). This distinction points to the complex role microglia play in modulating astrocyte behaviour and highlights the intricacies of their interactions within the context of brain aging.

Most age-related neurodegenerative studies have utilised microglia cultures from neonatal animals rather than from adult ones. Recently, a few studies have compared the microglial phenotype and characteristics using animals at different ages (Caldeira et al., 2014, Yanguas-Casás et al., 2020). This investigation extends

beyond merely comparing microglia at different developmental stages. It was examined how spinal microglia in adult and neonatal rats differ from their cortical counterparts. The spinal cord possesses its own unique microenvironment, markedly distinct from that found in the cerebral cortex, characterised by a specific cellular composition, vascular supply, and metabolic demands (Bartanusz et al., 2011, Schnell et al., 1999) Furthermore, the blood-spinal cord barrier exhibits properties different from those of the blood-brain barrier, which can influence the local microenvironment and the response to injury or disease (Bartanusz et al., 2011). Understanding how spinal microglia respond and express genes differently from cortical microglia is essential to comprehend regional variations in the CNS response.

3.2 Aims

The study reported in this chapter aimed to increase the understanding of the expression of PPARs and CNS-resident FABPs (5, 7, and 8) in glial cells. The functional phenotype of neonatal and adult microglia isolated from the rat brain and spinal cord was assessed. The influence of the developmental stage, location (cortical or spinal), and different types of stimuli, such as LPS and ATP, were examined on microglia and astrocytes to understand glial cell communication in neuroinflammation.

3.3 Results

3.3.1 Purity of Adult and Neonatal Primary Microglia Culture

The microglial isolation method, as described by (Imraish, 2018, Edan, 2019), is explained in Section 2.2. This method has been successful in producing highly enriched primary microglia cultures from both adult and neonate rat brain and spinal cord tissues. Through the use of immunocytochemistry, it has been determined that the microglia cultures are over 90% pure, in adult cortical (Figure 3. 1) and adult spinal (Figure 3. 2). Furthermore, staining for cell-specific markers, such as GFAP for astrocytes and NeuN for neurons, demonstrates minimal contamination.

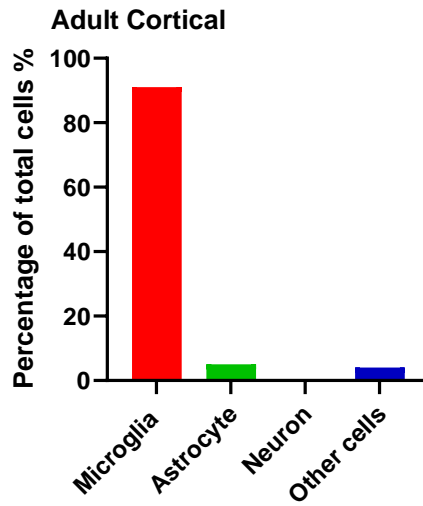
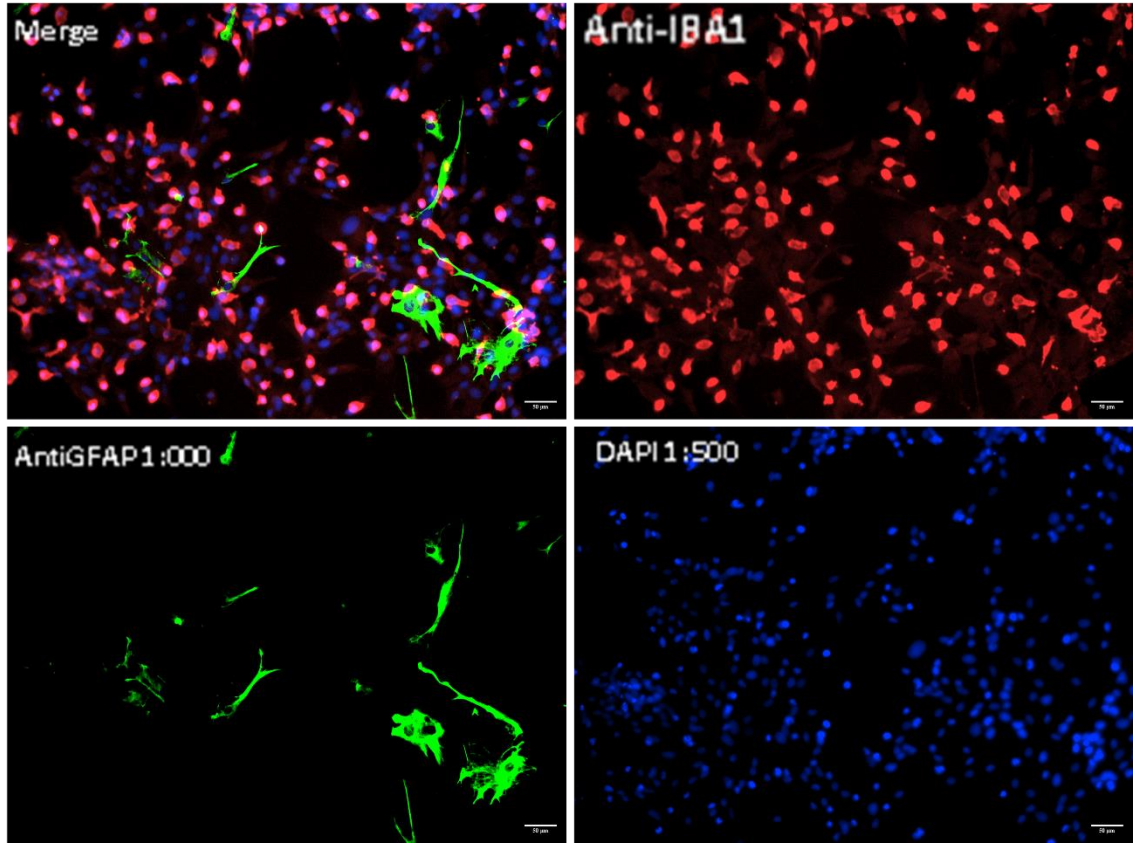


Figure 3. 1: Determination of adult cortical microglia culture purity. The purity of microglia cultures was determined through immunocytochemistry, employing markers selective for microglia (Iba1, red), astrocytes (GFAP, green), and neurons (NeuN, green). Nuclei were stained with DAPI (blue). Images are representative of three different wells from a single preparation. The scale bar represents 50µm.

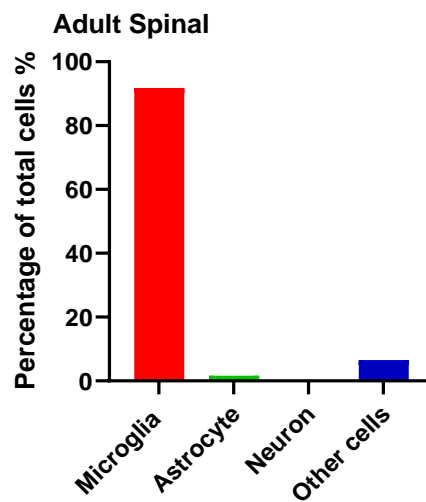
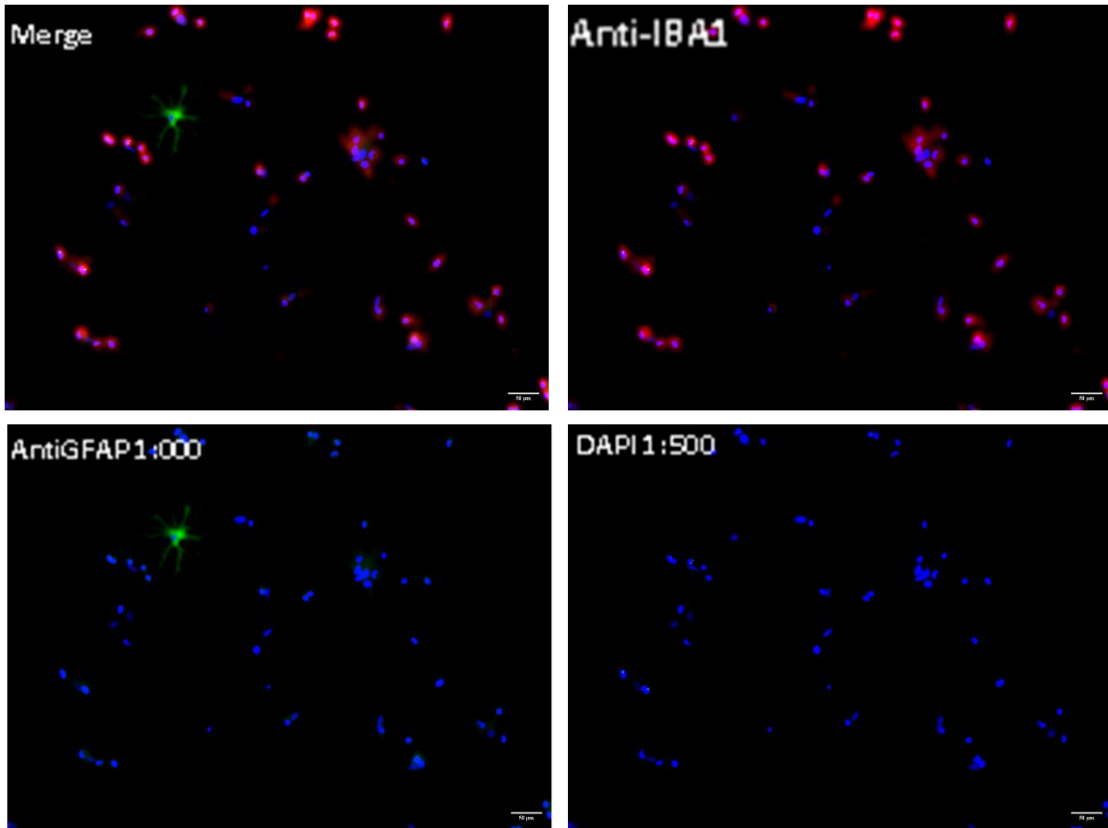


Figure 3. 2: Determination of adult spinal microglia culture purity. The purity of microglia cultures was determined through immunocytochemistry, employing markers selective for microglia (Iba1, red), astrocytes (GFAP, green), and neurons (NeuN, green). Nuclei were stained with DAPI (blue). Images are representative of three different wells from a single preparation. The scale bar is representative of 50 μ m.

3.3.2 Morphological Differences between Adult and Neonatal Microglia

In this investigation, distinct morphological differences were observed in microglia depending on their location within the tissue and their developmental stage. Notably, microglia in neonatal rats predominantly exhibited an amoeboid shape, indicative of a more reactive state during early development

In contrast, adult rat microglia were primarily characterised by a ramified morphology, with extensive thin processes extending into the surrounding environment, suggesting a surveillant role in the mature central nervous system. The employment of the immunopanning technique to isolate microglia from neonates revealed a mix of both ramified and amoeboid forms, suggesting a transitional state during early development (Figure 3.3).

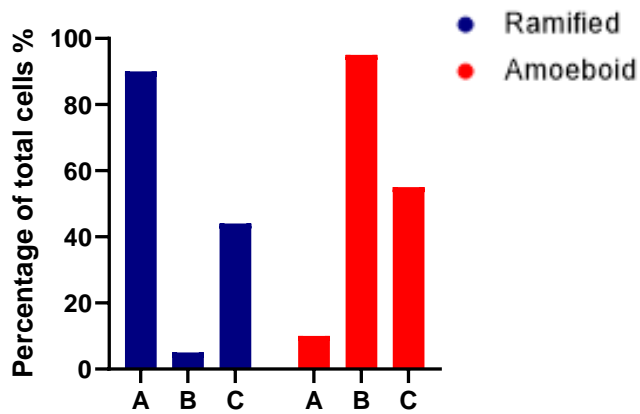
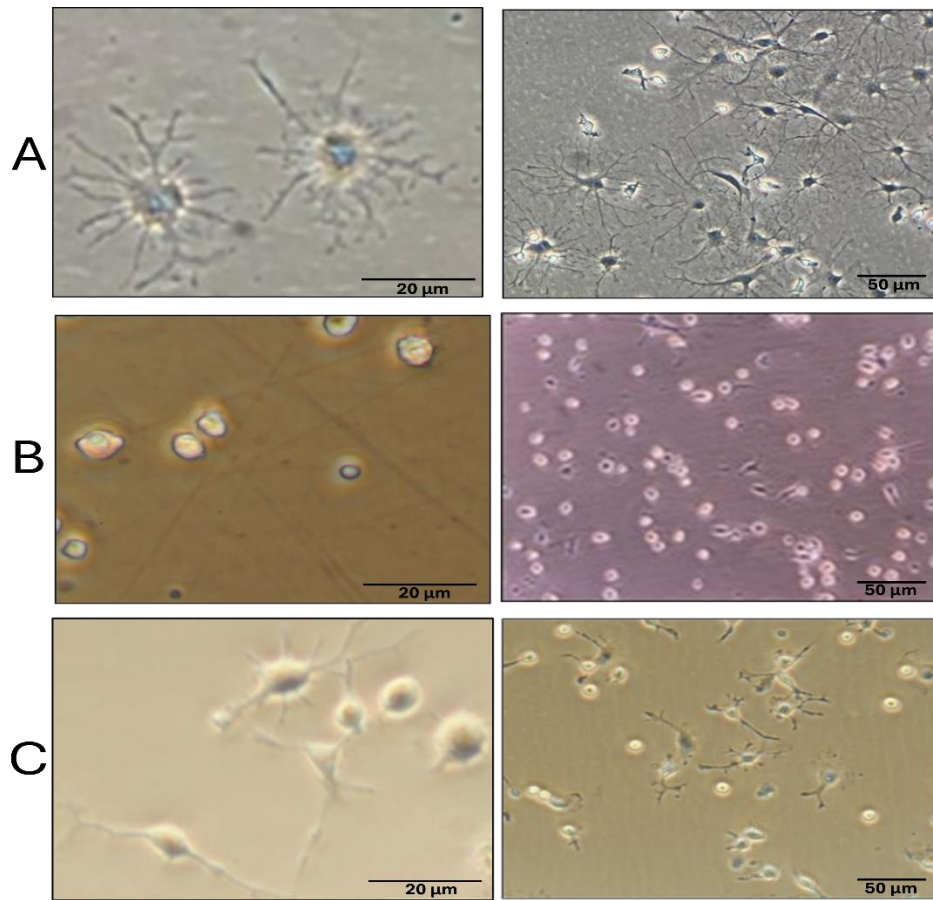


Figure 3. 3: The morphological characterization of isolated cortical neonatal and adult microglia. A light microscope was utilised to examine microglia morphology. (A) Ramified adult microglia, (B) amoeboid neonatal microglia, and (C) a mixture of both ramified and amoeboid neonatal microglia isolated through immunopanning. Images are representative of three different wells from a single preparation.

3.3.3 Assessment of Maintenance of Microglial Developmental Stage in Post-Isolation Culture

To confirm that the observed morphological differences accurately reflect the distinct stages of microglial development, the expression of developmental markers was assessed. MafB and Sall1 were indicative of adult microglia, while Psat1 and Scd2 signified neonatal microglia. These markers were selected for their differential expression levels, with MafB and Sall1 upregulated in adult microglia compared to neonatal stages, exemplifying the transition to mature microglial function. Conversely, Psat1 and Scd2 were shown to have heightened expression during the neonatal phase, delineating early microglial development stages. This expression pattern aligns with the findings of Matcovitch-Natan et al. (2016), who demonstrated an increase in MafB expression as microglia transition from pre-microglial to the adult stage, signifying its role in adult microglia homeostasis and emphasising the functional significance of these markers in delineating microglial maturation (Maticovitch-Natan et al., 2016).

In this investigation of microglial maturation markers, Figure 3.4 illustrates that MafB mRNA expression was markedly increased in adult cortical and spinal microglia compared to neonatal counterparts. Conversely, Psat1 mRNA was found to be expressed at significantly higher levels in neonatal microglia for both cortical and spinal regions. Not all markers followed this pattern of distinct expression between neonatal and adult microglia. For Sall1, while expression levels were comparable in cortical microglia across developmental stages, a significant enhancement of Sall1 mRNA expression was observed in adult spinal microglia compared to the neonatal stage. Scd2 showed no significant variance between neonatal and adult microglia in either cortical or spinal regions. The congruence between the findings presented in this thesis and published *in vivo* data substantiates the reliability of these developmental markers in reflecting the transformation of microglia as they mature, from their early presence in the neonatal phase to their fully realised state in adult microglia.

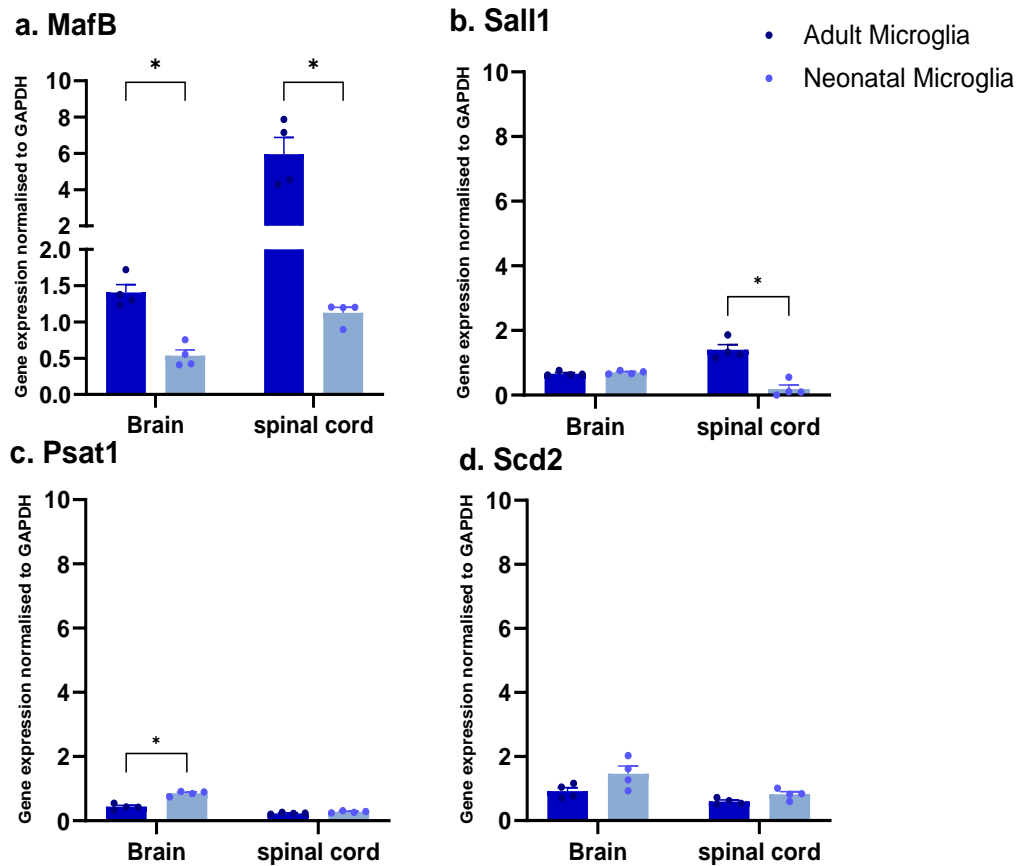


Figure 3. 4: The relative expression of biomarkers for adult and neonatal microglia. (a) MafB (v-maf avian musculoaponeurotic fibrosarcoma oncogene homolog B) and (b) Sall1 (Spalt Like Transcription Factor 1) for adult microglia; (c) Psat1 (Phosphoserine Aminotransferase 1) and (d) Scd2 (Stearoyl-CoA Desaturase 2) gene expression were normalised to GAPDH using the standard curve method as described in the methods section. Data represent mean \pm SEM from one representative experiment (n=4 wells). Results are representative of three independent experiments. Statistically significant differences are indicated by: (* $p < 0.05$, ** $p < 0.001$, *** $p < 0.0005$, **** $p < 0.0001$), using unpaired t-tests.

3.3.4 Evaluating Phagocytic Efficacy of Microglia Across Developmental Stages

This assay, designed to measure the phagocytic capabilities of microglia, demonstrated that a high percentage of fluorescent beads were engulfed by both adult and neonatal microglial cells. As illustrated in (Figure 3.5), in the adult microglia samples, there was an almost complete clearance of the beads, suggesting a robust phagocytic capability with 36% of cells demonstrated phagocytic activity under normal conditions. This increased marginally to 40% when treated with LPS, suggesting a slight enhancement of phagocytic function in response to an inflammatory stimulus. This implies that adult microglia possess a highly efficient phagocytic mechanism, likely reflective of their mature immunological function within the CNS. Contrastingly, in the neonatal microglia, some beads remained unengulfed, 29% of cells showed phagocytic activity under normal conditions. Interestingly, this percentage slightly decreased to 25% when treated with LPS, indicating less efficient clearance. The presence of these residual beads in neonatal samples could suggest that the phagocytic process in neonatal microglia is not as fully developed or active as in their adult counterparts.

The addition of LPS was intended to simulate an inflammatory environment to investigate whether this would modulate the phagocytic efficacy of microglia across different developmental stages. The observed complete clearance of beads by adult microglia even in the presence of LPS could indicate resilience and a capacity to maintain phagocytic function under inflammatory conditions, characteristics that may develop with maturation.

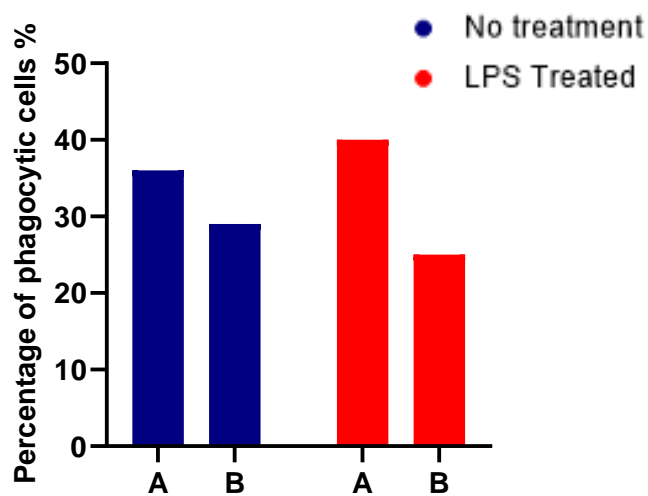
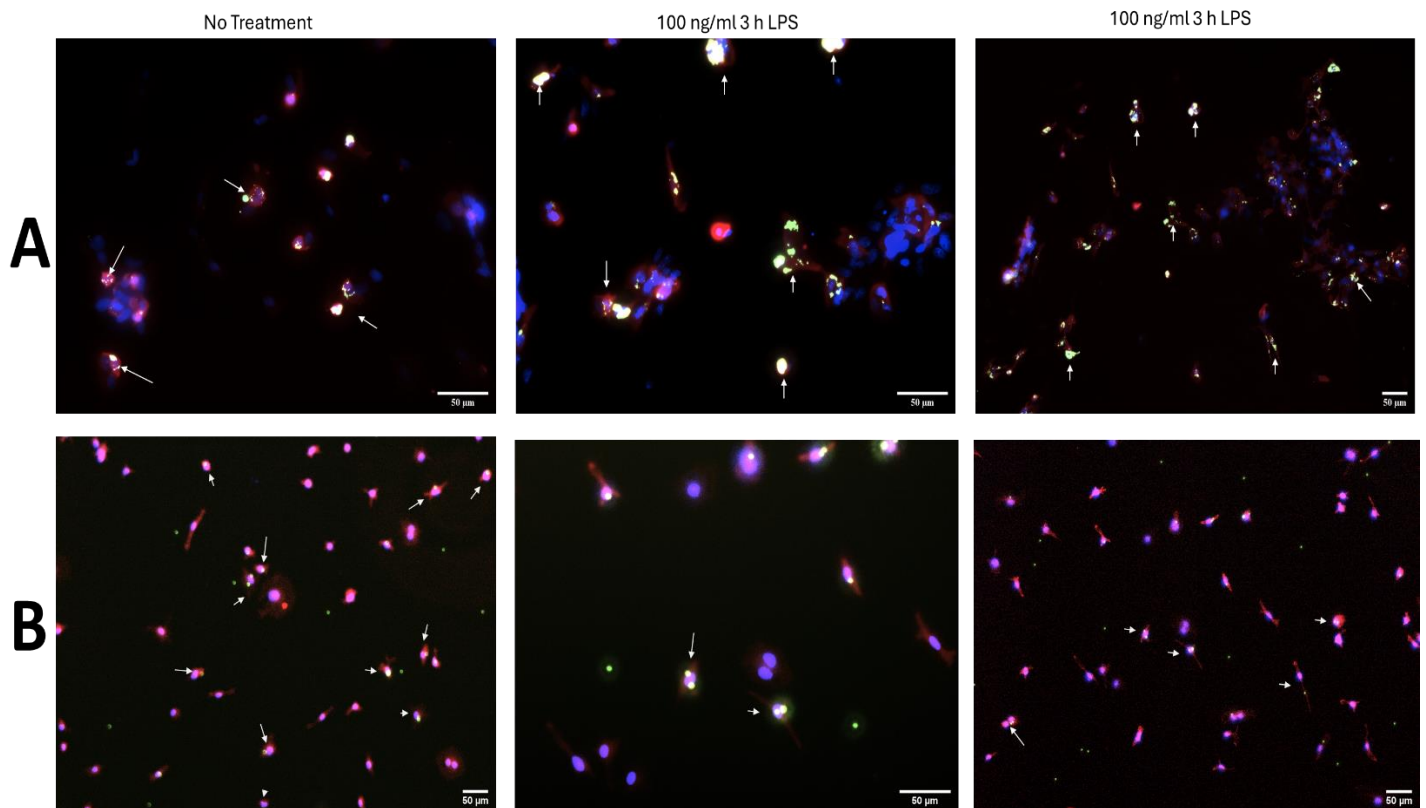


Figure 3. 5: Microglia phagocytic activity. (A) Primary adult microglial cells and (B) primary neonatal microglial cells were isolated by immunopanning. The cells were incubated with fluorescent beads (green) either alone or with 100 ng/ml LPS for 3 hours and incubated at 37°C with medium, then fixed and stained with DAPI (blue). Microglia with internalised beads are indicated by white arrows; red signals denote Iba1-positive microglia. Images are representative of three different wells from a single preparation.

3.3.5 Assessment of the Purity of Primary Astrocyte Culture

In this study, the astrocyte isolation process, post microglia removal, was refined using a methodology that facilitated the attainment of high purity in the astrocyte culture. Initially, after the microglial cells were isolated through the shaking method, the flasks containing the remaining cells were replenished with warm DMEM. This was followed by overnight incubation at 37 °C on an orbital shaker set to 120 rpm to facilitate the detachment of oligodendrocyte cells. To validate the purity of the isolated astrocyte cultures, immunocytochemistry was employed utilising GFAP to identify astrocytes (stained green), Iba1 for microglia (stained red), and NeuN for neurons (orange). This assessment confirmed that the astrocyte cultures achieved over 90% purity (Figure 3. 6).

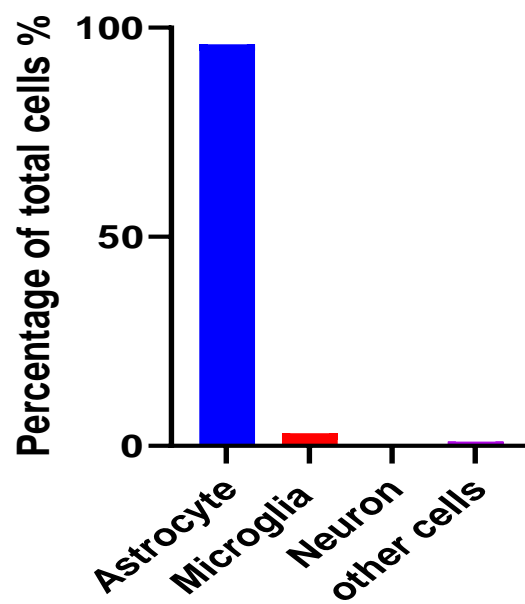
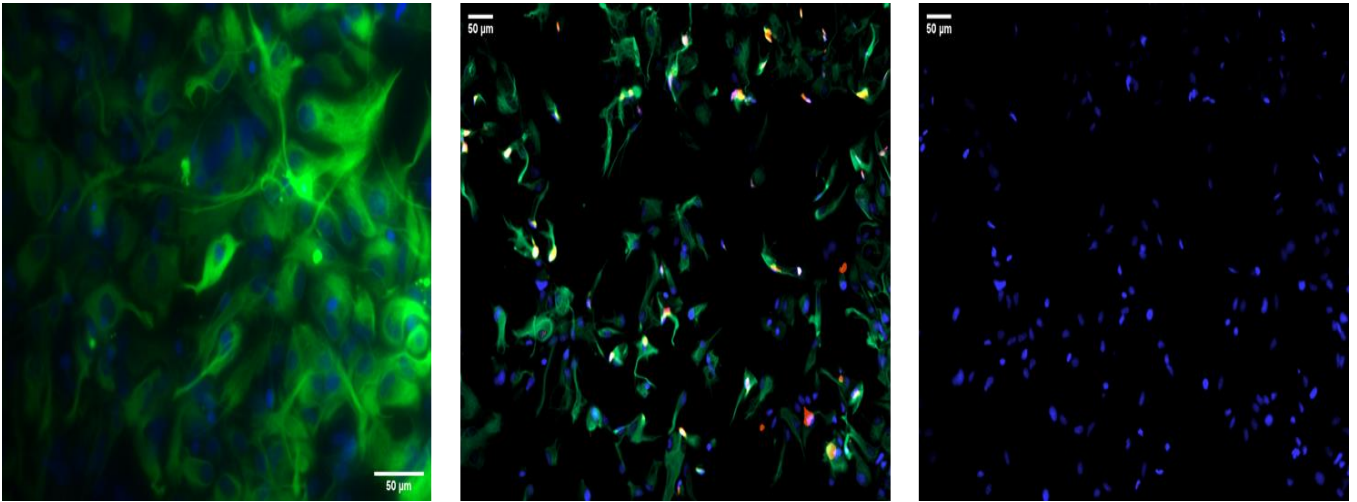


Figure 3. 6: Isolation of astrocyte culture purity. Astrocyte culture purity was determined by immunocytochemistry using markers specific to astrocytes (GFAP, green), microglia (Iba1, red), and neurons (NeuN, orange). Nuclei were also stained with DAPI (blue). Images are representative of three different wells from a single preparation.

3.3.6 Analysis of PPAR and FABP Gene Expression in Microglia from Different Developmental Stages and Tissue Locations

In a comparative gene expression analysis between neonatal and adult microglia within cortical and spinal cord tissues, as illustrated in Figure 3. 7 distinct profiles in PPAR and FABP family gene expressions were observed. FABP5 expression in neonatal cortical microglia was approximately 4-fold greater than in adult cortical microglia. In the spinal region, neonatal microglia also exhibited about a 1.5-fold higher expression of FABP5 compared to their adult counterparts. Similarly, PPAR α and PPAR β levels in neonatal cortical microglia were about 3-fold and 1.5-fold higher, respectively, than in adults. For spinal tissues, neonatal microglia demonstrated approximately a 3-fold and 1.3-fold increase in expression for both PPAR α and PPAR β over adults.

Notably, FABP7 showed an opposite trend, with adult spinal microglia expressing the gene at a 2-fold higher level than neonatal spinal microglia. Moreover, FABP8 expression in neonatal spinal microglia was strikingly elevated, over 8-fold and 12-fold higher than in neonatal and adult cortical microglia, respectively, demonstrating a pronounced regional specificity. Conversely, PPAR γ expression did not exhibit a significant change when comparing neonatal and adult microglia in either brain or spinal cord regions, indicating a consistent expression across developmental stages.

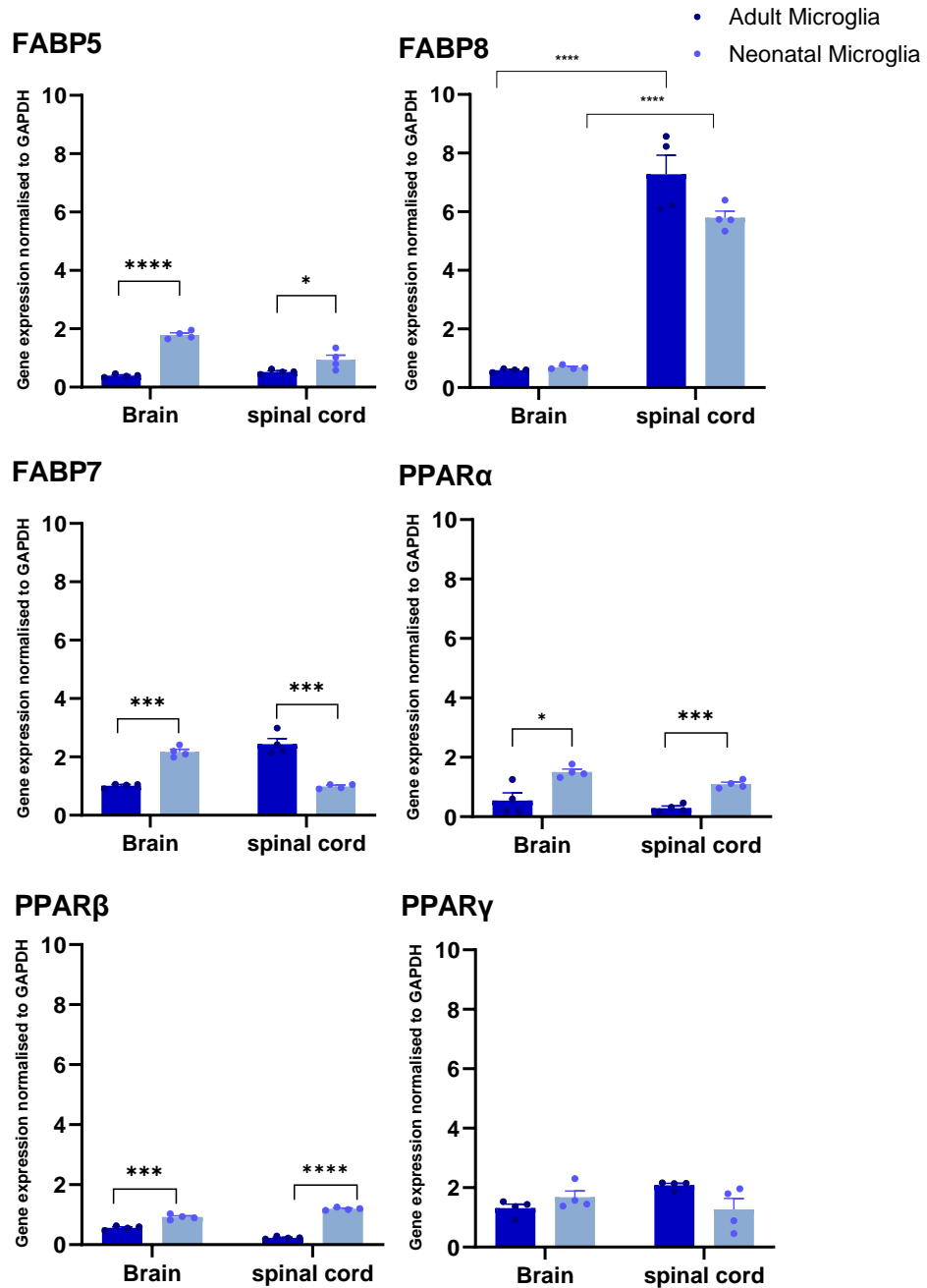


Figure 3. 7: Differential gene Expression in Adult and Neonatal Microglia: PPAR α , β , γ , FABP5, FABP7, and FABP8 (PMP2) gene expression in adult and neonatal microglia was measured using TaqMan qPCR and normalised to GAPDH. Microglia were isolated from rat cortical or spinal cords. Data represent mean \pm SEM from one representative experiment (n=4 wells). Results are representative of three independent experiments. Statistically significant differences are indicated by: (*p < 0.05, **p < 0.001, ***p < 0.0005, ****p < 0.0001), using unpaired t-tests.

3.3.7 Astrocyte Expression of PPARs and FABPs

Figure 3. 8 : demonstrates that astrocytes express FABP5, FABP7, and FABP8/PMP2, along with PPAR α and PPAR β . Spinal cord astrocytes express significantly higher levels of FABP5 and FABP8/PMP2 compared to their cortical counterparts, with expression levels showing about a 2.5-fold increase for FABP5 and about a 4-fold increase for FABP8/PMP2. There was no significant difference in the expression levels of FABP7 between spinal cord and cortical astrocytes. Similarly, PPAR α and PPAR β also do not exhibit significant variance, suggesting a consistent expression profile for these genes across the two astrocyte populations. Notably, PPAR γ expression was undetectable in astrocytes from both regions, highlighting its absence in the astrocyte gene expression repertoire in the contexts examined.

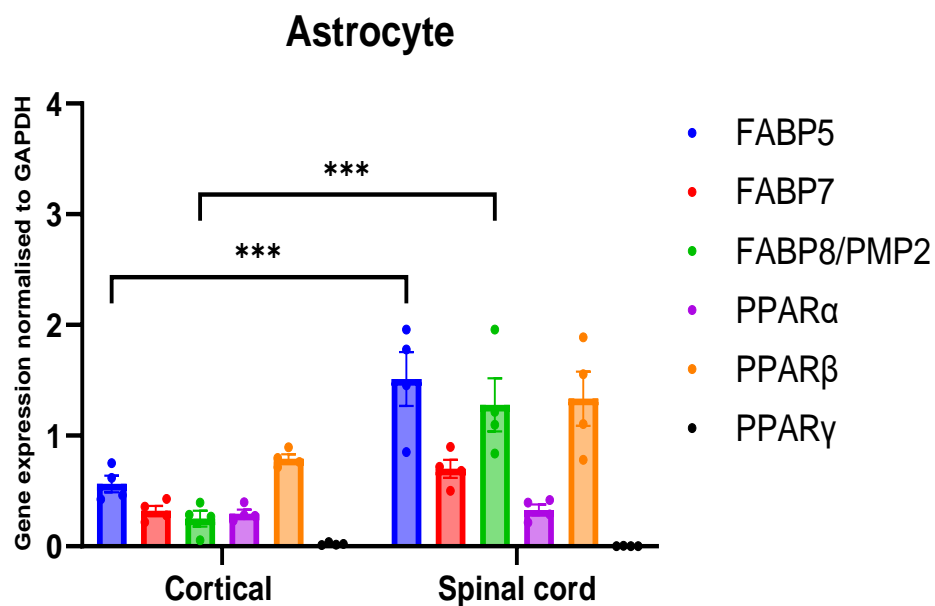


Figure 3. 8 : PPAR α , β , γ , FABP5, FABP7 and FABP8 (pmp2) gene expression in astrocytes. Gene Expression in Astrocytes. Gene expression was measured using TaqMan qPCR and normalised to GAPDH. Data represent mean \pm SEM from one representative experiment (n=4 wells). Results are representative of three independent experiments.. Results were analysed by two-way ANOVA followed by Bonferroni's multiple comparison test. Statistically significant differences are indicated by: (*p < 0.05, **p < 0.001, ***p < 0.0005, ****p < 0.0001).

Gene expression analysis highlighted a developmental and regional specificity in microglial and astrocytic expression of FABPs and PPARs. Notably, neonatal microglia exhibited increased expression of FABP5 and PPARs (both PPAR α and PPAR β) across cortical and spinal tissues. FABP8, on the other hand, was highly expressed in spinal microglia across both developmental stages as well as in spinal astrocytes, indicating its broad significance in the spinal region.

The elevated expression of FABP7 in the neonatal brain and in adult spinal microglia more than neonatal counterparts suggests a differential role that may be influenced by both the developmental stage and the microenvironment. The interaction of FABPs with specific PPARs, which show parallel increases in expression, raises the possibility of a synergistic role in lipid metabolism and signalling pathways that govern microglial responses.

3.3.8 Effects of Stimulating Microglia and Astrocytes with ATP and LPS

In this study, the inflammatory responses of microglia and astrocytes to examples of pathogen-associated molecular patterns (PAMPs) and damage-associated molecular patterns (DAMPs) were investigated using lipopolysaccharide (LPS) and adenosine triphosphate (ATP), respectively. LPS is widely recognised for its role in enhancing the production of inflammatory cytokines in microglia, serving as a potent stimulant for these cells (Go et al., 2016). Similarly, ATP, when released from damaged tissue or neurons, acts as a pro-inflammatory agent and a catalyst for microglial activation (Ferrari et al., 2006, Inoue, 2002, Tewari et al., 2024). Based on data from previous laboratory work, as documented by Imraish (2018) and Edan (2019), a concentration of 100 ng/ml for LPS and 100 μ M for ATP was employed.

3.3.8.1 Differential Temporal Responses to LPS Stimulation in Neonatal and Adult Microglia Across Cortical and Spinal Tissues

In this study, the inflammatory response of microglia to LPS stimulation was examined, comparing the effects across developmental stages (neonatal and adult) and locations (cortical and spinal). As Figure 3.9 shows, the findings reveal a pronounced increase in interleukin-1 beta (IL-1 β) mRNA expression across all tested groups, indicating a common activation of microglia in response to LPS. A robust upregulation of IL-1 β mRNA expression was detected in neonatal cortical microglia, showing a 470-fold increase at 3 hours and a 415-fold increase at 6 hours post-LPS stimulation. Similarly, neonatal spinal microglia showed a substantial response, albeit to a lesser extent, with a 283-fold increase at 3 hours. This comparison demonstrates a more pronounced inflammatory response in the cortical region compared to the spinal region in neonatal microglia. In adult microglia, the cortical cells displayed a significant upregulation of IL-1 β than their neonatal counterparts, with a 520-fold increase at 3 hours and a 660-fold increase at 6 hours. In contrast, adult spinal microglia showed a lower magnitude of IL-1 β induction (90-fold at 3 hours) compared to both adult and neonatal cortical microglia, as well as neonatal spinal microglia. These results illustrate a clear distinction in the inflammatory response between cortical and spinal microglia, with cortical cells demonstrating a higher sensitivity to LPS-induced activation. Furthermore, the developmental stage plays a crucial role, with adult microglia, particularly in the cortex, exhibiting a stronger response to LPS compared to neonatal microglia.

The absence of interleukin-10 (IL-10) and inducible nitric oxide synthase (iNOS) data for neonatal microglia, due to sample limitations, precludes a complete comparison across all parameters. However, the robust IL-1 β response provides valuable insights into the location-specific and developmental-stage-specific dynamics of microglial activation in the CNS.

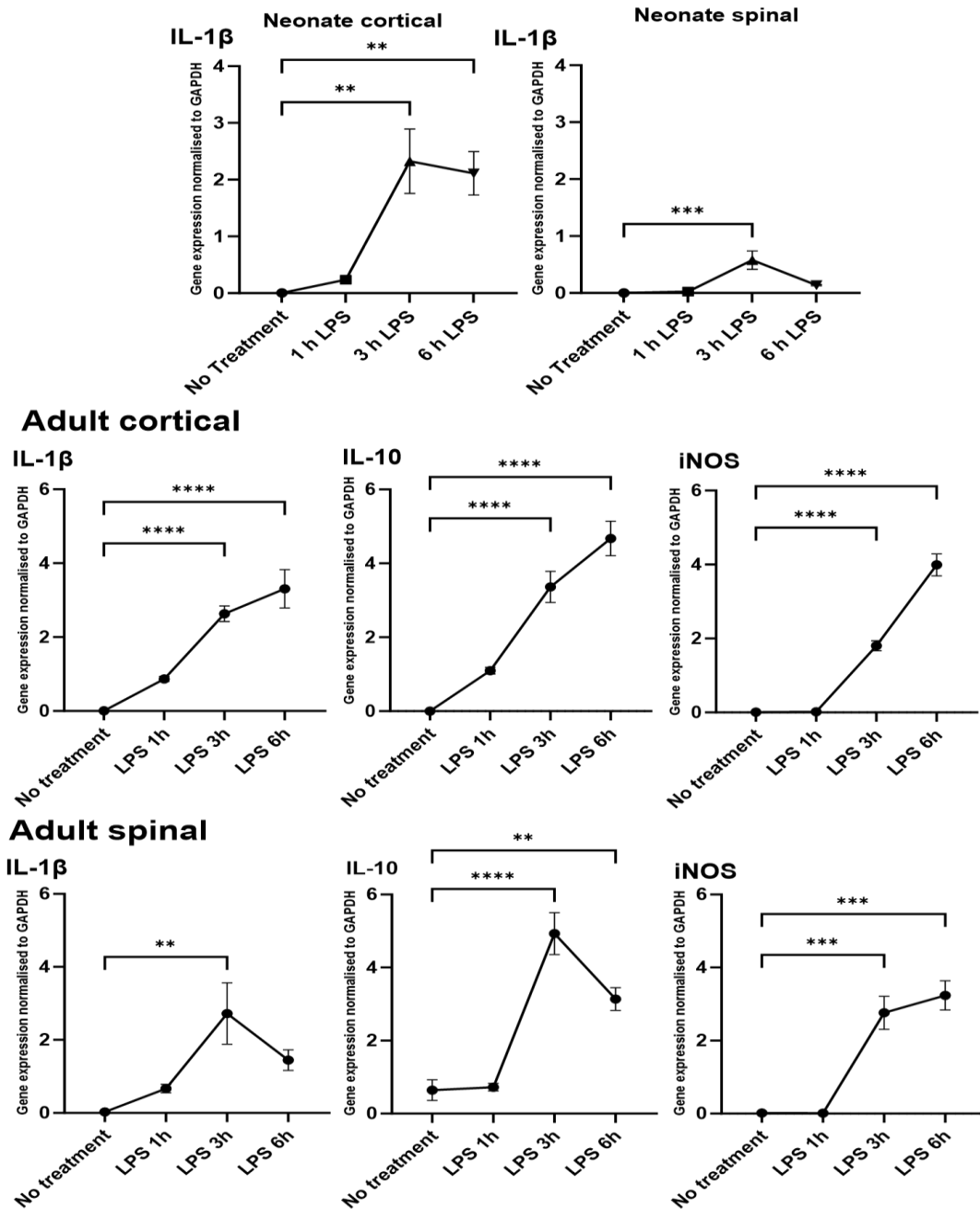


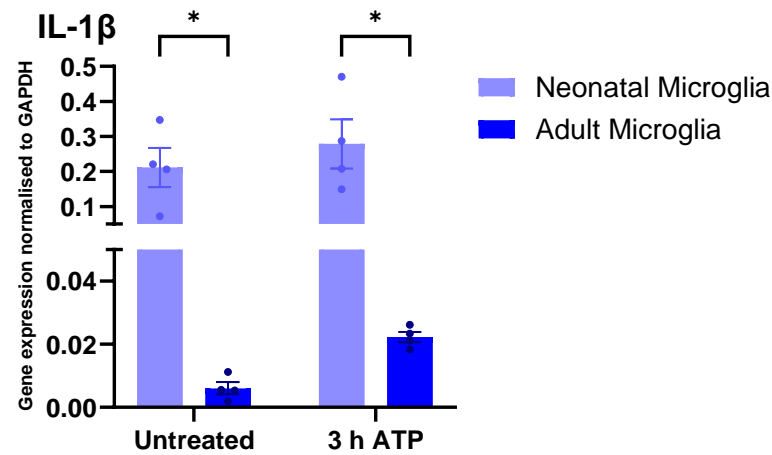
Figure 3. 9: Effects of 100 ng/mL LPS 1-6 h on inflammatory markers. Gene expression in adult and neonatal microglia was measured using TaqMan quantitative PCR (qPCR) and normalised to GAPDH. Microglia were isolated from rat cortical or spinal cords. Data represent mean \pm SEM from one representative experiment (n=4 wells). Results are representative of three independent experiments. Results were analysed by one-way analysis of variance (ANOVA) followed by Bonferroni's multiple comparison test. Statistically significant differences are indicated by: (*p < 0.05, **p < 0.001, ***p < 0.0005, ****p < 0.0001).

3.3.8.2 Differential Temporal Responses to ATP Stimulation in Neonatal and Adult Microglia Across Cortical and Spinal Tissues

ATP, identified as a damage-associated molecular pattern, was explored for its impact on the expression of IL-1 β in microglia across developmental stages and CNS regions. As illustrated in Figure 3. 10, for adult cortical microglia, exposure to 100 μ M ATP did not elicit a significant increase in IL-1 β mRNA expression after 3 hours compared to untreated cells. This suggests that ATP does not prompt cortical microglia to produce IL-1 β to the same extent as observed under other experimental conditions, such as LPS exposure. Similarly, when examining neonatal cortical microglia, there was no increase in IL-1 β mRNA levels following ATP stimulation, indicating a consistent absence of response to ATP between neonatal and adult cortical microglia.

Unfortunately, due to sample limitations, it was not possible to ascertain the response of neonatal spinal microglia to ATP. However, the data available from adult spinal microglia demonstrated a modest yet significant increase in IL-1 β expression, highlighting a potential regional difference in microglial sensitivity to ATP between the spinal cord and cortex. Overall, the absence of IL-1 β induction by ATP in both neonatal and adult cortical microglia, contrasting with the reactivity observed in adult spinal microglia, may have significant implications for the understanding of microglial activation and the CNS's regional specificity in damage response. The lack of data for neonatal spinal microglia represents a gap that future research will need to fill to provide a comprehensive picture of microglial reactivity across different developmental stages and CNS regions.

Cortical



Adult

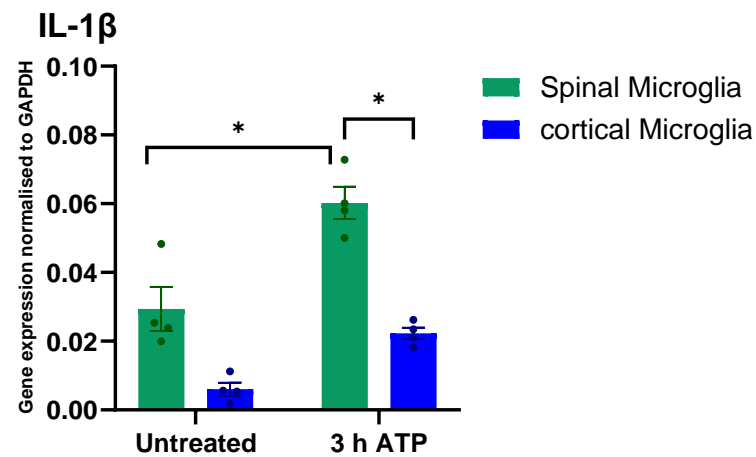


Figure 3. 10: Effects of 100 μ M ATP 3 h on Inflammatory Markers. IL-1 β gene expression in adult and neonatal microglia was measured using TaqMan quantitative PCR (qPCR) and normalised to GAPDH. Microglia were isolated from rat cortical or spinal cords. Data represent mean \pm SEM from one representative experiment (n=4 wells). Results are representative of three independent experiments. Results were analysed by one-way analysis of variance (ANOVA) followed by Bonferroni's multiple comparison test. Statistically significant differences are indicated by: (*p < 0.05, **p < 0.001, ***p < 0.0005, ****p < 0.0001).

3.3.8.2 Temporal Dynamics of Inflammatory Gene Expression in Astrocytes Following ATP Stimulation

The activation of astrocytes was evaluated over a shorter time frame, from 1 to 3 hours, to ascertain if such a duration would be sufficient to elicit an activation response. No significant increase in IL-1 β mRNA expression was detected following ATP addition, and only in spinal astrocytes was an increase in iNOS and IL-10 observed.

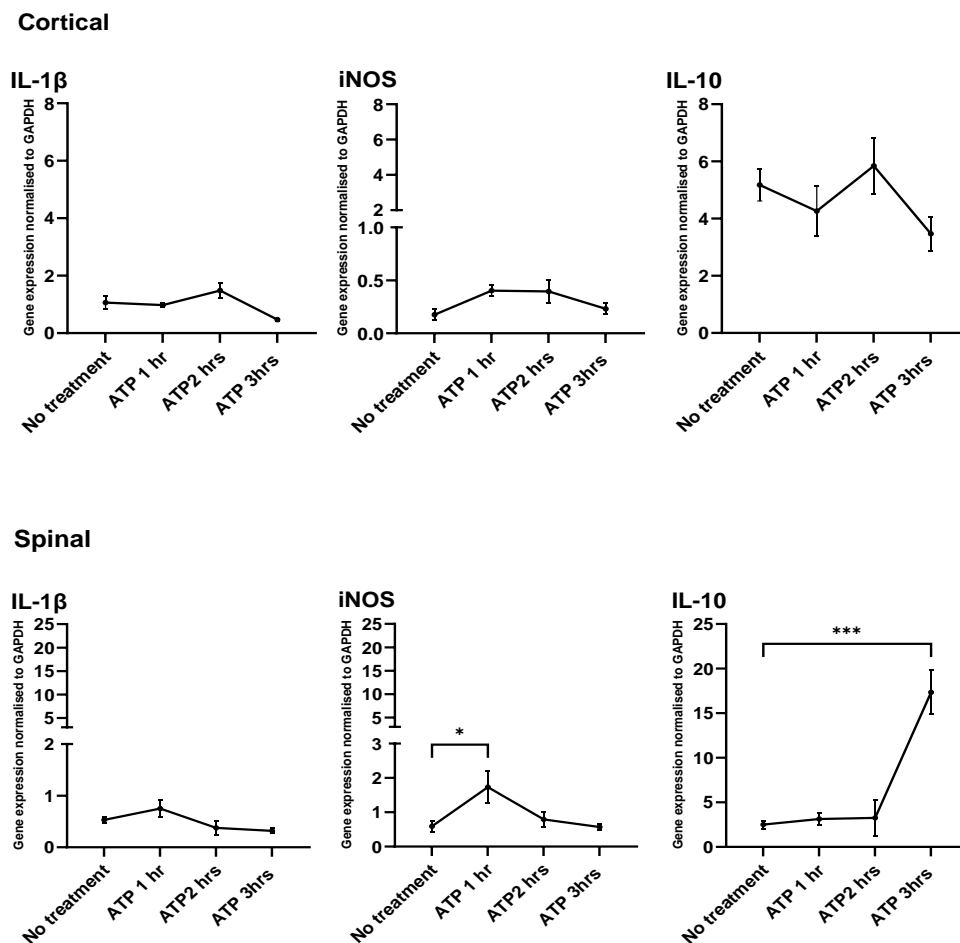


Figure 3. 11 Effects of 100 μ M ATP 1-3 h on Inflammatory Markers. Gene expression in cortical and spinal astrocytes was measured using TaqMan quantitative PCR (qPCR) and normalised to GAPDH. Data represent mean \pm SEM from one representative experiment (n=4 wells). Results are representative of three independent experiments. Results were analysed by one-way analysis of variance (ANOVA) followed by Bonferroni's multiple comparison test. Statistically significant differences are indicated by: (* $p < 0.05$, ** $p < 0.001$, *** $p < 0.0005$, **** $p < 0.0001$).

Collectively, the investigation into the inflammatory responses of microglia has demonstrated distinct profiles upon exposure to LPS, with differences observed between cortical and spinal regions as well as between developmental stages. It was observed that neonatal cortical microglia displayed an acute and pronounced increase in IL-1 β expression following LPS stimulation, markedly higher than the response observed in neonatal spinal microglia. In adults, cortical microglia not only sustained this heightened reactivity to LPS but amplified it further, indicating a potentiated inflammatory capacity with maturation.

Contrastingly, stimulation with ATP did not elicit a comparable increase in IL-1 β expression in cortical microglia of either age group. However, adult spinal microglia did exhibit a response to ATP, albeit with a modest increase in IL-1 β expression, revealing a possible regional variation in response to ATP. These findings collectively highlight the intricate nature of microglial activation patterns, which are influenced by both the microenvironment and the developmental context. They stress the importance of considering both age and anatomical location when addressing neuroinflammatory mechanisms.

3.4 Discussion

Emerging evidence about the crucial functions of glial cells in health and various pathological conditions has motivated researchers to explore the pathways that regulate their roles, especially in neuroinflammatory diseases. Although the distribution of peroxisome proliferator-activated receptors (PPARs) and fatty acid-binding proteins (FABPs) in the central nervous system (CNS) has been extensively investigated in mice and rats, few studies have focused on PPAR expression in specific cell types within the CNS. The present study sought to address this gap by investigating the expression of PPAR α , PPAR β , PPAR γ , and FABP5, 7, and 8 in the brains and spinal cords of both adult and neonatal rats.

Research on microglia has primarily concentrated on neonatal primary microglia from the cerebral cortex (Orre et al., 2014). This focus is due to the simpler isolation and cultivation processes, which yield higher numbers of cells compared to adult microglia (Tamashiro et al., 2012, Moussaud and Draheim, 2010). In this chapter, reliable and efficient methods for extracting both neonatal and adult pure microglia from the rat cortical and spinal cord are described.

Microglia exhibit diverse morphological, transcriptional, metabolic, and functional profiles in healthy and diseased CNS (Hanisch and Kettenmann, 2007). Their states are dynamic and multifaceted, determined by the surrounding environment. The quantification of gene expression by qPCR reveals that the basal levels of the activation marker IL-1 β remain unchanged in untreated microglia, suggesting that the extraction process does not induce an activation state in these cells. This ensures that microglia retain their responsiveness to various stimuli, such as LPS and ATP. IL-1 β expression, a principal inflammatory cytokine, is notably induced upon activation. Moreover, *in vitro* evidence demonstrates the ability of these isolated microglia to effectively phagocytize fluorescence beads. The extraction techniques consistently yield microglial samples of exceptional purity that retain essential functions. The age-dependent differences in microglial homeostasis and gene expression patterns (Matcovitch-Natan et al., 2016, Hammond et al., 2019)

highlight the importance of considering the developmental stage when studying microglial function. While adult microglia display less variability compared to their embryonic counterparts, regional differences in microglial properties persist throughout the CNS (Grabert et al., 2016, De Biase et al., 2017).

The findings of this study contribute to the understanding of the role of PPARs and FABPs in microglial function and neuroinflammation. The identification of PPAR β as a potential regulator of lipid metabolism and anti-inflammatory responses in microglia provides a foundation for future research exploring its therapeutic potential in neuroinflammatory and neurodegenerative diseases.

3.4.1 PPAR and FABP Expression in the Microglia and Astrocyte Cells

PPAR β is the most highly expressed isotype in the rat brain, followed by PPAR α and then PPAR γ (Warden et al., 2016). Although the expression of PPAR in microglia and astrocytes is not yet well defined, PPAR β has been reported to be highly expressed in several different neuronal areas, with PPAR α being more highly expressed than PPAR γ (Warden et al., 2016b, Moreno et al., 2004, Braissant et al., 1996, Braissant and Wahli, 1998). In the CNS, the expression of FABP3, FABP5, and FABP7, described as brain lipid-binding proteins, is a common phenomenon (Matsumata et al., 2012, Pelters et al., 2004). The expression patterns of these FABPs vary with development in the brain (Furuhashi and Hotamisligil, 2008, Liu et al., 1997, Owada et al., 1996, Sellner et al., 1995, Killoy et al., 2020). These reports are consistent with data in the current study that PPAR α , PPAR β , and PPAR γ were expressed in both neonatal and adult microglia in brains and spinal cords. Neonatal microglia express FABP5, FABP7, PPAR α , and PPAR β at a higher level than adult microglia in both cortical and spinal cord cultures. However, there was no difference in PPAR γ expression in terms of developmental stage or anatomical region. PPAR β/δ has been the subject of less research regarding its anti-inflammatory effects compared to PPAR α and PPAR γ , making it the least explored PPAR subtype in this context. Despite this, activation of PPAR β in various cell types has been linked to changes in genes related to lipid metabolism as well as an overall

anti-inflammatory response (Wang et al., 2003, Iwashita et al., 2007, Palomer et al., 2014).

The study's findings on the differential expression of FABPs and PPARs in microglia and astrocytes, according to developmental stage and tissue type, add to the growing body of evidence on the diverse roles of these molecules in the central nervous system. The heightened expression of FABP5 and PPARs in neonatal microglia, especially in cortical regions, aligns with studies suggesting a critical role for these factors in early brain development and inflammation response modulation (Falomir-Lockhart et al., 2019, Zolezzi et al., 2017, Liu et al., 2010). The consistent expression of FABP8 in spinal microglia and astrocytes points out its potential importance in spinal cord physiology and pathology (Zenker et al., 2014). This research contributes valuable insights into the spatial and temporal dynamics of FABP and PPAR expression, hinting at their intricate involvement in neurodevelopmental and neuroinflammatory processes.

3.4.2 Comparative Analysis of the Responses in Neonatal Versus Adult, and Spinal Cord Versus Cortical Microglia to ATP and LPS Exposure

This investigation emphasises the region-specific and age-related variations in microglial responses to LPS and ATP, with a significant age-progressive IL-1 β expression increase in cortical microglia post-LPS stimulation, contrasting with spinal microglia and the ATP response. This is supported by Crain et al. (2013), who found that microglial gene expression changed with age in C57Bl/6 mice, noting distinct profiles from neonatal stages to adulthood. For instance, P3 microglia exhibited high iNOS, TNF α , and arginase-I levels, whilst P21 microglia showed elevated CD11b and TLR4 expression. Adult microglia displayed low pro-inflammatory cytokine levels that rose by 12 months, indicating phenotypic shifts during development (Crain et al., 2013).

Extracellular ATP is described as a potent stimulator of TNF- α secretion, as observed in rat brain microglia primary cultures, with low ATP concentrations (<30 μ M) prompting plasminogen release. Plasminogen acts as a crucial neurotrophic

factor, enhancing synaptic transmission. Conversely, high ATP levels (3 mM) triggered IL-1 β release, leading to cell apoptosis or necrosis (Hide et al., 2000). Thus, microglia exhibit a varied secretion of substances, either neuroprotective or neurotoxic, such as plasminogen, TNF- α , and IL-1 β , depending on the ATP concentration (Hide et al., 2000, Ferrari et al., 2006). This indicates microglia's versatile roles, reacting distinctively to varying ATP levels. However, in this study, ATP stimulation did not significantly elevate IL-1 β expression in cortical microglia across different age groups. In contrast, adult spinal microglia responded to ATP with a slight increase in IL-1 β expression, suggesting a potential regional variation in microglial response to ATP. Therefore, assessing different ATP concentrations at varied time intervals and examining various cytokine gene expressions, like TNF- α , IL-6, and iNOS, is crucial.

Nevertheless, in discussing these observations on rat microglia, it is important to acknowledge a key limitation: the need for additional repeats to strengthen the validity of the results. The limited availability of neonatal spinal samples restricted the capacity to conduct a comprehensive comparative analysis with adult samples using various pro-inflammatory markers like IL-10 and iNOS. To further elucidate developmental and regional differences in microglial response, future studies should employ varied concentrations of LPS and ATP to effectively compare neonatal and adult microglia.

The rat microglia model has provided valuable insights into the complexities of the CNS immune response. However, the limitations of this model in translating findings to human physiology must be acknowledged. To bridge this gap, the next chapter will describe the development of a human microglia model using either human induced pluripotent stem cells (iPSCs) or peripheral blood mononuclear cells (PBMCs). This approach will enable the responses of microglia to be studied in a more realistic context, facilitating the development of therapies and interventions specifically tailored to human neurological conditions. The findings on the differential responses of adult and neonatal rat microglia, and the potential of

targeting specific molecular pathways, serve as a foundation for the next stage of investigation using a human microglia model. This transition is necessary for obtaining more translatable results and for a better understanding of how microglia respond in the context of human neurological disorders.

Covid-19 Impact

The global COVID-19 pandemic has had a significant impact on this research, leading to major modifications in the experimental approach. During the peak of the pandemic, all experiments were suddenly halted due to the implementation of strict safety protocols and lockdown measures. When I finally returned to the laboratory, I was required to shift away from animal models and explore alternative approaches, as the research was being conducted in a frame laboratory. This shift away from animal models presented new challenges, including adapting to new experimental designs and learning new techniques.

Chapter 4 Overcoming iPSCs Challenges with PBMCs:
Establishing a Functional In Vitro Human Microglia
Model for Neuroinflammation Studies

4.1 Introduction

Progress in neuroscience drug discovery has been hindered by the absence of suitable human cellular models. The limited availability of relevant human cell models poses significant obstacles to studying the fundamental pathophysiological mechanisms linking microglia to various brain diseases (O'Donnell et al., 2019, Keene et al., 2016). Induced pluripotent stem cells (iPSCs) represent a significant breakthrough in stem cell research, having the potential to differentiate into various cell types. iPSCs are generated when fibroblasts or PBMCs are reprogrammed to a pluripotent state using transcription factors such as OCT4, SOX2, KLF4, and C-MYC, applied through a viral vector (Takahashi et al., 2007, Takahashi and Yamanaka, 2006). Pluripotent stem cells can differentiate into the three primary germ layers, namely endoderm, ectoderm, and mesoderm. While these cells are present in early embryos for only a short period, they can be cultured continuously in a laboratory under specific conditions. The functional pluripotency of these cells is confirmed as they can be induced to differentiate into any cell type of an organism, including neurons, astrocytes, and the recently developed iPSC-derived microglia (McQuade et al., 2018, Powell et al., 2021).

Microglia are derived from yolk-sac hematopoietic precursors during embryogenesis, which then populate the brain. Replicating these developmental processes is essential for effective *in vitro* differentiation (Ginhoux et al., 2010, Ginhoux et al., 2013). The challenge lies in accurately mimicking the microglial developmental pathway in a laboratory setting. Recent advances in differentiation protocols have significantly improved this, enhancing the ability to study microglia *in vitro* with greater fidelity to their natural development (McQuade et al., 2018, Pandya et al., 2017, Abud et al., 2017, Haenseler et al., 2017). The initial experimental phase of this study was dedicated to the differentiation of iPSCs into microglial cells. Despite employing established protocols (McQuade et al., 2018, Haenseler et al., 2017, Douvaras et al., 2017, Pandya et al., 2017), attempts to

derive functional microglia from iPSCs faced significant challenges, reflecting the complex of directing iPSC differentiation.

This study aimed to differentiate iPSCs into dopaminergic neurons, integral to the brain's motor or reward pathways, and to induce neuronal death in these cells, thereby stimulating microglia activation, to replicate aspects of neurodegenerative conditions such as Parkinson's disease. This approach aligns with the growing interest in understanding neuron-glia interactions in neurodegeneration. Due to the obstacles in generating iPSC-derived microglia, an alternative cell source was investigated – peripheral blood mononuclear cells (PBMCs). PBMCs offered a more straightforward and less complex approach to microglia differentiation (Ohgidani et al., 2014, Banerjee et al., 2021). This shift not only demonstrated the adaptability required in scientific research but also highlighted the evolving nature of cellular reprogramming and differentiation techniques.

4.2 Aims

The objectives of this chapter were to:

1. Optimise the culture and maintenance of induced pluripotent stem cells (iPSCs) to ensure their viability and pluripotency. This includes refining the culture environment and passage techniques to preserve the undifferentiated state of iPSCs.
2. Differentiation of iPSCs into microglia-like cells by identifying the optimum combination of growth factors and culture conditions, subsequently testing for the expression of microglial markers.
3. Differentiate iPSCs into dopaminergic neurons.
4. Employ PBMCs as an alternative, more straightforward source for generating functional microglia. This involves adapting and optimising existing protocols to derive microglia-like cells from PBMCs, followed by a comprehensive characterisation. Assess the functional capabilities of these cells, particularly their response to various stimuli, to validate their functionality as models for neuroinflammatory and neurodegenerative processes.

4.3 Results: Development of a Human Microglia Derived Induced Pluripotent Stem Cells (iPSCs)

4.3.1 Assessment of iPSC Quality and Morphology

One of the primary indicators of iPSC quality is their morphology, which can be assessed routinely, even daily. Undifferentiated human iPSCs typically form compact, multicellular colonies with clear-cut borders. These cells are closely packed, displaying a prominent nuclear-to-cytoplasm ratio and distinct nucleoli. Cells are arranged in a 'cobblestone' uniform pattern as illustrated in (Figure 4.1/A). In healthy colonies, cells merge smoothly, often resulting in a multi-layered appearance at the centre and creating dense cell clusters visible under phase contrast microscopy (see Figure 4.1/B). It is important to note that spontaneous differentiation is a common occurrence in any human pluripotent stem cell (hPSC) culture. The absence of spontaneous differentiation does not imply that the cells are at optimal health. In fact, a small degree of differentiation, around 5-10%, is typical. Colonies that exhibit signs of differentiation are shown in (Figure 4.1/C).

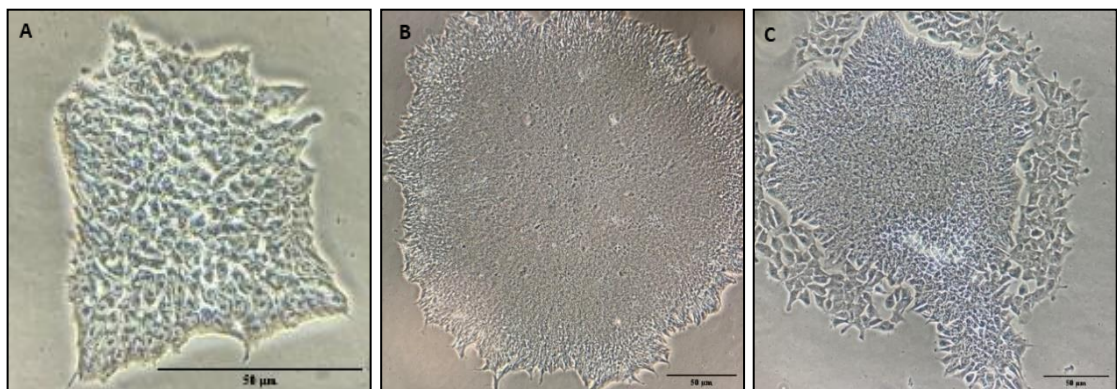


Figure 4. 1: Morphological Characteristics of iPSCs Grown in TeSR™-E8 Medium. (A) Exhibits healthy cell morphology. (B) Shows iPSC cells multi-layered at the appropriate stage for passaging. (C) Indicates a region of spontaneous differentiation. Representative images were collected using inverted light microscopy, with the scale bar representing 50μm.

4.3.2 Assessment of Various Basement Membranes for iPSC Culture

The successful culture of human iPSCs in TeSR™-E8™ necessitates the use of an appropriate matrix that facilitates the adherence of cell aggregates. Initially, iPSCs were cultured on Matrigel specifically qualified for stem cell use and sourced from mouse sarcoma. However, due to supply issues, various alternatives to Matrigel were explored. Matrigel, not optimised for culturing hPSCs, demonstrated low attachment after plating, emphasising the importance of selecting a matrix that is qualified for stem cell culture to ensure a healthy growth environment. Therefore, the matrix was switched to stem cell-qualified Cultrex, a matrix of the same origin (Figure 4. 2).

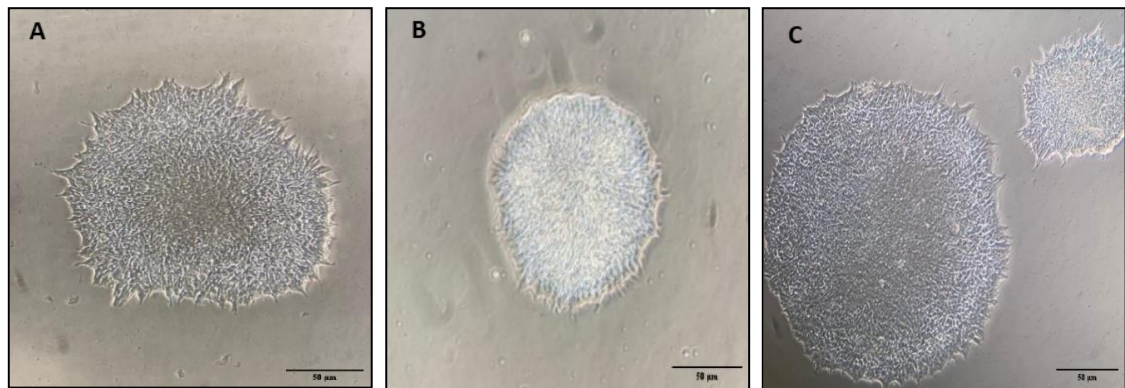


Figure 4. 2 Morphology of iPSCs Cultured on TESR-E8 media A. stem cell-qualified Matrigel, B. corning Matrgiel, C. iPSCs-qualified Cultrex. Representative images collected using inverted light microscopy, scale bar is representative of 50 µm.

4.3.3 Investigation of Different Methods for Splitting iPSCs

Regular microscopic examination of iPSC cultures is crucial, with a 24-hour period often being ideal for passaging, typically between the 5th and 7th day, depending on the initial size of the clumps seeded. The colonies are usually ready for passaging when they predominantly display a dense centre, covering about 75% of the colony. Adjusting the initial seeding density and clump sizes can modify the passaging schedule. During passaging, the colonies should appear densely packed with a multi-layered centre. However, the use of Y-27632, a Rho kinase inhibitor which enhances the survival of human pluripotent stem cells (hPSCs) during routine passaging, is advised against (Figure 4. 3). For passaging hPSCs, an enzyme-free passaging reagent, ReLeSR, was employed, offering a quick and efficient method for regular passaging of iPSCs by utilising the stronger adhesion properties of differentiated cells compared to undifferentiated ones. Unlike procedures involving Gentle Cell Dissociation Reagent, passaging with ReLeSR™ does not require manual picking of differentiated regions or scraping to dislodge cell aggregates before passaging.

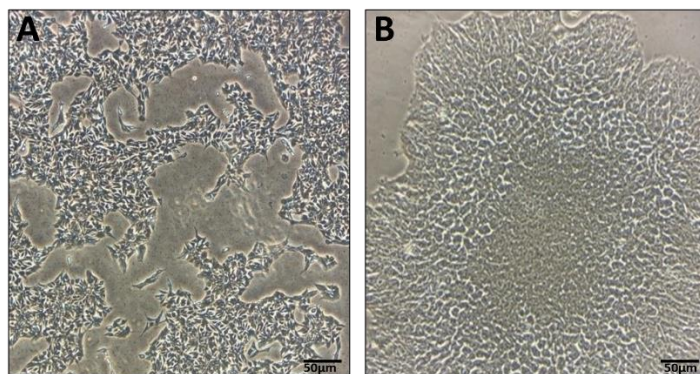


Figure 4. 3: Morphology of iPSCs cultures that have undergone passaging with ReLeSR: (A) iPSCs cultured with Rho kinase inhibitor (Y-27632) show elongated morphology and dispersed colony formation, characteristic of ROCK inhibition. This shape change promotes cell survival post-passaging. (B) iPSCs cultured without Rho kinase inhibitor display typical compact colony morphology with densely packed cells. Note the differences in cell shape, colony compactness, and overall attachment between the two conditions. Representative images were collected using inverted light microscopy, and the scale bar is 50 µm.

4.3.4 Assessment of Pluripotency of iPSCs

This assessment is crucial in ensuring that the iPSCs used in this study possess the required cellular properties for subsequent differentiation into specific cell types and tissues.

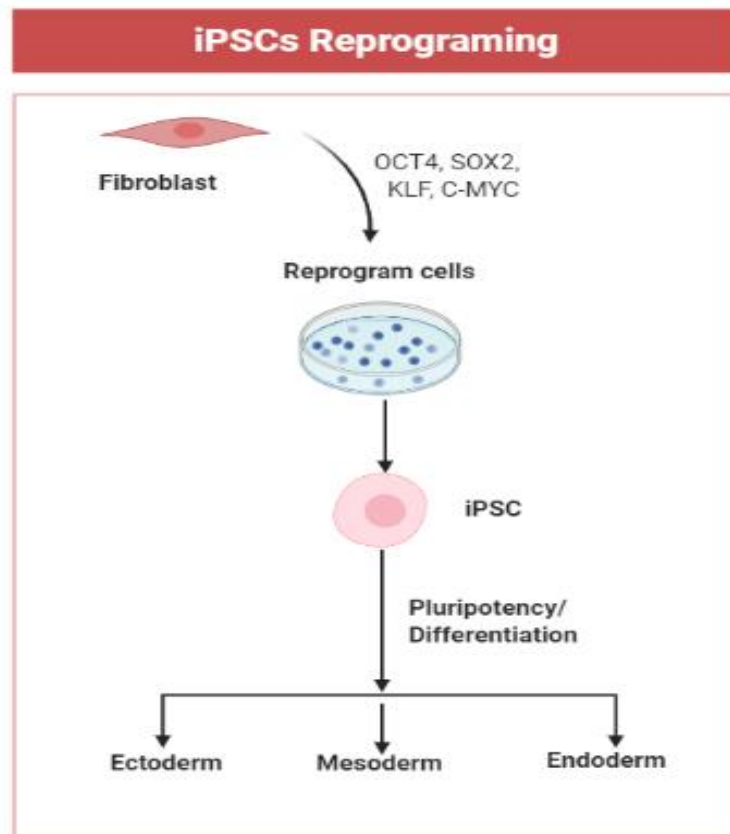


Figure 4. 4 Schematic Representation of iPSC Reprogramming and subsequent Trilineage Differentiation: The diagram illustrates the process from initial somatic cells (typically fibroblasts or blood cells) through reprogramming using defined factors (e.g., Oct4, Sox2, Klf4, c-Myc) to generate iPSCs. The pluripotent iPSCs are then shown differentiating into the three primary germ layers: endoderm, mesoderm, and ectoderm. This represents the standard method for generating and validating iPSCs. Generated using BioRender.

To evaluate the expression levels of key pluripotency markers in hPSCs, NANOG, OCT4, SOX2, TDGF1, and DNMT3B were selected (Chambers et al., 2003, Pomeroy et al., 2016). For this purpose, 18 samples, passages 2-20, were randomly chosen. The analysis demonstrated that each sample expressed pluripotency gene markers (see Figure 4. 5).

Additionally, the STEMdiff™ Trilineage Differentiation Kit was used to provide reproducible and directed differentiation to confirm the functional ability of hiPSCs to differentiate into the three germ layers: ectoderm, mesoderm, and endoderm. The differentiation procedure was conducted according to the guidelines provided by the kit's manufacturer. For lineage-specific marker analysis, cells were fixed with 4% PFA on day 5 for mesoderm and endoderm lineages and day 7 for ectoderm, to perform immunocytochemistry (ICC). The markers used for identifying each cell type were SOX17 for endoderm, OTX2 for ectoderm, and Brachyury for mesoderm. The results clearly indicated the iPSCs' capacity to differentiate into all three germ layers (Figure 4. 6). However, the potential for antibody cross-reactivity among different germ layers was not explored and warrants further investigation in subsequent studies.

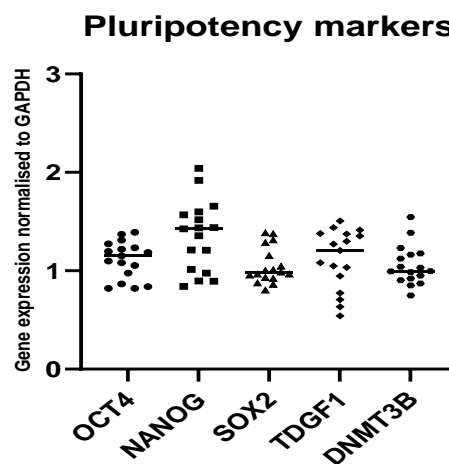


Figure 4. 5 Expression of Pluripotency Markers in iPSCs: Gene expression was measured using RT-qPCR and normalised to GAPDH. The results are presented as individual data points. A Grubbs test was conducted to identify outliers, with none detected ($\alpha = 0.05$).

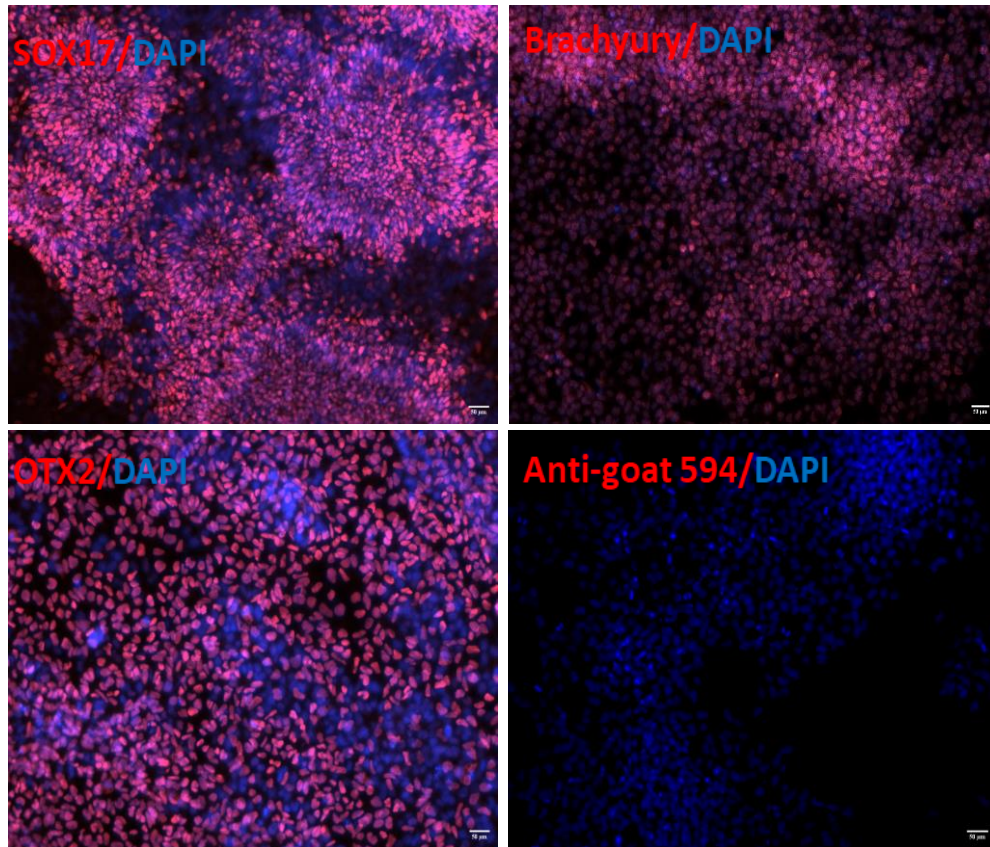


Figure 4. 6 Verification of Human Induced Pluripotent Stem Cell Pluripotency. The iPSCs were differentiated into mesoderm or endoderm for 5 days, or ectoderm for 7 days using the STEMdiff™ Trilineage Differentiation Kit. The cells were fixed with 4% PFA and then incubated with their respective primary antibody overnight. The following day, they were treated with anti-goat 594 as a secondary antibody for 60 minutes at room temperature. The nuclei were stained with DAPI (1 $\mu\text{g}/\text{mL}$) for 2 minutes. Control cells were incubated with only the Anti-goat 594 secondary antibody. Images were captured with a widefield microscope at 10x magnification and are representative of two independent experiments, scale bar is representative of 50 μm .

4.3.5 Routine Monitoring of iPSC Cultures

Routine checks of iPSC cultures, approximately every 10 to 20 passages, are essential to prevent the emergence of abnormal karyotypes. For more frequent screening of common abnormalities associated with iPSC cultures, the hPSC Genetic Analysis Kit (Stem Technologies) was utilised. This qPCR-based method is designed to detect recurrent chromosomal abnormalities in iPSCs. Employing the iPSC Genetic Analysis Kit from Stem cell Technologies, which screens for the eight most prevalent mutations in iPSCs, three samples from different passages were analysed. Data analysis was performed following the guidelines of Stem cell Technologies' analysis software. Unfortunately, only one sample exhibited entirely normal results, while the other two samples indicated a combination of deletion and amplification (Figure 4. 7). Future research should include comprehensive karyotype testing, such as G-banding analysis, to thoroughly ascertain the genomic integrity of the samples.

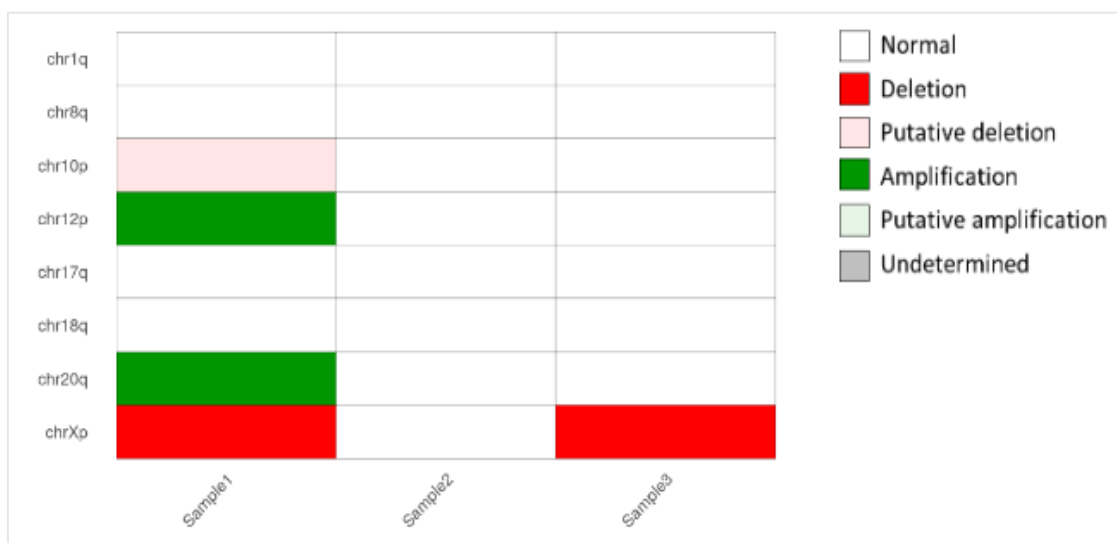


Figure 4. 7 Identification of iPSCs Abnormality: three iPSC samples were analysed using the Stem cell hPSC Genetic Analysis Kit. This kit is designed to detect the eight most frequently occurring chromosomal mutations in iPSCs. qPCR was used to measure gene expression, normalised against Chr4p and compared to a genomic DNA control. The identification of a chromosomal abnormality within a sample is indicated by a P-value <0.05 and a copy number <1.8 or >2.2.

4.3.6 Generation of iPSC-Derived Dopaminergic Neurons

To differentiate iPSCs into dopaminergic neurons, a methodological approach based on key studies (Powell et al., 2021, Theka et al., 2013) was followed. This approach involves a Single-Step Procedure using transcription factors (Ascl1, LMX1a/b, and Nurr1) through virus transduction to directly convert iPSCs into dopaminergic neurons. These factors are known for their critical roles in the development and function of dopaminergic neurons. Overexpression of three key transcription factors, Ascl1-LMX1B-Nurr1 (ALN), was achieved using an inducible polycistronic system. The polycistronic vector used, from Addgene (#43918 tetO-ALN, kindly gifted by John Gearhart), lacked the reverse tetracycline transactivator protein (rtTA), essential for the inducible expression of the ALN genes. Consequently, an additional vector containing rtTA, FUW-M2rtTA plasmids (Addgene, #20342), was incorporated. In this system, doxycycline interacts with rtTA, which then binds to the TetO promoter, initiating transcription of the ALN genes. Assessing the transduction efficiency in these iPSCs using the pINDUCER20-GFP vector and determining the most effective virus concentration was crucial. iPSCs were more efficiently transduced using virus concentrated by ultracentrifugation compared to non-concentrated virus (HEK293FT viral media). Determining the optimal volume of viral particles is critical for achieving high transduction efficiency and robust gene expression in transduced cells, which is variable and depends on the efficacy of the transduction process.

In these experiments, pINDUCER20-GFP lentiviral vectors were used as reporter viruses to transduce iPSCs with several viral volumes. After transduction, 1 µg/mL of doxycycline was added for 48 hours to induce GFP expression, as shown in (Figure 4. 8). GFP expression in successfully transduced cells was then assessed using fluorescence microscopy. The outcomes of these preliminary trials were instrumental in identifying the optimal viral volume needed to ensure that over 85% of the cells exhibited the desired protein expression.

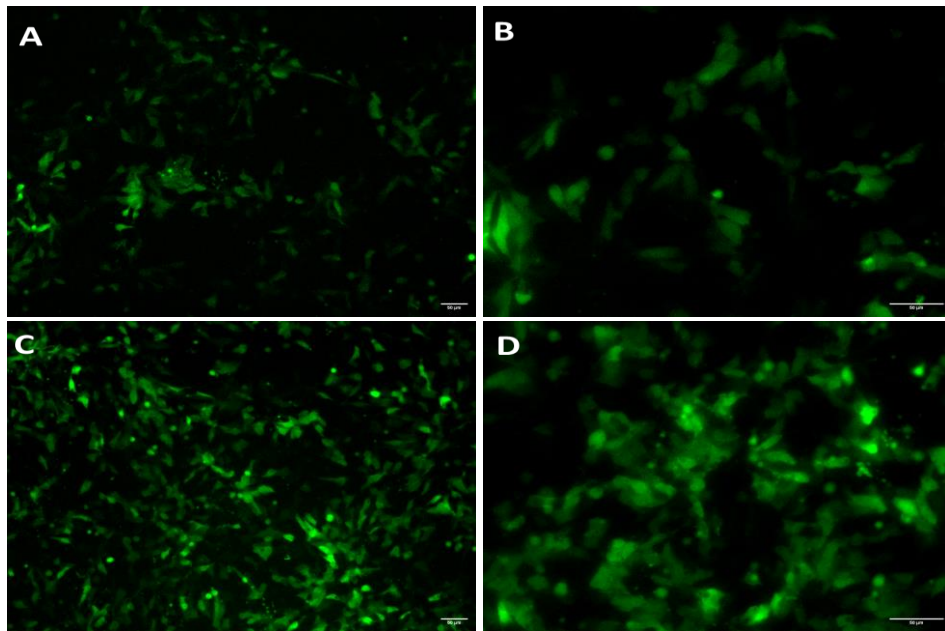


Figure 4. 8: Assessment of Optimal Viral Concentrations for Effective Transduction. A and B display the results of using a 20 µL viral volume at 10x and 20x magnification, respectively. C and D show the outcomes with a 50 µL viral volume at 10x and 20x magnification, respectively. Images were captured using a widefield inverted fluorescence microscope, with the scale bar representing 50 µm.

The iPSCs were transfected with the ALN vector for 24 hours, after which induction media containing 1µg/ml doxycycline were added. The culture was then evaluated to determine the optimal time to add Cytosine arabinoside (Ara-C), a known antimitotic agent effective against dividing cells, usually between day 5 and 6, to suppress the proliferation of non-neuronal cells.

In neuronal cultures, Ara-C is employed at low concentrations to achieve this effect without adversely impacting neurons. After a ten-day induction period with doxycycline, noticeable cellular processes began to appear, some resembling axonal structures (Figure 4. 9).

This observation served as an indicator of the transduction's efficiency; a lack of significant process development suggested suboptimal viral transduction. Subsequently, neuron maturation media, which included the B27 supplement but excluded doxycycline, was introduced. Ara-C treatment continued until day 11 but

at a reduced concentration. Unfortunately, upon discontinuation of Ara-C treatment, an increase in flat, non-neuronal cell growth was observed. Due to time constraints, it was not possible to repeat this experiment.

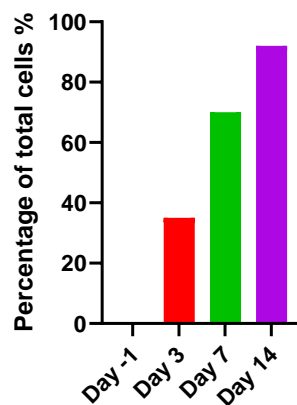
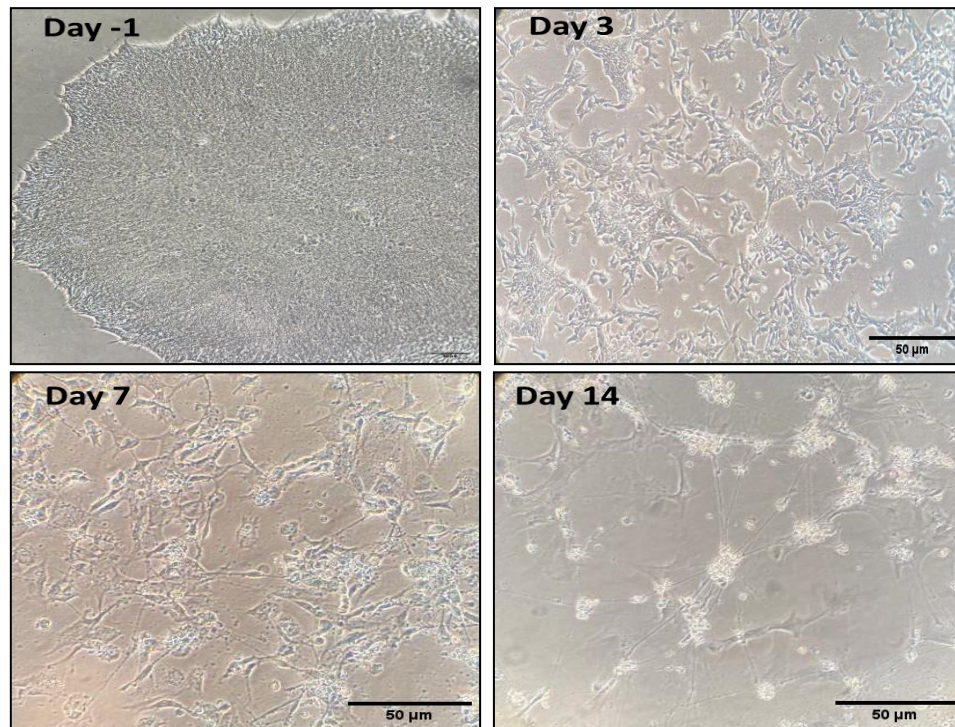


Figure 4. 9: Generation of Dopaminergic Neurones via ASCL1, LMX1B, and NURR1 Transduction: Morphology Development in Induced Dopaminergic Neurons. Quantification of the percentage of cells with visible processes over time. Images are representative of three different wells from a single preparation. Images were taken using an inverted light microscope, with the scale bar representing 50 µm.

4.3.7 Differentiation of Human iPSC-Derived Microglia

The methodology employed for differentiating iPSCs into microglia-like cells was based on and adapted from the protocol established by (McQuade et al., 2018), which closely mirrors the natural ontogeny of microglia *in vivo*. This differentiation process begins with the conversion of iPSCs into hematopoietic progenitor cells (HPCs), a phase that extends from 12 to 20 days. Following this initial stage, the HPCs are transitioned into a microglial differentiation medium, where they are cultured for about 22-30 days. The differentiation journey culminates with a final maturation phase lasting 5-10 days, during which neural and astrocytic factors are introduced to develop microglia within a simulated brain environment, ensuring the formation of a pure and homeostatic microglial population (Figure 4. 10)

Two distinct differentiation strategies were employed to derive HPCs from iPSCs. The first method used a commercial kit from Stemcell Technologies (STEMdiff™ Hematopoietic Kit), comprising two types of media: Media A for the first 2 days and Media B for the subsequent 10 days. The process began by seeding aggregates in TeSR-E8 medium, aiming for approximately 20 aggregates, each consisting of around 100 cells, per well in a 6-well plate. The seeding density was critical; too few aggregates resulted in low yields, while too many hindered efficient differentiation (McQuade et al., 2018). Following the manufacturer's guidelines for media change, the cells started to exhibit mesoderm characteristics by the fourth day, forming dense aggregates and an adherent monolayer. By day 10, floating hematopoietic cells became visible, increasing in quantity until their collection on day 12, with further collection of HPCs on day 14 (Table 4.1).

iPSCs to Microglia Differentiation

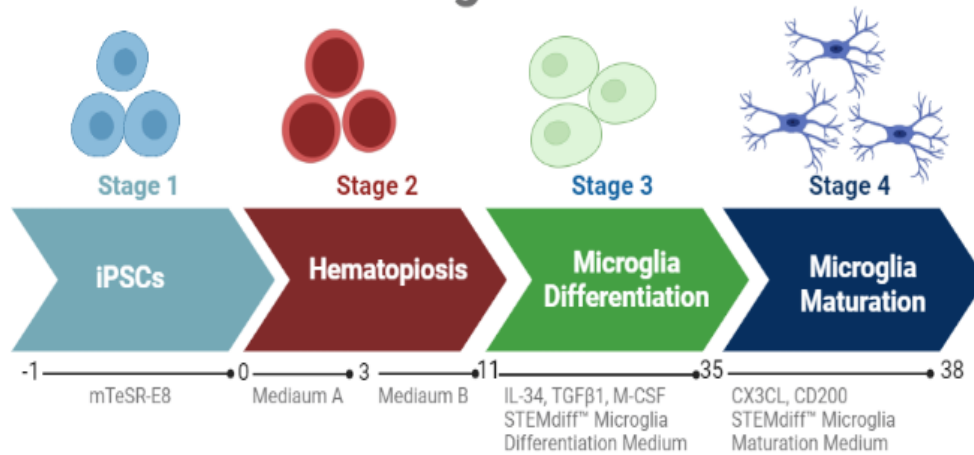

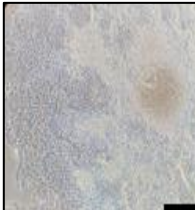

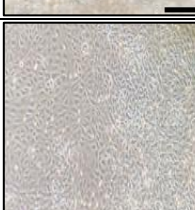
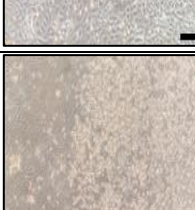



Figure 4. 10: Timeline for Induced Microglia Cell Differentiation Using iPSCs: Differentiation from iPSCs occurs through the mesoderm lineage (days 0–3), leading to haematopoiesis (days 3–11). Subsequently, floating HPCs are transferred to a new medium for 27 days to induce microglial differentiation. Additional neuronal and astrocytic ligands are added during the final three days of differentiation to aid in developing microglia that are more brain-like. This figure was created using BioRender.com.

Table 4. 1: Differentiation of iPSCs Using the STEMdiff Hematopoietic Kit. This series of images illustrates the process of generating hematopoietic cells from iPSCs over a 12-day period using the STEMdiff Hematopoietic Kit. Images captured on days -1, 3, 6, 9, 12, and 14 of the culture periods were obtained with an inverted light microscope, with the scale bar in each image corresponding to around 10 μm .

Day	Stage	Image	Key Visual Markers and Description
-1	iPSC colony		Dense, compact colony with smooth edges. Uniform cell morphology within the colony
3	Early differentiation		Colony edges become less defined. Cells start to spread out from the central mass
6	Mesoderm formation		Cells continue to spread and flatten. Formation of a cobblestone-like appearance
9	Hematopoietic progenitor emergence		Appearance of small, round cells at colony edges. These are early hematopoietic progenitors
12	Hematopoietic cell proliferation		Increase in number of small, round cells. Some cells begin to detach from the surface
14	Mature hematopoietic cells		Numerous small, round cells in suspension. The original colony structure no longer visible

Typically, following the production of hematopoietic cells from iPSCs, it is standard practice to sort these cells into subpopulations such as CD34+, CD43+, or CD45+ using FACS (fluorescence-activated cell sorting). However, according to (McQuade et al., 2018) such sorting is not necessary when using the specific Stem cell kit. They reported that HPs, whether sorted or unsorted, yielded almost identical iPSC-derived microglia. In line with this finding, FACS sorting on these HPs was not performed, so the gene expression of critical hematopoietic markers was used instead.

HPs expressed CD34, CD43, and CD45, in contrast to the undifferentiated iPSC controls, which did not show these markers. Conversely, the iPSC controls displayed the expression of pluripotency markers SOX2 and OCT4, which were absent in the HPs (Figure 4. 11). These data demonstrate that the HPs, generated using the Stem cell kit, have effectively transitioned from a pluripotent state and now exhibit essential hematopoietic markers, indicating successful differentiation.

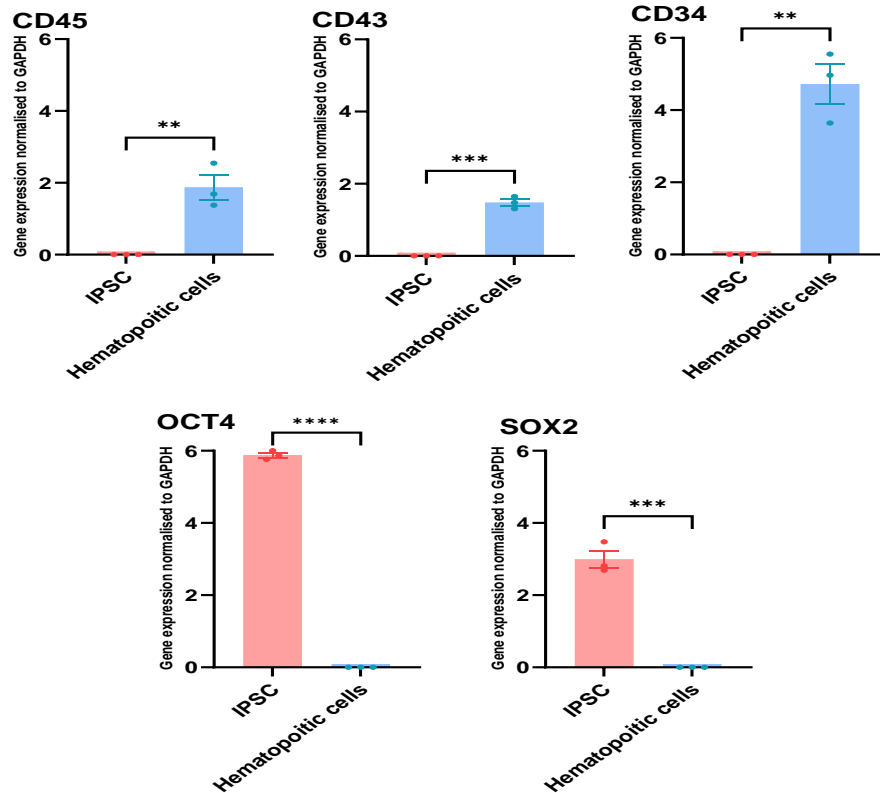


Figure 4. 11: Expression of Key Markers in Hematopoietic Cells Derived from iPSCs Using Stem Cell Kit: iPSCs were differentiated into hematopoietic cells following the manufacturer's guidelines. Gene expression was measured using RT-qPCR and normalised to GAPDH. Bars represent the standard error mean of the values.

An alternative approach for generating hematopoietic progenitors (HPs) involved using a mixture of cytokines over an 18-day period (Heo et al., 2018, Niwa et al., 2011, Douvaras et al., 2017, Fattorelli et al., 2021). This method was performed in two formats: a two-dimensional (2D) culture and a three-dimensional (3D) culture using embryonic bodies, with varying cytokine combinations and concentrations to identify the optimal method for generating HPCs. While the cell morphology observed with this cytokine cocktail method resembled that achieved using the Stemcell kit, notable differences were observed in the outcome, particularly on the harvest day (Figure 4. 12). An important observation was that many cells remained adherent at the time of harvest, leading to a substantially lower yield compared to the first method. Furthermore, these cells predominantly expressed only the CD45

hematopoietic progenitor cell marker (Figure 4. 13). In contrast, hematopoietic stem cells typically express a broader range of markers, including CD34, CD43, and CD45, when derived using the Stemcell kit (Figure 4. 11).

This cytokine-based approach was replicated twice, but both attempts resulted in similarly low yields and limited marker expression, reinforcing the initial observations. Due to these consistently disappointing outcomes, this method was considered unsuitable for the purpose and was therefore not employed in further experiments.

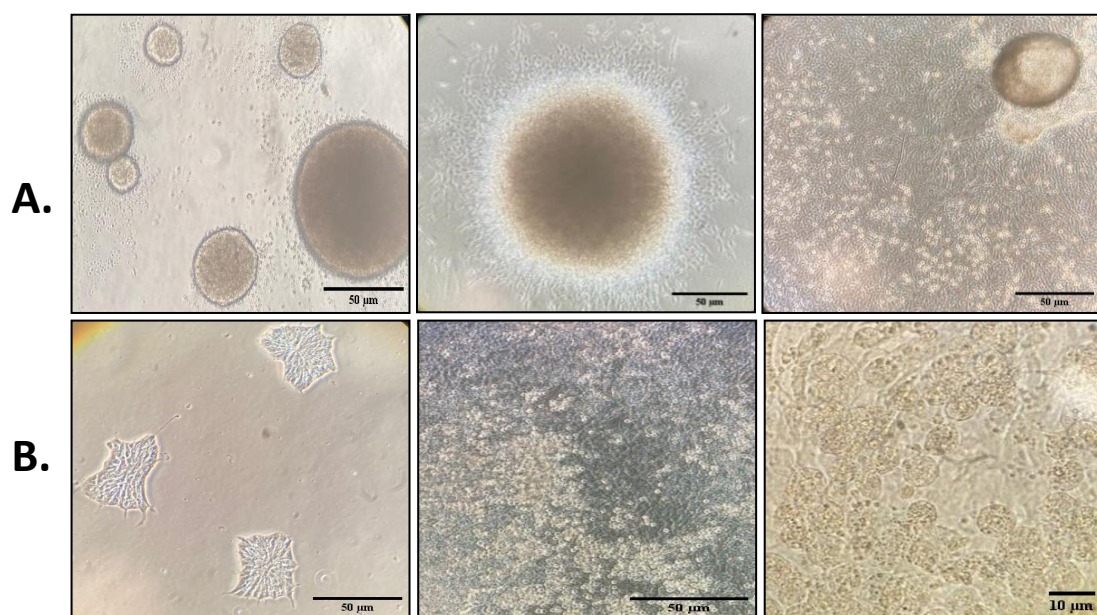


Figure 4. 12: Different Methods to Differentiate iPSCs Toward HPCs: iPSCs were cultured under two distinct conditions: **A.** (culture number V2/3D) as a 3D culture, and **B.** (Culture number V2/2D) in a 2D format. Both culture types were maintained in Stemline II serum-free medium with insulin, transferrin-selenium, and BMP4 (80 ng/ml) for the first 4 days, followed by media containing a mix of growth factors: VEGF (80 ng/ml) and SCF (100 ng/ml) for 2 days. From days 6 to 14, a cytokine cocktail comprising SCF, IL-3, G-CSF, FLT3 (each at 50 ng/ml), and TPO (5 ng/ml) was added. Subsequently, from day 14-25, G-CSF and FLT3 at 50 ng/ml were added to the renewed Stemline II serum-free medium. The culture process was carried out for a total of 18 days under these conditions.

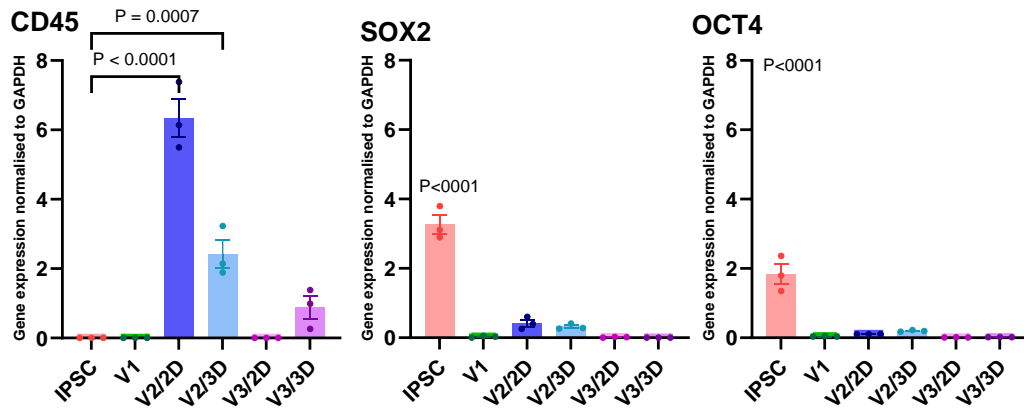


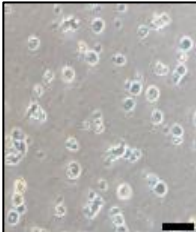

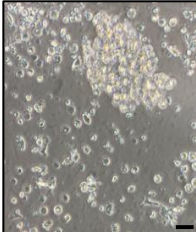
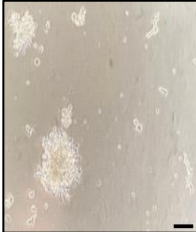
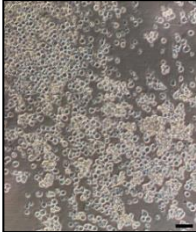
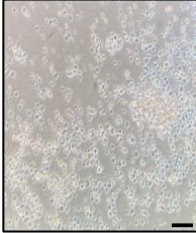
Figure 4. 13: Expression of Key Markers in Hematopoietic Cells Derived from iPSCs Using Cytokine Cocktail Method. Refer to Table 2-4 for details on culture cytokines and duration. Gene expression was measured using RT-qPCR and normalised to GAPDH. Bars represent the standard error mean of the values.

Subsequently, the hematopoietic progenitor cells (HPCs) derived from the stem cells were utilised in an attempt to differentiate them into microglia. The McQuade protocol was adapted, involving the use of differentiating cytokines for the first 25 days, supplementing the medium with 100 ng/mL IL-34, 50 ng/mL TGFβ1, and 25 ng/mL M-CSF (purchased from PeproTech), followed by the addition of maturation cytokines including 100 ng/mL IL-34, 50 ng/mL TGFβ1, 25 ng/mL M-CSF, 100 ng/mL CD200, and 100 ng/mL CX3CL1 for another 3 days. Unfortunately, this attempt encountered challenges: most cells remained in suspension, and the anticipated morphological changes were not observed.

In an alternative effort, a microglia differentiation kit from Stem Cell Technologies based on the McQuade protocol was used, which included both differentiation and maturation media. Initially, some morphological changes in the HPCs were noticed, such as the development of branch-like structures. However, as the culture progressed, the cells began to clump together, potentially indicative of cell death (Table 4. 2). Despite these unexpected morphological developments, cells were fixed for analysis; however, a significant number of cells were lost during this process.

The analysis of the remaining cells revealed expression of Iba1 and TMEM119, markers indicative of microglia. However, considerable debris that stained for these markers was noted, raising concerns about non-specific staining. This outcome suggested that the staining might not be exclusively identifying the target cells, especially since these cells didn't stain for the microglia-specific marker P2RY12 (Figure 4.14). This experiment, conducted only once due to the extensive culture duration (approximately 45 days) and the limited cell yield, highlighted several challenges.

Table 4. 2: Morphological Changes During Attempted iPSC-Derived Microglia Differentiation: Hematopoietic cells were differentiated into microglia using the STEMdiff Microglia Differentiation Kit for 27 days, followed by a 3-day maturation phase using the STEMdiff Microglia Maturation Kit. The scale bar in each image corresponds to around 10 μm .

Day	Stage	Image	Key Visual Markers and Description
-1	Initial hematopoietic cells		Cells appeared round and individual in suspension. Uniform size and shape were observed
4	Early differentiation		Cells began to form small clusters. Some adherence to the culture surface was visible.
6	Continued differentiation		Larger cell clusters had formed. A mix of adherent and floating cells was present
9	Mid-stage differentiation		Distinct colony-like structures were visible. Cells showed varied morphologies. Some single cells were observed due to media changes.
20	Late-stage differentiation		Large, dense cell aggregates were present. Some cells with elongated shapes were visible at colony edges. An increased number of single cells was noted due to media changes.
28	Final stage (post-maturation)		A heterogeneous cell population was observed. Many single, floating cells were present. Some dead cells were visible. Cells lacked typical microglial morphology.

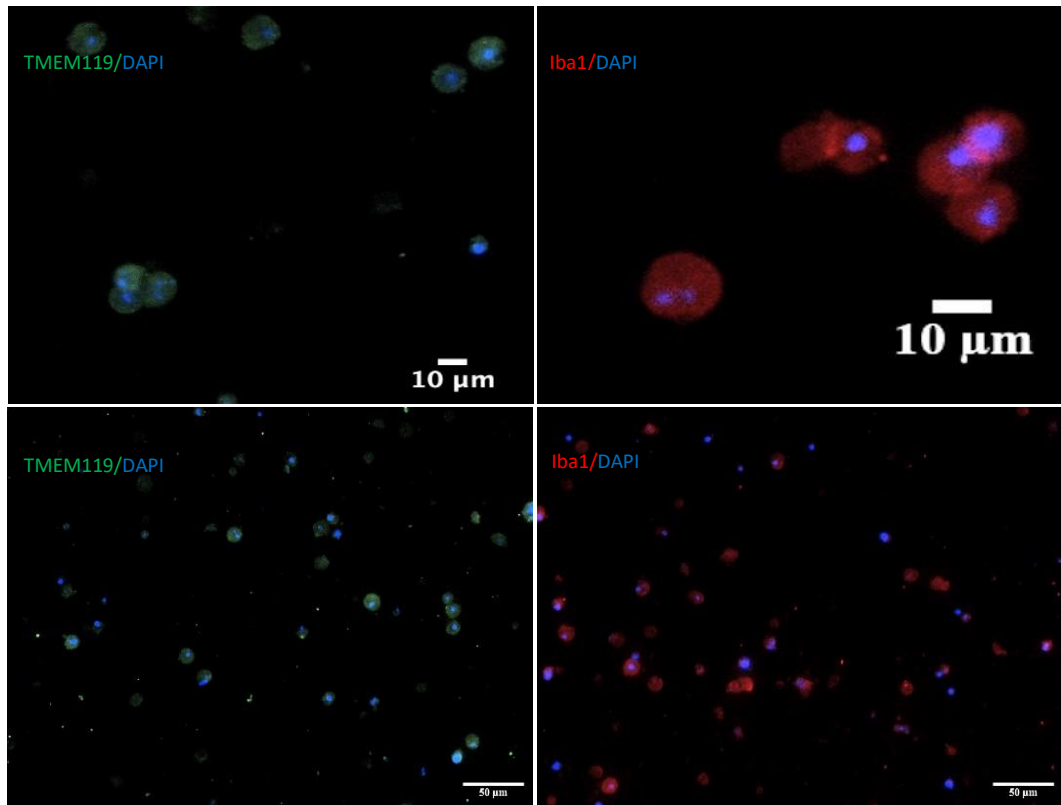
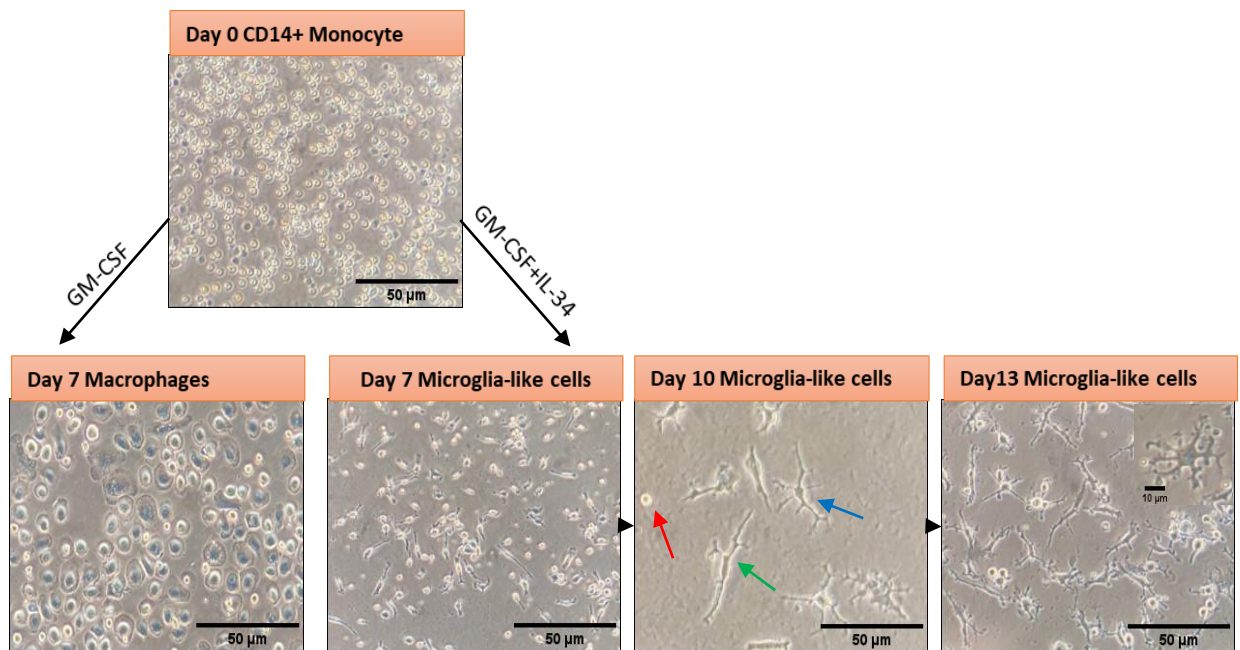


Figure 4. 14: Assessment of Microglial Markers in iPSC-Derived Human Microglia: Expression of microglial markers Iba1 and TMEM119. Hematopoietic cells were differentiated into microglia using the STEMdiff Microglia Differentiation Kit for 27 days, followed by a 3-day maturation phase using the STEMdiff Microglia Maturation Kit. After maturation, the cells were fixed and stained specifically for microglia with Iba1 and TMEM119 (red). Nuclei were also stained with DAPI (blue).

4.4 Generation of Human-Derived Microglia Using Peripheral Blood Mononuclear Cells (PBMCs)

In this study, either freshly isolated or frozen peripheral blood mononuclear cells (PBMCs) were used to produce human-induced microglia-like (iMG) cells. This process involved a mix of IL-34 (100 ng/ml) and GM-CSF (10 ng/ml), based on methods established by Ohgidani et al. (2014), Sellgren et al. (2017), and Banerjee et al. (2021). Initially, untreated monocytes were observed to display a round morphology, as shown in (Figure 4.16) During induction, it was observed that iMG cells began to develop branches around the 7th day, and by days 10-14, they exhibited heterogeneous morphologies characteristic of microglia, including ramified compact bodies with extensive branching, semi-ramified, and amoeboid morphologies, as demonstrated in the results (Figure 4.16). For the generation of macrophages, monocytes were exposed to GM-CSF for a period of 5-7 days. By the 6th day, phase-contrast microscopy clearly revealed the unique "fried-egg" shape of macrophages, marked by a large, rounded cell body, as confirmed in (Figure 4.16) and in alignment with the literature (Ohgidani et al., 2014, Banerjee et al., 2021).



iMG morphology Day 13

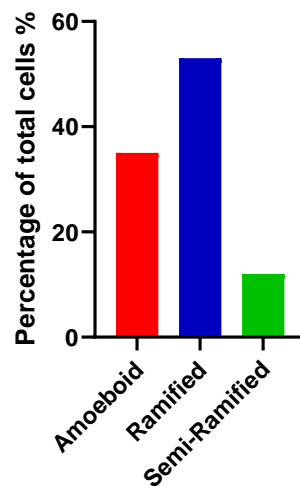


Figure 4. 15: Morphology of Primary Human Macrophage and Microglia-like Cells. Monocytes were isolated from human blood via density gradient and CD14+ sorting, followed by a 2-hour incubation at 37°C in 10% FBS for adherence. Nonadherent cells were washed away, leaving adherent monocytes. These were then differentiated into macrophages using GM-CSF (10 ng/ml) and 10% FBS, refreshed every three days. Alternatively, monocytes were transformed into microglia cells over 14 days using IL-34 (100 ng/ml) and GM-CSF (10 ng/ml), with media changes every three days. The resulting microglia exhibited heterogeneous morphology, marked by arrows: red for amoeboid, green for semi-ramified, and blue for ramified forms. Images are representative of three independent experiments. Images were taken using an inverted light microscope.

4.4.1 Functional Assessment and Validation of Human Monocyte-Derived Microglia

4.4.1.1 Expression of Microglia-Specific Markers in Induced Microglia-Like Cells

Both microglia and macrophages share certain markers such as Iba1, PU.1, CD45, and TREM2. However, markers such as HEXB, TMEM119, and the P2Y₁₂ receptor are reported to be unique to microglia and not found in macrophages (Schwabnland et al., 2021). In this study, the identity of induced microglia-like (iMG) cells was confirmed using both myeloid and microglia-specific markers. As expected, iMG cells demonstrated the presence of HEXB, TMEM119, and P2Y₁₂. Notably, TMEM119 and HEXB were expressed in induced macrophage-like (iMac) cells, while the P2Y₁₂ receptor was absent in iMacs. Both iMG cells and iMac cells exhibited the presence of myeloid lineage markers such as Iba1, PU.1, and TREM2 (Figure 4. 16).

Immunocytochemistry and qPCR results indicated that iMG cells and iMacs, both derived from monocytes, share typical markers of the myeloid lineage. However, only iMG cells display unique markers specific to microglia, notably the P2Y₁₂ receptor (Figure 4. 17). Thus, it is possible to distinguish iMG cells from monocyte-derived macrophages using this marker.

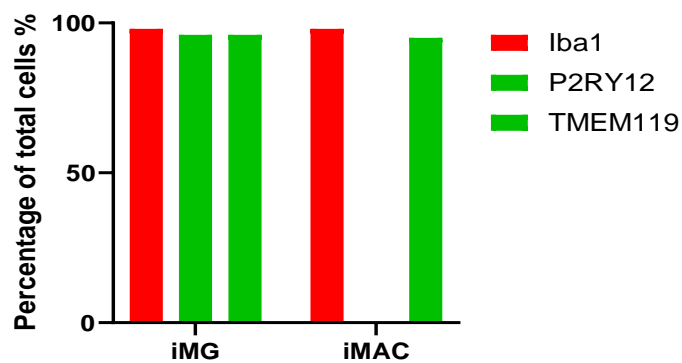
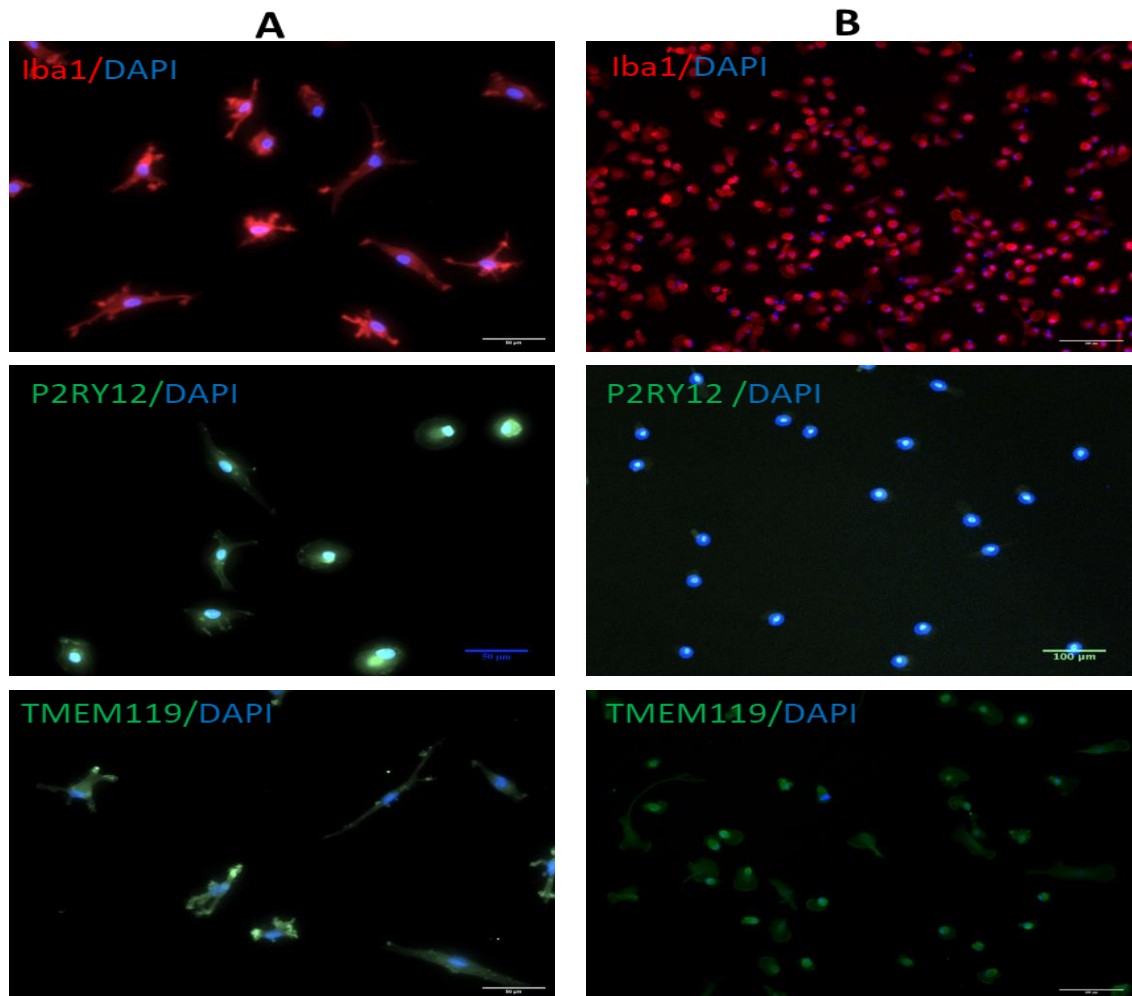


Figure 4. 16: Monocyte-derived Macrophage (iMAC) and monocyte-derived microglia (iMG) Cells express Surface Markers. The presence of surface markers on iMG cells (A) and iMAC cells (B) was evaluated using immunocytochemistry. Primary antibodies, including Anti-Iba1, Anti-P2RY12, and Anti-TMEM119, were applied and incubated overnight. iMG cultures exhibited heterogeneous morphologies. Imaging was collected with a widefield microscope at magnifications of 10x or 20x. Data are representative of three separate experiments.

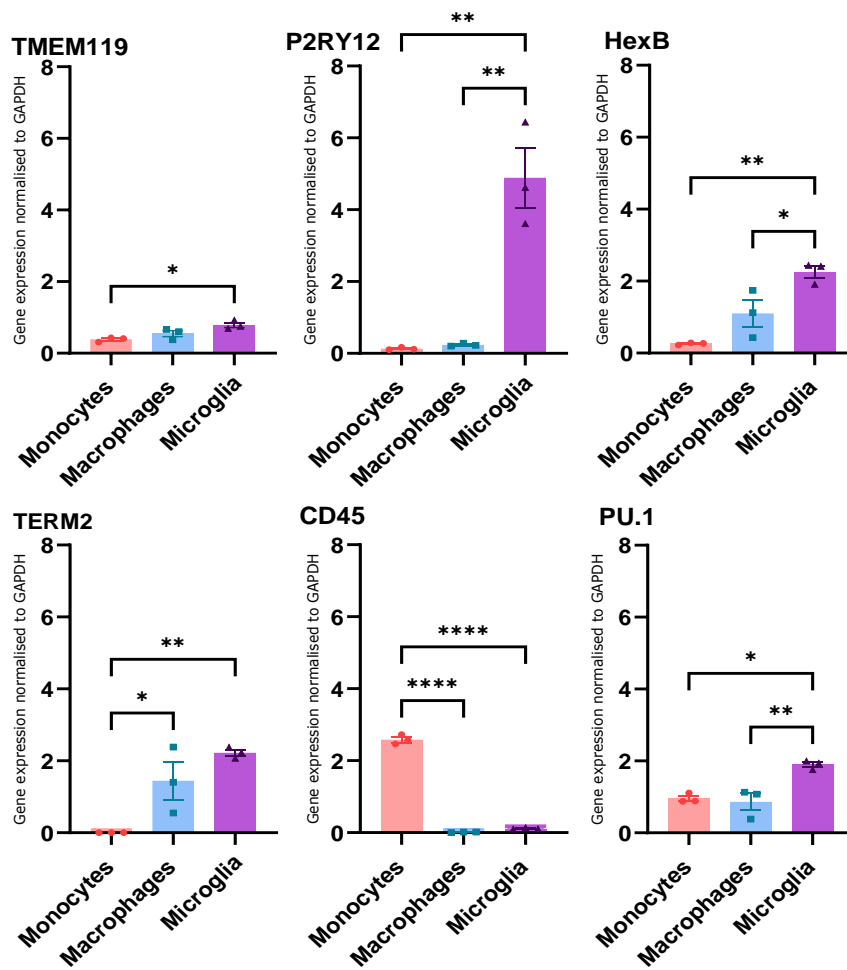


Figure 4. 17: Monocyte-Derived Macrophage (iMAC) and Monocyte-Derived Microglia (iMG) Cells Express Surface Markers: mRNA Expression of microglia-specific markers and myeloid markers was assessed in CD14+ Monocytes harvested after a 2-hour incubation at 37°C, as well as in macrophages (iMAC) and microglia-like cells (iMG) harvested after 6 and 13 days of differentiation, respectively. The differentiation media for iMAC contained 10ng/ml GM-CSF and 10% FBS, while for iMG cells, it included 10ng/ml GM-CSF and 100ng/ml IL-34. RT-PCR was used to measure key marker expression levels, which were then normalised using GAPDH mRNA expression. Results are from three independent experiments. Data are presented as the standard error of the mean.

4.4.1.2 Phagocytosis Capability of iMAC and iMG Cells

Phagocytosis, a critical function of immune cells, plays a pivotal role in the innate immune response. In this study, the phagocytic activity of iMAC and iMG cells was assessed to evaluate their phagocytic abilities using GFP-tagged fluorescent beads, a standard method for evaluating phagocytosis. This approach enabled the observation of the cells' ability to engulf these beads (Figure 4. 18).

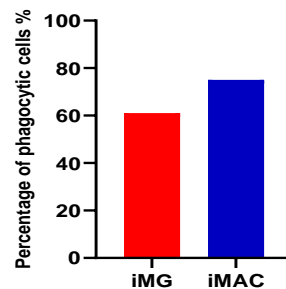
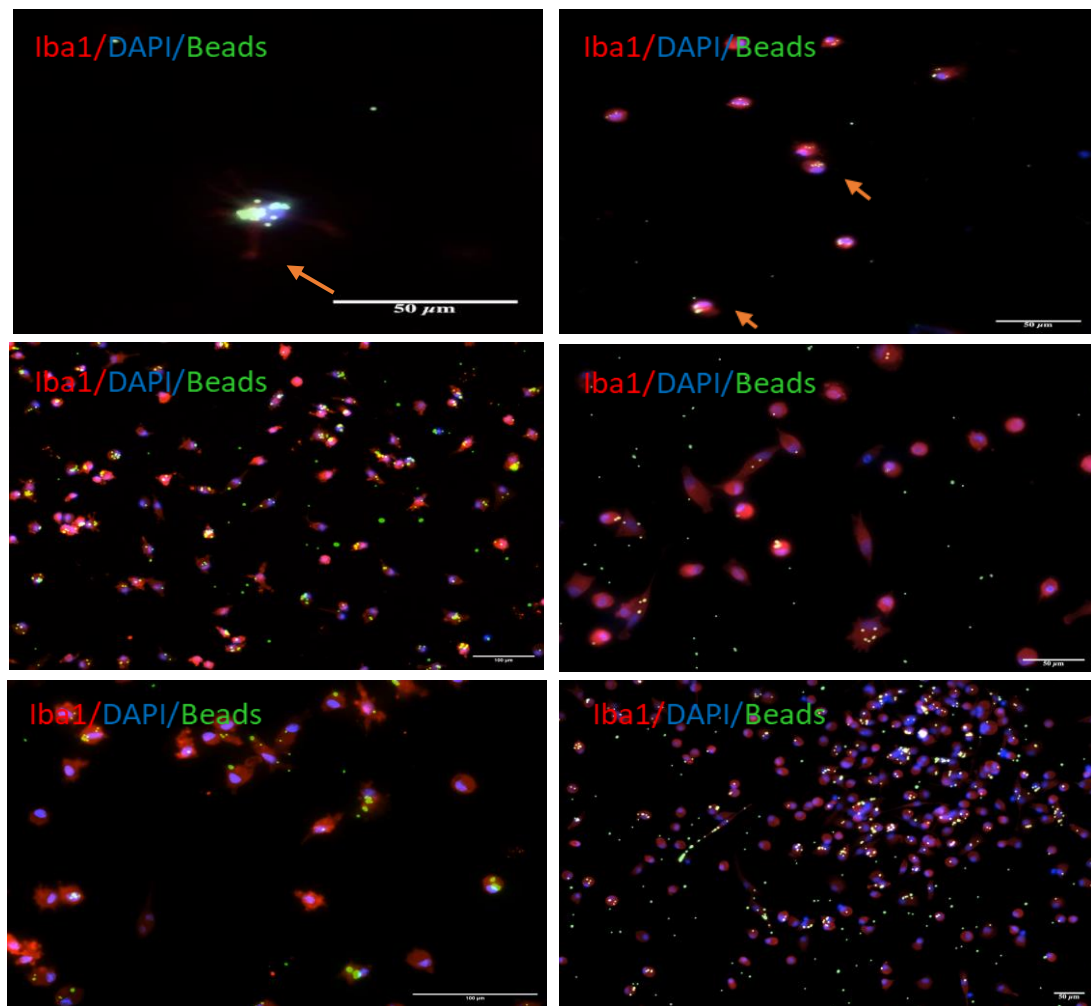


Figure 4. 18: Phagocytic Capability of iMAC and iMG Cells. After culturing iMG cells (left) for 13 days and iMACs (right) for 6 days, GFP-tagged latex beads opsonised in FBS were added to the culture medium, at a final concentration of 0.05% V/V. Cells were incubated for 24 hours at 37°C, then fixed with 4% PFA. Staining was performed using anti-Iba1 (Red) and DAPI (blue) for nuclear visualization. The image was collected with a widefield microscope at magnifications of 10x or 20x. These data represent findings from three independent experiments (N=3). Arrows indicate cells that phagocytosed GFP-tagged latex beads.

4.4.1.3 Unique PCA Clusters Demonstrate Effective Transformation of Monocytes into iMacs and iMG Cells

Peripheral blood mononuclear cells (PBMCs) were isolated from the three donors, and monocytes were purified using magnetic-activated cell sorting (MACS) with CD14 microbeads (Miltenyi Biotec). The CD14-positive monocytes were then differentiated into iMacs and iMG cells. To visualize the overall transcriptomic differences between monocytes, iMacs, and iMG cells, Principal Component Analysis (PCA) was used on the full-genome RNA sequencing data, the three distinct cell types involved in the induction process were examined: monocytes, iMacs, and iMG cells. The resulting PCA plot revealed three distinct clusters corresponding to monocytes, iMacs, and iMG cells. Principal Component 1 (PC1) accounted for 77% of the variance and 16% was due to Principal Component 2 (PC2), suggesting that the monocytes were effectively transformed into the two other cell types, iMacs and iMG cells, and that there were clear differences between iMAC and iMG cells in terms of the transcriptome (Figure 4. 19).

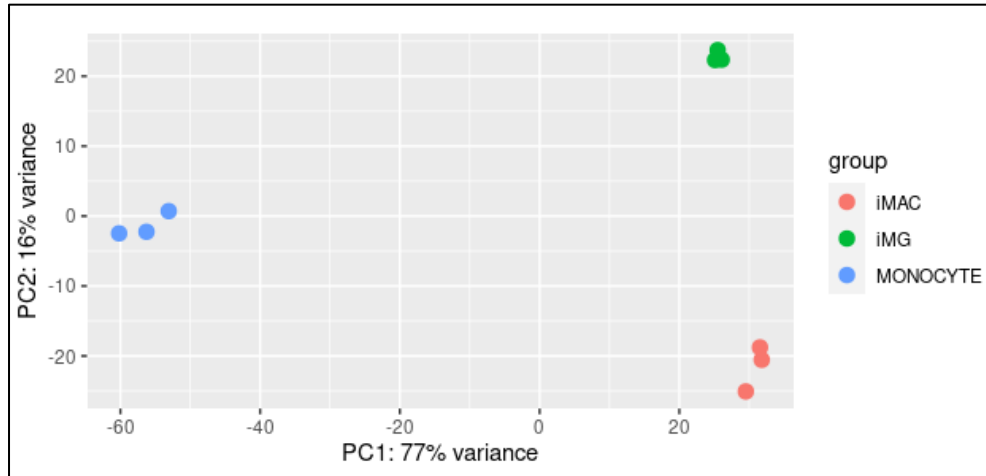


Figure 4. 19: PCA of Monocytes, iMACs, and iMG: Cell-type-specific segregation between monocytes, iMAC, and iMG samples. Macrophages (iMAC) were cultured in 10 ng/ml GM-CSF and microglia (iMG) in 10 ng/ml GM-CSF and 100 ng/ml IL34. CD14+ monocytes were harvested after a 2-hour incubation at 37°C, while macrophages and iMG cells were harvested after 6 and 13 days of differentiation, respectively. Blue: Monocytes; Red: iMacs; Green: iMG cells. Data were from 3 separate donors.

4.4.1.4 Comparative Venn and Differential Gene Analysis Among iMG Cells, iMacs, and Monocytes

Differential expression analysis was conducted to further investigate the specific genes and pathways that distinguish iMacs and iMG cells from CD14-positive monocytes. Microglia express a specific set of genes at much higher levels than macrophages. To understand the distinctions between monocytes, iMacs, and iMG cells, a Venn analysis was conducted of shared and unique genes expressed in these groups (Figure 4.21/A).

Specifically, 125 genes were found to be exclusively expressed in iMG cells, while iMacs and monocytes exhibited 50 and 269 unique genes, respectively. Additionally, there were 17,208 genes common to all three groups. The volcano plot provides an alternative view of the variations in gene expression between iMG cells and monocytes, iMAC and monocytes, and iMG and iMAC, highlighting significantly differentially expressed genes. These genes met the criteria of a False Discovery Rate (FDR) with p-values less than 1×10^{-16} and an absolute log₂ fold change ($|\log_2FC|$) greater than 2. These genes are marked in red for easy identification (Figure 4.21/B).

The gene enrichment analysis performed on the unique genes expressed in iMG cells revealed a significant overrepresentation of pathways associated with ion and neurotransmitter transporters and genes involved in synaptic function and neuron interaction. Notably, the analysis identified an enrichment of genes encoding solute carrier family proteins, including SLC25A41A7, which transports molecules across the mitochondrial membrane (Haitina et al., 2006), SLC52A1, a riboflavin transporter that may contribute to cellular metabolism and energy production (Colasuonno et al., 2022); and SLC30A2, a zinc transporter crucial for regulating zinc levels and synaptic function (De Benedictis et al., 2021). Moreover, the enrichment analysis highlighted several genes directly related to synaptic function and neuron interaction. These included DRD2, which encodes the dopamine receptor D2, a key

player in dopamine neurotransmission and various neuronal functions such as motivation, cognition, and motor control (Pike et al., 2022, Tritsch and Sabatini, 2012). Furthermore, the enrichment of GABRE, encoding a GABA receptor subunit, demonstrates the importance of inhibitory synaptic transmission in neural circuit functions (García-Martín et al., 2018). The enrichment of GDNF, a gene encoding glial cell line-derived neurotrophic factor, highlights the role of neurotrophic support in neuronal survival (Chang et al., 2006).

Expression of certain microglia-specific genes (Banerjee et al., 2021) was analysed, revealing high expression of genes related to synaptic remodelling in iMG cells, such as complement factors C1QA, C1QB, C1QC, C9, and SERPING1 (Figure 4.21/C). These data are consistent with the literature (Gosselin et al., 2017, Ryan et al., 2017, Banerjee et al., 2021). notably, these genes were uniquely upregulated in iMG cells but not in iMacs and reported to be microglia-specific (Ryan et al., 2017, Banerjee et al., 2021). These results corroborate previous findings and enhance the understanding of the unique genetic profile of iMG cells. Interestingly, astrotactin 2 (ASTN2), a gene that plays a role in modulating the efficacy of synaptic connections (Ito et al., 2023) was uniquely expressed only in iMG. Moreover, iMG uniquely expressed SYT1, SYT9, and SYT17 genes, which are notable for their roles in synaptic interactions and signalling. Using the DAVID bioinformatics resource, a specialised gene enrichment examination of iMG cells highlighted a concentration of distinctive genes within pathways associated with synaptic regulation and ion transport. See appendices(Figure 1).

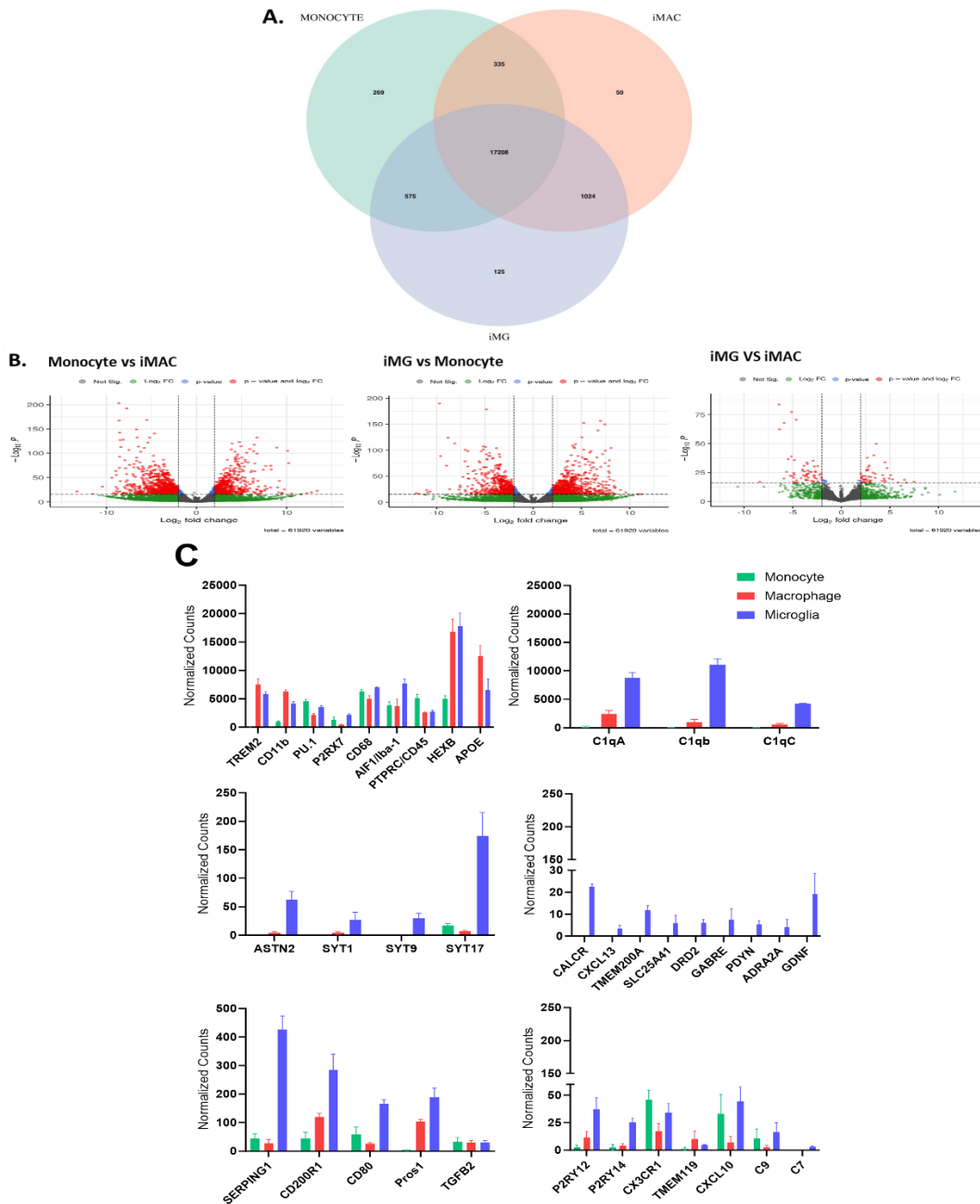


Figure 4. 20: The unique and differential gene expression among iMG, iMacs, and monocyte cell types was analysed through various methods. This analysis involved **A.** A Venn diagram comparing gene expression in iMG cells, iMacs, and monocytes, based on mean gene counts. Green represents monocytes; red signifies iMacs; blue denotes iMG cells. **B.** A Volcano Plot illustrating variations in gene expression between Monocyte vs iMAC, iMG Cells vs Monocyte, and iMG vs iMAC. The plot features a dashed line representing a threshold of $p < 1 \times 10^{-16}$ (horizontal line) and an absolute \log_2 fold change ($|\log_2FC|$) greater than 2 (vertical line). **C.** Unique and differential gene expression counts in iMG cells vs monocyte and iMAC. Data from 3 separate donors.

4.4.2 Stimulation of Microglia: An Investigation of the Effects of PAMPs and DAMPs Upon Microglial Phenotype and gene expression

This study aimed to identify the optimal stimulation time and the lowest effective concentration for microglial activation in a physiologically relevant manner, avoiding the extreme conditions associated with sepsis and death. In preliminary experiments, macrophages were examined due to a quicker and easier culture process. Macrophages were exposed to 100 ng/ml LPS at various time points: 1, 3, 6, and 24 hours. A peak in TNF α mRNA expression was observed at 6 hours, increasing by 90-fold, compared to a 25-fold increase at 1 hour and a decrease to 4-fold at 24 hours. Similarly, IL-1 β mRNA expression peaked at 6 hours (160-fold increase) but increased further at 24 hours (230-fold). IL-6 mRNA levels also peaked at 6 hours with a 175-fold increase but decreased at 24 hours. Interestingly, IL-10 mRNA expression only showed significant increases at 6 and 24 hours (Figure 4. 21/A). This timeframe precedes the peak of IL-10 expression, providing a view of early pro-inflammatory and subsequent anti-inflammatory responses.

Based on the observed peak in pro-inflammatory cytokine expression at this period. At 6 hours, TNF α showed a nearly maximum increase, and IL-1 β reached a significant level of expression, indicating a robust inflammatory response. Furthermore, IL-10, an anti-inflammatory cytokine, started showing a significant increase post-6 hour, providing a longitudinal perspective of the immune response. This time point thus captures a critical phase of both pro- and anti-inflammatory activity, making it ideal for assessing the efficacy of various LPS concentrations (10, 50, and 100ng/ml). At this time point, IL-1 β , TNF α , and IL-10 mRNA expressions significantly increased across all tested LPS concentrations (Figure 4. 21/B). This approach allowed us to effectively determine the minimum LPS concentration required to stimulate an observable response in macrophages, contributing valuable insights into microglial activation dynamics.

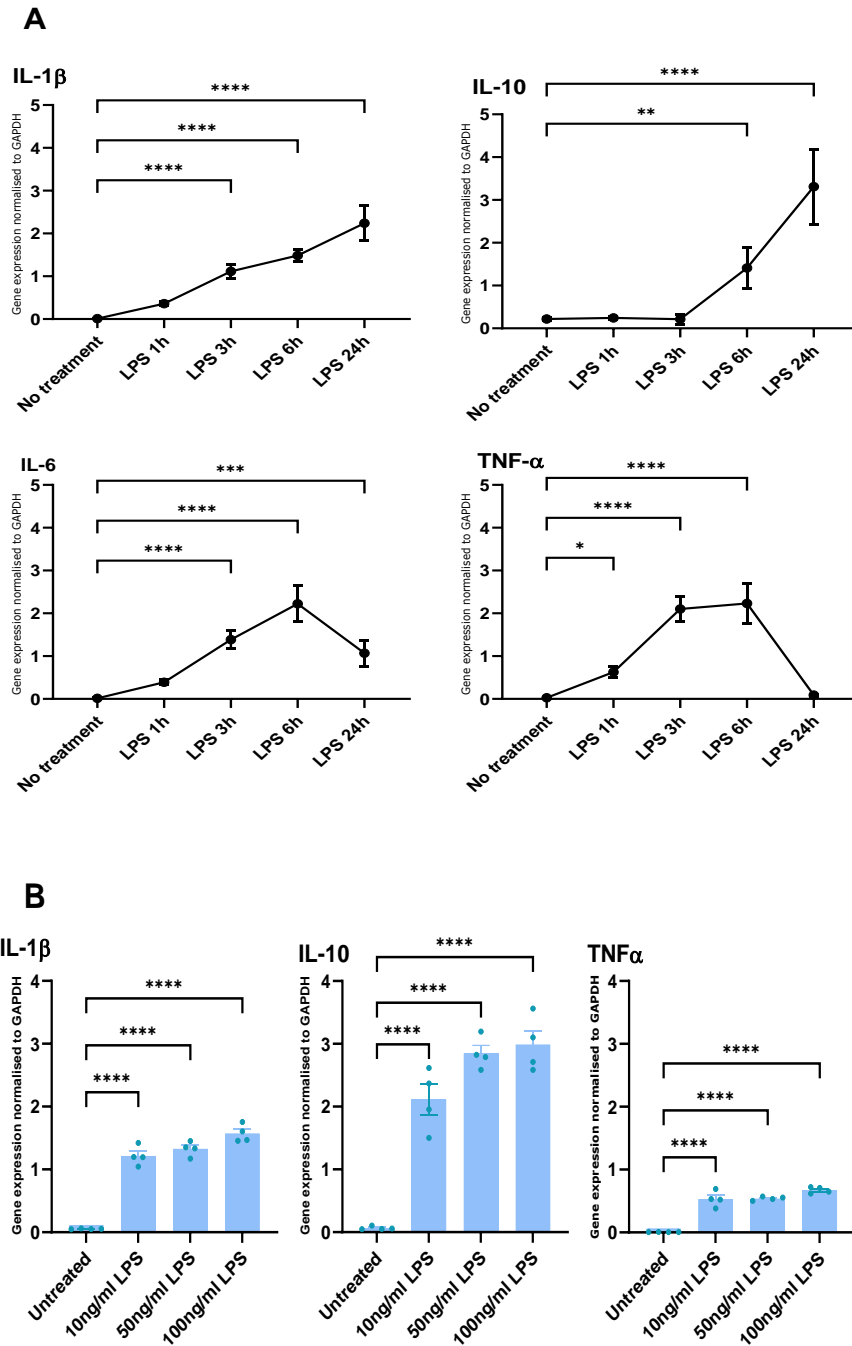


Figure 4. 21: The Optimal Concentration and Timing for Macrophage Stimulation.

A. Macrophages were stimulated with 100 ng/ml LPS at various time intervals – 1, 3, 6, and 24 hours. B. The impact of varying LPS concentrations (10, 50, and 100 ng/ml) on macrophages was assessed over a 6-hour period. The expression levels of mRNA were quantified using RT-qPCR and normalised using GAPDH gene expression. Data represent mean \pm SEM from one representative experiment (n=4 wells). Results are representative of three independent experiments.

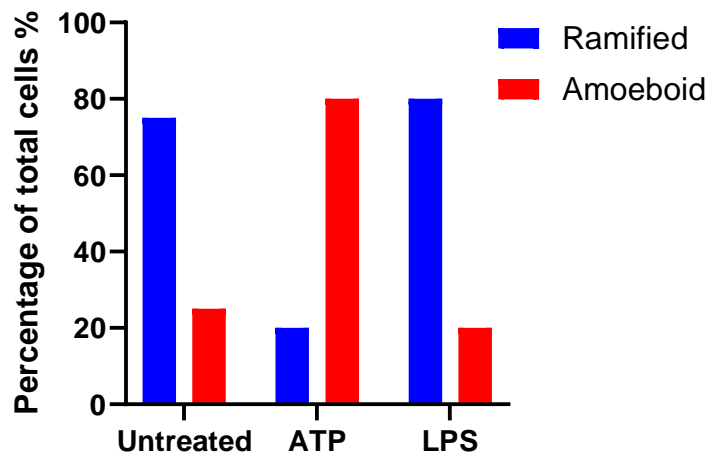
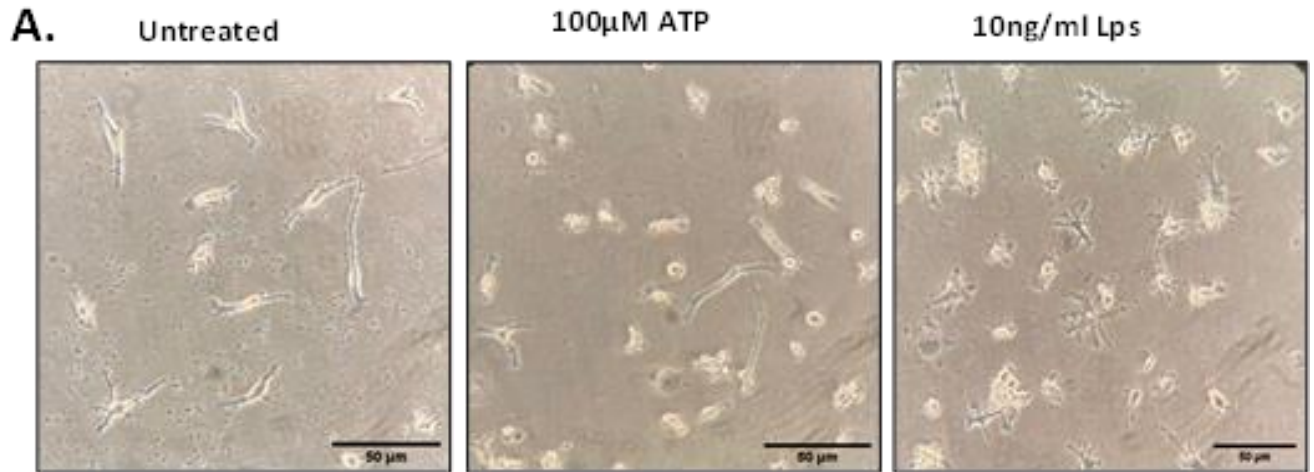
Microglia, upon stimulation, can transition across a range of activation states, from a pro-inflammatory state to an anti-inflammatory state. This polarisation involves changes in cell morphology, gene expression, and cytokine production (Ohgidani et al., 2014, Banerjee et al., 2021). From the preliminary data on macrophage stimulation, 2 hours for stimulation duration was chosen as it represented a midpoint where significant gene expression changes were observed without reaching the peak or declining phases. Additionally, in further work, the anti-inflammatory effects of PPAR β agonists, the use of low levels of inflammatory stimuli, which still show significant increases in gene expression, would represent a situation reflecting low-level, chronic neuroinflammation such as that present in human neurodegenerative diseases

Following 10 ng/mL LPS treatment for 2 hours, morphological alterations in iMG cells were noted, characterised by the development of extensively branched, elongated structures, as compared to untreated iMG cells. Conversely, iMG cells activated with 100 μ M ATP for 2 hours displayed a distinct amoeboid morphology, characterised by a rounder cytoplasm and the presence of shorter branches (Figure 4. 22/A). This highlights the variable morphological adaptations of iMG cells in response to different activating agents.

To gain insight into the microglial response, the LPS concentration was reduced to 5 and 10 ng/mL for 2 hours. IL-1 β mRNA levels showed a notable increase, with a 27-fold rise using 5 ng/ml and a 39-fold increase using 10 ng/ml (Figure 4. 22/B). IL-10 mRNA levels also rose, showing a 22-fold increase with 5 ng/ml LPS and a 15-fold with 10 ng/ml. IL-6 mRNA levels rose by 591-fold and further escalated to 1027-fold with 10 ng/ml LPS. TNF α expression experienced a relatively modest elevation, with 15-fold and 17-fold increases for 5 ng/ml and 10 ng/ml, respectively.

To investigate DAMP effects on microglia, ATP was employed from 10 to 100 μ M for 2 hours (Figure 4. 22/B) IL-1 β mRNA levels increased differently, showing increases of 2.6, 12, and 11-fold for 10, 50, and 100 μ M ATP, respectively. ATP treatment resulted in significant increases in IL-6 mRNA: a 12-fold increase with 10 μ M, 205-

fold with 50 μ M, and 388-fold with 100 μ M ATP. Interestingly, IL-10 mRNA levels increased 14-fold with either 50 or 100 μ M ATP, while TNF α did not show a significant increase with ATP treatment.



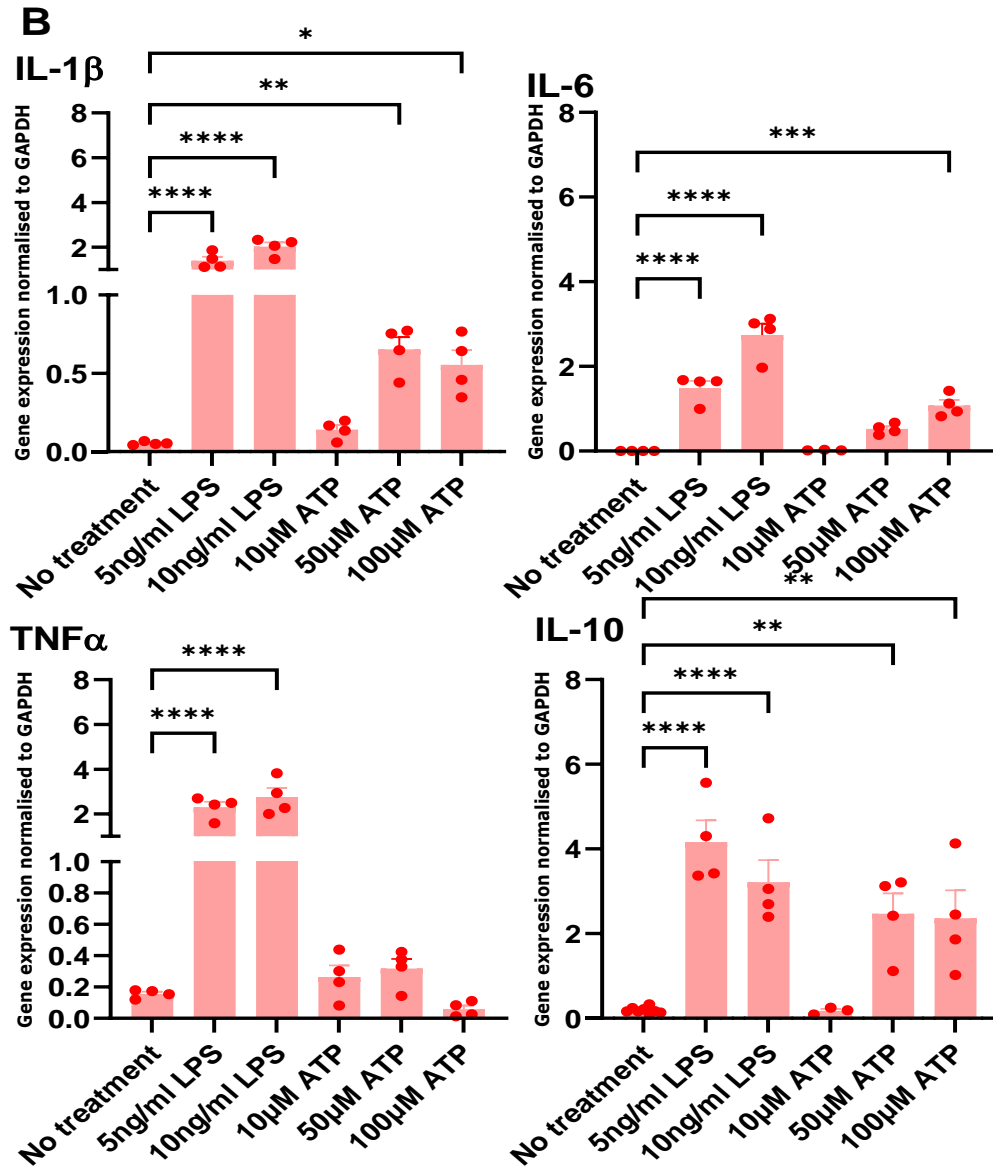


Figure 4. 22: Investigation of effects of LPS and ATP on Microglia. A. iMG cells underwent morphological analysis post-stimulation with LPS or ATP for 2 hours. The LPS-treated cells (10 ng/ml) demonstrated enhanced branching, indicating a state of activation. In contrast, ATP-treated cells (100 μ M) adopted an amoeboid structure, indicative of a heightened reactive state. B. iMG cells were exposed to 5 or 10 ng/ml LPS or 100 μ M ATP for 2 hours. Real-time qPCR analysis was employed to measure IL-1 β , TNF α , and IL-10 expression levels, with normalization against GAPDH expression. Data represent mean \pm SEM from one representative experiment (n=4 wells). Results are representative of three independent experiments.

4.5 Summary and Discussion

Numerous studies have utilised murine models to explore microglial phenotypes and functions, but it is crucial to acknowledge the differences in microglial transcriptomes between murine and humans (Deczkowska et al., 2018, Zhou et al., 2020, Galatro et al., 2017). Additionally, the efficacy of animal-based clinical trials often does not translate to human diseases, as exemplified by Alzheimer's Disease and stroke (Franco and Cedazo-Minguez, 2014). Alternatives, such as post-mortem brain examinations and *in vivo* imaging, have their limitations. Conducting *in vitro* studies with primary human microglia presents numerous technical and ethical challenges. As alternatives, researchers have utilised human microglial cell lines, such as HMO6 and HMC3 (Nagai et al., 2005, Janabi et al., 1995), which offer a substitute but may not fully capture human-specific microglial attributes, and their phenotypes can alter over time due to genetic manipulation and repeated culturing. Recent technological advancements have enabled researchers to develop human microglia-like cell models from human blood monocytes and hPSCs, as detailed in multiple studies (Ohgidani et al., 2014, Ryan et al., 2017, Sellgren et al., 2019, Banerjee et al., 2021, McQuade et al., 2018, Haenseler et al., 2017, Abud et al., 2017, Muffat et al., 2016, Fattorelli et al., 2021). Differentiating hPSC into microglia presents challenges due to the complex reprogramming involved. To mimic human microglial characteristics closely, it's important to generate an efficient model that is also based on simple and uncomplicated sample collection. Adapting methods from Ohgidani et al. (2014) and Banerjee et al. (2021), this study successfully produced a microglia-like model from human peripheral monocytes, aligning with findings from previous research.

The quality of iPSCs is important for successfully differentiating them into different cell types. In this study, a cell line kindly gifted from Dr. Nick Hannan's laboratory was used. The culture was maintained in TeSR-E8 media growing stem cells on qualified Cultrex using ReLeSR, an enzyme-free passaging reagent, this approach consistently yielded non-differentiated, stable cultures (McQuade et al., 2018, Powell et al., 2021). These cells were verified through the evaluation of key pluripotency markers and their ability to differentiate into all three germ layers (Takahashi et al., 2007, Takahashi and Yamanaka, 2006, Chambers et al., 2003, Pomeroy et al., 2016). Genetic analysis using the hPSC Genetic Analysis Kit (Stemcell Technologies) yielded variable results between samples, indicating the need in the future to focus on comprehensive karyotypic analysis using G-banding to confirm the genetic stability of the iPSC cultures.

The generation of dopaminergic neurons from iPSCs has been extensively explored, often involving multi-stage processes with complicated media formulations that result in inconsistent outcomes. A cost-effective approach for generating DA neurons has been employed by overexpressing key transcription factors *Nurr1*, *Ascl1*, and *LMX1B*, similar to the studies Powell et al. (2021) and Theka et al. (2013). Initially, neuron validation was conducted based solely on morphological criteria. However, further assessments are deemed essential for their confident identification as dopaminergic models, including assessments of dopamine synthesis and the expression of neuron-specific markers. These preliminary findings and morphologies are seen as encouraging, yet additional validation is required.

Although existing methods for differentiating iPSCs into iMGLs provide a valuable foundation, several challenges were encountered that hindered their direct application. Despite this, a protocol was successfully established for creating intermediate hematopoietic cells. Reflecting the complex nature of differentiating iPSCs into microglia, several commercial kits have been developed (McQuade et al., 2018). These kits manage the cells through sequential differentiation stages, reducing the variability associated with multi-cytokine media compositions.

Efforts to generate HPs using two different methods were successful only with the kit, which produced a sufficient yield of cells expressing key HP markers. However, upon subjecting these HPs to microglial differentiation and maturation using Stemcell Technologies kits, the resulting cells did not exhibit the typical ramified microglia morphology after 34 days. The cells appeared round, with many floating, which might indicate an activated state or cell death. Despite this atypical morphology, the cells were found to express Iba1 and the microglia-specific marker TMEM119, but not P2Y₁₂ receptors. Therefore, further analysis is needed to confirm their gene expression profile and phagocytic capabilities.

Experiences have suggested that, despite the initial cost, kits with pre-prepared media may be preferable to optimising multiple cytokine cocktails. The process of differentiating iPSCs into microglia appeared less promising. The challenge in scaling up culture generation to facilitate high-throughput experiments in drug discovery stems from variability in differentiation efficiency, yields, and cell quality across different iPSC lines, batches, and operators (Banerjee et al., 2021).

Due to the challenges in generating functional microglia and the time-intensive nature of the process, alternative methods were explored. Recent studies, such as those by Ohgidani et al. (2014) and Banerjee et al. (2021), have demonstrated that similar protocols can induce a microglia-like phenotype by adding key cytokines that mimic the CNS microenvironment. The microglia generated using this protocol are notably different from human blood monocytes, as they express typical surface markers of human microglia. These cells also exhibit heterogeneous morphologies, including ramified, semi-ramified, and amoeboid forms, and demonstrate active engagement in functional activities such as phagocytosis and cytokine release (Banerjee et al., 2021, Ohgidani et al., 2014). Using IL-34, reported to originate from neurons, human monocytes were transformed into iMG cells in just 14 days. Notably, IL-34 has been described as crucial for microglial proliferation (Noto et al., 2014, Gómez-Nicola et al., 2013, Mizuno et al., 2011, Wang et al., 2012). iMG cells formed a distinct cluster separate from macrophages and monocytes. They

exhibited high relative expression of genes that are either highly expressed or unique to microglia compared to other immune and brain cells. These observations align with the outcomes of a similar study conducted by (Banerjee et al., 2021), corroborating the unique genetic profile of iMG cells. Upon stimulation with low concentrations of LPS and ATP, iMG cells entered a pro-inflammatory state, leading to the release of cytokines such as IL-1 β , TNF- α , and neurotoxic factors, along with the anti-inflammatory cytokine IL-10. Several genes associated with the complement system, including C1QA, C1QB, C1QC, C9, *along with* SYT1, SYT9, SYT17, ASTN2, and SERPING1, were markedly upregulated.

This upregulation emphasises the successful transformation of monocytes into iMG cells, highlighting their acquisition of microglia-specific functions such as synaptic remodelling. Moreover, this expression pattern is indicative of the specialised functions of microglia in the CNS, distinguishing them from peripheral immune cells such as monocytes and macrophages (Wolfes and Dean, 2020). This observation is in line with the results reported by (Ryan et al., 2017, Gosselin et al., 2017, Banerjee et al., 2021), affirming the specialised brain functions these differentiated cells possess. Microglia express a variety of ion channels and neurotransmitter receptors that allow them to sense and respond to changes in neuronal activity and the extracellular environment (Kettenmann et al., 2011). The enrichment of genes related to these functions in iMG cells provides strong evidence for their microglia-like properties.

While monocyte-derived microglia monocultures are frequently described as human microglia-like cells, caution is advised when interpreting their outcomes. These cells are capable of responding to a variety of environmental signals and adapting their functions based on complex intercellular communication. Consequently, the functional outcomes observed in these monocultures might significantly differ from those seen in more complex settings, such as organoids or *in vivo* models, where cellular interplay is more representative of natural conditions.

This study encountered challenges such as variability between subjects and cell viability during induction, affecting the consistency of experimental results. Despite these limitations, the *in vitro* iMG cells demonstrated results compatible with those of other research groups. The findings confirm the iMG model's resemblance to human brain microglia in both cellular and molecular aspects, providing a validated, comprehensive RNA profile. This contributes to the existing body of research on human monocyte-derived microglial models.

Chapter 5 The Impact of PPAR β Agonists on Inflammation

5.1 Introduction

In the evolving landscape of neuroinflammatory research, the peroxisome proliferator-activated receptor beta (PPAR β), part of the nuclear receptor superfamily, has garnered attention for its capacity to influence a wide variety of cellular functions. These include processes related to inflammation, metabolism, and autophagy, thereby presenting a multifaceted approach to countering neuroinflammatory conditions (Wang et al., 2003, Iwashita et al., 2007, Palomer et al., 2014). This receptor has been identified as a potential therapeutic target for managing diverse conditions such as metabolic syndrome, dyslipidaemia, cancer development, and diabetes. While most research has focused on peripheral organs (Phua et al., 2020, Álvarez-Guardia et al., 2011, Odegaard et al., 2008, Tanaka et al., 2003), the presence of this receptor within various brain regions and cells is well-documented (Higashiyama et al., 2007, Xiao et al., 2010). However, its involvement in neurodegenerative and neuroinflammatory processes has yet to be fully explained.

Nuclear receptors, such as PPAR β , LXR, and PPAR γ , have been shown to undergo post-translational modifications, including SUMOylation, which can modulate their activity and function (Treuter and Venteclef, 2011). SUMOylation, the covalent attachment of small ubiquitin-like modifier (SUMO) proteins to target proteins, has emerged as a key regulatory mechanism in various cellular processes, including transcriptional regulation and inflammation (Treuter and Venteclef, 2011, Ghisletti et al., 2007). Interestingly, ligand binding has been reported to trigger SUMOylation of some nuclear receptors, such as LXR and PPAR γ , which in turn can mediate their anti-inflammatory effects (Ghisletti et al., 2007, Pascual et al., 2005). However, the role of SUMOylation in PPAR β -mediated anti-inflammatory effects remains to be elucidated.

The therapeutic promise of PPAR β agonists in microglia, primary immune cells in the CNS, lies in their ability to mitigate inflammatory responses, a hallmark of various neurodegenerative diseases. Activation of PPAR β by its selective ligands has been shown to exert an anti-inflammatory effect, primarily by downregulating the release of pro-inflammatory cytokines and upregulating anti-inflammatory mediators. This action likely occurs through the inhibition of the NF- κ B pathway, a key regulatory mechanism in the inflammatory response. This, in turn, decreases the expression of inflammatory genes and the secretion of cytokines that drive inflammation (Kuang et al., 2012).

Beyond their anti-inflammatory properties, PPAR β agonists may also affect microglial function through changes in cellular metabolism. By activating PPAR β , these compounds can shift the metabolic profile of microglia from a glycolytic, pro-inflammatory state to an oxidative metabolism, favouring an anti-inflammatory, neuroprotective state. This metabolic reprogramming is crucial for mitigating the bioenergetic demands of persistent inflammation and supporting the resolution of inflammation (Kruglov et al., 2024, Phua et al., 2020, Chehaibi et al., 2017).

While SUMOylation has been implicated in the anti-inflammatory effects of some nuclear receptors, such as LXR and PPAR γ , recent evidence suggests that changes in gene expression mediated by ABC transporters on the cell membrane may also contribute to these effects (Ito et al., 2015). The rapid nature of the anti-inflammatory effects observed with some nuclear receptor agonists has led to a controversy regarding the primary mechanism of action, as gene expression changes are typically considered to be slower processes (Ito et al., 2015).

Thus, the exploration of PPAR β as a therapeutic target highlights a novel approach to developing treatments aimed at the root causes of neuroinflammation. Investigating the potential mechanisms underlying the anti-inflammatory effects of PPAR β agonists, including SUMOylation, changes in gene expression, and metabolic reprogramming, is crucial for understanding their therapeutic potential and optimizing their application in the context of neuroinflammatory disorders.

5.2 Aims

This chapter investigates the anti-inflammatory effects of PPAR β on microglial cells, with a specific focus on the selective agonist GW0742. The methodology employed includes the use of real-time polymerase chain reaction (RT-PCR) to quantitatively assess changes in inflammatory and anti-inflammatory gene expression. Additionally, cytokine arrays are utilised to examine the cytokine secretion profiles, and RNA sequencing is conducted to capture a broad spectrum of transcriptional changes induced by PPAR β modulation. Furthermore, the SUMOylation of PPAR β is explored, continuing previous investigations in the FRAME laboratory, in order to assess how this post-translational modification is regulated in the presence and absence of GW0742. These objectives are designed to provide an integrated view of PPAR β 's capacity to mitigate inflammation in microglia and offer insights into the potential molecular mechanism involved. This approach enables this study to better understand PPAR β signalling pathways and their therapeutic implications in modulating microglial activity.

5.3 Results: Investigating The Role of PPAR β in Animal-Based Neuroinflammatory Models

5.3.1 Impact of LPS And ATP on PPAR β Expression in Adult and Neonatal Rat Microglia

Initially, the effect of LPS and ATP treatment upon PPAR β expression was quantified in neonatal and adult rat microglia. Upon stimulation with ATP, neonatal microglial cells exhibited a 3-fold increase in PPAR β expression, compared to a 2-fold increase when stimulated with LPS. In contrast, adult microglial cells demonstrated an equal 3-fold increase in PPAR β expression following ATP stimulation, however, a more pronounced 3.5-fold increase was observed with LPS stimulation (Figure 5. 1)). This differential expression pattern suggests that adult microglia may be more sensitive to pro-inflammatory stimuli such as LPS, potentially due to the mature immune system's more robust response mechanisms. However, the similar increases observed with ATP in both neonatal and adult microglia indicate a similar response to DAMP signals across different developmental stages.

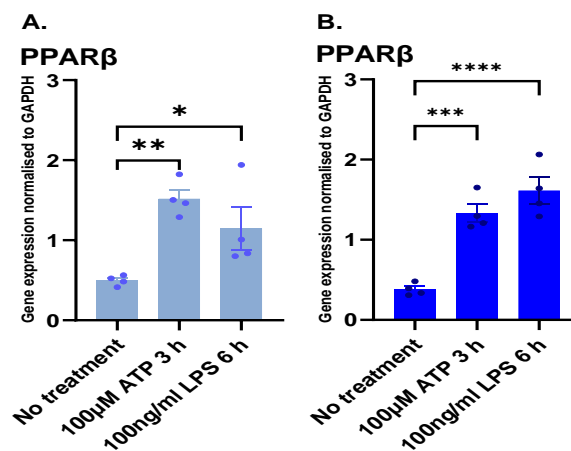


Figure 5. 1: Impact of ATP and LPS on PPAR β Expression in Neonatal vs Adult Cortical Microglia: The effects of ATP (100 μ M for 3 hours) and LPS (100 ng/mL for 6 hours) on PPAR β gene expression in **A.** neonatal and **B.** adult cortical microglia. Gene expression was quantified using TaqMan qPCR (normalised to GAPDH). Data represent mean \pm SEM from one representative experiment (n=4 wells). Results are representative of three independent experiments. Analysis via one-way ANOVA and Bonferroni's test revealed significant changes (*p < 0.05, **p < 0.001, ***p < 0.0005, ****p < 0.0001).

5.3.2 Investigation of PPAR β Activation in Adult and Neonatal Rat Microglia and its Effect on Inflammatory Cytokine Gene Expression.

5.3.2.1 Determining the Modulatory Effects of the PPAR β Ligand GW0742 on Inflammatory Responses in Cortical Microglia

The concentration-dependence of PPAR β agonist pre-treatment was investigated in relation to microglial responses to LPS in both neonatal and adult microglia. Pre-treatment with the PPAR β agonist GW0742 significantly modulated cytokine levels differently in neonatal versus adult microglia. The expression of the data as a percentage of the LPS+DMSO effect facilitates a clear comparison of the impact of PPAR β agonist on the inflammatory response.

In neonatal microglia, administration of GW0742 one hour before LPS stimulation resulted in a pronounced decrease in IL-1 β levels. Specifically, reductions of 50% at 10 nM, 60% at 50 nM, and 75% at 100 nM GW0742 were observed. Concurrently, IL-10 levels in neonatal microglia decreased by 51% at 10 nM, escalated to a 67% decrease at 50nM, and settled to a 63% decrease at 100 nM of GW0742 (Figure 5. 2/A).

On the other hand, adult microglia exhibited a more moderate response to PPAR β agonist pre-treatment in terms of IL-1 β reduction, showing no significant change with 10 nM, a 72% decrease with 50nM, and a 45% decrease with 100nM GW0742. Notably, IL-10 levels in adult microglia increased significantly, with a 150-fold rise observed at 50 nM and a 280-fold increase at 100 nM GW0742 (Figure 5. 2/B).

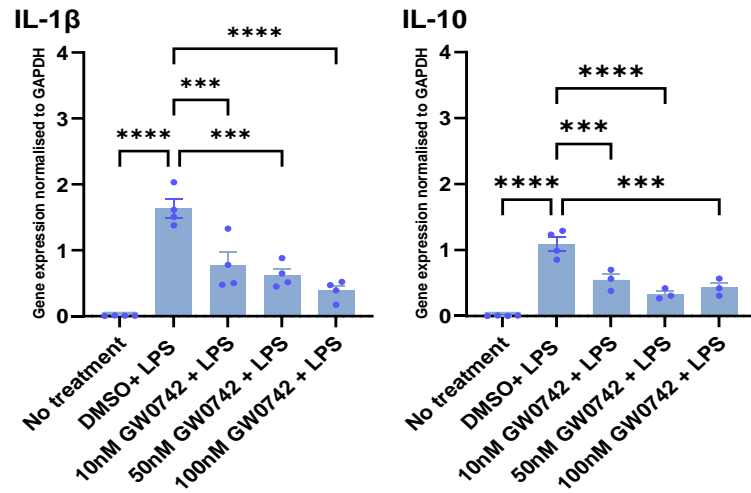
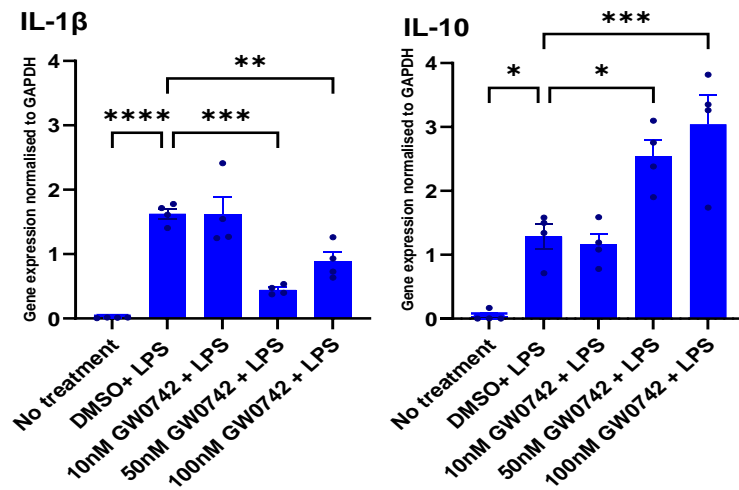
A**B**

Figure 5. 2: Impact of GW0742 on IL-1 β and IL-10 in Neonatal and Adult Microglia: Neonatal and adult cortical microglia were pre-treated with 10, 50, and 100 nM GW0742 for 1 hour before stimulation with 100 ng/mL LPS for 6 hours. Gene expression was quantified using TaqMan qPCR and normalised to GAPDH. Data represent mean \pm SEM from one representative experiment (n=4 wells). Results are representative of three independent experiments. Analysis via one-way ANOVA and Bonferroni's test revealed significant changes (*p < 0.05, **p < 0.001, ***p < 0.0005, ****p < 0.0001).

5.3.2.2 Assessing the Age-Dependent Effects of 50nM GW0742 Pre-treatment on Inflammatory Markers in Neonatal and Adult Cortical Microglia

Subsequent experiments employing 50 nM GW0742 as a pre-treatment before LPS exposure revealed distinct neonatal versus adult cortical microglia outcomes. In neonatal microglia, the intervention led to a marked decrease in inflammatory and anti-inflammatory markers: IL-1 β levels decreased by 15%, iNOS levels by 50%, and IL-10 levels by 45% (Figure 5. 3/A). On the other hand, in adult microglia, the reduction in IL-1 β was observed at a lower magnitude of 24%. Notably, IL-10 levels in adult microglia did not significantly change when comparing LPS stimulation alone to those pre-treated with GW0742. However, a significant reduction in iNOS expression was observed, with a decrease of 64% in adult microglia (Figure 5. 3/B), demonstrating a significant age-related variance in the response to PPAR β agonist GW0742 pre-treatment.

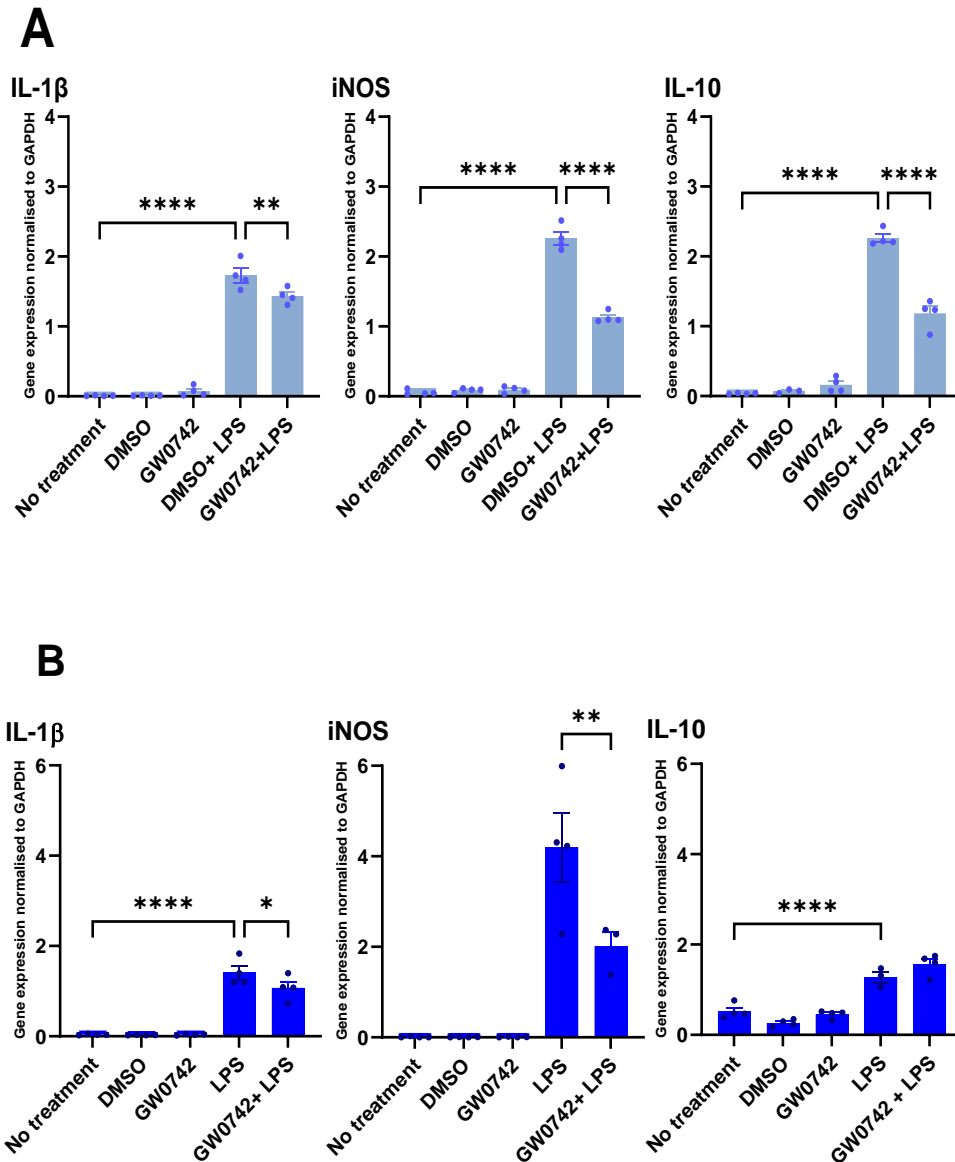


Figure 5. 3: Impact of 50 nM GW0742 Pre-treatment on IL-1 β , iNOS, and IL-10 Expression in Neonatal and Adult Cortical Microglia Following LPS Stimulation: The effects of GW0742 pre-incubation to neonatal and adult cortical microglia 1 hour before a 6-hour exposure to 100 ng/mL LPS on the expression levels of IL-1 β , iNOS, and IL-10. Gene expression was quantified using TaqMan qPCR and normalised to GAPDH. Data represent mean \pm SEM from one representative experiment (n=4 wells). Results are representative of three independent experiments. Analysis via one-way ANOVA and Bonferroni's test revealed significant changes (* $p < 0.05$, ** $p < 0.001$, *** $p < 0.0005$, **** $p < 0.0001$).

5.3.3 Investigating the Role of PPAR β in Adult Spinal Primary Rat Microglia

Adult spinal microglia exhibited a similar trend in the reduction of pro-inflammatory markers as seen in adult cortical microglia. Pre-treating adult spinal microglia with 50 nM GW0742 prior to LPS stimulation resulted in a significant decrease in pro-inflammatory mRNA levels, including a 45% decrease in IL-1 β and an 82% decrease in iNOS (Figure 5. 4). This comparison between spinal and cortical microglia highlights the consistent anti-inflammatory effect of GW0742 across different regions, although the magnitude of response varies, suggesting regional differences in microglial reactivity to treatment.

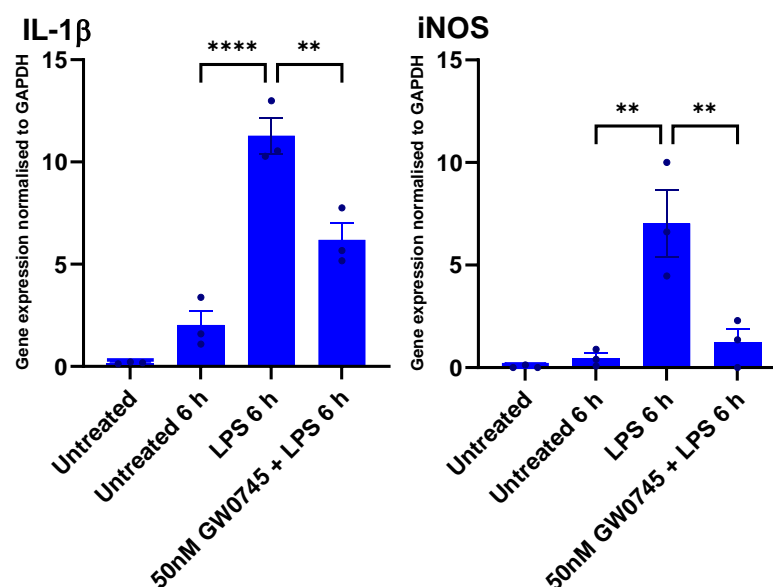


Figure 5. 4: Impact of 50 nM GW0742 Pre-treatment on IL-1 β and iNOS Expression in Adult Spinal Microglia Following LPS Stimulation: The effects of pre-treating adult spinal microglia with 50 nM GW0742 1 hour prior to a 6-hour stimulation with 100 ng/mL LPS. Gene expression was quantified using TaqMan qPCR, normalised to GAPDH. Data represent mean \pm SEM from one representative experiment (n=4 wells). Results are representative of three independent experiments. Analysis via one-way ANOVA and Bonferroni's test revealed significant changes (*p < 0.05, **p < 0.001, ***p < 0.0005, ****p < 0.0001).

5.3.4 Investigating the Role of PPAR β using Microglial Conditioned Media (MCM) on Cortical Astrocyte Activation as a Model of Glial Cell Neuroinflammation

In an investigation into the neuroprotective potential of GW0742, microglial conditioned media (MCM), obtained from microglia stimulated either with LPS or pre-treated with 50 nM GW0742 prior to LPS exposure, were examined for their effects on cultured astrocytes. Despite employing a rapid astrocyte isolation technique as detailed in Chapter 2, even untreated astrocyte samples exhibited activation markers and elevated levels of IL-1 β , iNOS, and IL-10 (Figure 3.13).

Nevertheless, the impact of neonatal cortical and spinal microglial conditioned media (MCM) on astrocytes was further explored. The MCM was prepared from microglia under four different conditions: untreated, LPS-stimulated, GW0742-treated, and GW0742 pre-treated followed by LPS stimulation. Following treatment, microglia were allowed to incubate for 24 hours for cytokine release, after which the media were filtered through a 0.45 μ m filter and stored at -80°C. Both cortical and spinal astrocytes were then exposed to their respective MCM, diluted in a 1:2 ratio with astrocyte media for 24 hours, with control astrocytes not receiving any MCM.

Treatment of activated cortical astrocytes with MCM resulted in a reduction in the levels of pro-inflammatory markers IL-1 β , iNOS, and IL-10 (Figure 5. 5/A). Spinal astrocytes treated with MCM showed a reduction in IL-1 β levels, while IL-10 levels remained unchanged. Notably, there was a 6-fold increase in iNOS levels in spinal astrocytes treated with LPS-stimulated MCM compared to controls (Figure 5. 5/B). Overall, addition of MCM regardless of treatment with GW0742 or LPS induced a significant decrease in cytokine expression in cortical astrocytes. The pattern was mixed in spinal astrocytes, and it is difficult to draw clear conclusions from this dataset.

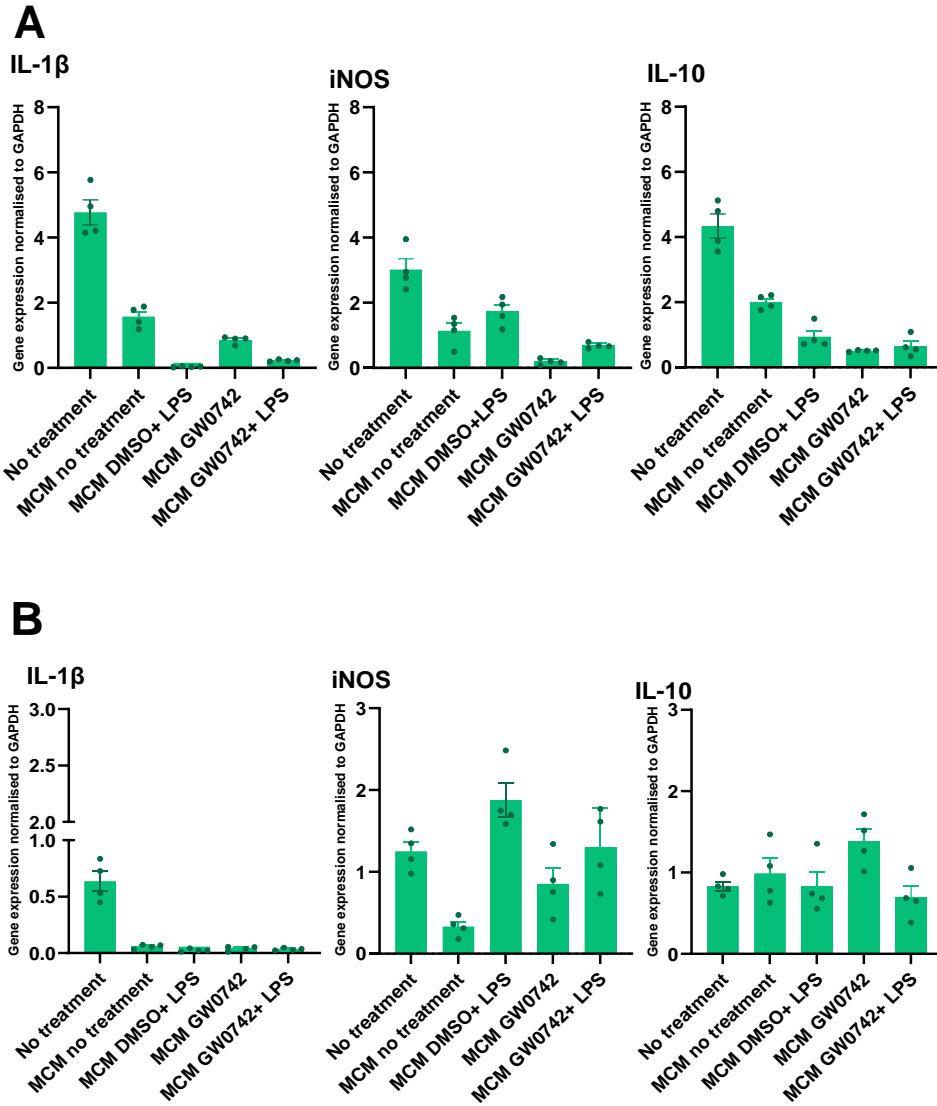


Figure 5. 5: Impact of Microglial Conditioned Media on Pro-inflammatory Marker Expression in Cortical and Spinal Astrocytes: Treatment of **A.** cortical or **B.** spinal astrocytes with their respective MCM for 24 hours. Gene expression was quantified using TaqMan qPCR, normalised to GAPDH. Data represent mean \pm SEM from one experiment (n=4 wells).

5.4 Investigating The role of PPAR β in a Human-Based Neuroinflammatory Model

5.4.1 Assessing Activation of PPAR β in Macrophages in Response to Low-Grade Inflammation Induced by DAMPs (ATP) and PAMPs (LPS)

Monocyte-derived macrophages (iMAC) were utilised as a parallel investigation to compare with monocyte-derived microglia. iMAC were pre-treated with GW0742 before being stimulated with LPS for 6 hours. This treatment significantly reduced inflammatory markers: IL-1 β levels decreased by 99%, TNF- α by 90%, and IL-6 by 96%. Additionally, the level of the anti-inflammatory marker IL-10 saw a 71% decrease (Figure 5. 6).

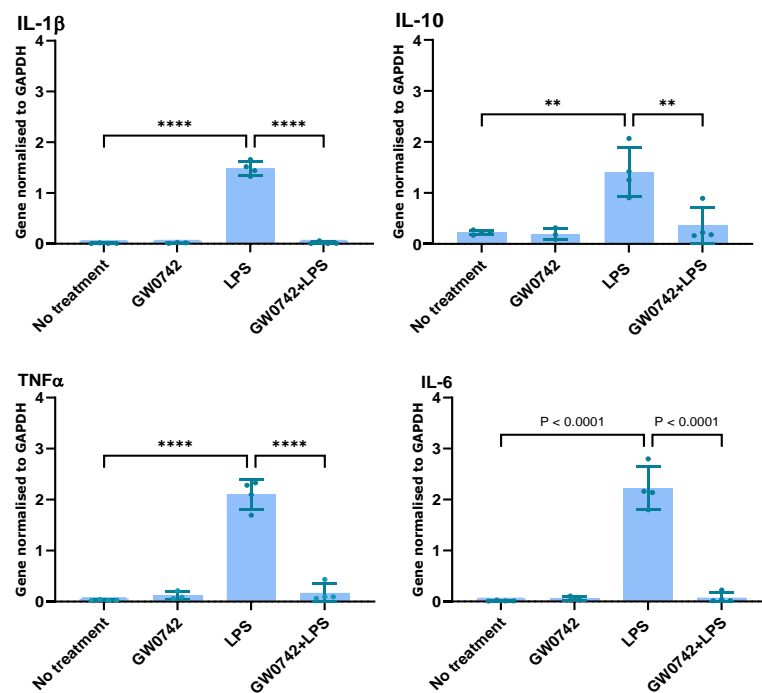


Figure 5. 6: GW0742 Pre-treatment Effects on Inflammatory and Anti-inflammatory Marker Levels in LPS-Stimulated Monocyte-Derived Macrophages: 50 nM GW0742 was pre-incubated with iMAC cells for 1 hour before a 6-hour exposure to 100 ng/mL LPS. Expression levels of IL-1 β , TNF α and IL-10 were quantified using TaqMan qPCR, normalised to GAPDH. Data represent mean \pm SEM from one representative experiment (n=4 wells). Results are representative of three independent experiments. Analysis via one-way ANOVA and Bonferroni's test revealed significant changes (*p < 0.05, **p < 0.001, ***p < 0.0005, ****p < 0.0001).

In this investigation, ATP was utilised as a Damage-Associated Molecular Pattern (DAMP) to stimulate macrophages at concentrations of 10, 50, and 100 μM for 2 hours. This approach led to a notable increase in IL-1 β expression, with the levels rising by 20-fold and 37-fold at 50 μM and 100 μM ATP concentrations, respectively. Pre-treatment with GW0742 prior to ATP stimulation significantly reduced IL-1 β levels, with a 67% decrease observed at 50 μM ATP and a 58% decrease at 100 μM ATP. Additionally, IL-10 levels significantly increased when macrophages were pre-treated with GW0742, showing increases of 2.4-fold, 2.2-fold, and 4-fold noted across varying ATP concentrations (Figure 5. 7).

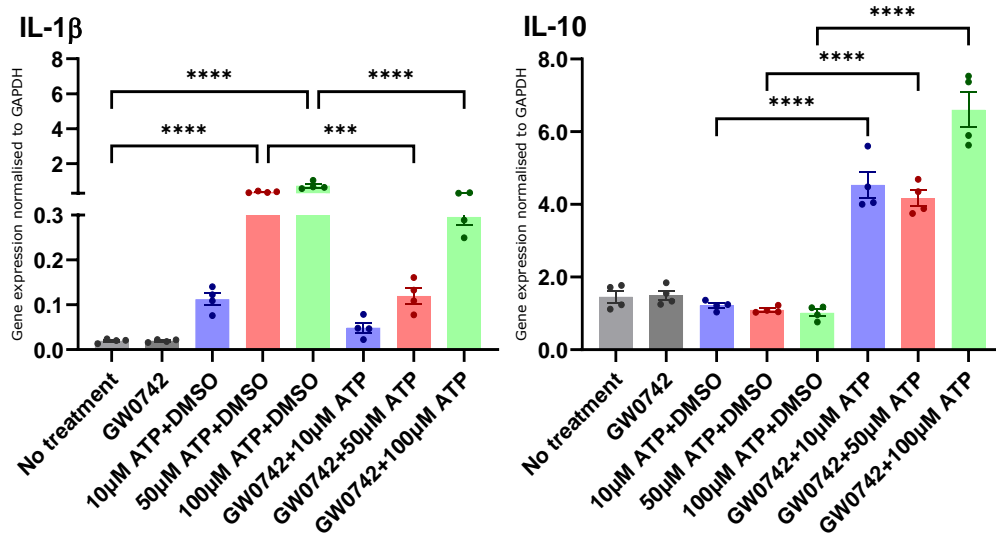


Figure 5. 7: Modulating Effects of GW0742 Pre-treatment on IL-1 β and IL-10 Levels in ATP-Stimulated Macrophages: 50nM GW0742 pre-treatment of iMAC cells 1 hour before a 2-hour exposure to 10-100 μM ATP. The expression levels of IL-1 β and IL-10 were quantified using TaqMan qPCR, and normalised to GAPDH. Data represent mean \pm SEM from one representative experiment (n=4 wells). Results are representative of three independent experiments. Analysis via one-way ANOVA and Bonferroni's test revealed significant changes (*p < 0.05, **p < 0.001, ***p < 0.0005, ****p < 0.0001).

5.4.2 Investigating the effect of inflammatory stimuli upon PPAR β expression in Monocyte-Derived Microglia

As illustrated in Figure 5. 8, stimulation with ATP, and LPS, evoked increases in PPAR β expression in monocyte-derived microglial cells.

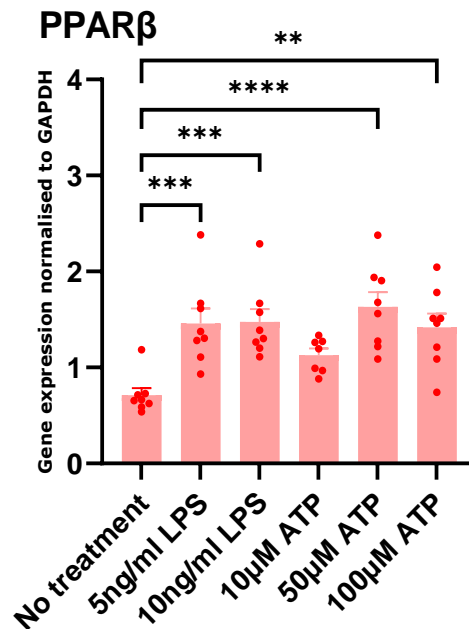


Figure 5. 8: The effects of ATP (10-100 μ M, 2 hours) and LPS (5 and 10 ng/mL, 2 hours) on PPAR β Gene Expression in Monocyte-Derived Microglia (iMG): Gene expression was quantified using TaqMan qPCR, normalised to GAPDH. Data represent mean \pm SEM from one representative experiment (n=4 wells). Results are representative of three independent experiments. Analysis via one-way ANOVA and Bonferroni's test revealed significant changes (*p < 0.05, **p < 0.001, ***p < 0.0005, ****p < 0.0001).

5.4.3 Examination of the Effects of GW0742 on mRNA Levels of PDK4 and ANGPTL4

To further investigate the mechanisms underlying the anti-inflammatory effects of PPAR β agonist, the impact of PPAR β ligand on the mRNA levels of pyruvate dehydrogenase kinase 4 (PDK4) and angiopoietin-like 4 (ANGPTL4) was examined, two genes known to be directly regulated by PPAR β (Adhikary et al., 2015, Staiger et al., 2009). PDK4 is involved in regulating glucose metabolism by inhibiting the pyruvate dehydrogenase complex, while ANGPTL4 plays a role in lipid metabolism and has been implicated in the regulation of inflammation (Zhang et al., 2014, Koliwad et al., 2009).

By assessing the expression of these PPAR β target genes in response to ligand treatment, The aimed to determine whether the anti-inflammatory effects of PPAR β agonists were mediated through the direct transcriptional regulation of PPAR β . This approach would help distinguish between the potential mechanisms of action, such as the direct regulation of gene expression through PPAR β activation, and other processes like SUMOylation or the direct inhibition of inflammatory gene promoters. Increased expression of PDK4 and ANGPTL4 over a short period of ligand treatment would suggest that the anti-inflammatory effects are, at least in part, mediated through the direct transcriptional regulation of PPAR β target genes.

Microglia (iMG) treated with GW0742 exhibited an up-regulation of genes associated with PPAR β activity, specifically (PDK4) and (ANGPTL4) (Adhikary et al., 2015), increasing 10-fold and 8-fold, respectively. These effects were apparent after just one hour of GW0742 treatment, demonstrating a rapid gene induction phenomenon (Figure 5. 9).

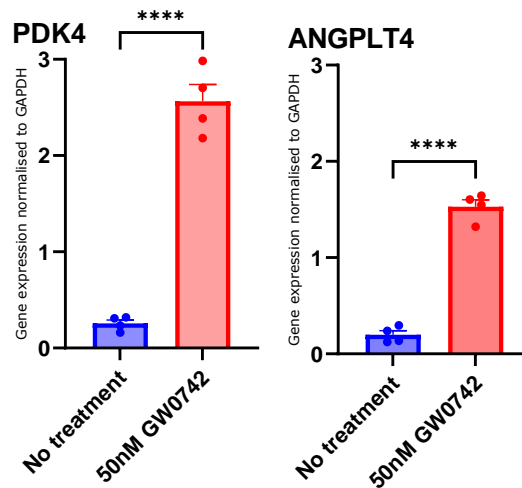


Figure 5. 9: Rapid Upregulation of PDK4 and ANGPTL4 in iMG Cells Following GW0742 Treatment: iMG cells were treated with 50 nM GW0742 for 1 hour then cells were harvested using Tri reagent, PDK4 and ANGPTL4 gene expression was quantified using TaqMan qPCR, normalised to GAPDH. Data represent mean \pm SEM from one representative experiment (n=4 wells). Results are representative of three independent experiments. Analysis via one-way ANOVA and Bonferroni's test revealed significant changes (* $p < 0.05$, ** $p < 0.001$, *** $p < 0.0005$, **** $p < 0.0001$).

5.4.4 Evaluation of the Impact of GW0742 on mRNA Levels of Inflammatory Cytokines in ATP-Stimulated Monocyte-Derived Microglia (iMG)

A 50 μ M ATP and GW0742 pre-treatment generated a uniform and significant reduction across all examined inflammatory markers (Figure 5. 10). Specifically, IL-1 β levels decreased by 80%, illustrating a pronounced anti-inflammatory effect. TNF α levels also showed a significant decrease, with a 43% reduction observed under these conditions. Similarly, IL-6 levels were substantially lowered by 68%, reinforcing the anti-inflammatory impact of GW0742 pre-treatment. In addition to these reductions, IL-10 levels, an anti-inflammatory marker, increased by 1.5-fold, further indicating a shift towards anti-inflammatory responses in microglia treated with GW0742 before 50 μ M ATP stimulation. This reduction in pro-inflammatory markers, coupled with the increase in IL-10, highlights the anti-inflammatory potential of GW0742 pre-treatment in microglial cells challenged with 50 μ M ATP.

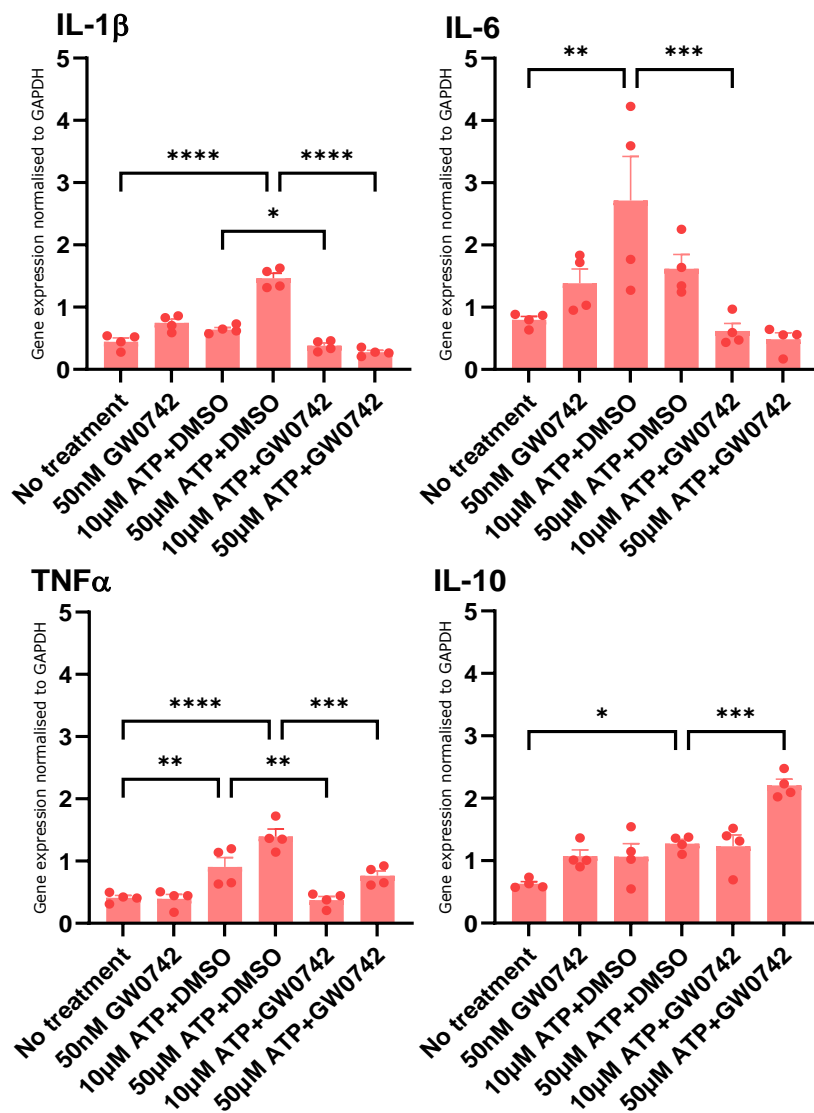


Figure 5. 10: Modulating Effects of 50 nM GW0742 Pre-treatment on Inflammatory Markers Levels in ATP-Stimulated iMG: 50 nM GW0742 was pre-incubated with iMG 1 hour before a 2-hour exposure to 10-100 μ M ATP. Expression levels of IL-1 β , TNF α , IL6 and IL-10 were quantified using TaqMan qPCR, normalised to GAPDH. Data represent mean \pm SEM from one representative experiment (n=4 wells). Results are representative of three independent experiments. Analysis via one-way ANOVA and Bonferroni's test revealed significant changes (*p < 0.05, **p < 0.001, ***p < 0.0005, ****p < 0.0001).

5.4.5 Assessment of the Impact of GW0742 on mRNA Levels of Inflammatory Cytokines in LPS-Stimulated Monocyte-Derived Microglia (iMG)

As shown in Figure 5. 11, iMG cells were pre-treated with 50nM GW0742 for 1 hour before being stimulated with 5ng/ml LPS. This pre-treatment led to a notable decrease in inflammatory markers: IL-1 β levels were reduced by 74%, IL-6 saw a dramatic 99% decrease, and TNF-alpha levels dropped by 88%. Additionally, the level of the anti-inflammatory cytokine IL-10 also decreased, albeit more modestly by 42%.

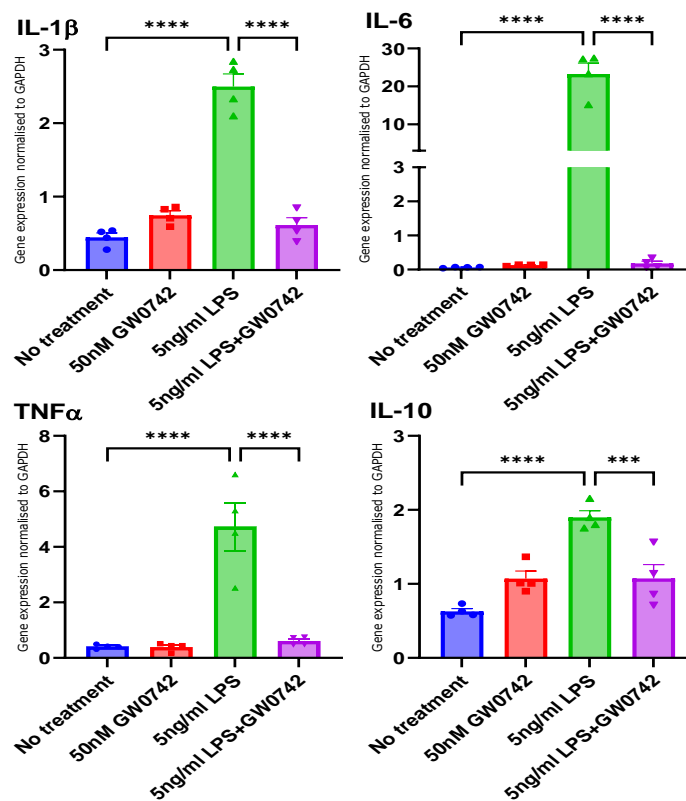


Figure 5. 11: GW0742 Pre-treatment Effects on Inflammatory and Anti-inflammatory Marker Levels in LPS-Stimulated Monocyte-Derived Microglia: 50 nM GW0742 was preincubated with iMG 1 hour before a 2-hour exposure to 100 ng/mL LPS. Expression levels of IL-1 β , TNF α and IL-10 were quantified using TaqMan qPCR, normalised to GAPDH. Data represent mean \pm SEM from one representative experiment (n=4 wells). Results are representative of three independent experiments. Analysis via one-way ANOVA and Bonferroni's test revealed significant changes (*p < 0.05, **p < 0.001, ***p < 0.0005, ****p < 0.0001).

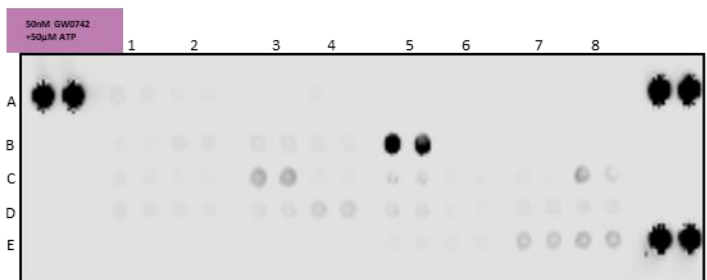
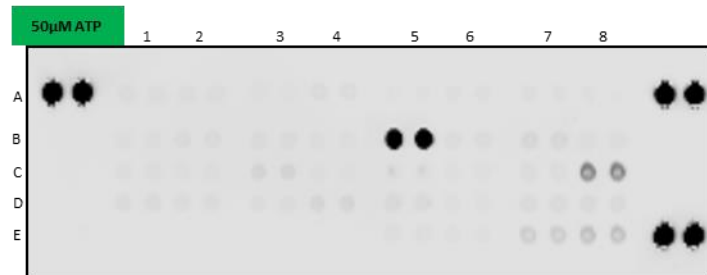
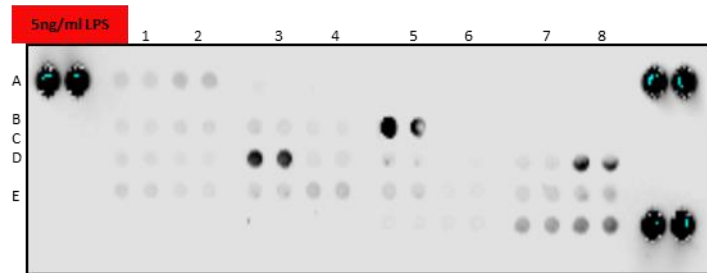
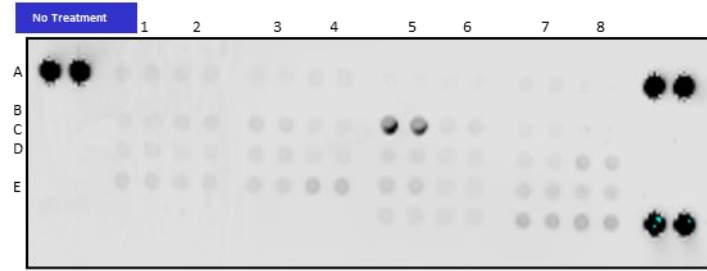
5.4.6 Cytokine Profiling of Monocyte-Derived Microglia: Effects of DAMP and PAMP Stimulation and Effects of PPAR β Agonist (GW0742)

This study utilised a 36-cytokine array to analyse the responses of monocyte-derived microglia under four different conditions: untreated, stimulated with 50 μ M ATP (to investigate the DAMP effect), stimulated with 5 ng/ml LPS (to investigate the PAMP effect), and cells pre-treated with 50 nM GW0742 prior to ATP stimulation (to confirm the ability of PPAR β activation to mitigate inflammatory responses). Each treatment was maintained for 2 hours, after which the media were replaced with fresh media containing fresh IL-34 and GM-CSF cytokines. The cells were then allowed to incubate for an additional 24 hours to facilitate cytokine release. Following this incubation period, cell supernatants were collected, centrifuged, and stored at -80°C for subsequent analysis.

Protein concentrations in the supernatant were quantified using the Proteome Profiler Human Cytokine Array Kit from R&D Systems, and membrane visualisation was performed with a Li-Cor Odyssey imaging system, ensuring consistent exposure times across all experiments. Interestingly, the untreated samples exhibited elevated levels of various cytokines and chemokines, including IL-1 β , TNF α , IL-1 α , IFN γ , IL-12, and IL-5, indicating pre-existing activation. This activation was likely induced by the refreshed media containing IL-34 and GM-CSF, suggesting that future experiments should exclude induction media to minimise unintended cell activation.

Despite these initial findings, the analysis provided valuable insights into the cytokine and chemokine production capabilities of monocyte-derived microglia, revealing secretion profiles of various inflammatory and regulatory molecules such as CXCL10, CCL5, CXCL1, and IL-17, as depicted in Figure 5. 12. This observation highlights the complexity of microglial responses to different stimuli and highlights the necessity for careful experimental design to accurately assess the impact of treatments on cytokine production.

A



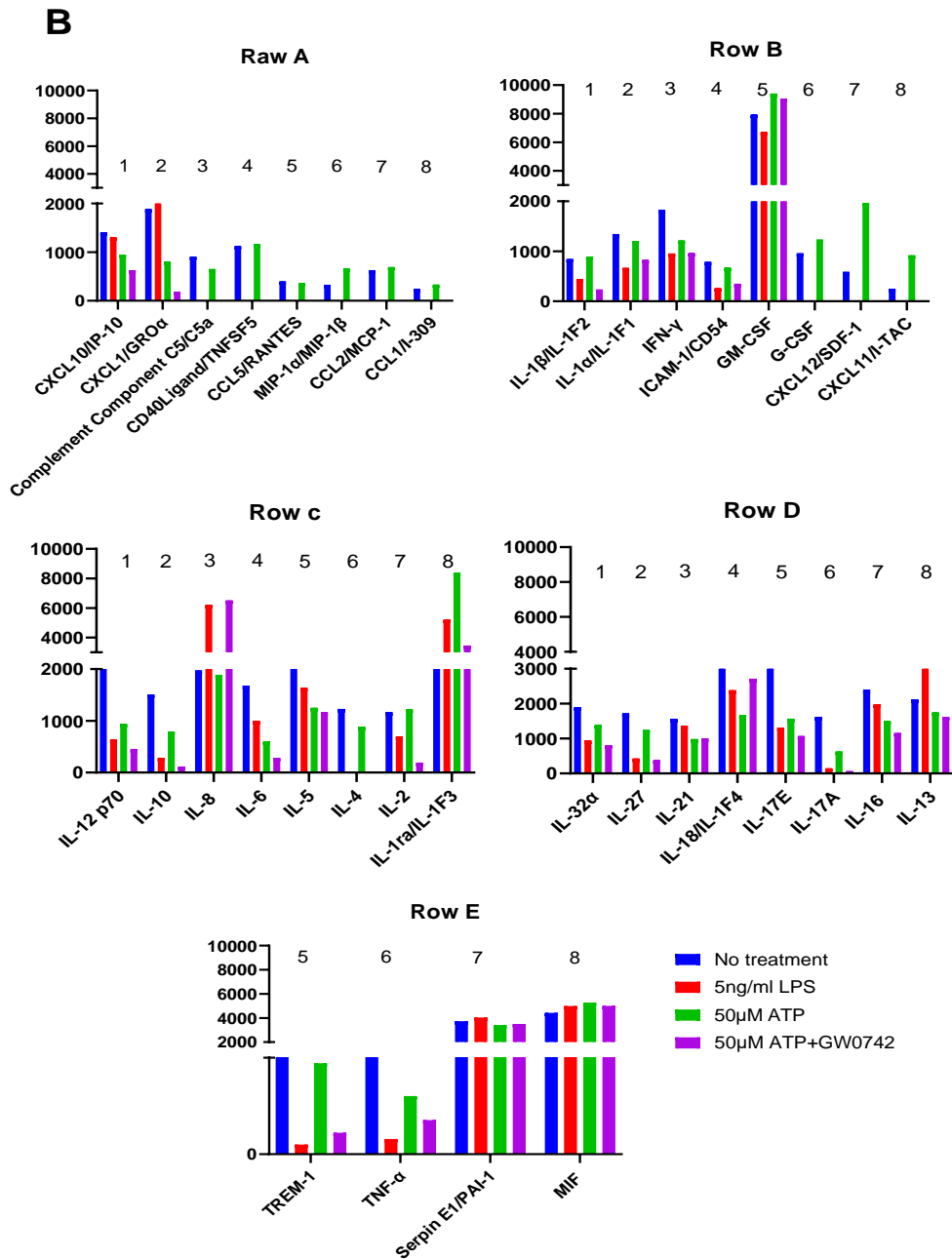


Figure 5. 12: Cytokine Expression in iMG Under Various Stimuli, A: The membrane panel displays direct visualisation of cytokine arrays from iMG subjected to four different treatment conditions: untreated, 50 µM ATP stimulation, 5 ng/ml LPS stimulation, and pre-treatment with 50 nM GW0742 followed by 50 µM ATP stimulation. Each membrane was processed to detect a wide array of cytokines and chemokines **B.** Quantitative analysis of the signal strength of each detected protein, providing a comparative analysis of cytokine levels across treatment groups. Measurements were conducted in duplicate, and the total pixel intensity for each cytokine was quantified using FIJI software.

5.4.7 Transcriptomic Profiling of microglia activated with ATP and effects of treatment with PPAR β Agonist (GW0742)

To investigate the transcriptional changes in monocyte derived microglia (iMG) upon ATP stimulation and the potential modulatory effects of the PPAR β agonist GW0742, RNA sequencing was performed on four experimental groups: (1) untreated iMG cells, (2) iMG cells pre-treated with GW0742 alone, (3) iMG cells stimulated with ATP alone, and (4) iMG cells pre-treated with GW0742 followed by ATP stimulation. The aim of this study was to identify differentially expressed genes and pathways associated with microglial activation and to assess the impact of PPAR β activation on the ATP-induced transcriptional response.

Principal Component Analysis (PCA) was performed on the RNA sequencing data to visualize the overall transcriptomic differences among the four experimental groups. The PCA plot illustrates the segregation of samples into four discrete clusters according to their gene expression signatures. The horizontal axis, labelled as Principal Component 1 (PC1), accounts for most of the dataset's variability, quantified at 59%. The vertical axis, Principal Component 2 (PC2), captures a further 20% of the variability, offering an additional dimension of differentiation among the samples (Figure 5.13).

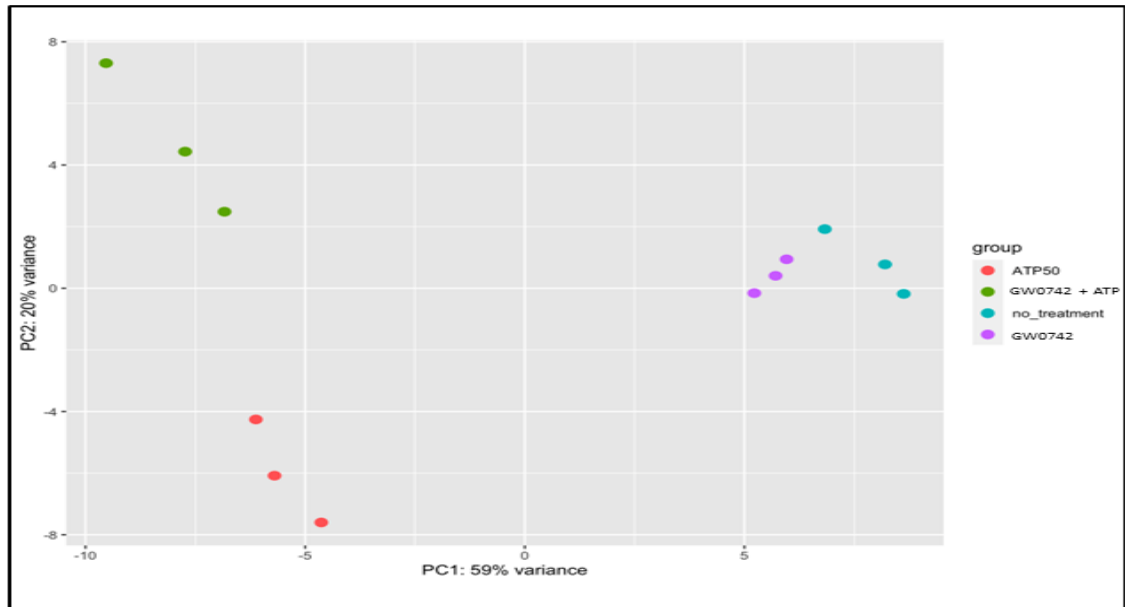


Figure 5. 13: PCA Plot Showing Extent of Clustering of Treatments Along the First Two Principal Components: iMG cells were subjected to four different conditions: untreated, exposed to 50 nM GW0742 for 1 hour, activated with 50 μ M ATP for 2 hours, or treated with 50 nM GW0742 for 1 hour prior to 2 hours induction with 50 μ M ATP.

5.4.8 Identification of Genes Significantly Modulated by GW0742 and ATP Treatment in iMG Cells.

As shown in Figure 5. 14, the volcano plots display differential gene expression across four treatment groups: untreated, GW0742 treatment, ATP stimulation, and GW0742 pre-treatment followed by ATP stimulation. These plots highlight genes with statistically significant changes in expression, illustrating both the p-value and the magnitude of change (fold change). For GW0742 versus untreated conditions, there are relatively few significantly altered genes. In contrast, ATP stimulation alone shows pronounced changes with many genes significantly upregulated or downregulated. Furthermore, the GW0742+ATP versus ATP plot reveals additional alterations in gene expression attributable to GW0742 pre-treatment, distinct from ATP stimulation alone. These findings suggest that GW0742 modulates gene expression and alters the cellular response to ATP stimulation, indicating specific regulatory pathways impacted by these treatments.

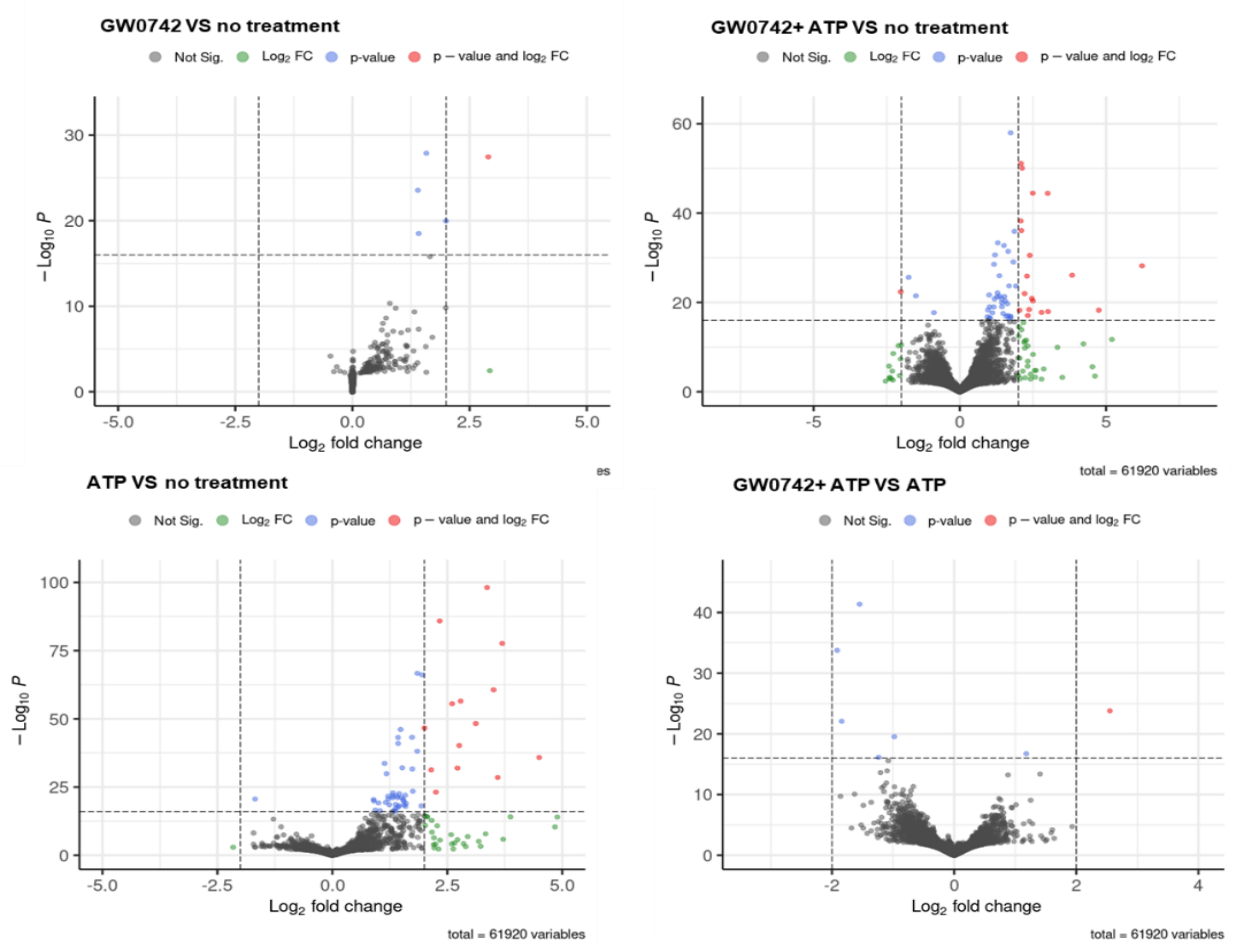


Figure 5. 14: Volcano Plot Analysis of iMG Cell Response to Treatments: The volcano plots compare gene expression profiles of iMG cells across four conditions: untreated (control), 50 nM GW0742 pre-treatment, 50 μ M ATP 2 hours stimulation, and combined 50 nM GW0742 pre-treatment for 1 hour before 50 μ M ATP stimulation for 2 hours. Each plot illustrates the magnitude of gene expression changes (\log_2 fold change) against the statistical significance ($-\log_{10}$ p-value). Significant upregulated and downregulated genes are highlighted, demonstrating the distinct transcriptional impact of each treatment condition on iMG cells.

A. ATP vs Untreated (Control)

Upon ATP stimulation, a distinct gene expression profile was observed, with notable increases in specific genes compared to untreated controls. Table 5. 1 shows the top 20 upregulated genes. The early growth response genes EGR3 and EGR4 exhibited the most significant upregulation, showing log₂ fold changes (LFC) of 7.16 and 6.36, respectively. These genes are critical in cellular stress responses and play a pivotal role in the regulation of inflammatory processes (Wieland et al., 2005, Liu et al., 2008). Additionally, the nuclear receptors NR4A1 (Nur77) and NR4A2 (Nurr1) also demonstrated notable increases in expression. These receptors are implicated in diverse cellular processes, including metabolism, inflammation, and immune responses, and are known to exert anti-inflammatory effects. They are rapidly induced as immediate early genes in response to various stimuli and can act as transcriptional regulators to modulate the expression of target genes involved in the inflammatory response, primarily to limit the level of increase in inflammatory gene expression (Pei et al., 2005, McEvoy et al., 2002, Mahajan et al., 2015, Saijo et al., 2009).

Other genes associated with stress and inflammation were also upregulated. For example, the chemokines CCL3L1, CCL4L2, and CCL4 are involved in immune responses by attracting immune cells to sites of inflammation. MMP19, a matrix metalloproteinase that degrades extracellular matrix components, was also upregulated. The increased expression of MMP19 might suggest remodelling or alteration of the extracellular environment in the brain, which can occur during inflammation or in response to injury, indicating an activated cellular state (Kataoka et al., 2009, Bonecchi et al., 2009, Van Horssen et al., 2006, Maurer and Von Stebut, 2004, Mantovani et al., 2004).

The signaling pathways that were activated in microglial cells upon stimulation with ATP, as determined by the analysis of significantly upregulated genes using the DAVID bioinformatics resource. The pathways are sourced from the Kyoto

Encyclopedia of Genes and Genomes (KEGG) database. The most significant activation was observed in the NF-kappa B signaling pathway, suggesting a prominent inflammatory response (Hayden and Ghosh, 2008). See appendices (Figure 2). Additionally, the MAPK and TNF signaling pathways were notably upregulated, emphasising their roles in microglial activation and inflammation (Arthur and Ley, 2013, Parameswaran and Patial, 2010). These data suggest that ATP acts as a potent stimulator of microglial activation, influencing a variety of signalling pathways relevant to immune responses and inflammation within the CNS.

Table 5. 1 : ATP Stimulated iMG vs Untreated (Control) iMG: Top 20 UP-Regulated Genes: (significantly changed only, sorted by LFC).

Gene ID	Gene Name	log2FoldChange	padj
ENSG00000179388	EGR3	7.160476	6.45E-35
ENSG00000135625	EGR4	6.36939	1.09E-08
ENSG00000123358	NR4A1	5.647512	1.02E-23
ENSG00000198576	ARC	5.117027	1.52E-20
ENSG00000125740	FOSB	4.896078	7.73E-13
ENSG00000164949	GEM	4.844042	2.91E-09
ENSG00000120738	EGR1	4.496664	6.45E-35
ENSG00000153234	NR4A2	3.877219	5.36E-13
ENSG00000244242	IFITM10	3.731175	4.34E-05
ENSG00000276085	CCL3L1	3.695495	3.99E-75
ENSG00000276070	CCL4L2	3.596406	1.46E-26
ENSG00000113070	HBEGF	3.509037	3.79E-59
ENSG00000275302	CCL4	3.363331	7.94E-94
ENSG00000143333	RGS16	3.335672	3.62E-07
ENSG00000228013	IL6R-AS1	3.270309	8.78E-03
ENSG00000177374	HIC1	3.195226	2.14E-04
ENSG00000155090	KLF10	3.118846	2.47E-46
ENSG00000115641	FHL2	2.952522	3.80E-06
ENSG00000287553	ENSG00000287553	2.902872	1.04E-03
ENSG00000123342	MMP19	2.790616	1.65E-53

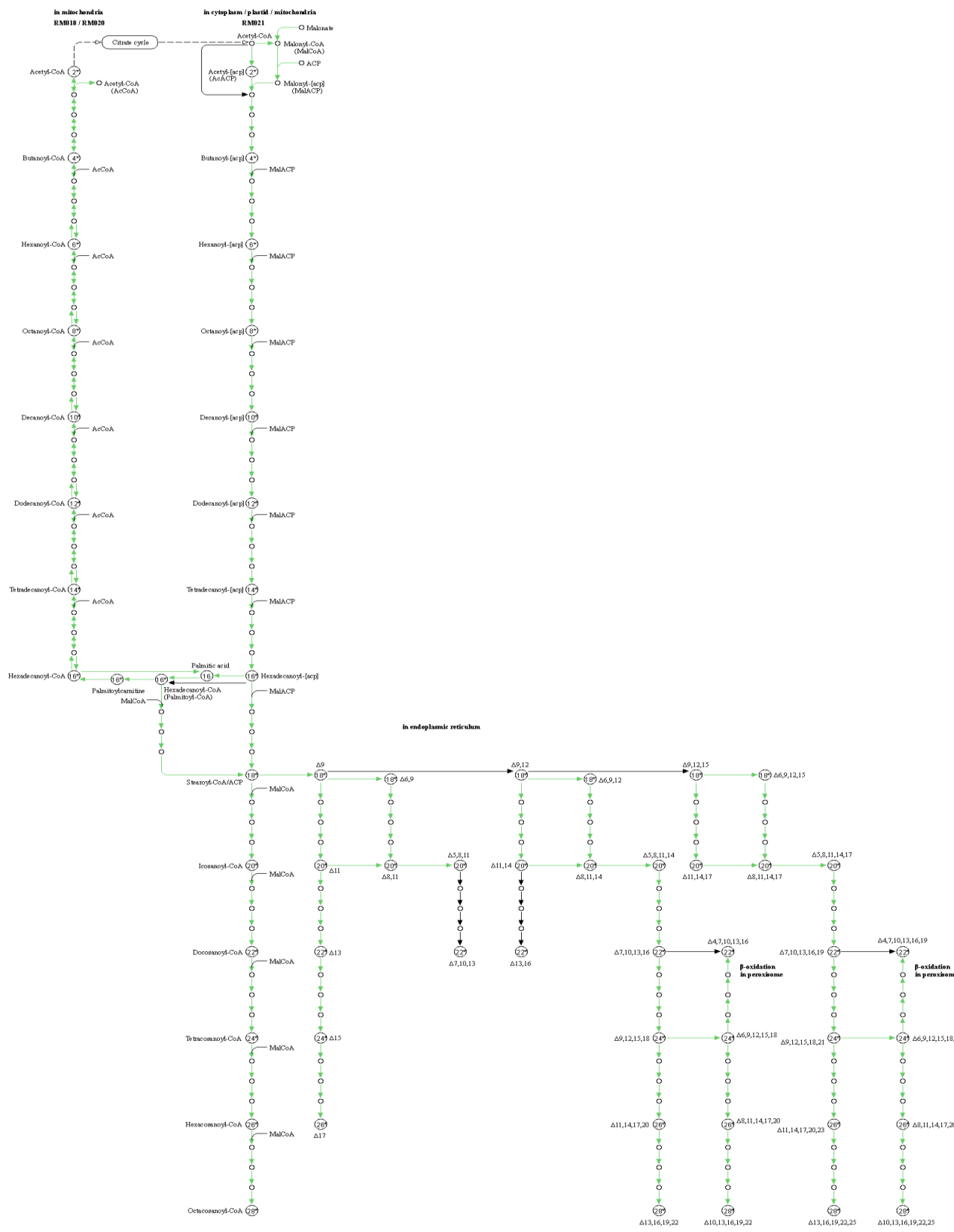
B. GW0742+ ATP vs ATP UP-regulated Gene Analysis

Table 5. 2 displays a list of genes that were significantly upregulated in microglial cells pre-treated with 50 nM GW0742 before a 2-hour stimulation with 50 μ M ATP, compared to cells stimulated with ATP alone. Notable genes such as CXCL10, RB1CC1, CCL22, MERTK, IL17RB, and PDK4, which are associated with inflammation resolution and metabolic enhancement, were upregulated. PDK4, a target gene for the PPAR β agonist, plays a crucial role in regulating glucose and lipid metabolism by inhibiting the pyruvate dehydrogenase complex (PDC) (Sugden and Holness, 2006). The upregulation of PDK4 in GW0742-treated microglia is particularly interesting as it confirms the activation of the PPAR β pathway (Adhikary et al., 2015) and suggests a shift towards fatty acid oxidation, which may help meet the increased energy demands of activated microglia while conserving glucose for other CNS cells (Ghosh et al., 2018). Moreover, the metabolic reprogramming induced by PDK4 may contribute to the resolution of inflammation by modulating the production of inflammatory mediators and the phenotype of microglia cells (Diskin and Pålsson-McDermott, 2018). CXCL10 (C-X-C motif chemokine ligand 10) is known for its role in mediating immune responses by recruiting leukocytes to sites of inflammation (Sørensen et al., 2002, Cui et al., 2023). RB1CC1 (RB1-inducible coiled-coil 1) has been implicated in autophagy, which is a crucial process for clearing damaged organelles and proteins, and may contribute to cellular homeostasis and neuroprotection (Jülg et al., 2021). CCL22, known for its chemotactic ability to attract regulatory T cells, showed a significant increase in expression, which may contribute to the resolution of inflammation and neuroprotection in the CNS (Michels et al., 2020, Mantovani et al., 2004). MERTK, a receptor tyrosine kinase, is important for the phagocytosis of apoptotic cells and debris by microglia, a process vital for mitigating neuroinflammation and promoting tissue repair (Du et al., 2021). IL17RB (Interleukin 17 receptor B) is a cytokine receptor which, when activated, can initiate signalling pathways leading to anti-inflammatory response (Rickel et al., 2008).

As determined by the analysis of significantly upregulated genes using the DAVID bioinformatics resource. The GW0742 treatment on ATP-stimulated microglial cells significantly influenced several metabolic and signalling pathways. The PPAR signalling pathway, known for regulating genes involved in energy homeostasis, was prominently activated. This is in line with the role of PPAR β agonists in modulating lipid metabolism and inflammatory responses. Furthermore, as shown in pathways related to fatty acid metabolism and biosynthesis, such as pantothenate and CoA biosynthesis, fatty acid degradation, and the biosynthesis of unsaturated fatty acids, were activated. These pathways are integral to cellular energy production and

regulatory processes. See appendices (

FATTY ACID METABOLISM



01212.5/019
© Kozhikash Laboratories

Current Gene List: List_2
 Current Background: Homo sapiens
 522 DAVID IDs
 12 record(s)

 [Download File](#)

ENSEMBL_GENE_ID	GENE NAME	Related Genes	Species
ENSG00000188921	3-hydroxyacyl-CoA dehydratase 4(HACD4)	RG	Homo sapiens
ENSG0000012660	ELOVL fatty acid elongase 5(ELOVL5)	RG	Homo sapiens
ENSG00000120437	acetyl-CoA acetyltransferase 2(ACAT2)	RG	Homo sapiens
ENSG00000167315	acetyl-CoA acyltransferase 2(ACAA2)	RG	Homo sapiens
ENSG00000151726	acyl-CoA synthetase long chain family member 1(ACSL1)	RG	Homo sapiens
ENSG00000110090	carnitine palmitoyltransferase 1A(CPT1A)	RG	Homo sapiens
ENSG00000138029	hydroxyacyl-CoA dehydrogenase trifunctional multienzyme complex subunit beta(HADHB)	RG	Homo sapiens
ENSG00000138796	hydroxyacyl-CoA dehydrogenase(HADH)	RG	Homo sapiens
ENSG00000149084	hydroxysteroid 17-beta dehydrogenase 12(HSD17B12)	RG	Homo sapiens
ENSG00000133835	hydroxysteroid 17-beta dehydrogenase 4(HSD17B4)	RG	Homo sapiens
ENSG00000099194	stearoyl-CoA desaturase(SCD)	RG	Homo sapiens
ENSG00000116171	sterol carrier protein 2(SCP2)	RG	Homo sapiens

Figure 3).

Additionally, oxidative phosphorylation, a crucial component of cellular respiration and ATP production, showed significant activation, which suggests an increased metabolic demand or enhanced energy efficiency in the treated microglial cells. The activation of cholesterol metabolism and broader metabolic pathways further reflects the extensive influence of GW0742 on cellular metabolism in microglia. The upregulation of specific gene expression and the subsequent activation of related pathways following treatment with GW0742 suggests the multifaceted role of PPAR β activation in microglia, encompassing the regulation of both inflammatory states and metabolic functions.

Table 5. 2 : GW0742+ATP vs ATP: Top 20 UP-regulated genes (significantly changed only, sorted by LFC).

Gene ID	Gene Name	log2FoldChange	padj
ENSG00000004799	PKD4	2.5533276	8.22E-22
ENSG000000085265	FCN1	1.6290631	1.99E-03
ENSG00000168488	ATXN2L	1.516262	2.44E-02
ENSG00000117594	HSD11B1	1.406884	1.87E-11
ENSG00000163453	IGFBP7	1.2902813	1.53E-04
ENSG00000169245	CXCL10	1.2764234	2.57E-02
ENSG00000064726	BTBD1	1.255628	1.48E-07
ENSG00000156508	EEF1A1	1.241427	7.57E-05
ENSG00000087460	GNAS	1.1806388	6.09E-14
ENSG00000056736	IL17RB	1.0584699	4.85E-03
ENSG00000210164	MT-TG	1.0228021	8.57E-03
ENSG00000086300	SNX10	1.0144546	7.02E-07
ENSG00000102962	CCL22	1.0075031	1.51E-03
ENSG00000162636	FAM102B	0.975724	3.32E-03
ENSG00000110013	SIAE	0.9595058	3.84E-04
ENSG00000112304	ACOT13	0.9484436	2.38E-06
ENSG00000153208	MERTK	0.9457111	2.38E-03
ENSG00000023287	RB1CC1	0.9454641	3.16E-04
ENSG00000118242	MREG	0.9393711	1.80E-06
ENSG00000210195	MT-TT	0.9330281	1.08E-04

C. GW0742+ ATP vs ATP Down-regulated Genes

Treatment with the PPAR β agonist GW0742, followed by ATP stimulation, led to notable downregulation of several genes implicated in inflammatory processes within microglial cells, as listed in (Table 5.3). Among the most significantly downregulated genes were CCL3L1, TNF, and CCL3, all of which are recognised for their roles in mediating inflammation. CCL3L1 and CCL3 encode chemokines that recruit immune cells to sites of inflammation, while TNF is a key cytokine that mediates systemic inflammation (Bonecchi et al., 2009). Additionally, the downregulation of EGR4, a transcription factor involved in cellular response to stimuli, and NR4A2, which is associated with inflammation and cell survival pathways, demonstrates the anti-inflammatory effect of PPAR β agonist treatment.

Various signalling pathways have been inhibited in ATP-stimulated microglial cells that have been pretreated with GW0742. The pathways affected include those involved in neurodegenerative diseases such as Parkinson's, Alzheimer's, and Huntington's disease, suggesting that GW0742 may have a role in modulating pathways related to neurodegeneration. See appendices (Figure 4).

These results suggest that GW0742 may exert its neuroprotective effects by inhibiting genes typically upregulated in response to inflammation or metabolic dysfunction, thereby potentially mitigating inflammatory responses and improving metabolism in microglial cells.

Table 5. 3: GW0742+ATP vs ATP: Top 20 Down-Regulated Genes (significantly changed only, sorted by LFC).

Gene ID	Gene Name	log2FoldChange	padj
ENSG00000276085	CCL3L1	-1.914416	4.89E-31
ENSG00000144655	CSRNP1	-1.865536	1.57E-08
ENSG00000232810	TNF	-1.841256	4.40E-20
ENSG00000198576	ARC	-1.635775	8.58E-09
ENSG00000277632	CCL3	-1.547588	4.69E-36
ENSG00000135625	EGR4	-1.537029	1.34E-04
ENSG00000053438	NNAT	-1.498288	6.84E-04
ENSG00000179094	PER1	-1.493405	4.78E-07
ENSG00000128965	CHAC1	-1.442871	3.11E-03
ENSG00000160888	IER2	-1.360624	1.88E-07
ENSG00000153234	NR4A2	-1.321958	1.17E-04
ENSG00000112699	GMDS	-1.292237	3.52E-03
ENSG00000166169	POLL	-1.262236	8.80E-04
ENSG00000105676	ARMC6	-1.243853	9.62E-05
ENSG00000275302	CCL4	-1.233567	1.47E-13
ENSG00000101400	SNTA1	-1.223666	4.96E-03
ENSG00000099625	CBARP	-1.218404	4.30E-03
ENSG00000033627	ATP6V0A1	-1.205665	1.87E-11
ENSG00000241553	ARPC4	-1.203119	2.22E-04
ENSG00000163739	CXCL1	-1.192743	3.16E-05

5.4.9 Investigation of GW0742-Mediated Anti-Inflammatory Effects

Heatmap analysis (Figure 5. 15) revealed a distinctive gene expression profile in microglial cells pre-treated with GW0742 prior to ATP stimulation. Notably, there was an upregulation of several genes associated with neuroprotective pathways, including *ATG3*, *RB1CC1*, *BNIP3L*, *UBQLN2*, *ABCA1*, *CPT1A*, *ALDH2*, *CCL22*, and *PPAR γ* , following GW0742 pretreatment. These genes are known for their roles in autophagy, lipid metabolism, detoxification, immune modulation, and peroxisome proliferator-activated receptor signalling, respectively. Their increased expression suggests that GW0742 may confer a protective effect against ATP-induced inflammatory stress in microglial cells (Bonecchi et al., 2009, Jülg et al., 2021, Köberlin et al., 2016, Schlaepfer and Joshi, 2020, Hjerpe et al., 2016, Li et al., 2021, Joshi et al., 2019, Mantovani et al., 2004, Korbecki et al., 2019, Graham et al., 2005, Tanaka et al., 2003, Dressel et al., 2003, Oliver Jr et al., 2001).

In contrast, genes typically upregulated in response to DAMP stimuli, such as *CXCL1*, *CCL1*, *CCL3*, *CCL2*, *IL-1 β* , *IL-1 α* , *ICAM-1*, *MIF*, *RELA*, *RELB*, *TNF α* , *CXCL3*, *CXCL16*, *CXCL8*, *NR4A1*, *NR4A2*, *NR4A3*, and *Serpin E1*, showed increased expression with ATP treatment alone. However, these genes were downregulated in cells pretreated with GW0742 before ATP exposure. This downregulation is indicative of GW0742's role in modifying the pro-inflammatory response induced by ATP.

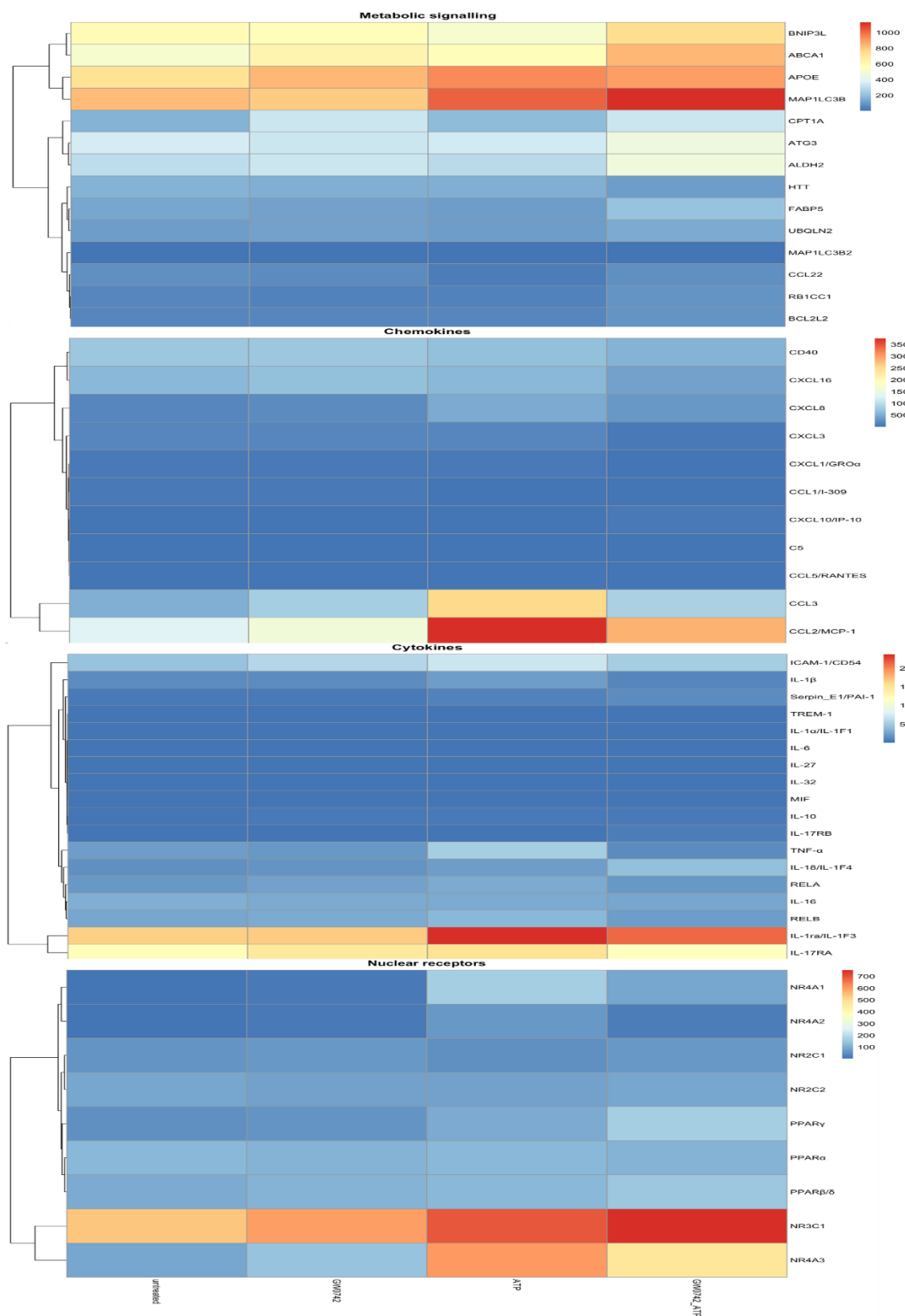


Figure 5. 15: Heatmap of Key Gene Expression from RNA-Seq Data: iMG cells across four different experimental conditions: untreated cells (control), cells treated

with 50 nM GW0742, cells activated with 50 μ M ATP for 2 hours, and cells pre-treated with GW0742 followed by ATP stimulation.

5.4.10 Investigating SUMOylation of PPAR β in response to ligand treatment as a potential mechanism involved in inhibition of inflammatory gene expression.

To date, PPAR β SUMOylation at single lysine, K104, has been identified by Koo et al. This modification reduces transcriptional activation by PPAR β and is reversed by the SUMO-Specific Protease 2 (SEN2), which facilitates the activation of fatty acid oxidation (FAO) gene expression in muscle tissues (Koo et al., 2015). In other nuclear receptors, ligand-activated SUMOylation has been proposed as a mechanism involved in the inhibition of inflammatory gene promoters. The potential role of SUMOylation in mediating the anti-inflammatory effects of PPAR β was examined through a series of validation experiments utilizing LXR β , a nuclear receptor known for its substantial SUMOylation. Enhanced SUMOylation of LXR β was confirmed by the overexpression of Ubc9, SUMO, and E3 ligase PIAS1, thus establishing the assay's efficacy (Figure 5. 17). Studies of LXR β SUMOylation repeated previous observations by a PhD student in the FRAME laboratories, with the synthetic agonist GW3965 reducing SUMOylation, contrasting the enhancement seen with the natural ligand 22(R)HC (Figure 5.16). Following the SUMO pulldown protocol as described by (Pourcet et al., 2013) transfections were conducted in HeLa cells to introduce HA-tagged PPAR β , alongside His-tagged SUMO isoforms 2 or 3, PIAS1, PIASy or HDAC4, and Ubc9. After transfection, a nickel-nitrilotriacetic acid (Ni-NTA) affinity matrix was used to isolate SUMO-modified proteins from cellular lysates. Subsequent Western blot analysis was performed using anti-HA to detect PPAR β , with anti- β -actin antibodies as loading controls.

PPAR β revealed minimal SUMOylation, suggesting a stark contrast in the SUMOylation profile of PPAR β as compared to LXR β , even with the overexpression of the SUMOylation machinery. The resulting immunoblots, as shown in Figure 5. 17, exhibit bands indicative of the unmodified form at approximately 49 kDa and SUMOylated (~55 kDa) PPAR β . The presence of multiple bands in this region suggests that PPAR β undergoes poly-SUMOylation. Notably, the SUMO3-modified version of the receptor displayed more pronounced bands, particularly in the presence of PIAS1.

Further investigations into whether the activation of PPAR β could influence SUMOylation patterns showed no increase in SUMOylation levels post-treatment with PPAR β agonist (GW0742); in fact, a slight decrease in the already low levels of SUMOylation was noted. As depicted in Figure 5. 18, it appears that PPAR β was slightly SUMOylated, and this was reduced in the presence of GW0742. These results suggest that SUMOylation does not play a major role in the anti-inflammatory effects exerted by PPAR β agonists.

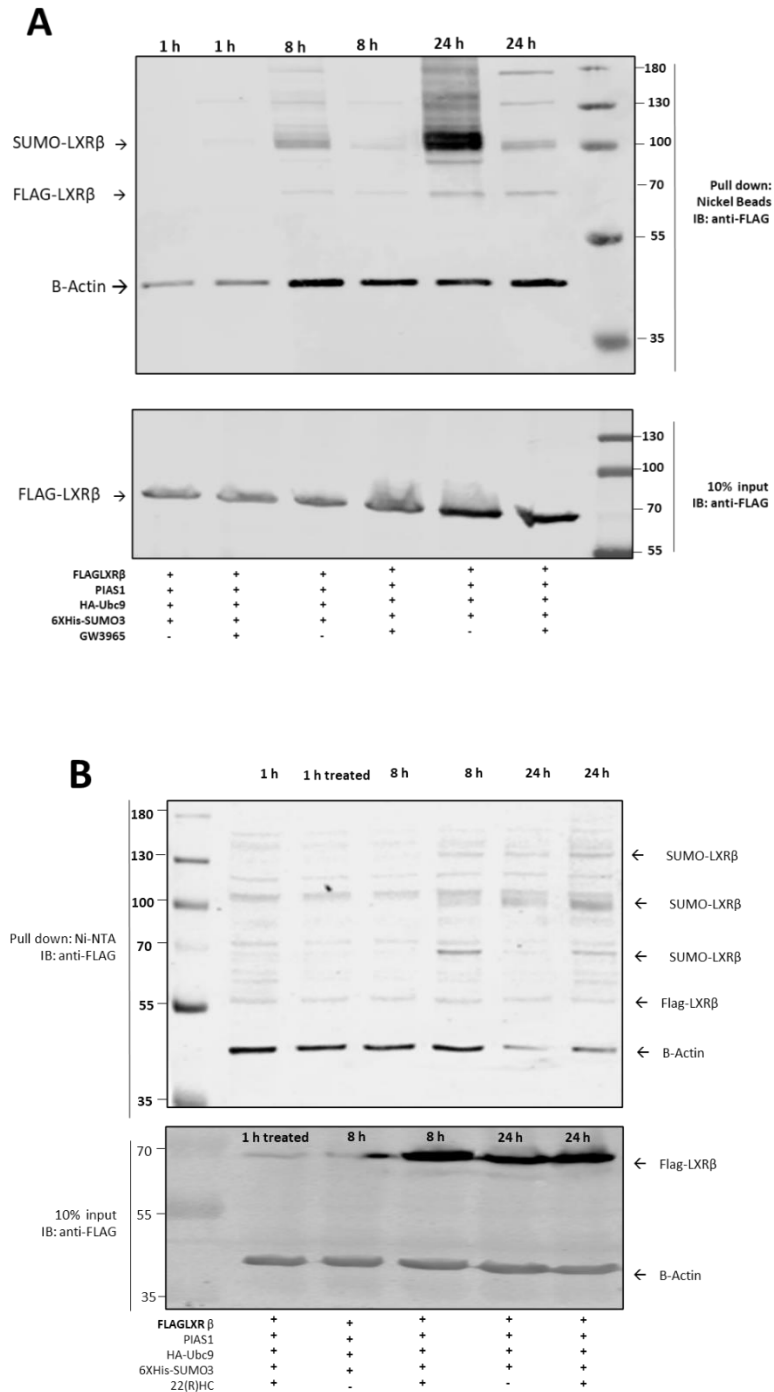


Figure 5. 16: LXR β Response to Synthetic and Natural Agonists: HeLa cells were transfected with FLAG-LXR β for 48 hours and treated with: **A.** 1 μ M GW3965 1-24 h **B.** 10 μ M 22(R)HC 1-24 hours. 90% of the cell lysate was purified using nickel beads and then analysed using a 10% acrylamide SDS-PAGE gel. The rest (10%) was used directly as a total input sample for similar electrophoretic analysis. Western blot analysis utilised anti-Flag and anti- β -actin antibodies at dilutions of 1:1000 and 1:5000, respectively. Data represents two independent experiments.

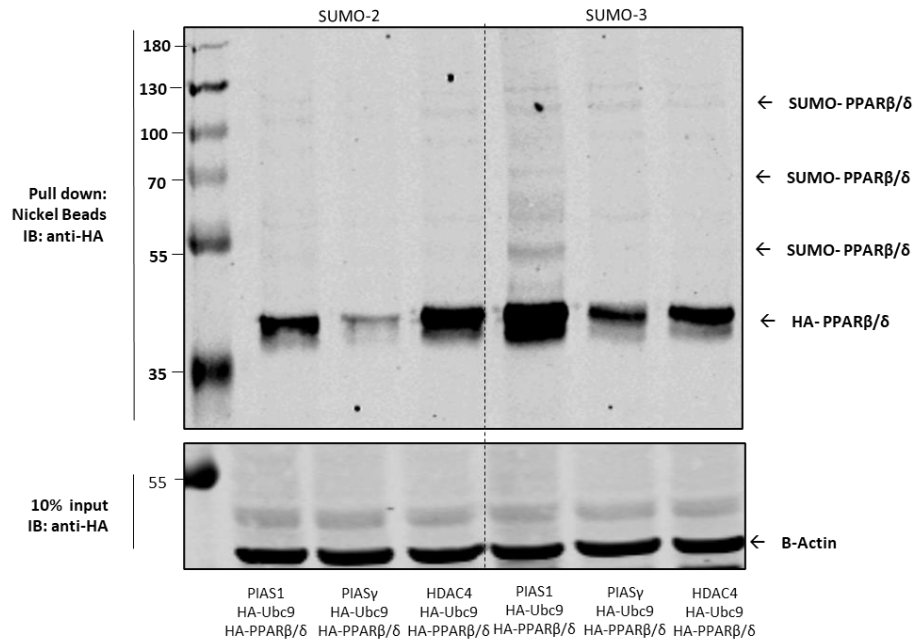


Figure 5. 17: SUMOylation Analysis in HeLa Cells: HeLa cells were transfected to express HA-tagged PPARβ along with Ubc9, and co-transfectants PIAS1, PIASy, or HDAC4, and either His-tagged SUMO 2 or 3. Ninety percent of the cell lysate was purified using nickel beads and analysed using a 10% acrylamide SDS-PAGE gel. The remaining 10% was used directly as a total input sample for similar electrophoretic analysis. Western blot analysis utilised anti-HA and anti-β-actin antibodies at dilutions of 1:1000 and 1:5000, respectively. Data represents two independent experiments.

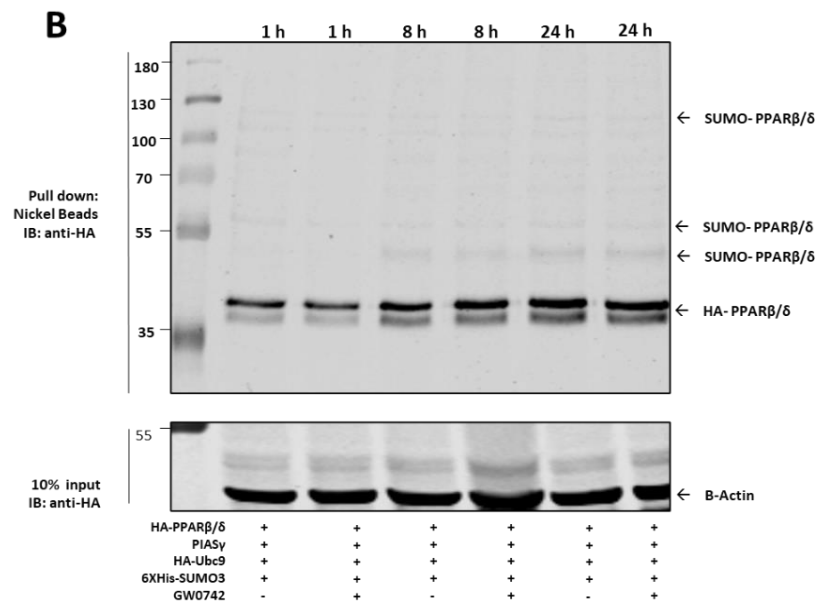
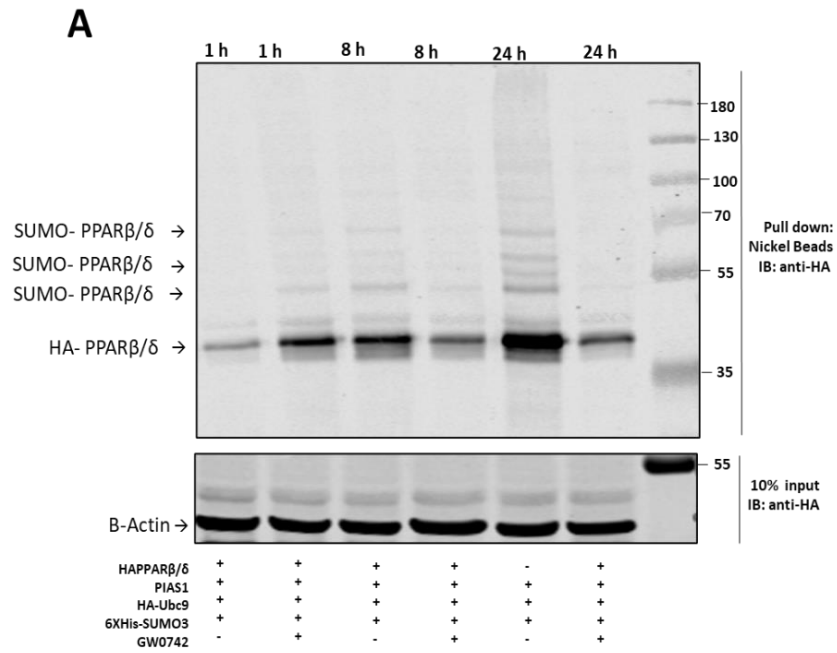


Figure 5. 18: Influence of GW0742 on PPARβ SUMOylation: HeLa cells were transfected with HA-PPARβ for 48 hours and treated with 50 nM GW0742 for 1-24 hours: **A.** PIAS1. **B.** PIASy. 90% of the cell lysate was purified using nickel beads and then analysed using a 10% acrylamide SDS-PAGE gel. The rest (10%) was used directly as a total input sample for similar electrophoretic analysis. Western blot analysis utilised anti-HA and anti-β-actin antibodies at dilutions of 1:1000 and 1:5000, respectively. Data represents two independent experiments.

5.5 Discussion

This study explored the modulation of inflammatory responses in microglial cells using LPS and ATP as stimulants, with effects assessed through RT-qPCR. Expression of PPAR β is influenced by inflammatory stimuli, with significant upregulation of PPAR β mRNA observed in response to LPS or ATP-induced activation in both adult and neonatal cortical microglia and monocyte-derived microglia.

This study demonstrated the upregulation of PPAR β in microglia in response to inflammatory stimuli, which is a novel finding that has not been extensively investigated in previous research. This observation is particularly interesting when considering how inflammation affects the expression of other nuclear receptors, such as PPAR α , PPAR γ , and LXRs, in macrophages and microglia.

In macrophages, inflammatory stimuli have been shown to generally decrease the expression of nuclear receptors, including PPAR α , PPAR γ , and LXRs. For example, (Barish et al., 2005) demonstrated that LPS stimulation reduced the expression of PPAR α , PPAR γ , and LXR α in mouse macrophages. Similarly, (Ghisletti et al., 2007) reported that LPS treatment decreased the expression of PPAR γ and LXR α in human macrophages. These findings suggest that inflammation may suppress these nuclear receptors' anti-inflammatory and metabolic regulatory functions in macrophages.

This research demonstrated a significant inhibition in pro-inflammatory cytokines TNF α and IL-1 β expression across various models, including primary adult and neonatal rat microglia, human monocyte-derived macrophages (iMAC), and human monocyte-derived microglia (iMG). This supports previous findings that highlight the anti-inflammatory capabilities of PPAR β agonists. Notably, while most studies have focused on muscle and various peripheral tissues, there has been limited exploration within the CNS, despite the high expression of this isoform in the CNS (Phua et al., 2020, Wang et al., 2020).

The initial discovery of the anti-inflammatory impacts of PPAR β occurred in macrophage cells. It was found that the PPAR β activator, GW0742, suppressed the

induction of inflammatory gene expression, including cyclooxygenase-2 (COX-2) and iNOS, in response to LPS stimulation in primary macrophages derived from mice (Welch et al., 2003). PPAR β has been reported to modulate NF- κ B activity through several mechanisms, including the inhibition of the nuclear translocation of the p65 subunit, direct binding to p65, and reduction of p65 acetylation via AMPK and SIRT1 activation (Odegaard and Chawla, 2008, Planavila et al., 2005, Kapoor et al., 2010, Barroso et al., 2011).

This study used low levels of ATP to stimulate human monocyte-derived microglia and highlighted the impact of the PPAR β agonist GW0742 on cellular transcriptomics. Notably, pretreatment with GW0742 altered the gene expression landscape, elevating genes tied to neuroprotection while dampening those associated with inflammation in response to ATP.

Specifically, GW0742 upregulated the expression of ATG3, RB1CC1, and BNIP3L, which are involved in autophagy processes Figure 5. 19. Autophagy is a cellular process implicated in the degradation and recovery of cellular components. Autophagy can help to clear damaged organelles and proteins, including those that might contribute to inflammatory processes, thereby exerting an anti-inflammatory effect (Palomer et al., 2014, Pomilio et al., 2020). ATG3 (Autophagy Related 3) is an essential component of the autophagy machinery, participating in the lipidation of LC3 and the formation of autophagosomes (Nath et al., 2014). RB1CC1 (RB1 Inducible Coiled-Coil 1), also known as FIP200, is a key regulator of autophagy initiation and is required for the formation of the ULK1 complex (Hara et al., 2008). BNIP3L (BCL2 Interacting Protein 3 Like), also known as NIX, is a mitophagy receptor that mediates the selective clearance of damaged mitochondria (Li et al., 2021). The upregulation of these genes by GW0742 suggests that PPAR β activation may promote neuroprotection by enhancing autophagy and mitophagy, which are crucial processes for maintaining cellular homeostasis and preventing the accumulation of toxic protein aggregates and dysfunctional mitochondria in the context of

neuroinflammation and neurodegeneration (Plaza-Zabala et al., 2017, Soto-Avellaneda and Morrison, 2020).

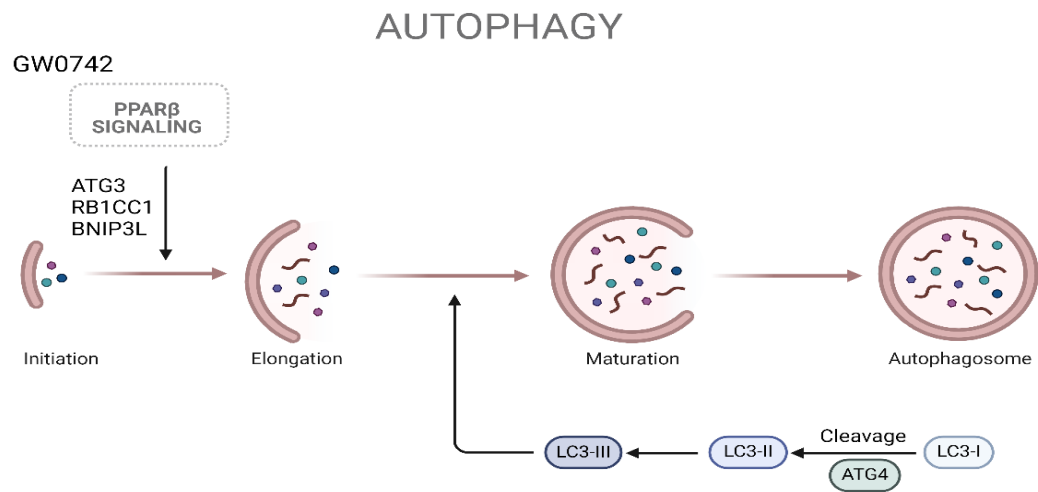


Figure 5. 19: The stages of the autophagic process and the role of specific genes upregulated by GW0742, which are crucial for autophagy. GW0742, an agonist of PPAR β , increase the expression of genes pivotal to autophagy, such as ATG3, RB1CC1, and BNIP3L. ATG3 is integral to the lipidation of LC3, facilitating autophagosome formation. Generated using Biorender.

In the other hand, the PPAR β agonist GW0742 significantly decreased the expression of several pro-inflammatory genes, including IL-1 β , TNF α , CCL2, ICAM, RELA, RELB, and CXCL3, 8, and 16. One possible mechanism by which PPAR β agonists like GW0742 could downregulate pro-inflammatory gene expression is through the inhibition of the NF- κ B signaling pathway. NF- κ B is a key transcription factor that regulates the expression of numerous inflammatory genes, including cytokines (e.g., IL-1 β and TNF α), chemokines (e.g., CCL2, CXCL3, 8, and 16), and adhesion molecules (e.g., ICAM) (Liu et al., 2017). The decreased expression of RELA and RELB, two subunits of the NF- κ B complex, in response to GW0742 treatment, suggests that PPAR β activation may directly interfere with NF- κ B signalling. This is consistent with previous studies demonstrating that PPAR β agonists can inhibit NF- κ B activation and downstream inflammatory gene expression in various cell types, including macrophages and endothelial cells (Fan et al., 2008) (Storer et al., 2005).

To investigate the potential role of SUMOylation in mediating the anti-inflammatory effects of PPAR β , the SUMOylation assay was first validated using LXR β , a nuclear receptor known to be heavily SUMOylated (Ghisletti et al., 2007). By overexpressing Ubc9, SUMO, and E3 ligase (PIAS1), robust SUMOylation of LXR β was observed, confirming the functionality of the assay. In contrast, when the same approach was applied to PPAR β , minimal SUMOylation was found compared to LXR β , even when overexpressing the SUMOylation machinery. Furthermore, treatment with a PPAR β agonist did not increase SUMOylation and, if anything, slightly decreased the already low levels observed. These findings indicate that SUMOylation is unlikely to be a primary mechanism mediating the anti-inflammatory effects of PPAR β agonists, in contrast to other nuclear receptors like LXR β (Figure 5. 20).

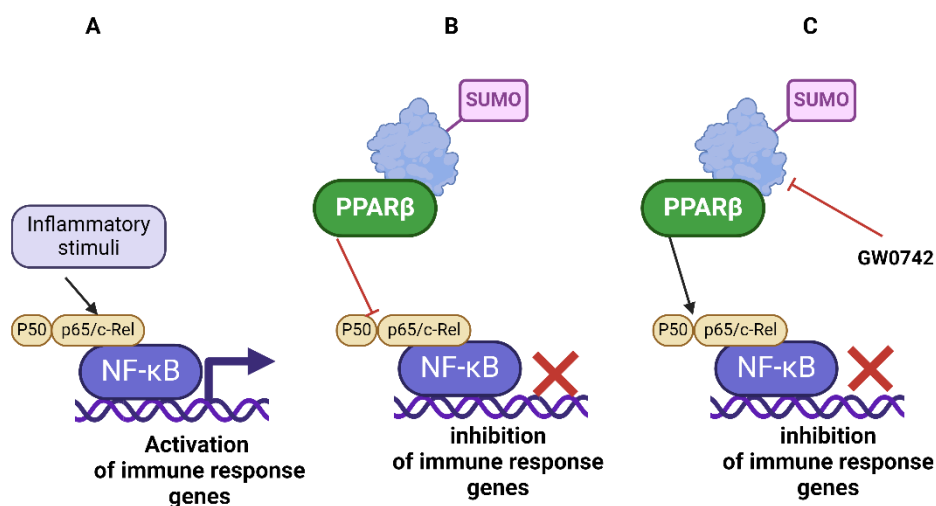


Figure 5. 20: The Effect of PPAR β Activation on Inflammatory Response.

A: Illustrates the activation of the NF- κ B pathway by inflammatory stimuli. **B:** According to the SUMOylation Hypothesis, SUMOylation of PPAR β leads to the repression of NF- κ B, thereby inhibiting the expression of immune response genes, suggesting that SUMOylation plays a role in the anti-inflammatory activity of PPAR β . **C:** Despite the inhibition of PPAR β SUMOylation by the PPAR β agonist GW0742, the NF- κ B pathway remains inhibited. This suggests that the anti-inflammatory effects of GW0742 are achieved through a mechanism that does not rely on SUMOylation. Generated using Biorender.

Next, the rapid changes in gene expression induced by PPAR β activation were examined. Despite the assumption that gene expression changes would be too slow to account for the fast anti-inflammatory effects observed, significant increases in PPAR β target genes were found within 30 minutes of ligand addition. These target genes, such as PDK4 and ANGPTL4, are involved in lipid metabolism and immune regulation (Zhang et al., 2014, Koliwad et al., 2009, Adhikary et al., 2015) suggesting that their upregulation may contribute to the anti-inflammatory actions of PPAR β agonists.

One potential mechanism by which PPAR β activation could modulate inflammation is through changes in cholesterol metabolism. Upregulation of genes like ABCA1 could increase cholesterol efflux from the cell membrane, thereby reducing the availability of cholesterol for lipid raft formation and TLR4 signaling (Figure 5. 21). This, in turn, could dampen the inflammatory response to stimuli like LPS (Ito et al., 2015).

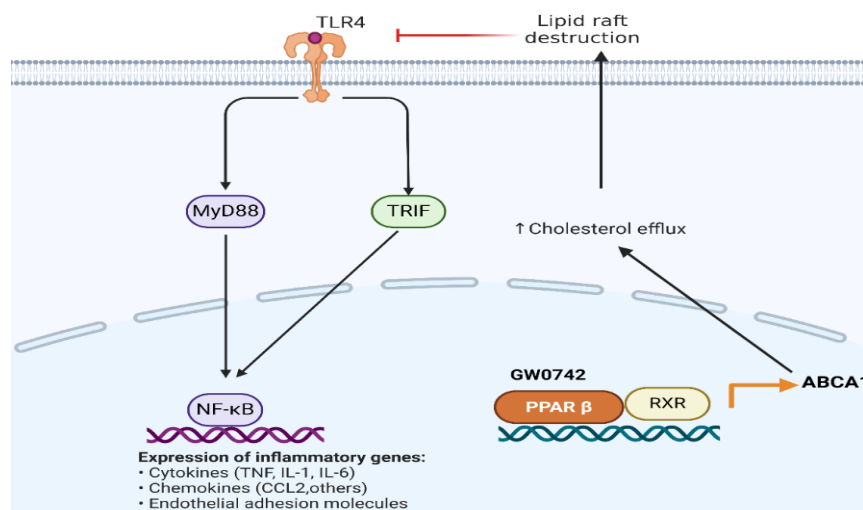


Figure 5. 21: Increased transcription of the ABCA1 gene. The signalling diagram illustrates the mechanism by which PPAR β , when activated by an agonist such as GW0742, leads to increased transcription of the ABCA1 gene. The elevated ABCA1 levels promote the efflux of cholesterol from the cell membrane. This decrease in membrane cholesterol results in the destabilisation of lipid rafts, which are critical for TLR4 signalling. As a consequence, TLR4-mediated inflammatory pathways, which would typically be activated in response to inflammatory stimuli such as LPS, are suppressed. Generated using Biorender.

Another possibility is that PPAR β activation shifts cellular metabolism towards a more oxidative state, which is associated with a less inflammatory phenotype in macrophages and microglia (Odegaard and Chawla, 2011). This metabolic reprogramming may enhance mitochondrial function and reduce the production of reactive oxygen species, thereby mitigating inflammation (Wang et al., 2004). In a study by Ghosh et al. (2018), the authors demonstrated that microglia can oxidize fatty acids, particularly during periods of energy stress. They found that when glucose levels were low, microglia increased their uptake and oxidation of fatty acids to maintain their energy demands. PPAR β plays a crucial role in lipid metabolism and energy homeostasis.

This study found that PPAR β agonists increased the levels of CPT1a a key regulator of fatty acid oxidation, and its upregulation has been associated with increased energy expenditure, reduced inflammation, and improved metabolic health (Schlaepfer and Joshi, 2020). The upregulation of CPT1a by PPAR β agonists suggests that these compounds may enhance fatty acid oxidation in microglia, potentially shifting their energy metabolism towards a more oxidative state.

In addition to promoting fatty acid oxidation, PPAR β agonists also increased the levels of ALDH2, a mitochondrial enzyme responsible for the detoxification of reactive aldehydes generated during oxidative stress and lipid peroxidation (Chen et al., 2014). Reactive aldehydes, such as 4-hydroxynonenal (4-HNE) and malondialdehyde (MDA), have been implicated in the pathogenesis of neurodegenerative diseases, including Alzheimer's disease (AD) (Joshi et al., 2019). These aldehydes can form adducts with proteins, lipids, and DNA, leading to cellular dysfunction and inflammation. Joshi et al. (2019) demonstrated that reduced ALDH2 activity and increased aldehydic load contribute to neuroinflammation and AD-related pathology in both human AD brains and mouse models of AD. By upregulating ALDH2, PPAR β agonists may help to reduce oxidative stress and inflammation in microglia by enhancing the clearance of these toxic aldehydes.

Recent studies, such as those by Chehaibi et al. (2017) and Tang et al. (2020), highlight the promising neuroprotective and anti-inflammatory impacts of PPAR β agonists in brain ischemia models, showcasing their potential in neurodegenerative disease management by promoting neurotrophic support, enhancing calcium balance, and supporting mitochondrial function and neuronal regeneration. Anti-inflammatory properties have been observed with PPAR β agonists, leading to the downregulation of pro-inflammatory genes like iNOS, and various chemokines such as CXCL1, CXCL2, along with interleukins IL1, and IL6, as well as additional cytokines like TNF- α and IFN- γ , while upregulating anti-inflammatory markers such as IL10 (Chehaibi et al., 2017, Kuang et al., 2012, Tang et al., 2020). Specifically, PPAR β agonists, including GW0742, have shown potential in reducing brain neutrophil entry during ischemic events and combating neuroinflammation (Chehaibi et al., 2017). PPAR β agonists exhibit a broad spectrum of molecular effects, from anti-inflammatory actions to myelin sheath stabilisation and reduction in A β deposits (Collino et al., 2008, Dunn et al., 2010, Kalinin et al., 2009). Depleting PPAR- β/δ experimentally has indicated not just an uptick in neuroinflammation but also in astrogliosis, oxidative stress, and A β accumulation (Barroso et al., 2013). Consistently, in an Alzheimer's disease (AD) mouse model (5XFAD), the PPAR β agonist GW0742 demonstrated the ability to lower A β deposits in the brain, alongside reducing several inflammatory cytokines and microglial activation near A β clusters (An et al., 2016, Malm et al., 2015).

The studies mentioned demonstrate the anti-inflammatory effects of GW0742, a PPAR β agonist, in various in vivo models of neurological disorders. For example, in a rat model of spinal cord injury, Ahmad et al. (2018) showed that intraperitoneal injection of GW0742 for 14 days post-injury reduced the expression of IL-6, TNF- α , and IL-1 β in the spinal cord, as well as decreased the activation of microglia and astrocytes. They proposed that GW0742 exerts anti-inflammatory effects by inhibiting the glial cells' NF- κ B and MAPK signalling pathways.

It is important to note that while these studies provide valuable insights into the anti-inflammatory effects of GW0742 in various neurological disorders, they differ from the current research in a crucial aspect. These studies demonstrate the effects of GW0742 in *in vivo* models, where the anti-inflammatory effects may occur through indirect mechanisms involving multiple cell types and complex interactions within the brain. In contrast, this study focuses on the direct effects of PPAR β ligands on isolated microglia, providing evidence for the cell-autonomous role of PPAR β in regulating microglial inflammatory responses. This distinction highlights the novelty and significance of the findings, as it demonstrates a direct link between PPAR β activation and the modulation of microglial function, which may have important implications for the development of targeted therapies for neuroinflammatory and neurodegenerative diseases.

Comparatively, the understanding of PPAR β 's neuroprotective mechanisms is extended by this study. While previous research has highlighted the receptor's role in reducing neuroinflammation, this work further elucidates its regulatory effects on autophagy and inflammation via detailed transcriptomic analysis, particularly under low ATP conditions mimicking neurodegenerative disease states. Moreover, the application of human primary microglia-like cells in these experiments offers a more physiologically relevant model to study these mechanisms. This model allows for a closer approximation to the *in vivo* human condition, thereby enhancing the translational potential of the findings. The observed downregulation of pro-inflammatory genes upon treatment with GW0742 aligns with previous observations of PPAR β 's neuroprotective effects, supporting its role in attenuating neuroinflammatory pathways and possibly ameliorating neurodegenerative disease progression.

The anti-inflammatory effects of PPAR β agonists are potentially multifaceted, involving the direct modulation of gene expression, inhibition of pro-inflammatory signalling pathways, shifts in cellular metabolism towards less inflammatory states, and the induction of autophagy (Figure 5. 22). These mechanisms highlight the

potential of PPAR β agonists as therapeutic agents in conditions characterised by excessive inflammation.

While providing valuable insights into the effects of PPAR β agonists on human microglial cells *in vitro*, this study encounters certain limitations inherent to its design and scope. Firstly, the investigation was conducted using a simplified system that does not fully capture the intricate cellular interactions occurring in the brain. This study demonstrates the potential for targeting PPAR β to counter pro-inflammatory effects in primary microglia. Whether these effects are replicated *in vivo* requires further study. Future research would benefit from employing more complex models, such as co-cultures involving neurons and astrocytes or the use of brain organoids. These advanced models would offer a deeper understanding of the cellular dynamics and the potential neuroprotective effects of PPAR β agonists in a more physiologically relevant context.

Additionally, the study's focus on microglial cells alone limits the exploration of how these cells interact with other brain components in response to pathological stimuli. Introducing alpha-synuclein as a stimulant in future experiments could shed light on the specific role of PPAR β agonists in modulating microglial activation and neuroinflammation in the context of synucleinopathies, a group of neurodegenerative disorders characterized by the abnormal accumulation of alpha-synuclein protein in the brain (Goedert et al., 2017), further elucidating their therapeutic potential. Another avenue for future research involves the comparison of different PPAR β agonists. The current study's reliance on a single agonist leaves open the question of whether other compounds, such as GW501516, would elicit similar anti-inflammatory and neuroprotective responses. Expanding the range of PPAR β agonists tested could provide a broader understanding of their mechanisms of action and effectiveness.

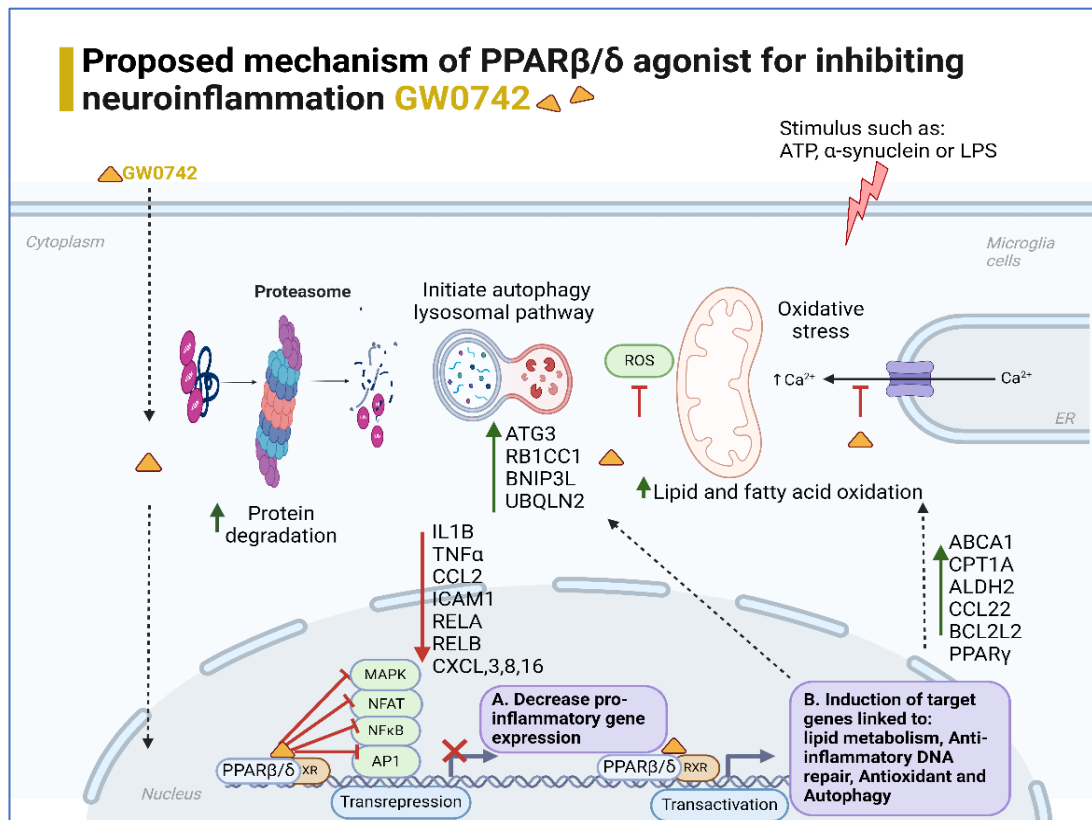


Figure 5. 22: Proposed Mechanism of PPAR β Agonists in Inhibiting Neuroinflammation: The mechanism involves the downregulation of pro-inflammatory gene expression through inhibition of key signalling pathways, including NF- κ B, MAPK, AP-1, and NFAT (**A**). PPAR β activation induced the expression of genes involved in protective processes: ABCA1 and ALDH2 enhance lipid metabolism and antioxidant defence, CCL22 contribute to anti-inflammatory responses, BCL2L2, ATG3, RB1CC1, and BNIP3L promote autophagy, aiding in the clearance of damaged cellular components; UBQLN2 regulate protein degradation (**B**). These actions lead to a reduction in neuroinflammation and create a neuroprotective environment, which is potentially beneficial in mitigating neuroinflammatory and neurodegenerative disorders. Generated using Biorender.

Chapter 6 Assessment of the Role of ABCG2/BCRP in PPAR β Drug Delivery to the Central Nervous System

6.1 Introduction

This research was funded by the Saudi Cultural Bureau; as part of the funding requirements, this study assessed whether PPAR β agonists are substrates for the ABC transporter BCRP, which could limit their CNS penetration. The Peroxisome Proliferator-Activated Receptor beta (PPAR β) has been identified as a promising therapeutic target for reducing inflammation within the Central Nervous System (CNS). Given the nuclear receptor nature of PPAR β , the transverse of its ligands across the plasma membrane and the nuclear membrane to reach the nucleus and bind to the receptor is essential for their efficacy. Moreover, the traversal of the blood-brain barrier (BBB) by potential anti-inflammatory drugs is imperative to achieve any potential therapeutic outcomes in neuroinflammation.

The ATP-binding cassette (ABC) efflux transporters, including the Breast Cancer Resistance Protein (BCRP/ABCG2), play a pivotal role in this context. This transmembrane protein facilitates the export of chemicals from cells via ATP hydrolysis, thereby influencing the pharmacokinetics of drugs, including their absorption, distribution, metabolism, and excretion (ADME) (Natarajan et al., 2012). Notably, ABCG2 is expressed on the luminal surface of brain microvessel endothelial cells forming the BBB, where it serves as a barrier to the cerebral penetration of substrate drugs, potentially limiting their therapeutic efficacy (Mahringer et al., 2009, Römermann et al., 2013, Kerr et al., 2011). Several studies have demonstrated the importance of ABCG2 in limiting the CNS penetration of various therapeutic agents. For example, (Enokizono et al., 2007) showed that ABCG2 restricts the brain uptake of the tyrosine kinase inhibitor gefitinib, which is used to treat non-small cell lung cancer. The authors found that gefitinib accumulation in the brain was significantly higher in *Abcg2*-deficient mice compared to wild-type mice, suggesting that ABCG2 plays a key role in limiting the CNS penetration of this drug.

Similarly, (Agarwal et al., 2010) investigated the role of ABCG2 in the brain distribution of the antibiotic fluoroquinolones, such as ciprofloxacin and norfloxacin. Using in vitro and in vivo models, they demonstrated that ABCG2 actively effluxes these antibiotics at the BBB, thereby reducing their brain penetration and potentially limiting their efficacy in the treatment of CNS infections. These examples highlight the importance of considering the role of ABCG2 in the brain penetration of therapeutic agents, particularly when targeting CNS disorders. Compounds that are substrates of ABCG2 may have limited brain exposure, which could impact their efficacy in treating neurological conditions. Therefore, understanding the interaction between potential therapeutic agents and ABCG2 is crucial for the development of effective CNS drugs.

To determine the interactions between drugs and ABC transporters, fluorescent substrate accumulation assays are widely employed. These assays involve incubating cells, which overexpress a specific transporter, with a fluorescent substrate designed to be exported by the transporter. The presence or absence of test compounds can influence the intracellular concentration of the fluorescent substrate, inversely proportional to the activity of the transporter. Consequently, the fluorescence spectrophotometry quantification of intracellular substrate accumulation provides insights into the competitive dynamics between the test compound and the fluorescent substrate, indicating potential drug-transporter interactions. If a test compound competes with the fluorescent substrate for efflux, this competition manifests as an increase in intracellular fluorescence, offering a quantitative measure of the compound's affinity for the transporter.

6.2 Aim

The objective of this study was to assess whether PPAR ligands function as substrates for the BCRP/ABCG2 efflux transporter. This transporter could play a significant role in hindering the passage of these ligands through the blood-brain barrier (BBB) thus affecting their capacity to reach therapeutic levels within the CNS. To this end, through employing a cell line overexpressing BCRP/ABCG2, this investigation aimed to evaluate the potential of PPAR ligands to interact with this transporter by competing with a known fluorescent BCRP substrate. Thus, serving as an indicator of the ligands' ability to be effluxed by BCRP/ABCG2, thereby offering insights into the pharmacokinetic challenges that could be faced in CNS drug delivery.

6.3 Results

This study identified the role of PPAR ligands as potential substrates for the BCRP/ABCG2 transporter, focusing on their capacity to traverse the BBB. The investigation utilised HEK293T cells (Cox et al., 2018), overexpressing BCRP/ABCG2 to explore the interaction between these ligands and the fluorescent BCRP substrate, mitoxantrone. The cells were incubated with 8 μM mitoxantrone for 60 minutes in the presence of varying concentrations (1-10 μM) of PPAR β agonists (GW0742 and GW01516), the PPAR α agonist (WY14643), and the PPAR γ agonist (rosiglitazone), followed by the measurement of intracellular mitoxantrone fluorescence as a marker of BCRP activity.

6.3.1 Impact of PPAR β Agonists on Mitoxantrone Accumulation in BCRP-Overexpressing Cells

The efficacy of the assay was validated through a significant increase in intracellular mitoxantrone fluorescence upon administration of the selective BCRP inhibitor Ko143 (Allen et al., 2002), in comparison to mitoxantrone alone (* $p < 0.05$), confirming the functionality of the assay. On the other hand, aspirin, a known non-substrate of BCRP, did not alter mitoxantrone accumulation, serving as a negative control (Figure 6.1).

Subsequent analyses, as shown in Figure 6.2, demonstrated that the PPAR β agonists GW0742 and GW01516 did not significantly alter mitoxantrone accumulation across the tested concentration range. This lack of effect suggests that these agonists do not act as substrates for the BCRP transporter under the conditions tested. A similar observation was noted with the PPAR α agonist WY14643 and the PPAR γ agonist rosiglitazone, as shown in Figure 6.3, where neither compound significantly influenced mitoxantrone fluorescence. These results collectively indicate that the examined PPAR agonists are unlikely to be BCRP substrates, at least within the parameters of this assay system.

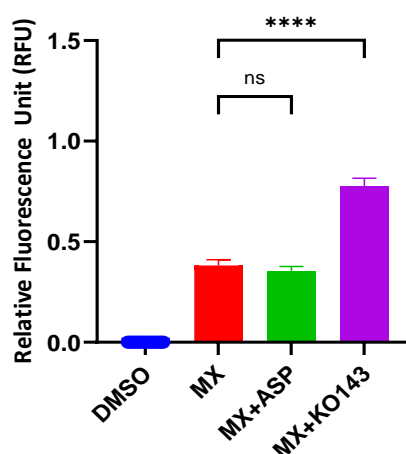


Figure 6.1: Assay Validation: BCRP/ABCG2-overexpressing HEK293T cells were incubated with 8 μ M mitoxantrone alone (MX) or in combination with 500 nM of the known BCRP inhibitor Ko143 (positive control), aspirin (ASP; negative substrate control), or 0.1% DMSO (vehicle control) for 60 minutes. Data are mean \pm SEM from three independent experiments. * $p < 0.05$ vs. MX alone.

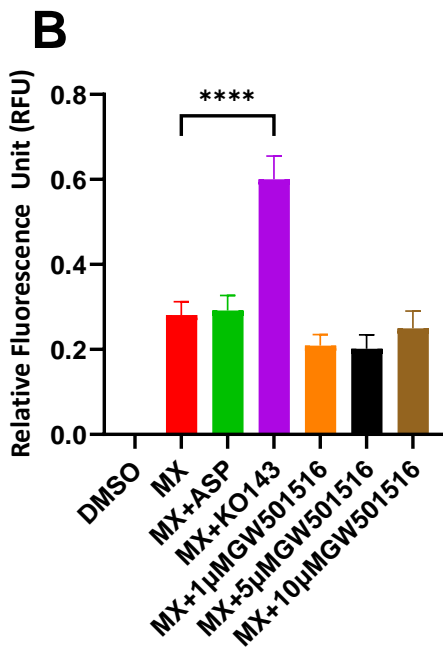
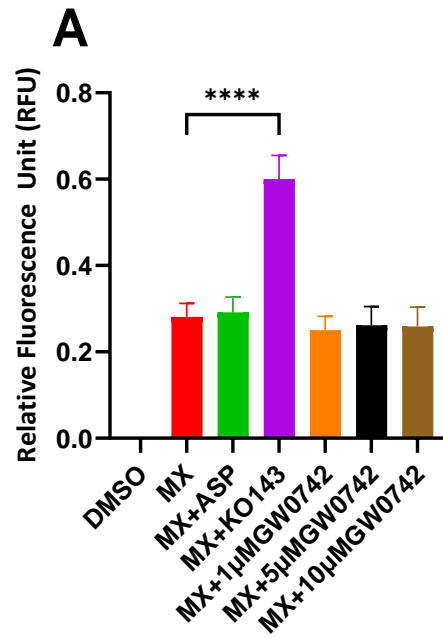


Figure 6.2: Lack of Impact by PPAR β Agonists GW0742 and GW01516 on Mitoxantrone Accumulation: BCRP/ABCG2-overexpressing HEK293 cells were treated with 8 μ M mitoxantrone and (1-10) μ M of the PPAR β ligands GW0742 (**A**) or GW01516 (**B**) for 60 minutes. Data are mean \pm SEM from three independent experiments.

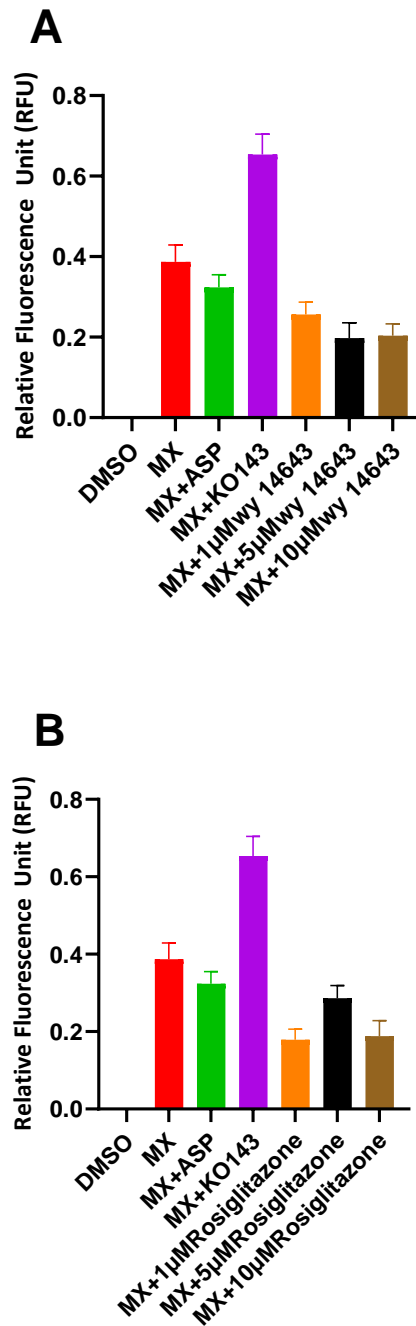


Figure 6.3: Evaluation of PPAR α and PPAR γ Agonists WY14643 and Rosiglitazone on Mitoxantrone Fluorescence: BCRP/ABCG2-overexpressing HEK293 cells were incubated with 8 μ M mitoxantrone and 1-10 μ M of the PPAR α agonist WY14643 (**A**) or the PPAR γ agonist rosiglitazone (**B**) for 60 minutes. Data are mean \pm SEM from three independent experiments.

6.4 Discussion

ABC transporters, located both in the gastrointestinal tract and at the BBB, are critical in regulating the absorption of drugs and their penetration into the CNS. Notably, the BCRP/ABCG2 plays a significant role as an efflux transporter involved in mediating multidrug resistance and limiting the entry of substrate drugs into the brain (Hartz and Bauer, 2010, Kerr et al., 2011). ABCG2 is known to transport a wide range of structurally diverse compounds, including both hydrophobic and hydrophilic molecules (Ni et al., 2010). However, many ABCG2 substrates are relatively hydrophobic and share common structural features, such as planar aromatic rings and the presence of electron donor groups (Matsson et al., 2007). This suggests that hydrophobicity may be an important factor in determining compounds' affinity for ABCG2, although other structural and physicochemical properties also play a role.

Regulatory bodies, including the Food and Drug Administration (FDA), stress the importance of assessing the interaction of new investigational drugs with major efflux transporters, such as P-glycoprotein and BCRP (Hartz and Bauer, 2010). Gaining insights into whether a compound acts as a substrate or inhibitor of these transporters is crucial for predicting its clinical implications. This includes predictions regarding pharmacokinetic behaviour, therapeutic efficacy, and potential adverse effects, thus informing drug development and approval processes. However, the current study only focused on BCRP and did not investigate the potential interaction of PPAR agonists with P-glycoprotein, which is another major efflux transporter at the BBB. Future studies should address this limitation by evaluating the interaction of PPAR agonists with P-glycoprotein to provide a more comprehensive understanding of their CNS delivery potential.

In the present study, a fluorescent substrate accumulation assay was employed in cells overexpressing BCRP to screen selected PPAR agonists for potential

interactions with this transporter. The assay's validity was confirmed through the use of Ko143, a known BCRP inhibitor, which resulted in a significant increase in intracellular mitoxantrone fluorescence. However, it was observed that neither the PPAR β agonists GW0742 and GW01516, the PPAR α agonist WY14643, nor the PPAR γ agonist rosiglitazone significantly influenced mitoxantrone accumulation, suggesting their unlikely role as BCRP substrates under the tested conditions. These findings differ from those of (Weiss et al., 2009), who investigated the interaction between rosiglitazone and ABCG2 using an ABCG2 inhibition assay. In their study, rosiglitazone was found to interact with ABCG2, although it did not reach a plateau effect in the inhibition assay. The lack of a significant effect in the substrate accumulation assay does not necessarily exclude the possibility of an interaction between PPAR agonists and BCRP. The interaction may be dependent on various factors, such as the concentration of the compounds, assay conditions, and cellular context. It is important to note that the concentrations used in this study may not fully represent the physiologically relevant concentrations achieved in vivo, and other factors, such as protein binding, metabolism, and competing transport mechanisms, can influence the overall disposition of these compounds.

Furthermore, the present study focused on a single transporter, BCRP, while in vivo, multiple transporters and metabolic pathways may work in concert to determine the pharmacokinetics and brain penetration of PPAR agonists. To fully understand the role of transporters in the disposition of these compounds, it is necessary to investigate their interactions with other relevant transporters, such as P-glycoprotein (P-gp) and multidrug resistance-associated proteins (MRPs).

Several studies have investigated the interaction of small-molecule hydrophobic drugs with efflux transporters at the BBB. For example, (Agarwal et al., 2010) used in vitro assays and in vivo studies in transporter-deficient mice to demonstrate that both P-gp and BCRP restrict the brain penetration of gefitinib, a small molecule tyrosine kinase inhibitor used in the treatment of non-small cell lung cancer. They

found that the brain distribution of gefitinib was significantly higher in mice lacking both P-gp and BCRP compared to wild-type mice, highlighting the importance of these transporters in limiting the CNS penetration of this hydrophobic drug. These findings underscore the need to consider the role of multiple efflux transporters when assessing the brain penetration potential of small molecule drugs, including PPAR agonists. These *in vitro* findings align with previous *in vivo* research, indicating the CNS effects of peripherally administered PPAR agonists, implying their capacity to cross the BBB to a certain extent. For example, it was demonstrated that oral administration of the PPAR β agonist GW0742 reduced amyloid plaque load and neuroinflammation in a mouse model of Alzheimer's disease (Malm et al., 2015). Similarly, the systemic delivery of PPAR α and PPAR γ agonists was reported to have neuroprotective effects in various models of CNS injury and disease (Villapol, 2018). However, it is important to note that the observed CNS effects of PPAR agonists *in vivo* may not be solely attributed to their direct action in the brain, as they may also influence peripheral processes that indirectly modulate CNS function. For example, PPAR agonists have been shown to reduce systemic inflammation (Straus and Glass, 2007) and improve insulin sensitivity (Soccio et al., 2014), which could indirectly contribute to their neuroprotective effects.

In conclusion, the absence of a significant interaction between the examined PPAR agonists and BCRP in this *in vitro* assay suggests that this specific efflux transporter may not significantly impede their CNS penetration *in vivo*. Nevertheless, these preliminary findings should be approached with caution. Further investigations are necessary to directly evaluate the BBB permeability of these compounds and to examine potential interactions with other efflux transporters present at the BBB, such as ABCB1/P-glycoprotein and ABCC1/multidrug resistance protein 1, which are also integral to regulating drug access to the brain (Mahringer et al., 2009). Despite these considerations, the findings offer initial support for the concept of targeting neuroinflammation with PPAR agonists and highlight the importance of continued research into their mechanisms of CNS drug delivery.

Chapter 7 General Discussion and Future Directions

7.1 Summary of Findings

Original Findings
<ol style="list-style-type: none">1. Expression and Function of PPARs and FABPs in Rat Microglia:<ul style="list-style-type: none">• PPARα, PPARβ, and PPARγ are expressed in both neonatal and adult rats within the brain and spinal cord regions.• Compared to their adult counterparts, neonatal microglia in cortical and spinal cord cultures exhibit elevated levels of FABP5, FABP7, PPARα, and PPARβ.2. Microglial Responses to Inflammatory Stimuli:<ul style="list-style-type: none">• Activation of microglia and an increase in PPARβ mRNA expression in adult and neonatal cortical microglia, as well as in monocyte-derived microglia, have been observed following exposure to LPS and ATP.• The discovery of age-related and region-specific differences in microglial responses to LPS and ATP highlights the significance of considering both the developmental stage and the specific CNS region in the study of microglial function.3. Anti-inflammatory Effects of PPAR Agonists:<ul style="list-style-type: none">• The use of the PPARβ agonist GW0742 has been shown to inhibit the expression of pro-inflammatory cytokines TNFα and IL-1β in various models, including primary rat microglia, human monocyte-derived macrophages, and human monocyte-derived microglia.• Pretreatment of iMG cells with the PPARβ agonist GW0742 before low-level ATP stimulation alters the gene expression landscape across the entire transcriptome, elevating neuroprotective genes and suppressing inflammation-related genes.• The anti-inflammatory mechanisms of PPARβ agonists have been investigated, with gene expression analysis indicating that the modulation of NF-κB activity, shifting of cellular metabolism, and the promotion of autophagy may all be involved.4. ABCG2 transporters have been found not to significantly impede the CNS penetration of tested PPAR agonists, including GW0742, GW01516, WY14643, and rosiglitazone.5. Initial evidence suggests SUMOylation of PPARβ is minimal and the PPARβ agonist GW0742 appears to decrease rather than increase the low level SUMOylation observed.

7.2 Discussion

In the thesis investigations have shed light on the expression and functionalities of PPARs within microglia, the innate immune cells of the (CNS). The pivotal roles of microglia include the maintenance of brain homeostasis, the response to injury and infection, and the modulation of neuroinflammation, as identified by (Hanisch and Kettenmann, 2007). The dysregulation of microglial activation has been associated with a variety of neurodegenerative diseases, demonstrating the significance of uncovering pathways that modulate microglial functions as a primary research objective (Deczkowska et al., 2018).

The findings obtained demonstrate the presence of PPAR α , PPAR β , and PPAR γ in microglia from both neonatal and adult rats, derived from cortex and spinal cord tissues. This finding corroborates prior studies that have documented the expression of PPARs within the CNS (Warden et al., 2016a, Moreno et al., 2004, Braissant et al., 1996). It is particularly noteworthy that neonatal microglia display elevated expression levels of FABP5, FABP7, PPAR α , and PPAR β in comparison to adult microglia, suggesting that the expression of these proteins is regulated developmentally. This observation is in harmony with research highlighting the essential roles played by FABPs and PPARs in early brain development and the modulation of inflammation (Falomir-Lockhart et al., 2019, Zolezzi et al., 2017, Liu et al., 2010). Furthermore, the uniform expression of FABP8 observed in spinal microglia and astrocytes indicates its possible role in the physiology and pathology of the spinal cord, as proposed by (Zenker et al., 2014). These findings enrich the comprehension of the spatial and temporal dynamics governing the expression of FABP and PPAR within the CNS, alongside their potential contributions to neurodevelopmental and neuroinflammatory processes.

Microglial responses to inflammatory stimuli such as LPS and ATP were observed to differ, contingent upon the developmental stage and CNS region. It was found that microglia from the cortex of adult rats exhibited a more marked upregulation of the proinflammatory cytokine IL-1 β following LPS stimulation, compared to neonatal

and spinal cord microglia. This is in agreement with the findings reported by (Crain et al., 2013) and (Go et al., 2016). Such observations highlight the criticality of considering both age and tissue-specific factors in the investigation of microglial activation, thereby highlighting the exigency for further research that employs a broader array of inflammatory markers and variations in stimulus concentrations. Nevertheless, the limited sample size and the absence of a comprehensive comparative analysis between neonatal and adult spinal cord microglia, owing to constraints in sample availability, represent significant limitations of the study.

A principal discovery of this thesis is the upregulation of PPAR β mRNA expression in response to LPS or ATP stimulation, observed in both primary rat microglia and human monocyte-derived microglia (iMG). Despite PPAR β being less extensively studied relative to other PPAR isotypes, the findings imply a substantial role for this receptor in the modulation of microglial inflammatory responses. This notion is supported by previous research conducted by (Defaux et al., 2009) and (Dickey et al., 2017). The administration of the PPAR β agonist GW0742 was found to effectively diminish the expression of proinflammatory cytokines TNF- α and IL-1 β across various cellular models, including rat microglia, human monocyte-derived macrophages, and iMG cells. Additionally, RNA sequencing analyses disclosed that pretreatment with GW0742 altered the transcriptional profile of ATP-stimulated iMG cells, promoting the upregulation of neuroprotective genes whilst suppressing inflammation-related pathways. These results accentuate the anti-inflammatory and potentially neuroprotective implications of activating PPAR β in microglia. This aligns with earlier studies which have elucidated the anti-inflammatory properties of PPAR β agonists across different cell types and disease models (Kuang et al., 2012, Chehaibi et al., 2017, Tang et al., 2020).

In conjunction with the examination of PPAR roles within microglia, this thesis further delved into the potential interactions between selected PPAR agonists and the ABCG2 transporter, an eminent efflux transporter known for its contribution to multidrug resistance and the limitation it imposes on the brain entry of substrate

drugs (Hartz and Bauer, 2010, Kerr et al., 2011). Understanding the interaction between investigational drugs and major efflux transporters is deemed essential for the prediction of their pharmacokinetics, efficacy, and toxicity (Hartz and Bauer, 2010). Through the utilisation of a fluorescent substrate accumulation assay in cells overexpressing ABCG2, the study screened PPAR β agonists (GW0742 and GW01516), a PPAR α agonist (WY14643), and a PPAR γ agonist (rosiglitazone) for potential ABCG2 interactions. Notably, under the conditions tested, none of the evaluated PPAR agonists were observed to significantly influence the intracellular accumulation of the ABCG2 substrate, mitoxantrone, implying their unlikely role as ABCG2 substrates.

These *in vitro* observations are in harmony with prior *in vivo* research, which has documented the CNS effects of peripherally administered PPAR agonists, suggesting their ability to modulate neuroinflammation. For example, oral administration of the PPAR β agonist GW0742 has been shown to mitigate amyloid plaque load and neuroinflammation in a mouse model of Alzheimer's disease (Malm et al., 2015). Similarly, the systemic delivery of PPAR α and PPAR γ agonists has been associated with neuroprotective effects across various models of CNS injury and disease (Villapol, 2018). These *in vivo* studies do not, however, demonstrate that the effects observed are as a result of direct activation of PPARs in the CNS. Activation of PPARs in peripheral tissues may affect whole-body inflammatory status, which has indirect effects on the CNS. Although these preliminary outcomes imply that ABCG2 may not significantly hinder the CNS penetration of the tested PPAR agonists, further investigative efforts are needed to directly evaluate their BBB permeability and to explore possible interactions with other efflux transporters present at the BBB, such as P-glycoprotein (Mahringer et al., 2009). Nonetheless, these results provide initial evidence supporting the viability of targeting neuroinflammation with PPAR agonists and highlights the necessity for further exploration into their CNS drug delivery properties.

This thesis also investigated the role of post-translational modifications, specifically SUMOylation, in regulating PPAR β activity. SUMOylation has been implicated in modulating the stability, localization, and transcriptional activity of various nuclear receptors. Ligand-activated SUMOylation of nuclear receptors such as PPAR γ and LXR has been proposed as the mechanism underlying the anti-inflammatory actions of nuclear receptors in terms of inhibition of inflammatory cytokine transcription. (Treuter and Venteclef, 2011). Previous research (Koo et al., 2015) identified K104 as a SUMOylation site in PPAR β , reversed by SUMO-Specific Protease 2 (SEN2P), facilitating the activation of fatty acid oxidation (FAO) gene expression in muscle tissues.

These experiments aimed to further investigate the SUMOylation of PPAR β and its potential regulation by ligands. Using a SUMO pulldown protocol described by (Pourcet et al., 2013). Western blot analysis of the isolated SUMO-modified proteins revealed bands indicative of unmodified (~49-kDa) and SUMOylated (~55-kDa) PPAR β . The presence of multiple bands in this region suggests that PPAR β may undergo poly-SUMOylation, with SUMO3-modified versions of the receptor displaying more pronounced bands, particularly in the presence of PIAS1. This study suggests that PPAR β is slightly SUMOylated when compared to LXR, and this was reduced in the presence of GW0742. Given that the SUMOylation assay used involves overexpression of SUMO ligases and SUMO2/3, the very low level of SUMOylated PPAR β observed, and the reduction of SUMOylation in response to ligand, suggests that SUMOylation does not play a major role in the anti-inflammatory effects exerted by PPAR β agonists.

The development and validation of human microglia-like cell models derived from monocytes (iMG) or induced pluripotent stem cells (iPSCs) mark significant progress in the domain of neurological research. These models facilitate the investigation of human-specific microglial responses and genetic factors, addressing the constraints posed by animal models and primary human microglia (Abud et al., 2017, Muffat et al., 2016, Fattorelli et al., 2021). The incorporation of genetic risk factors, identified

in genome-wide association studies, such as variants in TREM2 and APOE, into human models enables the examination of their functional impact on microglia (McQuade et al., 2018, Claes et al., 2019). For example, research by Claes et al. (2019) involving iPSC-derived microglia from individuals carrying different TREM2 variants, probed into the repercussions of TREM2 deficiency on microglial function. It was discovered that microglia deficient in TREM2 showcased compromised phagocytosis of amyloid-beta plaques and exhibited altered inflammatory responses. These findings provide insight into the mechanisms through which TREM2 variants amplify the risk of Alzheimer's disease.

The findings of this study indicate that iMG cells, developed using protocols adapted from (Ohgidani et al., 2014) and (Banerjee et al., 2021), exhibit gene expression profiles that are distinct from those of peripheral monocytes and macrophages, featuring high relative expression of microglia-specific genes. Moreover, iMG cells were found to react to inflammatory stimuli by secreting cytokines and elevating microglial activation markers, mirroring the essential functional characteristics of brain-resident microglia. Although iPSC-derived microglia offer considerable potential, the experiences recounted in this study points out the complexities involved in refining differentiation protocols and the imperative for exhaustive validation of cellular phenotypes. This need for rigorous validation is echoed by findings from other research groups (McQuade et al., 2018, Haenseler et al., 2017).

7.3 Limitations and Future Work

Microglia originate from the foetal yolk sac, rendering microglia derived from monocytes distinct from brain-resident microglia (Ginhoux et al., 2010, Lenz and Nelson, 2018). While blood monocyte-derived microglia-like cells facilitate scalable production, they may be reflective of foetal/neonatal stages in terms of differentiation. Techniques to induce ageing could yield cell models that more closely resemble adult microglia (Banerjee et al., 2021). The utilisation of each

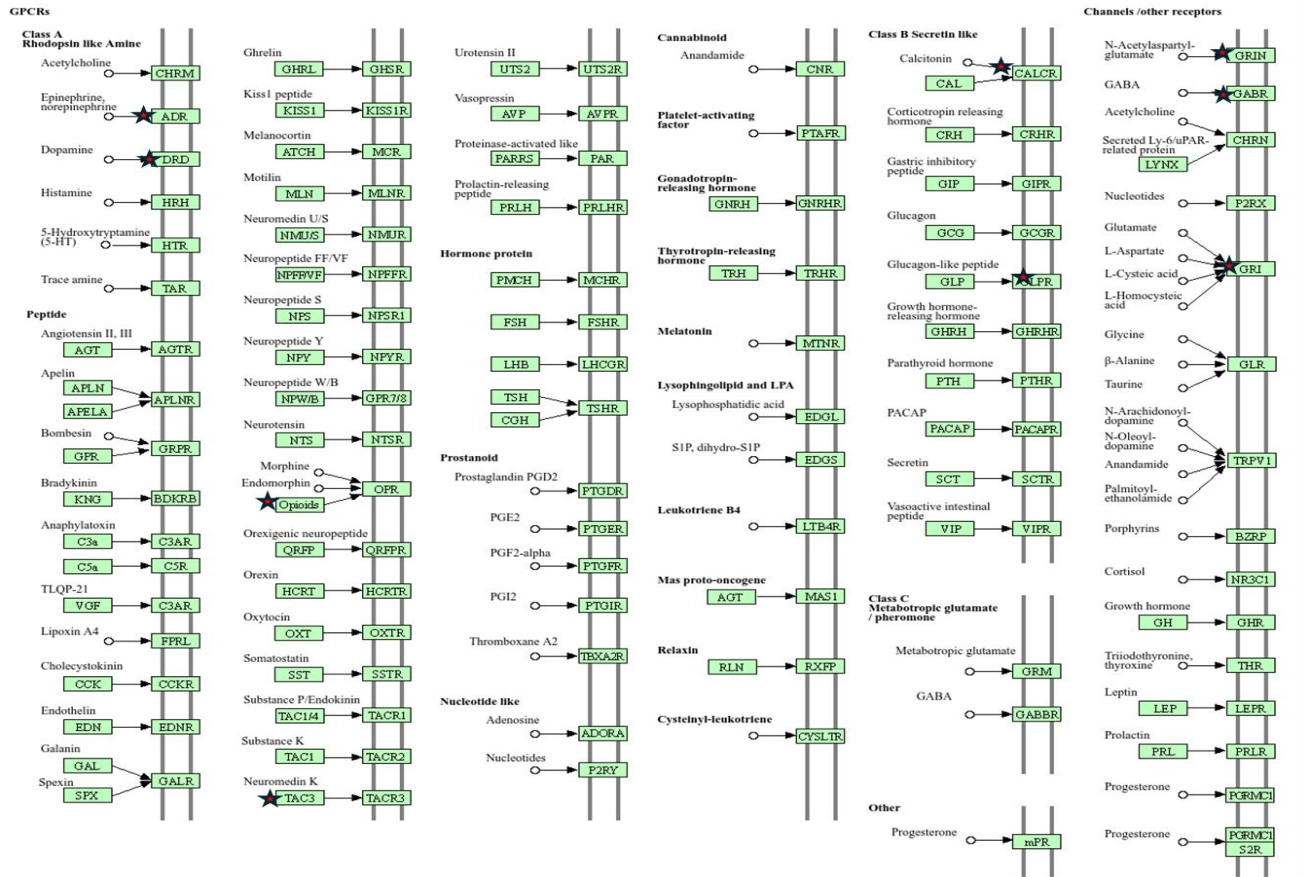
model system, with its unique advantages, collectively enriches the comprehension of human microglia biology. Furthermore, the focus of the current study on microglial monocultures will not encapsulate the intricate cellular interactions present within the brain. Future investigations should incorporate more sophisticated models, such as co-cultures with neurons, astrocytes, or brain organoids, to better simulate the brain's complexity (Abud et al., 2017, Haenseler et al., 2017).

Moreover, additional validation of iPSC-derived dopaminergic neurons and refinement of differentiation protocols are requisite for the establishment of reliable human cell models pertinent to the study of neurodegenerative diseases (Powell et al., 2021, Theka et al., 2013). Despite these limitations, the research demonstrates the therapeutic potential of targeting PPAR β in the modulation of neuroinflammation within neurological conditions. Models of human microglia derived from patient-specific monocytes could pave the way for personalised drug screening and the crafting of targeted therapies for neurodegenerative ailments.

In conclusion, this thesis contributes significantly to the elucidation of PPAR and FABP expression and functionality in microglia, the anti-inflammatory properties of PPAR β agonists, and the innovation of human microglia-like cell models. It underscores the therapeutic potential of modulating neuroinflammation through PPAR β targeting and lays the groundwork for future explorations utilising advanced human cell models for the investigation of disease mechanisms and the development of targeted treatments for neurological disorders. The RNA sequencing data derived from human monocyte-derived microglia not only validates the iMG model but also unveils the influence of PPAR β agonists on the microglial transcriptome, offering novel insights into the neuroprotective and anti-inflammatory mechanisms they harbour.

Appendices

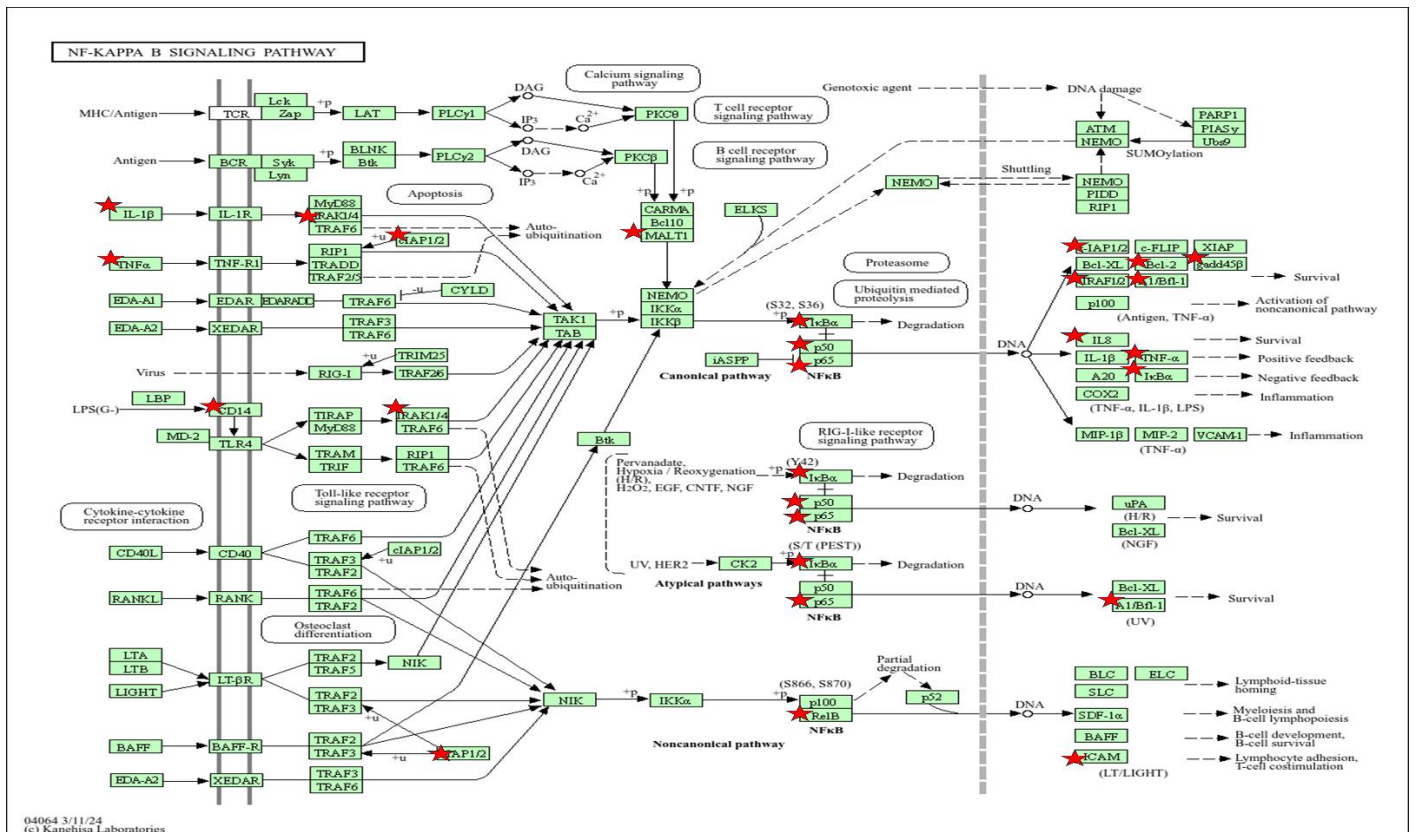
NEUROACTIVE LIGAND-RECEPTOR INTERACTION



04080 11/30/22
(c) Kamahisa Laboratories

ENSEMBL_GENE_ID	GENE NAME	Related Genes	Species
ENSG00000150594	adrenoceptor alpha 2A(ADRA2A)	RG	Homo sapiens
ENSG00000004948	calcitonin receptor(CALCR)	RG	Homo sapiens
ENSG00000149295	dopamine receptor D2(DRD2)	RG	Homo sapiens
ENSG00000102287	gamma-aminobutyric acid type A receptor subunit epsilon(GABRE)	RG	Homo sapiens
ENSG00000112164	glucagon like peptide 1 receptor(GLP1R)	RG	Homo sapiens
ENSG00000176884	glutamate ionotropic receptor NMDA type subunit 1(GRIN1)	RG	Homo sapiens
ENSG00000101327	prodynorphin(PDYN)	RG	Homo sapiens
ENSG00000166863	tachykinin precursor 3(TAC3)	RG	Homo sapiens

Figure 1: The unique and differential gene expression among iMG, iMacs, and monocyte cell types was analysed through various methods. An enrichment analysis with the unique genes expressed in iMG cells.



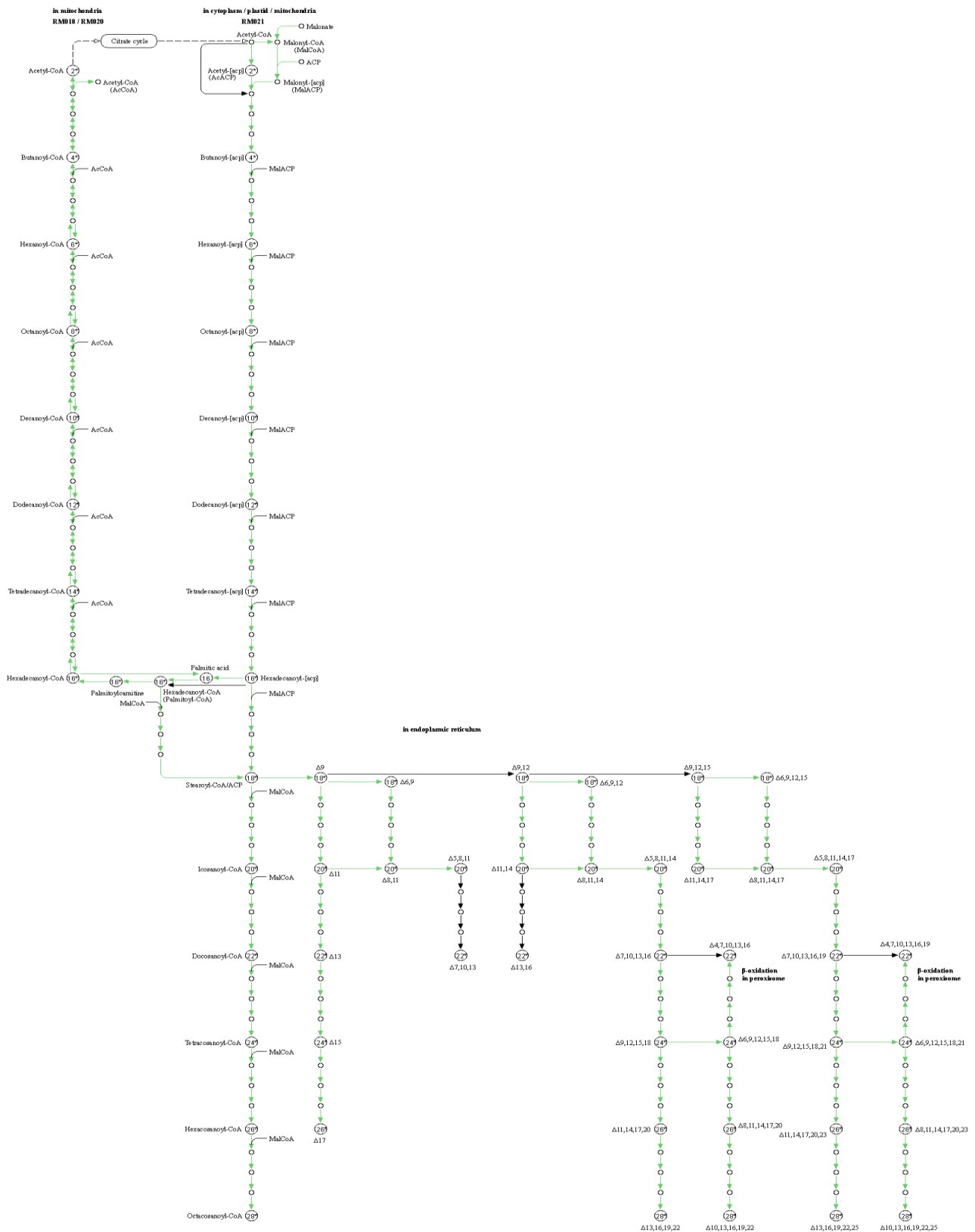
Current Gene List: List_1
Current Background: Homo sapiens
574 DAVID IDs
20 record(s)

[Download File](#)

ENSEMBL_GENE_ID	GENE NAME	Related Genes	Species
ENSG00000171791	BCL2 apoptosis regulator(BCL2)	RG	Homo sapiens
ENSG00000140379	BCL2 related protein 1(BCL2A1)	RG	Homo sapiens
ENSG00000276070	C-C motif chemokine ligand 4 like 2(CCL4L2)	RG	Homo sapiens
ENSG00000275302	C-C motif chemokine ligand 4(CCL4)	RG	Homo sapiens
ENSG00000169429	C-X-C motif chemokine ligand 8(CXCL8)	RG	Homo sapiens
ENSG00000170458	CD14 molecule(CD14)	RG	Homo sapiens
ENSG00000172175	MALT1 paracaspase(MALT1)	RG	Homo sapiens
ENSG00000100906	NFKB inhibitor alpha(NFKBIA)	RG	Homo sapiens
ENSG00000173039	RELA proto-oncogene, NF-kB subunit(RELA)	RG	Homo sapiens
ENSG00000104856	RELB proto-oncogene, NF-kB subunit(RELB)	RG	Homo sapiens
ENSG00000056558	TNF receptor associated factor 1(TRAF1)	RG	Homo sapiens
ENSG00000125735	TNF superfamily member 14(TNFSF14)	RG	Homo sapiens
ENSG00000023445	baculoviral IAP repeat containing 3(BIRC3)	RG	Homo sapiens
ENSG00000099860	growth arrest and DNA damage inducible beta(GADD45B)	RG	Homo sapiens
ENSG00000130222	growth arrest and DNA damage inducible gamma(GADD45G)	RG	Homo sapiens
ENSG00000090339	intercellular adhesion molecule 1(ICAM1)	RG	Homo sapiens
ENSG00000125538	interleukin 1 beta(IL1B)	RG	Homo sapiens
ENSG00000184216	interleukin 1 receptor associated kinase 1(IRAK1)	RG	Homo sapiens
ENSG00000109320	nuclear factor kappa B subunit 1(NFKB1)	RG	Homo sapiens
ENSG00000232810	tumor necrosis factor(TNF)	RG	Homo sapiens

Figure 2: Enrichment Analysis of Significantly Up-regulated Genes in KEGG Pathway: iMG treated with 50 μM ATP for 2 hours vs untreated cells. Genes were selected for GO analysis based on significant differential expression (adjusted p-value < 0.05).

FATTY ACID METABOLISM



Current Gene List: List_2
 Current Background: Homo sapiens
 522 DAVID IDs
 12 record(s)

 [Download File](#)

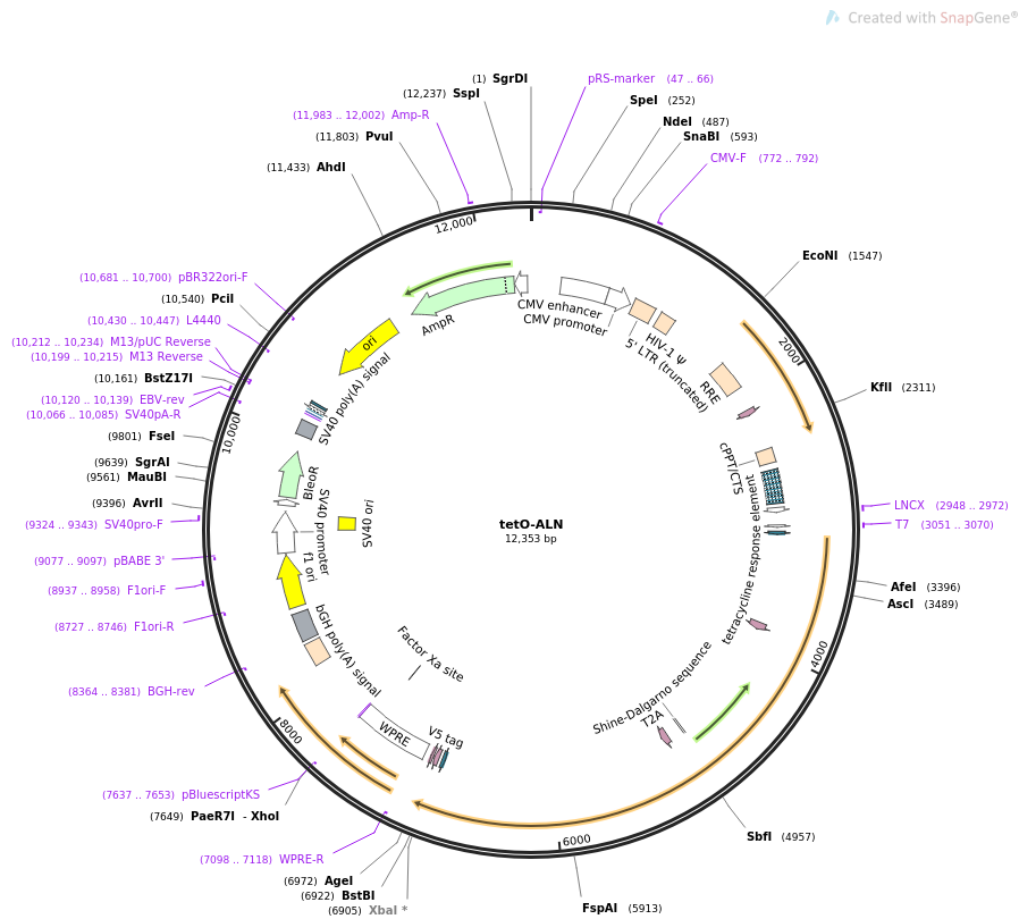
ENSEMBL_GENE_ID	GENE NAME	Related Genes	Species
ENSG00000188921	3-hydroxyacyl-CoA dehydratase 4(HACD4)	RG	Homo sapiens
ENSG00000012660	ELOVL fatty acid elongase 5(ELOVL5)	RG	Homo sapiens
ENSG00000120437	acetyl-CoA acetyltransferase 2(ACAT2)	RG	Homo sapiens
ENSG00000167315	acetyl-CoA acyltransferase 2(ACAA2)	RG	Homo sapiens
ENSG00000151726	acyl-CoA synthetase long chain family member 1(ACSL1)	RG	Homo sapiens
ENSG00000110090	carnitine palmitoyltransferase 1A(CPT1A)	RG	Homo sapiens
ENSG00000138029	hydroxyacyl-CoA dehydrogenase trifunctional multienzyme complex subunit beta(HADHB)	RG	Homo sapiens
ENSG00000138796	hydroxyacyl-CoA dehydrogenase(HADH)	RG	Homo sapiens
ENSG00000149084	hydroxysteroid 17-beta dehydrogenase 12(HSD17B12)	RG	Homo sapiens
ENSG00000133835	hydroxysteroid 17-beta dehydrogenase 4(HSD17B4)	RG	Homo sapiens
ENSG00000099194	stearoyl-CoA desaturase(SCD)	RG	Homo sapiens
ENSG00000116171	sterol carrier protein 2(SCP2)	RG	Homo sapiens

Figure 3: Enrichment Analysis of Significantly Up-regulated Genes in KEGG Pathways: iMG Pretreated with GW0742 for 1 hour then stimulated with 50 μ M ATP for 2 hours vs iMG stimulated with 50 μ M ATP only. Genes were selected for GO analysis based on significant differential only expression (adjusted p-value < 0.05).

ENSEMBL_GENE_ID	GENE NAME	Related Genes	Species
ENSG00000099624	ATP synthase F1 subunit delta(ATP5F1D)	RG	Homo sapiens
ENSG00000159199	ATP synthase membrane subunit c locus 1(ATP5MC1)	RG	Homo sapiens
ENSG00000135390	ATP synthase membrane subunit c locus 2(ATP5MC2)	RG	Homo sapiens
ENSG00000105327	BCL2 binding component 3(BBC3)	RG	Homo sapiens
ENSG00000115286	NADH:ubiquinone oxidoreductase core subunit S7(NDUFS7)	RG	Homo sapiens
ENSG00000110717	NADH:ubiquinone oxidoreductase core subunit S8(NDUFS8)	RG	Homo sapiens
ENSG00000167792	NADH:ubiquinone oxidoreductase core subunit V1(NDUFV1)	RG	Homo sapiens
ENSG00000130414	NADH:ubiquinone oxidoreductase subunit A10(NDUFA10)	RG	Homo sapiens
ENSG00000174886	NADH:ubiquinone oxidoreductase subunit A11(NDUFA11)	RG	Homo sapiens
ENSG00000139180	NADH:ubiquinone oxidoreductase subunit A9(NDUFA9)	RG	Homo sapiens
ENSG00000140990	NADH:ubiquinone oxidoreductase subunit B10(NDUFB10)	RG	Homo sapiens
ENSG00000099795	NADH:ubiquinone oxidoreductase subunit B7(NDUFB7)	RG	Homo sapiens
ENSG00000166136	NADH:ubiquinone oxidoreductase subunit B8(NDUFB8)	RG	Homo sapiens
ENSG00000145494	NADH:ubiquinone oxidoreductase subunit S6(NDUFS6)	RG	Homo sapiens
ENSG00000181222	RNA polymerase II subunit A(POLR2A)	RG	Homo sapiens
ENSG00000168002	RNA polymerase II subunit G(POLR2G)	RG	Homo sapiens
ENSG00000105258	RNA polymerase II subunit I(POLR2I)	RG	Homo sapiens
ENSG00000005075	RNA polymerase II subunit J(POLR2J)	RG	Homo sapiens
ENSG00000099817	RNA polymerase II, I and III subunit E(POLR2E)	RG	Homo sapiens
ENSG00000138107	actin related protein 1A(ACTR1A)	RG	Homo sapiens
ENSG00000161203	adaptor related protein complex 2 subunit mu 1(AP2M1)	RG	Homo sapiens
ENSG00000042753	adaptor related protein complex 2 subunit sigma 1(AP2S1)	RG	Homo sapiens
ENSG00000123395	autophagy related 101(ATG101)	RG	Homo sapiens
ENSG00000107175	cAMP responsive element binding protein 3(CREB3)	RG	Homo sapiens
ENSG00000146592	cAMP responsive element binding protein 5(CREB5)	RG	Homo sapiens
ENSG00000175416	clathrin light chain B(CLTB)	RG	Homo sapiens
ENSG00000131143	cytochrome c oxidase subunit 4I1(COX4I1)	RG	Homo sapiens
ENSG00000135940	cytochrome c oxidase subunit 5B(COX5B)	RG	Homo sapiens
ENSG00000126267	cytochrome c oxidase subunit 6B1(COX6B1)	RG	Homo sapiens
ENSG00000176340	cytochrome c oxidase subunit 8A(COX8A)	RG	Homo sapiens
ENSG00000175203	dynactin subunit 2(DCTN2)	RG	Homo sapiens
ENSG00000166847	dynactin subunit 5(DCTN5)	RG	Homo sapiens
ENSG00000233276	glutathione peroxidase 1(GPX1)	RG	Homo sapiens
ENSG00000116478	histone deacetylase 1(HDAC1)	RG	Homo sapiens
ENSG00000197386	huntingtin(HTT)	RG	Homo sapiens
ENSG00000126214	kinesin light chain 1(KLC1)	RG	Homo sapiens
ENSG00000228253	mitochondrially encoded ATP synthase 8(MT-ATP8)	RG	Homo sapiens
ENSG00000212907	mitochondrially encoded NADH 4L dehydrogenase(MT-ND4L)	RG	Homo sapiens
ENSG00000198695	mitochondrially encoded NADH dehydrogenase 6(MT-ND6)	RG	Homo sapiens
ENSG00000198938	mitochondrially encoded cytochrome c oxidase III(MT-CO3)	RG	Homo sapiens
ENSG00000137841	phospholipase C beta 2(PLCB2)	RG	Homo sapiens
ENSG00000149782	phospholipase C beta 3(PLCB3)	RG	Homo sapiens
ENSG00000277791	proteasome 20S subunit beta 3(PSMB3)	RG	Homo sapiens
ENSG00000100804	proteasome 20S subunit beta 5(PSMB5)	RG	Homo sapiens
ENSG00000013275	proteasome 26S subunit, ATPase 4(PSMC4)	RG	Homo sapiens
ENSG00000185627	proteasome 26S subunit, non-ATPase 13(PSMD13)	RG	Homo sapiens
ENSG00000169100	solute carrier family 25 member 6(SLC25A6)	RG	Homo sapiens
ENSG00000188229	tubulin beta 4B class IVb(TUBB4B)	RG	Homo sapiens
ENSG00000196230	tubulin beta class I(TUBB1)	RG	Homo sapiens
ENSG00000164405	ubiquinol-cytochrome c reductase complex III subunit VII(UQCRO)	RG	Homo sapiens

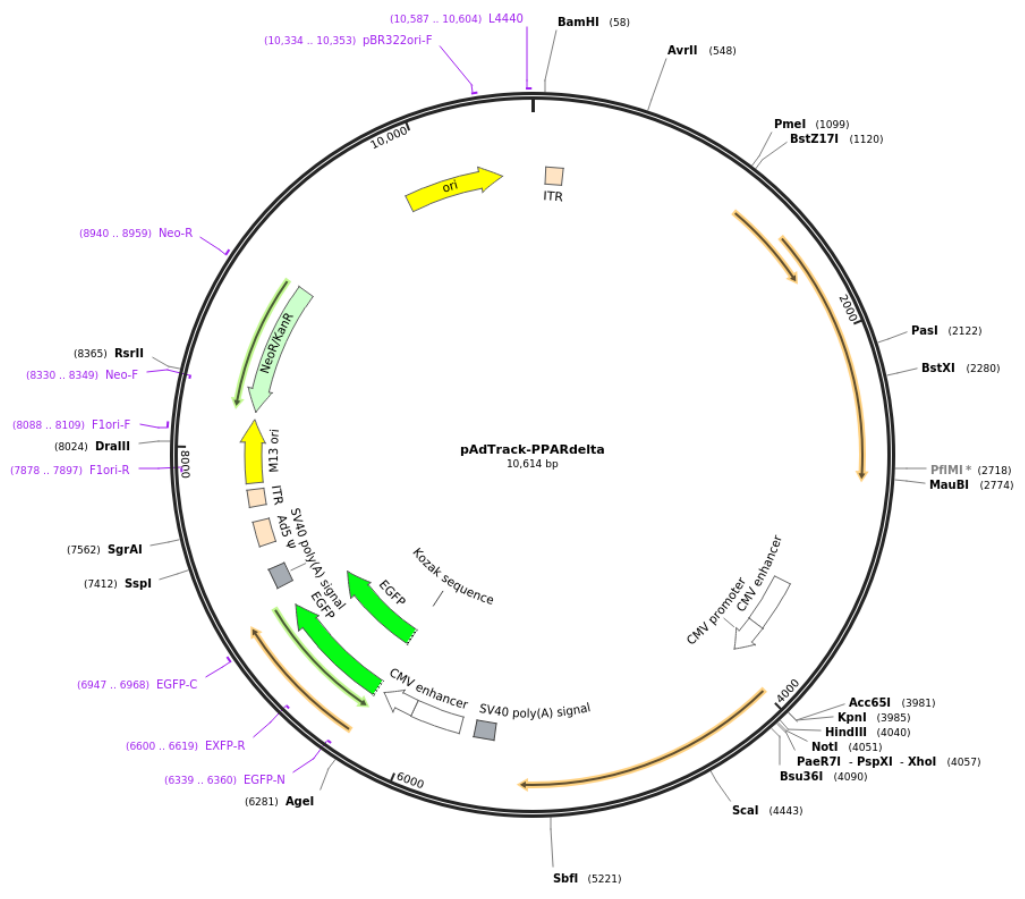
Figure 4: Enrichment Analysis of Significantly Down-regulated Genes in KEGG Pathways: iMG pretreated with GW0742 for 1 hour then stimulated with 50 μ M ATP for 2 hours to iMG stimulated with 50 μ M ATP only. Genes were selected for GO analysis based on significant differential expression only (adjusted p-value < 0.05).

Plasmid map for tetO-ALN (ASCL1-2A-LMX1B-2A-NURR1) was a gift from John Gearhart (Addgene plasmid # 43918 ; <http://n2t.net/addgene:43918> ; RRID:Addgene_43918) (Addis et al., 2011).



pAdTrack-PPARdelta pAdTrack-PPARdelta was a gift from Bert Vogelstein (Addgene plasmid # 16529; <http://n2t.net/addgene:16529> ; RRID:Addgene_16529) (He et al., 1999).

Created with SnapGene®



References

- ABBOTT, N. J., RÖNNBÄCK, L. & HANSSON, E. 2006. Astrocyte–endothelial interactions at the blood–brain barrier. *Nature reviews neuroscience*, 7, 41-53.
- ABUD, E. M., RAMIREZ, R. N., MARTINEZ, E. S., HEALY, L. M., NGUYEN, C. H., NEWMAN, S. A., YEROMIN, A. V., SCARFONE, V. M., MARSH, S. E. & FIMBRES, C. 2017. iPSC-derived human microglia-like cells to study neurological diseases. *Neuron*, 94, 278-293. e9.
- ADDIS, R. C., HSU, F.-C., WRIGHT, R. L., DICHTER, M. A., COULTER, D. A. & GEARHART, J. D. 2011. Efficient conversion of astrocytes to functional midbrain dopaminergic neurons using a single polycistronic vector. *PLoS one*, 6, e28719.
- ADHIKARY, T., WORTMANN, A., SCHUMANN, T., FINKERNAGEL, F., LIEBER, S., ROTH, K., TOH, P. M., DIEDERICH, W. E., NIST, A. & STIEWE, T. 2015. The transcriptional PPAR β/δ network in human macrophages defines a unique agonist-induced activation state. *Nucleic acids research*, 43, 5033-5051.
- AGARWAL, S., SANE, R., GALLARDO, J. L., OHLFEST, J. R. & ELMQUIST, W. F. 2010. Distribution of gefitinib to the brain is limited by P-glycoprotein (ABCB1) and breast cancer resistance protein (ABCG2)-mediated active efflux. *Journal of Pharmacology and Experimental Therapeutics*, 334, 147-155.
- AKIRA, S., UEMATSU, S. & TAKEUCHI, O. 2006. Pathogen recognition and innate immunity. *Cell*, 124, 783-801.
- ALLEN, J. D., VAN LOEVEZIJN, A., LAKHAI, J. M., VAN DER VALK, M., VAN TELLINGEN, O., REID, G., SCHELLENS, J. H., KOOMEN, G.-J. & SCHINKEL, A. H. 2002. Potent and specific inhibition of the breast cancer resistance protein multidrug transporter in vitro and in mouse intestine by a novel analogue of fumitremorgin C. *Molecular cancer therapeutics*, 1, 417-425.
- ALLEN, N. J., BENNETT, M. L., FOO, L. C., WANG, G. X., CHAKRABORTY, C., SMITH, S. J. & BARRES, B. A. 2012. Astrocyte glypicans 4 and 6 promote formation of excitatory synapses via GluA1 AMPA receptors. *Nature*, 486, 410-414.
- ALOISI, F. 2001. Immune function of microglia. *Glia*, 36, 165-179.
- ÁLVAREZ-GUARDIA, D., PALOMER, X., COLL, T., SERRANO, L., RODRÍGUEZ-CALVO, R., DAVIDSON, M. M., MERLOS, M., EL KOCHAIRI, I., MICHALIK, L. & WAHLI, W. 2011. PPAR β/δ activation blocks lipid-induced inflammatory pathways in mouse heart and human cardiac cells. *Biochimica et Biophysica Acta (BBA)-Molecular and Cell Biology of Lipids*, 1811, 59-67.

- AN, Y.-Q., ZHANG, C. T., DU, Y., ZHANG, M., TANG, S. S., HU, M., LONG, Y., SUN, H. B. & HONG, H. 2016. PPAR δ agonist GW0742 ameliorates A β 1-42-induced hippocampal neurotoxicity in mice. *Metabolic brain disease*, 31, 663-671.
- ARONOWSKI, J. & ZHAO, X. 2011. Molecular pathophysiology of cerebral hemorrhage: secondary brain injury. *Stroke*, 42, 1781-1786.
- ARTHUR, J. S. C. & LEY, S. C. 2013. Mitogen-activated protein kinases in innate immunity. *Nature Reviews Immunology*, 13, 679-692.
- BALISTRERI, C. R., COLONNA-ROMANO, G., LIO, D., CANDORE, G. & CARUSO, C. 2009. TLR4 polymorphisms and ageing: implications for the pathophysiology of age-related diseases. *Journal of clinical immunology*, 29, 406-415.
- BANERJEE, A., LU, Y., DO, K., MIZE, T., WU, X., CHEN, X. & CHEN, J. 2021. Validation of induced microglia-like cells (iMG Cells) for future studies of brain diseases. *Frontiers in Cellular Neuroscience*, 15, 629279.
- BARGER, S. W., GOODWIN, M. E., PORTER, M. M. & BEGGS, M. L. 2007. Glutamate release from activated microglia requires the oxidative burst and lipid peroxidation. *Journal of neurochemistry*, 101, 1205-1213.
- BARISH, G. D., DOWNES, M., ALAYNICK, W. A., YU, R. T., OCAMPO, C. B., BOOKOUT, A. L., MANGELSDORF, D. J. & EVANS, R. M. 2005. A nuclear receptor atlas: macrophage activation. *Molecular endocrinology*, 19, 2466-2477.
- BARROSO, E., DEL VALLE, J., PORQUET, D., SANTOS, A. M. V., SALVADÓ, L., RODRÍGUEZ-RODRÍGUEZ, R., GUTIÉRREZ, P., ANGLADA-HUGUET, M., ALBERCH, J. & CAMINS, A. 2013. Tau hyperphosphorylation and increased BACE1 and RAGE levels in the cortex of PPAR β/δ -null mice. *Biochimica et Biophysica Acta (BBA)-Molecular Basis of Disease*, 1832, 1241-1248.
- BARROSO, E., EYRE, E., PALOMER, X. & VÁZQUEZ-CARRERA, M. 2011. The peroxisome proliferator-activated receptor β/δ (PPAR β/δ) agonist GW501516 prevents TNF- α -induced NF- κ B activation in human HaCaT cells by reducing p65 acetylation through AMPK and SIRT1. *Biochemical pharmacology*, 81, 534-543.
- BARTANUSZ, V., JEZOVA, D., ALAJAJIAN, B. & DIGICAYLIOGLU, M. 2011. The blood-spinal cord barrier: morphology and clinical implications. *Annals of neurology*, 70, 194-206.
- BATISTA, F. A., TRIVELLA, D. B., BERNARDES, A., GRATIERI, J., OLIVEIRA, P. S., FIGUEIRA, A. C. M., WEBB, P. & POLIKARPOV, I. 2012. Structural insights into human peroxisome proliferator activated receptor delta (PPAR-delta) selective ligand binding. *PloS one*, 7, e33643.

- BAZINET, R. P. & LAYÉ, S. 2014. Polyunsaturated fatty acids and their metabolites in brain function and disease. *Nature reviews neuroscience*, 15, 771-785.
- BÉLANGER, M., ALLAMAN, I. & MAGISTRETTI, P. J. 2011. Brain energy metabolism: focus on astrocyte-neuron metabolic cooperation. *Cell metabolism*, 14, 724-738.
- BERGER, J. & MOLLER, D. E. 2002. The mechanisms of action of PPARs. *Annual review of medicine*, 53, 409-435.
- BERNAL, C., ARAYA, C., PALMA, V. & BRONFMAN, M. 2015. PPAR β/δ and PPAR γ maintain undifferentiated phenotypes of mouse adult neural precursor cells from the subventricular zone. *Frontiers in Cellular Neuroscience*, 9, 78.
- BERNARDO, A. & MINGHETTI, L. 2006. PPAR- γ agonists as regulators of microglial activation and brain inflammation. *Current pharmaceutical design*, 12, 93-109.
- BERNARDO, A. & MINGHETTI, L. 2008. Regulation of glial cell functions by PPAR- γ natural and synthetic agonists. *PPAR research*, 2008.
- BERNIER, L.-P. 2012. Purinergic regulation of inflammasome activation after central nervous system injury. *Journal of General Physiology*, 140, 571-575.
- BIANCHI, M. E. 2007. DAMPs, PAMPs and alarmins: all we need to know about danger. *Journal of Leucocyte Biology*, 81, 1-5.
- BIANCHI, R., GIAMBANCO, I. & DONATO, R. 2010. S100B/RAGE-dependent activation of microglia via NF- κ B and AP-1: Co-regulation of COX-2 expression by S100B, IL-1 β and TNF- α . *Neurobiology of aging*, 31, 665-677.
- BONECCHI, R., GALLIERA, E., BORRONI, E. M., CORSI, M. M., LOCATI, M. & MANTOVANI, A. 2009. Chemokines and chemokine receptors: an overview. *Frontiers in Bioscience-Landmark*, 14, 540-551.
- BONEVA, N. B., KAPLAMADZHIEV, D. B., SAHARA, S., KIKUCHI, H., PYKO, I. V., KIKUCHI, M., TONCHEV, A. B. & YAMASHIMA, T. 2011. Expression of fatty acid-binding proteins in adult hippocampal neurogenic niche of postischemic monkeys. *Hippocampus*, 21, 162-171.
- BRAISSANT, O., FOUFELLE, F., SCOTTO, C., DAUÇA, M. & WAHLI, W. 1996. Differential expression of peroxisome proliferator-activated receptors (PPARs): tissue distribution of PPAR-alpha, -beta, and -gamma in the adult rat. *Endocrinology*, 137, 354-366.
- BRAISSANT, O. & WAHLI, W. 1998. Differential expression of peroxisome proliferator-activated receptor- α , - β , and - γ during rat embryonic development. *Endocrinology*, 139, 2748-2754.

- BROWN, A. M. & RANSOM, B. R. 2007. Astrocyte glycogen and brain energy metabolism. *Glia*, 55, 1263-1271.
- BURGUILLOS, M. A., DEIERBORG, T., KAVANAGH, E., PERSSON, A., HAJJI, N., GARCIA-QUINTANILLA, A., CANO, J., BRUNDIN, P., ENGLUND, E. & VENERO, J. L. 2011. Caspase signalling controls microglia activation and neurotoxicity. *Nature*, 472, 319-324.
- BUTOVSKY, O., JEDRYCHOWSKI, M. P., MOORE, C. S., CIALIC, R., LANSER, A. J., GABRIELY, G., KOEGLSPERGER, T., DAKE, B., WU, P. M. & DOYKAN, C. E. 2014. Identification of a unique TGF- β -dependent molecular and functional signature in microglia. *Nature neuroscience*, 17, 131-143.
- BUTOVSKY, O., ZIV, Y., SCHWARTZ, A., LANDA, G., TALPALAR, A. E., PLUCHINO, S., MARTINO, G. & SCHWARTZ, M. 2006. Microglia activated by IL-4 or IFN- γ differentially induce neurogenesis and oligodendrogenesis from adult stem/progenitor cells. *Molecular and Cellular Neuroscience*, 31, 149-160.
- CALDEIRA, C., OLIVEIRA, A. F., CUNHA, C., VAZ, A. R., FALCÃO, A. S., FERNANDES, A. & BRITES, D. 2014. Microglia change from a reactive to an age-like phenotype with the time in culture. *Frontiers in cellular neuroscience*, 8, 152.
- CHAMBERS, I., COLBY, D., ROBERTSON, M., NICHOLS, J., LEE, S., TWEEDIE, S. & SMITH, A. 2003. Functional expression cloning of Nanog, a pluripotency sustaining factor in embryonic stem cells. *Cell*, 113, 643-655.
- CHANG, Y. P., FANG, K. M., LEE, T. I. & TZENG, S. F. 2006. Regulation of microglial activities by glial cell line derived neurotrophic factor. *Journal of cellular biochemistry*, 97, 501-511.
- CHEHAIBI, K., LE MAIRE, L., BRADONI, S., ESCOLA, J. C., BLANCO-VACA, F. & SLIMANE, M. N. 2017. Effect of PPAR- β/δ agonist GW0742 treatment in the acute phase response and blood-brain barrier permeability following brain injury. *Translational Research*, 182, 27-48.
- CHEN, C.-H., FERREIRA, J. C. B., GROSS, E. R. & MOCHLY-ROSEN, D. 2014. Targeting aldehyde dehydrogenase 2: new therapeutic opportunities. *Physiological reviews*, 94, 1-34.
- CHEN, W. W., ZHANG, X. & HUANG, W. J. 2016. Role of neuroinflammation in neurodegenerative diseases. *Molecular medicine reports*, 13, 3391-3396.
- CHHOR, V., LE CHARPENTIER, T., LEBON, S., ORÉ, M.-V., CELADOR, I. L., JOSSERAND, J., DEGOS, V., JACOTOT, E., HAGBERG, H. & SÄVMAN, K. 2013. Characterization of phenotype markers and neuronotoxic potential of polarised primary microglia in vitro. *Brain, behavior, and immunity*, 32, 70-85.

- CHOI, S. S., LEE, H. J., LIM, I., SATOH, J.-I. & KIM, S. U. 2014. Human astrocytes: secretome profiles of cytokines and chemokines. *PLoS one*, 9, e92325.
- CHRISTOPHERSON, K. S., ULLIAN, E. M., STOKES, C. C., MULLOWNEY, C. E., HELL, J. W., AGAH, A., LAWLER, J., MOSHER, D. F., BORNSTEIN, P. & BARRES, B. A. 2005. Thrombospondins are astrocyte-secreted proteins that promote CNS synaptogenesis. *Cell*, 120, 421-433.
- CLAES, C., VAN DEN DAELE, J., BOON, R., SCHOUTEDEN, S., COLOMBO, A., MONASOR, L. S., FIERIS, M., ORDOVÁS, L., NAMI, F. & BOHRMANN, B. 2019. Human stem cell-derived monocytes and microglia-like cells reveal impaired amyloid plaque clearance upon heterozygous or homozygous loss of TREM2. *Alzheimer's & Dementia*, 15, 453-464.
- CLARKE, L. E., LIDDELOW, S. A., CHAKRABORTY, C., MÜNCH, A. E., HEIMAN, M. & BARRES, B. A. 2018. Normal aging induces A1-like astrocyte reactivity. *Proceedings of the National Academy of Sciences*, 115, E1896-E1905.
- COLASUONNO, F., MARIOLI, C., TARTAGLIA, M., BERTINI, E., COMPAGNUCCI, C. & MORENO, S. 2022. New insights into the neurodegeneration mechanisms underlying riboflavin transporter deficiency (RTD): involvement of energy dysmetabolism and cytoskeletal derangement. *Biomedicines*, 10, 1329.
- COLL, T., RODRÍGUEZ-CALVO, R., BARROSO, E., SERRANO, L., EYRE, E., PALOMER, X. & VÁZQUEZ-CARRERA, M. 2009. Peroxisome proliferator-activated receptor (PPAR) β/δ : a new potential therapeutic target for the treatment of metabolic syndrome. *Current molecular pharmacology*, 2, 46-55.
- COLLIER, T. J., KANAAN, N. M. & KORDOWER, J. H. 2017. Aging and Parkinson's disease: Different sides of the same coin? *Movement Disorders*, 32, 983-990.
- COLLINO, M., PATEL, N. S. & THIEMERMANN, C. 2008. PPARs as new therapeutic targets for the treatment of cerebral ischemia/reperfusion injury. *Therapeutic Advances in Cardiovascular Disease*, 2, 179-197.
- COMBS, C. K., JOHNSON, D. E., KARLO, J. C., CANNADY, S. B. & LANDRETH, G. E. 2000. Inflammatory mechanisms in Alzheimer's disease: inhibition of β -amyloid-stimulated proinflammatory responses and neurotoxicity by PPAR γ agonists. *Journal of Neuroscience*, 20, 558-567.
- CORE, R. T. 2019. R: A language and environment for statistical computing. (No Title).

- COX, M. H., KAPOOR, P., BRIGGS, D. A. & KERR, I. D. 2018. Residues contributing to drug transport by ABCG2 are localised to multiple drug-binding pockets. *Biochemical Journal*, 475, 1553-1567.
- CRAIN, J. M., NIKODEMOVA, M. & WATTERS, J. J. 2013. Microglia express distinct M1 and M2 phenotypic markers in the postnatal and adult central nervous system in male and female mice. *Journal of neuroscience research*, 91, 1143-1151.
- CUI, P., LU, W., WANG, J., WANG, F., ZHANG, X., HOU, X., XU, F., LIANG, Y., CHAI, G. & HAO, J. 2023. Microglia/macrophages require vitamin D signaling to restrain neuroinflammation and brain injury in a murine ischemic stroke model. *Journal of Neuroinflammation*, 20, 1-20.
- DALLAS, S., MILLER, D. S. & BENDAYAN, R. 2006. Multidrug resistance-associated proteins: expression and function in the central nervous system. *Pharmacological reviews*, 58, 140-161.
- DAMANI, M. R., ZHAO, L., FONTAINHAS, A. M., AMARAL, J., FARISS, R. N. & WONG, W. T. 2011. Age-related alterations in the dynamic behavior of microglia. *Aging cell*, 10, 263-276.
- DAVALOS, D., GRUTZENDLER, J., YANG, G., KIM, J. V., ZUO, Y., JUNG, S., LITTMAN, D. R., DUSTIN, M. L. & GAN, W.-B. 2005. ATP mediates rapid microglial response to local brain injury in vivo. *Nature neuroscience*, 8, 752-758.
- DE BENEDICTIS, C. A., HAFFKE, C., HAGMEYER, S., SAUER, A. K. & GRABRUCKER, A. M. 2021. Expression analysis of zinc transporters in nervous tissue cells reveals neuronal and synaptic localization of ZIP4. *International Journal of Molecular Sciences*, 22, 4511.
- DE BIASE, L. M., SCHUEBEL, K. E., FUSFELD, Z. H., JAIR, K., HAWES, I. A., CIMBRO, R., ZHANG, H.-Y., LIU, Q.-R., SHEN, H. & XI, Z.-X. 2017. Local cues establish and maintain region-specific phenotypes of basal ganglia microglia. *Neuron*, 95, 341-356. e6.
- DE LANGE, P., LOMBARDI, A., SILVESTRI, E., GOGLIA, F., LANNI, A. & MORENO, M. 2008. Peroxisome proliferator-activated receptor delta: a conserved director of lipid homeostasis through regulation of the oxidative capacity of muscle. *PPAR research*, 2008.
- DE WIT, N. M., DEN HOEDT, S., MARTINEZ-MARTINEZ, P., ROZEMULLER, A. J., MULDER, M. T. & DE VRIES, H. E. 2019. Astrocytic ceramide as possible indicator of neuroinflammation. *Journal of neuroinflammation*, 16, 48.
- DECZKOWSKA, A., KEREN-SHAUL, H., WEINER, A., COLONNA, M., SCHWARTZ, M. & AMIT, I. 2018. Disease-associated microglia: a universal immune sensor of neurodegeneration. *Cell*, 173, 1073-1081.

- DEFAUX, A., ZURICH, M.-G., BRAISSANT, O., HONEGGER, P. & MONNET-TSCHUDI, F. 2009. Effects of the PPAR- β agonist GW501516 in an in vitro model of brain inflammation and antibody-induced demyelination. *Journal of neuroinflammation*, 6, 1-13.
- DEPLANQUE, D., GELÉ, P., PÉTRAUULT, O., SIX, I., FURMAN, C., BOULY, M., NION, S., DUPUIS, B., LEYS, D. & FRUCHART, J.-C. 2003. Peroxisome proliferator-activated receptor- α activation as a mechanism of preventive neuroprotection induced by chronic fenofibrate treatment. *Journal of Neuroscience*, 23, 6264-6271.
- DI VIRGILIO, F., SARTI, A. C. & COUTINHO-SILVA, R. 2020. Purinergic signaling, DAMPs, and inflammation. *American Journal of Physiology-Cell Physiology*, 318, C832-C835.
- DICKEY, A. S., SANCHEZ, D. N., ARREOLA, M., SAMPAT, K. R., FAN, W., ARBEZ, N., AKIMOV, S., VAN KANEGAN, M. J., OHNISHI, K. & GILMORE-HALL, S. K. 2017. PPAR δ activation by bexarotene promotes neuroprotection by restoring bioenergetic and quality control homeostasis. *Science translational medicine*, 9, eaal2332.
- DIEZKO, R. & SUSKE, G. 2013. Ligand binding reduces SUMOylation of the peroxisome proliferator-activated receptor γ (PPAR γ) activation function 1 (AF1) domain. *PLoS One*, 8, e66947.
- DISKIN, C. & PÅLSSON-MCDERMOTT, E. M. 2018. Metabolic modulation in macrophage effector function. *Frontiers in immunology*, 9, 336365.
- DOBIN, A., DAVIS, C. A., SCHLESINGER, F., DRENKOW, J., ZALESKI, C., JHA, S., BATUT, P., CHAISSON, M. & GINGERAS, T. R. 2013. STAR: ultrafast universal RNA-seq aligner. *Bioinformatics*, 29, 15-21.
- DOUGHERTY, K. D., DREYFUS, C. F. & BLACK, I. B. 2000. Brain-derived neurotrophic factor in astrocytes, oligodendrocytes, and microglia/macrophages after spinal cord injury. *Neurobiology of disease*, 7, 574-585.
- DOUVARAS, P., SUN, B., WANG, M., KRUGLIKOV, I., LALLOS, G., ZIMMER, M., TERRENOIRE, C., ZHANG, B., GANDY, S. & SCHADT, E. 2017. Directed differentiation of human pluripotent stem cells to microglia. *Stem cell reports*, 8, 1516-1524.
- DRESSEL, U., ALLEN, T. L., PIPPAL, J. B., ROHDE, P. R., LAU, P. & MUSCAT, G. E. 2003. The peroxisome proliferator-activated receptor β/δ agonist, GW501516, regulates the expression of genes involved in lipid catabolism and energy uncoupling in skeletal muscle cells. *Molecular endocrinology*, 17, 2477-2493.
- DREW, P. D., XU, J. & RACKE, M. K. 2008. PPAR- γ : therapeutic potential for multiple sclerosis. *PPAR research*, 2008.
- DU, Y., LU, Z., YANG, D., WANG, D., JIANG, L., SHEN, Y., DU, Q. & YU, W. 2021. MerTK inhibits the activation of the NLRP3 inflammasome

after subarachnoid hemorrhage by inducing autophagy. *Brain Research*, 1766, 147525.

- DUNN, S. E., BHAT, R., STRAUS, D. S., SOBEL, R. A., AXTELL, R., JOHNSON, A., NGUYEN, K., MUKUNDAN, L., MOSHKOVA, M. & DUGAS, J. C. 2010. Peroxisome proliferator-activated receptor δ limits the expansion of pathogenic Th cells during central nervous system autoimmunity. *Journal of Experimental Medicine*, 207, 1599-1608.
- EDAN, R. 2019. Microglia respond to exogenous and endogenous activating stimuli differently during development. *PhD thesis, The University of Nottingham*.
- ELMORE, M. R., NAJAFI, A. R., KOIKE, M. A., DAGHER, N. N., SPANGENBERG, E. E., RICE, R. A., KITAZAWA, M., MATUSOW, B., NGUYEN, H. & WEST, B. L. 2014. Colony-stimulating factor 1 receptor signaling is necessary for microglia viability, unmasking a microglia progenitor cell in the adult brain. *Neuron*, 82, 380-397.
- ENOKIZONO, J., KUSUHARA, H. & SUGIYAMA, Y. 2007. Effect of breast cancer resistance protein (Bcrp/Abcg2) on the disposition of phytoestrogens. *Molecular pharmacology*, 72, 967-975.
- ESCARTIN, C., GALEA, E., LAKATOS, A., O'CALLAGHAN, J. P., PETZOLD, G. C., SERRANO-POZO, A., STEINHÄUSER, C., VOLTERRA, A., CARMIGNOTO, G. & AGARWAL, A. 2021. Reactive astrocyte nomenclature, definitions, and future directions. *Nature neuroscience*, 24, 312-325.
- FALOMIR-LOCKHART, L. J., CAVAZZUTTI, G. F., GIMÉNEZ, E. & TOSCANI, A. M. 2019. Fatty Acid Signaling Mechanisms in Neural Cells: Fatty Acid Receptors. *Frontiers in Cellular Neuroscience*, 13.
- FALOMIR LOCKHART, L. J., CAVAZZUTTI, G. F., GIMÉNEZ, E. & TOSCANI, A. M. 2019. Fatty Acid Signaling Mechanisms in Neural Cells: Fatty Acid Receptors. *Frontiers in cellular neuroscience*, 13, 162.
- FAN, Y., WANG, Y., TANG, Z., ZHANG, H., QIN, X., ZHU, Y., GUAN, Y., WANG, X., STAELS, B. & CHIEN, S. 2008. Suppression of pro-inflammatory adhesion molecules by PPAR- δ in human vascular endothelial cells. *Arteriosclerosis, thrombosis, and vascular biology*, 28, 315-321.
- FATTORELLI, N., MARTINEZ-MURIANA, A., WOLFS, L., GERIC, I., DE STROOPER, B. & MANCUSO, R. 2021. Stem-cell-derived human microglia transplanted into mouse brain to study human disease. *Nature protocols*, 16, 1013-1033.
- FENTON, M. J. & GOLENBOCK, D. T. 1998. LPS-binding proteins and receptors. *Journal of leukocyte biology*, 64, 25-32.

- FERRARI, D., PIZZIRANI, C., ADINOLFI, E., LEMOLI, R. M., CURTI, A., IDZKO, M., PANTHER, E. & DI VIRGILIO, F. 2006. The P2X7 receptor: a key player in IL-1 processing and release. *The Journal of Immunology*, 176, 3877-3883.
- FIDALEO, M., FANELLI, F., PAOLA CERU, M. & MORENO, S. 2014. Neuroprotective properties of peroxisome proliferator-activated receptor alpha (PPAR α) and its lipid ligands. *Current medicinal chemistry*, 21, 2803-2821.
- FLOTHO, A. & MELCHIOR, F. 2013. Sumoylation: a regulatory protein modification in health and disease. *Annual review of biochemistry*, 82, 357-385.
- FORMAN, B. M., CHEN, J. & EVANS, R. M. 1997. Hypolipidemic drugs, polyunsaturated fatty acids, and eicosanoids are ligands for peroxisome proliferator-activated receptors α and δ . *Proceedings of the National Academy of Sciences*, 94, 4312-4317.
- FRANCO, R. & CEDAZO-MINGUEZ, A. 2014. Successful therapies for Alzheimer's disease: why so many in animal models and none in humans? *Frontiers in pharmacology*, 5, 146.
- FU, R., SHEN, Q., XU, P., LUO, J. J. & TANG, Y. 2014. Phagocytosis of microglia in the central nervous system diseases. *Molecular neurobiology*, 49, 1422-1434.
- FURUHASHI, M. & HOTAMISLIGIL, G. S. 2008. Fatty acid-binding proteins: role in metabolic diseases and potential as drug targets. *Nature reviews Drug discovery*, 7, 489-503.
- GALATRO, T. F., HOLTMAN, I. R., LERARIO, A. M., VAINCHTEIN, I. D., BROUWER, N., SOLA, P. R., VERAS, M. M., PEREIRA, T. F., LEITE, R. E. & MÖLLER, T. 2017. Transcriptomic analysis of purified human cortical microglia reveals age-associated changes. *Nature neuroscience*, 20, 1162-1171.
- GARCÍA-MARTÍN, E., ESGUEVILLAS, G., SERRADOR, M., ALONSO-NAVARRO, H., NAVACERRADA, F., AMO, G., GARCÍA-ALBEA, E., AGÚNDEZ, J. A. & JIMÉNEZ-JIMÉNEZ, F. J. 2018. Gamma-aminobutyric acid (GABA) receptors GABRA4, GABRE, and GABRQ gene polymorphisms and risk for migraine. *Journal of Neural Transmission*, 125, 689-698.
- GHISLETTI, S., HUANG, W., OGAWA, S., PASCUAL, G., LIN, M.-E., WILLSON, T. M., ROSENFELD, M. G. & GLASS, C. K. 2007. Parallel SUMOylation-dependent pathways mediate gene-and signal-specific transrepression by LXRs and PPAR γ . *Molecular cell*, 25, 57-70.
- GHOSH, S., CASTILLO, E., FRIAS, E. S. & SWANSON, R. A. 2018. Bioenergetic regulation of microglia. *Glia*, 66, 1200-1212.

- GINHOUX, F., GRETER, M., LEBOEUF, M., NANDI, S., SEE, P., GOKHAN, S., MEHLER, M. F., CONWAY, S. J., NG, L. G. & STANLEY, E. R. 2010. Fate mapping analysis reveals that adult microglia derive from primitive macrophages. *Science*, 330, 841-845.
- GINHOUX, F., LIM, S., HOEFFEL, G., LOW, D. & HUBER, T. 2013. Origin and differentiation of microglia. *Frontiers in cellular neuroscience*, 7, 45.
- GLASS, C. K., SAIJO, K., WINNER, B., MARCHETTO, M. C. & GAGE, F. H. 2010. Mechanisms underlying inflammation in neurodegeneration. *Cell*, 140, 918-934.
- GO, M., KOU, J., LIM, J.-E., YANG, J. & FUKUCHI, K.-I. 2016. Microglial response to LPS increases in wild-type mice during aging but diminishes in an Alzheimer's mouse model: implication of TLR4 signaling in disease progression. *Biochemical and biophysical research communications*, 479, 331-337.
- GOEDERT, M., JAKES, R. & SPILLANTINI, M. G. 2017. The synucleinopathies: twenty years on. *Journal of Parkinson's disease*, 7, S51-S69.
- GÓMEZ-NICOLA, D., FRANSEN, N. L., SUZZI, S. & PERRY, V. H. 2013. Regulation of microglial proliferation during chronic neurodegeneration. *Journal of Neuroscience*, 33, 2481-2493.
- GOMEZ-NICOLA, D. & PERRY, V. H. 2015. Microglial dynamics and role in the healthy and diseased brain: a paradigm of functional plasticity. *The Neuroscientist*, 21, 169-184.
- GOSELIN, D., SKOLA, D., COUFAL, N. G., HOLTMAN, I. R., SCHLACHETZKI, J. C., SAJTI, E., JAEGER, B. N., O'CONNOR, C., FITZPATRICK, C. & PASILLAS, M. P. 2017. An environment-dependent transcriptional network specifies human microglia identity. *Science*, 356, eaal3222.
- GRABERT, K., MICHOEL, T., KARAVOLOS, M. H., CLOHISEY, S., BAILLIE, J. K., STEVENS, M. P., FREEMAN, T. C., SUMMERS, K. M. & MCCOLL, B. W. 2016. Microglial brain region– dependent diversity and selective regional sensitivities to aging. *Nature neuroscience*, 19, 504-516.
- GRAHAM, T. L., MOOKHERJEE, C., SUCKLING, K. E., PALMER, C. N. & PATEL, L. 2005. The PPAR δ agonist GW0742X reduces atherosclerosis in LDLR $-/-$ mice. *Atherosclerosis*, 181, 29-37.
- GROSS, O., THOMAS, C. J., GUARDA, G. & TSCHOPP, J. 2011. The inflammasome: an integrated view. *Immunological reviews*, 243, 136-151.

- GUO, H., CALLAWAY, J. B. & TING, J. P. 2015. Inflammasomes: mechanism of action, role in disease, and therapeutics. *Nature medicine*, 21, 677-687.
- GUO, Q., WANG, G. & NAMURA, S. 2010. Fenofibrate improves cerebral blood flow after middle cerebral artery occlusion in mice. *Journal of Cerebral Blood Flow & Metabolism*, 30, 70-78.
- GYONEVA, S., DAVALOS, D., BISWAS, D., SWANGER, S. A., GARNIER-AMBLARD, E., LOTH, F., AKASSOGLU, K. & TRAYNELIS, S. F. 2014. Systemic inflammation regulates microglial responses to tissue damage in vivo. *Glia*, 62, 1345-1360.
- HAENSELER, W., ZAMBON, F., LEE, H., VOWLES, J., RINALDI, F., DUGGAL, G., HOULDEN, H., GWINN, K., WRAY, S. & LUK, K. C. 2017. Excess α -synuclein compromises phagocytosis in iPSC-derived macrophages. *Scientific reports*, 7, 9003.
- HAITINA, T., LINDBLOM, J., RENSTRÖM, T. & FREDRIKSSON, R. 2006. Fourteen novel human members of mitochondrial solute carrier family 25 (SLC25) widely expressed in the central nervous system. *Genomics*, 88, 779-790.
- HALL, M., QUIGNODON, L. & DESVERGNE, B. 2008. Peroxisome proliferator-activated receptor β/δ in the brain: facts and hypothesis. *PPAR research*, 2008.
- HAMMOND, T. R., DUFORT, C., DISSING-OLESEN, L., GIERA, S., YOUNG, A., WYSOKER, A., WALKER, A. J., GERGITS, F., SEGEL, M. & NEMESH, J. 2019. Single-cell RNA sequencing of microglia throughout the mouse lifespan and in the injured brain reveals complex cell-state changes. *Immunity*, 50, 253-271. e6.
- HANISCH, U.-K. & KETTENMANN, H. 2007. Microglia: active sensor and versatile effector cells in the normal and pathologic brain. *Nature neuroscience*, 10, 1387-1394.
- HANISCH, U. K. 2002. Microglia as a source and target of cytokines. *Glia*, 40, 140-155.
- HARA, T., TAKAMURA, A., KISHI, C., IEMURA, S.-I., NATSUME, T., GUAN, J.-L. & MIZUSHIMA, N. 2008. FIP200, a ULK-interacting protein, is required for autophagosome formation in mammalian cells. *The Journal of cell biology*, 181, 497-510.
- HARTZ, A. & BAUER, B. 2010. Regulation of ABC transporters at the blood-brain barrier: new targets for CNS therapy. *Molecular interventions*, 10, 293.
- HAYDEN, M. S. & GHOSH, S. 2008. Shared principles in NF- κ B signaling. *Cell*, 132, 344-362.

- HE, T.-C., CHAN, T. A., VOGELSTEIN, B. & KINZLER, K. W. 1999. PPAR δ is an APC-regulated target of nonsteroidal anti-inflammatory drugs. *Cell*, 99, 335-345.
- HEFENDEHL, J. K., NEHER, J. J., SÜHS, R. B., KOHSAKA, S., SKODRAS, A. & JUCKER, M. 2014. Homeostatic and injury-induced microglia behavior in the aging brain. *Aging cell*, 13, 60-69.
- HENDRICKX, D. A., VAN EDEN, C. G., SCHUURMAN, K. G., HAMANN, J. & HUITINGA, I. 2017. Staining of HLA-DR, Iba1 and CD68 in human microglia reveals partially overlapping expression depending on cellular morphology and pathology. *Journal of neuroimmunology*, 309, 12-22.
- HENEKA, M. T., CARSON, M. J., EL KHOURY, J., LANDRETH, G. E., BROSSERON, F., FEINSTEIN, D. L., JACOBS, A. H., WYSS-CORAY, T., VITORICA, J. & RANSOHOFF, R. M. 2015. Neuroinflammation in Alzheimer's disease. *The Lancet Neurology*, 14, 388-405.
- HENEKA, M. T. & LANDRETH, G. E. 2007. PPARs in the brain. *Biochimica et biophysica acta (BBA)-molecular and cell biology of lipids*, 1771, 1031-1045.
- HENEKA, M. T., SASTRE, M., DUMITRESCU-OZIMEK, L., HANKE, A., DEWACHTER, I., KUIPERI, C., O'BANION, K., KLOCKGETHER, T., VAN LEUVEN, F. & LANDRETH, G. E. 2005. Acute treatment with the PPAR γ agonist pioglitazone and ibuprofen reduces glial inflammation and A β 1-42 levels in APPV717I transgenic mice. *Brain*, 128, 1442-1453.
- HENNEBERGER, C., PAPOUIN, T., OLIET, S. H. & RUSAKOV, D. A. 2010. Long-term potentiation depends on release of D-serine from astrocytes. *Nature*, 463, 232-236.
- HEO, H.-R., SONG, H., KIM, H.-R., LEE, J. E., CHUNG, Y. G., KIM, W. J., YANG, S.-R., KIM, K.-S., CHUN, T. & LEE, D. R. 2018. Reprogramming mechanisms influence the maturation of hematopoietic progenitors from human pluripotent stem cells. *Cell Death & Disease*, 9, 1090.
- HICKMAN, S. E., ALLISON, E. K. & EL KHOURY, J. 2008. Microglial dysfunction and defective β -amyloid clearance pathways in aging Alzheimer's disease mice. *Journal of Neuroscience*, 28, 8354-8360.
- HIDE, I., TANAKA, M., INOUE, A., NAKAJIMA, K., KOHSAKA, S., INOUE, K. & NAKATA, Y. 2000. Extracellular ATP triggers tumor necrosis factor- α release from rat microglia. *Journal of neurochemistry*, 75, 965-972.
- HIGASHIYAMA, H., BILLIN, A. N., OKAMOTO, Y., KINOSHITA, M. & ASANO, S. 2007. Expression profiling of peroxisome proliferator-activated receptor-delta (PPAR-delta) in mouse tissues using tissue microarray. *Histochemistry and cell biology*, 127, 485-494.

- HJERPE, R., BETT, J. S., KEUSS, M. J., SOLOVYOVA, A., MCWILLIAMS, T. G., JOHNSON, C., SAHU, I., VARGHESE, J., WOOD, N. & WIGHTMAN, M. 2016. UBQLN2 mediates autophagy-independent protein aggregate clearance by the proteasome. *Cell*, 166, 935-949.
- HOCKEMEYER, D., SOLDNER, F., COOK, E. G., GAO, Q., MITALIPOVA, M. & JAENISCH, R. 2008. A drug-inducible system for direct reprogramming of human somatic cells to pluripotency. *Cell stem cell*, 3, 346-353.
- HOFFMEYER, S., BURK, O., VON RICHTER, O., ARNOLD, H. P., BROCKMÖLLER, J., JOHNE, A., CASCORBI, I., GERLOFF, T., ROOTS, I. & EICHELBAUM, M. 2000. Functional polymorphisms of the human multidrug-resistance gene: multiple sequence variations and correlation of one allele with P-glycoprotein expression and activity in vivo. *Proceedings of the National Academy of Sciences*, 97, 3473-3478.
- IGLESIAS, J., MORALES, L. & BARRETO, G. E. 2017. Metabolic and inflammatory adaptation of reactive astrocytes: role of PPARs. *Molecular neurobiology*, 54, 2518-2538.
- IMRAISH, A. 2018. Age-Related Changes in the Phenotype of Microglia. *PhD thesis, The University of Nottingham*.
- INOUE, K. 2002. Microglial activation by purines and pyrimidines. *Glia*, 40, 156-163.
- ITO, A., HONG, C., RONG, X., ZHU, X., TARLING, E. J., HEDDE, P. N., GRATTON, E., PARKS, J. & TONTONOZ, P. 2015. LXRs link metabolism to inflammation through Abca1-dependent regulation of membrane composition and TLR signaling. *elife*, 4, e08009.
- ITO, T., YOSHIDA, M., AIDA, T., KUSHIMA, I., HIRAMATSU, Y., ONO, M., YOSHIMI, A., TANAKA, K., OZAKI, N. & NODA, Y. 2023. Astrotactin 2 (ASTN2) regulates emotional and cognitive functions by affecting neuronal morphogenesis and monoaminergic systems. *Journal of Neurochemistry*, 165, 211-229.
- IWASHITA, A., MURAMATSU, Y., YAMAZAKI, T., MURAMOTO, M., KITA, Y., YAMAZAKI, S., MIHARA, K., MORIGUCHI, A. & MATSUOKA, N. 2007. Neuroprotective efficacy of the peroxisome proliferator-activated receptor δ -selective agonists in vitro and in vivo. *Journal of Pharmacology and Experimental Therapeutics*, 320, 1087-1096.
- JANABI, N., PEUDENIER, S., HÉRON, B., NG, K. H. & TARDIEU, M. 1995. Establishment of human microglial cell lines after transfection of primary cultures of embryonic microglial cells with the SV40 large T antigen. *Neuroscience letters*, 195, 105-108.
- JHA, M. K., JO, M., KIM, J.-H. & SUK, K. 2019. Microglia-astrocyte crosstalk: an intimate molecular conversation. *The Neuroscientist*, 25, 227-240.

- JOSHI, A. U., VAN WASSENHOVE, L. D., LOGAS, K. R., MINHAS, P. S., ANDREASSON, K. I., WEINBERG, K. I., CHEN, C.-H. & MOCHLY-ROSEN, D. 2019. Aldehyde dehydrogenase 2 activity and aldehydic load contribute to neuroinflammation and Alzheimer's disease related pathology. *Acta neuropathologica communications*, 7, 1-18.
- JÜLG, J., STROHM, L. & BEHRENDTS, C. 2021. Canonical and noncanonical autophagy pathways in microglia. *Molecular and cellular biology*, 41, e00389-20.
- KAGAWA, Y., YASUMOTO, Y., SHARIFI, K., EBRAHIMI, M., ISLAM, A., MIYAZAKI, H., YAMAMOTO, Y., SAWADA, T., KISHI, H. & KOBAYASHI, S. 2015. Fatty acid-binding protein 7 regulates function of caveolae in astrocytes through expression of caveolin-1. *Glia*, 63, 780-794.
- KALININ, S., RICHARDSON, J. C. & FEINSTEIN, D. L. 2009. A PPARdelta agonist reduces amyloid burden and brain inflammation in a transgenic mouse model of Alzheimer's disease. *Current Alzheimer Research*, 6, 431-437.
- KAMINSKA, B., GOZDZ, A., ZAWADZKA, M., ELLERT-MIKLASZEWSKA, A. & LIPKO, M. 2009. MAPK signal transduction underlying brain inflammation and gliosis as therapeutic target. *The Anatomical Record: Advances in Integrative Anatomy and Evolutionary Biology: Advances in Integrative Anatomy and Evolutionary Biology*, 292, 1902-1913.
- KAPOOR, A., COLLINO, M., CASTIGLIA, S., FANTOZZI, R. & THIEMERMANN, C. 2010. Activation of peroxisome proliferator-activated receptor- β/δ attenuates myocardial ischemia/reperfusion injury in the rat. *Shock*, 34, 117-124.
- KATAOKA, A., TOZAKI-SAITOH, H., KOGA, Y., TSUDA, M. & INOUE, K. 2009. Activation of P2X7 receptors induces CCL3 production in microglial cells through transcription factor NFAT. *Journal of neurochemistry*, 108, 115-125.
- KAWAI, T. & AKIRA, S. 2010. The role of pattern-recognition receptors in innate immunity: update on Toll-like receptors. *Nature immunology*, 11, 373-384.
- KEENE, C. D., DARVAS, M., KRAEMER, B., LIGGITT, D., SIGURDSON, C. & LADIGES, W. 2016. Neuropathological assessment and validation of mouse models for Alzheimer's disease: applying NIA-AA guidelines. Taylor & Francis.
- KERR, I. D., HAIDER, A. J. & GELISSEN, I. C. 2011. The ABCG family of membrane-associated transporters: you don't have to be big to be mighty. *British journal of pharmacology*, 164, 1767-1779.
- KETTENMANN, H., HANISCH, U.-K., NODA, M. & VERKHRATSKY, A. 2011. Physiology of microglia. *Physiological reviews*, 91, 461-553.

- KIELIAN, T. 2004. Microglia and chemokines in infectious diseases of the nervous system: views and reviews. *Front Biosci*, 9, 50.
- KIGERL, K. A., DE RIVERO VACCARI, J. P., DIETRICH, W. D., POPOVICH, P. G. & KEANE, R. W. 2014. Pattern recognition receptors and central nervous system repair. *Experimental neurology*, 258, 5-16.
- KILLOY, K. M., HARLAN, B. A., PEHAR, M. & VARGAS, M. R. 2020. FABP7 upregulation induces a neurotoxic phenotype in astrocytes. *Glia*, 68, 2693-2704.
- KÖBERLIN, M. S., HEINZ, L. X. & SUPERTI-FURGA, G. 2016. Functional crosstalk between membrane lipids and TLR biology. *Current Opinion in Cell Biology*, 39, 28-36.
- KODAIRA, H., KUSUHARA, H., USHIKI, J., FUSE, E. & SUGIYAMA, Y. 2010. Kinetic analysis of the cooperation of P-glycoprotein (P-gp/Abcb1) and breast cancer resistance protein (Bcrp/Abcg2) in limiting the brain and testis penetration of erlotinib, flavopiridol, and mitoxantrone. *Journal of Pharmacology and Experimental Therapeutics*, 333, 788-796.
- KOIZUMI, S., OHSAWA, K., INOUE, K. & KOHSAKA, S. 2013. Purinergic receptors in microglia: functional modal shifts of microglia mediated by P2 and P1 receptors. *Glia*, 61, 47-54.
- KOLIWAD, S. K., KUO, T., SHIPP, L. E., GRAY, N. E., BACKHED, F., SO, A. Y.-L., FARESE, R. V. & WANG, J.-C. 2009. Angiopoietin-like 4 (ANGPTL4, fasting-induced adipose factor) is a direct glucocorticoid receptor target and participates in glucocorticoid-regulated triglyceride metabolism. *Journal of Biological Chemistry*, 284, 25593-25601.
- KÖNIG, J., MÜLLER, F. & FROMM, M. F. 2013. Transporters and drug-drug interactions: important determinants of drug disposition and effects. *Pharmacological reviews*, 65, 944-966.
- KOO, Y. D., CHOI, J. W., KIM, M., CHAE, S., AHN, B. Y., KIM, M., OH, B. C., HWANG, D., SEOL, J. H. & KIM, Y.-B. 2015. SUMO-specific protease 2 (SEN2) is an important regulator of fatty acid metabolism in skeletal muscle. *Diabetes*, 64, 2420-2431.
- KORBECKI, J., BOBIŃSKI, R. & DUTKA, M. 2019. Self-regulation of the inflammatory response by peroxisome proliferator-activated receptors. *Inflammation research*, 68, 443-458.
- KRUGLOV, V., JANG, I. H. & CAMELL, C. D. 2024. Inflammaging and fatty acid oxidation in monocytes and macrophages. *Immunometabolism*, 6, e00038.
- KUANG, G., HE, Q., ZHANG, Y., ZHUANG, R., XIANG, A., JIANG, Q., LUO, Y. & YANG, J. 2012. Modulation of preactivation of PPAR- β on memory and learning dysfunction and inflammatory response in the

- hippocampus in rats exposed to global cerebral ischemia/reperfusion. *PPAR research*, 2012.
- LEE, Y. B., NAGAI, A. & KIM, S. U. 2002. Cytokines, chemokines, and cytokine receptors in human microglia. *Journal of neuroscience research*, 69, 94-103.
- LENZ, K. M. & NELSON, L. H. 2018. Microglia and beyond: innate immune cells as regulators of brain development and behavioral function. *Frontiers in immunology*, 9, 343454.
- LI, Y., ZHENG, W., LU, Y., ZHENG, Y., PAN, L., WU, X., YUAN, Y., SHEN, Z., MA, S. & ZHANG, X. 2021. BNIP3L/NIX-mediated mitophagy: molecular mechanisms and implications for human disease. *Cell Death & Disease*, 13, 14.
- LIAN, H., ROY, E. & ZHENG, H. 2016. Microglial phagocytosis assay. *Bio-protocol*, 6, e1988-e1988.
- LIAO, Y., SMYTH, G. K. & SHI, W. 2014. featureCounts: an efficient general purpose program for assigning sequence reads to genomic features. *Bioinformatics*, 30, 923-930.
- LIDDELOW, S. A. & BARRES, B. A. 2017. Reactive astrocytes: production, function, and therapeutic potential. *Immunity*, 46, 957-967.
- LIDDELOW, S. A., GUTTENPLAN, K. A., CLARKE, L. E., BENNETT, F. C., BOHLEN, C. J., SCHIRMER, L., BENNETT, M. L., MÜNCH, A. E., CHUNG, W.-S. & PETERSON, T. C. 2017. Neurotoxic reactive astrocytes are induced by activated microglia. *Nature*, 541, 481.
- LIU, D., EVANS, I., BRITTON, G. & ZACHARY, I. 2008. The zinc-finger transcription factor, early growth response 3, mediates VEGF-induced angiogenesis. *Oncogene*, 27, 2989-2998.
- LIU, R.-Z., MITA, R., BEAULIEU, M., GAO, Z. & GODBOUT, R. 2010. Fatty acid binding proteins in brain development and disease. *International Journal of Developmental Biology*, 54, 1229-1239.
- LIU, T., ZHANG, L., JOO, D. & SUN, S.-C. 2017. NF- κ B signaling in inflammation. *Signal transduction and targeted therapy*, 2, 1-9.
- LIU, Y., MOLINA, C. A., WELCHER, A. A., LONGO, L. D. & DE LEÓN, M. 1997. Expression of DA11, a neuronal-injury-induced fatty acid binding protein, coincides with axon growth and neuronal differentiation during central nervous system development. *Journal of neuroscience research*, 48, 551-562.
- LÖSCHER, W. & POTSCHKA, H. 2005. Role of drug efflux transporters in the brain for drug disposition and treatment of brain diseases. *Progress in neurobiology*, 76, 22-76.

- LOVE, M. I., HUBER, W. & ANDERS, S. 2014. Moderated estimation of fold change and dispersion for RNA-seq data with DESeq2. *Genome biology*, 15, 1-21.
- LOVETT-RACKE, A. E., HUSSAIN, R. Z., NORTHROP, S., CHOY, J., ROCCHINI, A., MATTHES, L., CHAVIS, J. A., DIAB, A., DREW, P. D. & RACKE, M. K. 2004. Peroxisome proliferator-activated receptor α agonists as therapy for autoimmune disease. *The Journal of Immunology*, 172, 5790-5798.
- MAHAJAN, S., SAINI, A., CHANDRA, V., NANDURI, R., KALRA, R., BHAGYARAJ, E., KHATRI, N. & GUPTA, P. 2015. Nuclear Receptor Nr4a2 Promotes Alternative Polarization of Macrophages and Confers Protection in Sepsis* \diamond . *Journal of Biological Chemistry*, 290, 18304-18314.
- MAHRINGER, A., DELZER, J. & FRICKER, G. 2009. A fluorescence-based in vitro assay for drug interactions with breast cancer resistance protein (BCRP, ABCG2). *European journal of pharmaceuticals and biopharmaceutics*, 72, 605-613.
- MALM, T., MARIANI, M., DONOVAN, L. J., NEILSON, L. & LANDRETH, G. E. 2015. Activation of the nuclear receptor PPAR δ is neuroprotective in a transgenic mouse model of Alzheimer's disease through inhibition of inflammation. *Journal of neuroinflammation*, 12, 1-15.
- MANDREKAR-COLUCCI, S., KARLO, J. C. & LANDRETH, G. E. 2012. Mechanisms underlying the rapid peroxisome proliferator-activated receptor- γ -mediated amyloid clearance and reversal of cognitive deficits in a murine model of Alzheimer's disease. *Journal of Neuroscience*, 32, 10117-10128.
- MANTOVANI, A., SICA, A., SOZZANI, S., ALLAVENA, P., VECCHI, A. & LOCATI, M. 2004. The chemokine system in diverse forms of macrophage activation and polarization. *Trends in immunology*, 25, 677-686.
- MARTIN, M. 2011. Cutadapt removes adapter sequences from high-throughput sequencing reads. *EMBnet. journal*, 17, 10-12.
- MATCOVITCH-NATAN, O., WINTER, D. R., GILADI, A., VARGAS AGUILAR, S., SPINRAD, A., SARRAZIN, S., BEN-YEHUDA, H., DAVID, E., ZELADA GONZÁLEZ, F. & PERRIN, P. 2016. Microglia development follows a stepwise program to regulate brain homeostasis. *Science*, 353, aad8670.
- MATEJUK, A. & RANSOHOFF, R. M. 2020. Crosstalk between astrocytes and microglia: an overview. *Frontiers in immunology*, 11, 1416.
- MATIAS, I., MORGADO, J. & GOMES, F. C. A. 2019. Astrocyte heterogeneity: impact to brain aging and disease. *Frontiers in aging neuroscience*, 11.

- MATSSON, P., ENGLUND, G., AHLIN, G., BERGSTRÖM, C. A., NORINDER, U. & ARTURSSON, P. 2007. A global drug inhibition pattern for the human ATP-binding cassette transporter breast cancer resistance protein (ABCG2). *Journal of Pharmacology and Experimental Therapeutics*, 323, 19-30.
- MATSUMATA, M., SAKAYORI, N., MAEKAWA, M., OWADA, Y., YOSHIKAWA, T. & OSUMI, N. 2012. The effects of Fabp7 and Fabp5 on postnatal hippocampal neurogenesis in the mouse. *Stem cells*, 30, 1532-1543.
- MAURER, M. & VON STEBUT, E. 2004. Macrophage inflammatory protein-1. *The international journal of biochemistry & cell biology*, 36, 1882-1886.
- MCEVOY, A. N., MURPHY, E. A., PONNIO, T., CONNEELY, O. M., BRESNIHAN, B., FITZGERALD, O. & MURPHY, E. P. 2002. Activation of nuclear orphan receptor NURR1 transcription by NF- κ B and cyclic adenosine 5'-monophosphate response element-binding protein in rheumatoid arthritis synovial tissue. *The Journal of Immunology*, 168, 2979-2987.
- MCQUADE, A., COBURN, M., TU, C. H., HASSELMANN, J., DAVTYAN, H. & BLURTON-JONES, M. 2018. Development and validation of a simplified method to generate human microglia from pluripotent stem cells. *Molecular neurodegeneration*, 13, 1-13.
- MECHA, M., IÑIGO, P. M., MESTRE, L., HERNANGÓMEZ, M., BORRELL, J. & GUAZA, C. 2011. An easy and fast way to obtain a high number of glial cells from rat cerebral tissue: A beginners approach.
- MELIEF, J., KONING, N., SCHUURMAN, K. G., VAN DE GARDE, M. D., SMOLDERS, J., HOEK, R. M., VAN EIJK, M., HAMANN, J. & HUITINGA, I. 2012. Phenotyping primary human microglia: tight regulation of LPS responsiveness. *Glia*, 60, 1506-1517.
- MICHALIK, L. & WAHLI, W. 2006. Involvement of PPAR nuclear receptors in tissue injury and wound repair. *The Journal of clinical investigation*, 116, 598-606.
- MICHELS, M., ABATTI, M. R., ÁVILA, P., VIEIRA, A., BORGES, H., CARVALHO JUNIOR, C., WENDHAUSEN, D., GASPAROTTO, J., TIEFENSEE RIBEIRO, C. & MOREIRA, J. C. F. 2020. Characterization and modulation of microglial phenotypes in an animal model of severe sepsis. *Journal of cellular and molecular medicine*, 24, 88-97.
- MINKIEWICZ, J., DE RIVERO VACCARI, J. P. & KEANE, R. W. 2013. Human astrocytes express a novel NLRP2 inflammasome. *Glia*, 61, 1113-1121.
- MIZEE, M. R., MIEDEMA, S. S., VAN DER POEL, M., ADELIA, SCHUURMAN, K. G., VAN STRIEN, M. E., MELIEF, J., SMOLDERS, J., HENDRICKX,

- D. A. & HEUTINCK, K. M. 2017. Isolation of primary microglia from the human post-mortem brain: effects of ante-and post-mortem variables. *Acta neuropathologica communications*, 5, 1-14.
- MIZUNO, T., DOI, Y., MIZOGUCHI, H., JIN, S., NODA, M., SONOBE, Y., TAKEUCHI, H. & SUZUMURA, A. 2011. Interleukin-34 selectively enhances the neuroprotective effects of microglia to attenuate oligomeric amyloid- β neurotoxicity. *The American journal of pathology*, 179, 2016-2027.
- MORENO, S., FARIOLI-VECCHIOLI, S. & CERU, M. 2004. Immunolocalization of peroxisome proliferator-activated receptors and retinoid X receptors in the adult rat CNS. *Neuroscience*, 123, 131-145.
- MOSHER, K. I. & WYSS-CORAY, T. 2014. Microglial dysfunction in brain aging and Alzheimer's disease. *Biochemical pharmacology*, 88, 594-604.
- MOUSSAUD, S. & DRAHEIM, H. J. 2010. A new method to isolate microglia from adult mice and culture them for an extended period of time. *Journal of neuroscience methods*, 187, 243-253.
- MUFFAT, J., LI, Y., YUAN, B., MITALIPOVA, M., OMER, A., CORCORAN, S., BAKIASI, G., TSAI, L.-H., AUBOURG, P. & RANSOHOFF, R. M. 2016. Efficient derivation of microglia-like cells from human pluripotent stem cells. *Nature medicine*, 22, 1358-1367.
- NAGAI, A., MISHIMA, S., ISHIDA, Y., ISHIKURA, H., HARADA, T., KOBAYASHI, S. & KIM, S. U. 2005. Immortalized human microglial cell line: phenotypic expression. *Journal of neuroscience research*, 81, 342-348.
- NAKAJIMA, K., HONDA, S., TOHYAMA, Y., IMAI, Y., KOHSAKA, S. & KURIHARA, T. 2001. Neurotrophin secretion from cultured microglia. *Journal of neuroscience research*, 65, 322-331.
- NATARAJAN, K., XIE, Y., BAER, M. R. & ROSS, D. D. 2012. Role of breast cancer resistance protein (BCRP/ABCG2) in cancer drug resistance. *Biochemical pharmacology*, 83, 1084-1103.
- NATH, S., DANCOURT, J., SHTEYN, V., PUENTE, G., FONG, W. M., NAG, S., BEWERSDORF, J., YAMAMOTO, A., ANTONNY, B. & MELIA, T. J. 2014. Lipidation of the LC3/GABARAP family of autophagy proteins relies on a membrane-curvature-sensing domain in Atg3. *Nature cell biology*, 16, 415-424.
- NI, Z., BIKADI, Z., F ROSENBERG, M. & MAO, Q. 2010. Structure and function of the human breast cancer resistance protein (BCRP/ABCG2). *Current drug metabolism*, 11, 603-617.
- NIWA, A., HEIKE, T., UMEDA, K., OSHIMA, K., KATO, I., SAKAI, H., SUEMORI, H., NAKAHATA, T. & SAITO, M. K. 2011. A novel serum-

- free monolayer culture for orderly hematopoietic differentiation of human pluripotent cells via mesodermal progenitors. *PLoS One*, 6, e22261.
- NORDEN, D. M., FENN, A. M., DUGAN, A. & GODBOUT, J. P. 2014. TGF β produced by IL-10 redirected astrocytes attenuates microglial activation. *Glia*, 62, 881-895.
- NORDEN, D. M. & GODBOUT, J. 2013. Microglia of the aged brain: primed to be activated and resistant to regulation. *Neuropathology and applied neurobiology*, 39, 19-34.
- NOTO, D., SAKUMA, H., TAKAHASHI, K., SAIKA, R., SAGA, R., YAMADA, M., YAMAMURA, T. & MIYAKE, S. 2014. Development of a culture system to induce microglia-like cells from haematopoietic cells. *Neuropathology and applied neurobiology*, 40, 697-713.
- O'SHEA, J. J. & PLENGE, R. 2012. JAK and STAT signaling molecules in immunoregulation and immune-mediated disease. *Immunity*, 36, 542-550.
- O'DONNELL, P., ROSEN, L., ALEXANDER, R., MURTHY, V., DAVIES, C. H. & RATTI, E. 2019. Strategies to address challenges in neuroscience drug discovery and development. *International Journal of Neuropsychopharmacology*, 22, 445-448.
- ODEGAARD, J. I. & CHAWLA, A. 2008. Mechanisms of macrophage activation in obesity-induced insulin resistance. *Nature clinical practice endocrinology & metabolism*, 4, 619-626.
- ODEGAARD, J. I. & CHAWLA, A. 2011. Alternative macrophage activation and metabolism. *Annual Review of Pathology: Mechanisms of Disease*, 6, 275-297.
- ODEGAARD, J. I., RICARDO-GONZALEZ, R. R., EAGLE, A. R., VATS, D., MOREL, C. R., GOFORTH, M. H., SUBRAMANIAN, V., MUKUNDAN, L., FERRANTE, A. W. & CHAWLA, A. 2008. Alternative M2 activation of Kupffer cells by PPAR δ ameliorates obesity-induced insulin resistance. *Cell metabolism*, 7, 496-507.
- OHGIDANI, M., KATO, T. A., SETOYAMA, D., SAGATA, N., HASHIMOTO, R., SHIGENOBU, K., YOSHIDA, T., HAYAKAWA, K., SHIMOKAWA, N. & MIURA, D. 2014. Direct induction of ramified microglia-like cells from human monocytes: dynamic microglial dysfunction in Nasu-Hakola disease. *Scientific reports*, 4, 4957.
- OLIVER JR, W. R., SHENK, J. L., SNAITH, M. R., RUSSELL, C. S., PLUNKET, K. D., BODKIN, N. L., LEWIS, M. C., WINEGAR, D. A., SZNAIDMAN, M. L. & LAMBERT, M. H. 2001. A selective peroxisome proliferator-activated receptor δ agonist promotes reverse cholesterol transport. *Proceedings of the national academy of sciences*, 98, 5306-5311.

- ORRE, M., KAMPHUIS, W., OSBORN, L. M., MELIEF, J., KOOIJMAN, L., HUITINGA, I., KLOOSTER, J., BOSSERS, K. & HOL, E. M. 2014. Acute isolation and transcriptome characterization of cortical astrocytes and microglia from young and aged mice. *Neurobiology of aging*, 35, 1-14.
- OWADA, Y., YOSHIMOTO, T. & KONDO, H. 1996. Spatio-temporally differential expression of genes for three members of fatty acid binding proteins in developing and mature rat brains. *Journal of chemical neuroanatomy*, 12, 113-122.
- PALOMER, X., CAPDEVILA-BUSQUETS, E., BOTTERI, G., SALVADÓ, L., BARROSO, E., DAVIDSON, M. M., MICHALIK, L., WAHLI, W. & VÁZQUEZ-CARRERA, M. 2014. PPAR β/δ attenuates palmitate-induced endoplasmic reticulum stress and induces autophagic markers in human cardiac cells. *International journal of cardiology*, 174, 110-118.
- PAN, Y., SCANLON, M. J., OWADA, Y., YAMAMOTO, Y., PORTER, C. J. & NICOLAZZO, J. A. 2015. Fatty acid-binding protein 5 facilitates the blood-brain barrier transport of docosahexaenoic acid. *Molecular pharmacology*, 12, 4375-4385.
- PANATIER, A., THEODOSIS, D. T., MOTHET, J.-P., TOUQUET, B., POLLEGIONI, L., POULAIN, D. A. & OLIET, S. H. 2006. Glia-derived D-serine controls NMDA receptor activity and synaptic memory. *Cell*, 125, 775-784.
- PANDYA, H., SHEN, M. J., ICHIKAWA, D. M., SEDLOCK, A. B., CHOI, Y., JOHNSON, K. R., KIM, G., BROWN, M. A., ELKAHLOUN, A. G. & MARIC, D. 2017. Differentiation of human and murine induced pluripotent stem cells to microglia-like cells. *Nature neuroscience*, 20, 753-759.
- PAOLICELLI, R. C., BOLASCO, G., PAGANI, F., MAGGI, L., SCIANNI, M., PANZANELLI, P., GIUSTETTO, M., FERREIRA, T. A., GUIDUCCI, E. & DUMAS, L. 2011. Synaptic pruning by microglia is necessary for normal brain development. *science*, 333, 1456-1458.
- PARAMESWARAN, N. & PATIAL, S. 2010. Tumor necrosis factor- α signaling in macrophages. *Critical Reviews™ in Eukaryotic Gene Expression*, 20.
- PARDRIDGE, W. M. 2012. Drug transport across the blood-brain barrier. *Journal of cerebral blood flow & metabolism*, 32, 1959-1972.
- PASCUAL, G., FONG, A. L., OGAWA, S., GAMLIEL, A., LI, A. C., PERISSI, V., ROSE, D. W., WILLSON, T. M., ROSENFELD, M. G. & GLASS, C. K. 2005. A SUMOylation-dependent pathway mediates transrepression of inflammatory response genes by PPAR- γ . *Nature*, 437, 759-763.

- PASCUAL, O., BEN ACHOUR, S., ROSTAING, P., TRILLER, A. & BESSIS, A. 2012. Microglia activation triggers astrocyte-mediated modulation of excitatory neurotransmission. *Proceedings of the National Academy of Sciences*, 109, E197-E205.
- PATERNITI, I., ESPOSITO, E., MAZZON, E., GALUPPO, M., DI PAOLA, R., BRAMANTI, P., KAPOOR, A., THIEMERMANN, C. & CUZZOCREA, S. 2010. Evidence for the role of peroxisome proliferator-activated receptor- β/δ in the development of spinal cord injury. *Journal of Pharmacology and Experimental Therapeutics*, 333, 465-477.
- PEI, L., CASTRILLO, A., CHEN, M., HOFFMANN, A. & TONTONOZ, P. 2005. Induction of NR4A orphan nuclear receptor expression in macrophages in response to inflammatory stimuli. *Journal of biological chemistry*, 280, 29256-29262.
- PELLERIN, L. & MAGISTRETTI, P. J. 1994. Glutamate uptake into astrocytes stimulates aerobic glycolysis: a mechanism coupling neuronal activity to glucose utilization. *Proceedings of the National Academy of Sciences*, 91, 10625-10629.
- PELSERS, M. M., HANHOFF, T., VAN DER VOORT, D., ARTS, B., PETERS, M., PONDS, R., HONIG, A., RUDZINSKI, W., SPENER, F. & DE KRUIJK, J. R. 2004. Brain-and heart-type fatty acid-binding proteins in the brain: tissue distribution and clinical utility. *Clinical chemistry*, 50, 1568-1575.
- PERRY, V. H. & HOLMES, C. 2014. Microglial priming in neurodegenerative disease. *Nature Reviews Neurology*, 10, 217-224.
- PHUA, W. W. T., TAN, W. R., YIP, Y. S., HEW, I. D., WEE, J. W. K., CHENG, H. S., LEOW, M. K. S., WAHLI, W. & TAN, N. S. 2020. PPAR β/δ agonism upregulates forkhead box A2 to reduce inflammation in C2C12 myoblasts and in skeletal muscle. *International Journal of Molecular Sciences*, 21, 1747.
- PICKERING, M., CUMISKEY, D. & O'CONNOR, J. J. 2005. Actions of TNF- α on glutamatergic synaptic transmission in the central nervous system. *Experimental physiology*, 90, 663-670.
- PIKE, A. F., LONGHENA, F., FAUSTINI, G., VAN EIK, J.-M., GOMBERT, I., HERREBOUT, M. A., FAYED, M. M., SANDRE, M., VARANITA, T. & TEUNISSEN, C. E. 2022. Dopamine signaling modulates microglial NLRP3 inflammasome activation: implications for Parkinson's disease. *Journal of neuroinflammation*, 19, 50.
- PLANAVALA, A., RODRÍGUEZ-CALVO, R., JOVÉ, M., MICHALIK, L., WAHLI, W., LAGUNA, J. C. & VÁZQUEZ-CARRERA, M. 2005. Peroxisome proliferator-activated receptor β/δ activation inhibits hypertrophy in neonatal rat cardiomyocytes. *Cardiovascular research*, 65, 832-841.

- PLAZA-ZABALA, A., SIERRA-TORRE, V. & SIERRA, A. 2017. Autophagy and microglia: novel partners in neurodegeneration and aging. *International journal of molecular sciences*, 18, 598.
- POMEROY, J. E., HOUGH, S. R., DAVIDSON, K. C., QUAAS, A. M., REES, J. A. & PERA, M. F. 2016. Stem cell surface marker expression defines late stages of reprogramming to pluripotency in human fibroblasts. *Stem Cells Translational Medicine*, 5, 870-882.
- POMILIO, C., GOROJOD, R. M., RIUDAUVETS, M., VINUESA, A., PRESA, J., GREGOSA, A., BENTIVEGNA, M., ALAIMO, A., ALCON, S. P. & SEVLEVER, G. 2020. Microglial autophagy is impaired by prolonged exposure to β -amyloid peptides: evidence from experimental models and Alzheimer's disease patients. *Geroscience*, 42, 613-632.
- POURCET, B., PINEDA-TORRA, I., DERUDAS, B., STAELS, B. & GLINEUR, C. 2010. SUMOylation of human peroxisome proliferator-activated receptor α inhibits its trans-activity through the recruitment of the nuclear corepressor NCoR. *Journal of Biological Chemistry*, 285, 5983-5992.
- POURCET, B., STAELS, B. & GLINEUR, C. 2013. PPAR SUMOylation: some useful experimental tips. *Peroxisome Proliferator-Activated Receptors (PPARs) Methods and Protocols*, 145-161.
- POWELL, S. K., O'SHEA, C., TOWNSLEY, K., PRYTKOVA, I., DOBRINDT, K., ELAHI, R., ISKHAKOVA, M., LAMBERT, T., VALADA, A. & LIAO, W. 2021. Induction of dopaminergic neurons for neuronal subtype-specific modeling of psychiatric disease risk. *Molecular Psychiatry*, 1-13.
- RANSOHOFF, R. M. 2016. How neuroinflammation contributes to neurodegeneration. *Science*, 353.
- RICKEL, E. A., SIEGEL, L. A., YOON, B.-R. P., ROTTMAN, J., KUGLER, D., SWART, D., ANDERS, P., TOCKER, J. E., COMEAU, M. R. & BUDELSKY, A. L. 2008. 217 Identification of functional roles for both IL-17RB and IL-17RA in mediating IL-25 induced activities. *Cytokine*, 3, 291.
- RÖMERMANN, K., WANEK, T., BANKSTAHL, M., BANKSTAHL, J. P., FEDROWITZ, M., MÜLLER, M., LÖSCHER, W., KUNTNER, C. & LANGER, O. 2013. (R)-[11C] verapamil is selectively transported by murine and human P-glycoprotein at the blood-brain barrier, and not by MRP1 and BCRP. *Nuclear medicine and biology*, 40, 873-878.
- ROTHSTEIN, J. D., DYKES-HOBERG, M., PARDO, C. A., BRISTOL, L. A., JIN, L., KUNCL, R. W., KANAI, Y., HEDIGER, M. A., WANG, Y. & SCHIELKE, J. P. 1996. Knockout of glutamate transporters reveals a major role for astroglial transport in excitotoxicity and clearance of glutamate. *Neuron*, 16, 675-686.

- ROZOVSKY, I., FINCH, C. & MORGAN, T. 1998. Age-related activation of microglia and astrocytes: in vitro studies show persistent phenotypes of aging, increased proliferation, and resistance to down-regulation. *Neurobiology of aging*, 19, 97-103.
- RUSTENHOVEN, J., PARK, T. I., SCHWEDER, P., SCOTTER, J., CORREIA, J., SMITH, A. M., GIBBONS, H. M., OLDFIELD, R. L., BERGIN, P. S. & MEE, E. W. 2016. Isolation of highly enriched primary human microglia for functional studies. *Scientific reports*, 6, 19371.
- RYAN, K. J., WHITE, C. C., PATEL, K., XU, J., OLAH, M., REPLOGLE, J. M., FRANGIEH, M., CIMPEAN, M., WINN, P. & MCHENRY, A. 2017. A human microglia-like cellular model for assessing the effects of neurodegenerative disease gene variants. *Science translational medicine*, 9, eaai7635.
- SAIJO, K., WINNER, B., CARSON, C. T., COLLIER, J. G., BOYER, L., ROSENFELD, M. G., GAGE, F. H. & GLASS, C. K. 2009. A Nurr1/CoREST pathway in microglia and astrocytes protects dopaminergic neurons from inflammation-induced death. *Cell*, 137, 47-59.
- SARRUF, D. A., YU, F., NGUYEN, H. T., WILLIAMS, D. L., PRINTZ, R. L., NISWENDER, K. D. & SCHWARTZ, M. W. 2009. Expression of peroxisome proliferator-activated receptor- γ in key neuronal subsets regulating glucose metabolism and energy homeostasis. *Endocrinology*, 150, 707-712.
- SAVCHENKO, V., MCKANNA, J., NIKONENKO, I. & SKIBO, G. 2000. Microglia and astrocytes in the adult rat brain: comparative immunocytochemical analysis demonstrates the efficacy of lipocortin 1 immunoreactivity. *Neuroscience*, 96, 195-203.
- SCHAFFER, D. P., LEHRMAN, E. K., KAUTZMAN, A. G., KOYAMA, R., MARDINLY, A. R., YAMASAKI, R., RANSOHOFF, R. M., GREENBERG, M. E., BARRES, B. A. & STEVENS, B. 2012. Microglia sculpt postnatal neural circuits in an activity and complement-dependent manner. *Neuron*, 74, 691-705.
- SCHAFFER, D. P. & STEVENS, B. 2015. Microglia function in central nervous system development and plasticity. *Cold Spring Harbor perspectives in biology*, 7, a020545.
- SCHAIN, M. & KREISL, W. C. 2017. Neuroinflammation in Neurodegenerative Disorders—a Review. *Current Neurology and Neuroscience Reports*, 17, 25.
- SCHINKEL, A. H. 1999. P-Glycoprotein, a gatekeeper in the blood-brain barrier. *Advanced drug delivery reviews*, 36, 179-194.
- SCHLAEPFER, I. R. & JOSHI, M. 2020. CPT1A-mediated fat oxidation, mechanisms, and therapeutic potential. *Endocrinology*, 161, bqz046.

- SCHNEGG, C. I., KOOSHKI, M., HSU, F.-C., SUI, G. & ROBBINS, M. E. 2012. PPAR δ prevents radiation-induced proinflammatory responses in microglia via transrepression of NF- κ B and inhibition of the PKC α /MEK1/2/ERK1/2/AP-1 pathway. *Free Radical Biology and Medicine*, 52, 1734-1743.
- SCHNEGG, C. I. & ROBBINS, M. E. 2011. Neuroprotective mechanisms of PPAR δ : Modulation of oxidative stress and inflammatory processes. *PPAR research*, 2011.
- SCHNELL, L., FEARN, S., KLASSEN, H., SCHWAB, M. E. & PERRY, V. H. 1999. Acute inflammatory responses to mechanical lesions in the CNS: differences between brain and spinal cord. *European Journal of Neuroscience*, 11, 3648-3658.
- SCHWABENLAND, M., BRÜCK, W., PRILLER, J., STADELMANN, C., LASSMANN, H. & PRINZ, M. 2021. Analyzing microglial phenotypes across neuropathologies: a practical guide. *Acta neuropathologica*, 1-14.
- SELLGREN, C. M., GRACIAS, J., WATMUFF, B., BIAG, J. D., THANOS, J. M., WHITTREDGE, P. B., FU, T., WORRINGER, K., BROWN, H. E. & WANG, J. 2019. Increased synapse elimination by microglia in schizophrenia patient-derived models of synaptic pruning. *Nature neuroscience*, 22, 374-385.
- SELLNER, P. A., CHU, W., GLATZ, J. F. & BERMAN, N. E. 1995. Developmental role of fatty acid-binding proteins in mouse brain. *Developmental brain research*, 89, 33-46.
- SIERRA, A., GOTTFRIED-BLACKMORE, A. C., MCEWEN, B. S. & BULLOCH, K. 2007. Microglia derived from aging mice exhibit an altered inflammatory profile. *Glia*, 55, 412-424.
- SMATHERS, R. L. & PETERSEN, D. R. 2011. The human fatty acid-binding protein family: evolutionary divergences and functions. *Human genomics*, 5, 1-22.
- SOCCIO, R. E., CHEN, E. R. & LAZAR, M. A. 2014. Thiazolidinediones and the promise of insulin sensitization in type 2 diabetes. *Cell metabolism*, 20, 573-591.
- SØRENSEN, T. L., TREBST, C., KIVISÄKK, P., KLAEGE, K. L., MAJMUDAR, A., RAVID, R., LASSMANN, H., OLSEN, D. B., STRIETER, R. M. & RANSOHOFF, R. M. 2002. Multiple sclerosis: a study of CXCL10 and CXCR3 co-localization in the inflamed central nervous system. *Journal of neuroimmunology*, 127, 59-68.
- SOTO-AVELLANEDA, A. & MORRISON, B. E. 2020. Signaling and other functions of lipids in autophagy: a review. *Lipids in Health and Disease*, 19, 214.

- SPITTAU, B. 2017. Aging microglia—phenotypes, functions and implications for age-related neurodegenerative diseases. *Frontiers in aging neuroscience*, 9, 194.
- STAIGER, H., HAAS, C., MACHANN, J., WERNER, R., WEISSER, M., SCHICK, F., MACHICAO, F., STEFAN, N., FRITSCHKE, A. & HÄRING, H.-U. 2009. Muscle-derived angiopoietin-like protein 4 is induced by fatty acids via peroxisome proliferator-activated receptor (PPAR)- δ and is of metabolic relevance in humans. *Diabetes*, 58, 579-589.
- STANLEY, B., POST, J. & HENSLEY, K. 2012. A comparative review of cell culture systems for the study of microglial biology in Alzheimer's disease. *Journal of neuroinflammation*, 9, 1-8.
- STENCE, N., WAITE, M. & DAILEY, M. E. 2001. Dynamics of microglial activation: A confocal time-lapse analysis in hippocampal slices. *Glia*, 33, 256-266.
- STEVENS, B., ALLEN, N. J., VAZQUEZ, L. E., HOWELL, G. R., CHRISTOPHERSON, K. S., NOURI, N., MICHEVA, K. D., MEHALOW, A. K., HUBERMAN, A. D. & STAFFORD, B. 2007. The classical complement cascade mediates CNS synapse elimination. *Cell*, 131, 1164-1178.
- STORCH, J. & CORSICO, B. 2008. The emerging functions and mechanisms of mammalian fatty acid-binding proteins. *Annu. Rev. Nutr.*, 28, 73-95.
- STORER, P. D., XU, J., CHAVIS, J. & DREW, P. D. 2005. Peroxisome proliferator-activated receptor-gamma agonists inhibit the activation of microglia and astrocytes: implications for multiple sclerosis. *Journal of neuroimmunology*, 161, 113-122.
- STRAUS, D. S. & GLASS, C. K. 2007. Anti-inflammatory actions of PPAR ligands: new insights on cellular and molecular mechanisms. *Trends in immunology*, 28, 551-558.
- SUGDEN, M. C. & HOLNESS, M. J. 2006. Mechanisms underlying regulation of the expression and activities of the mammalian pyruvate dehydrogenase kinases. *Archives of physiology and biochemistry*, 112, 139-149.
- SYVÄNEN, S., LINDHE, Ö., PALNER, M., KORNUM, B. R., RAHMAN, O., LÅNGSTRÖM, B., KNUDSEN, G. M. & HAMMARLUND-UDENAES, M. 2009. Species differences in blood-brain barrier transport of three positron emission tomography radioligands with emphasis on P-glycoprotein transport. *Drug metabolism and disposition*, 37, 635-643.
- TAKAHASHI, K., OKITA, K., NAKAGAWA, M. & YAMANAKA, S. 2007. Induction of pluripotent stem cells from fibroblast cultures. *Nature protocols*, 2, 3081-3089.

- TAKAHASHI, K. & YAMANAKA, S. 2006. Induction of pluripotent stem cells from mouse embryonic and adult fibroblast cultures by defined factors. *cell*, 126, 663-676.
- TAMASHIRO, T. T., DALGARD, C. L. & BYRNES, K. R. 2012. Primary microglia isolation from mixed glial cell cultures of neonatal rat brain tissue. *JoVE (Journal of Visualized Experiments)*, e3814.
- TAN, N.-S., SHAW, N. S., VINCKENBOSCH, N., LIU, P., YASMIN, R., DESVERGNE, B., WAHLI, W. & NOY, N. 2002. Selective cooperation between fatty acid binding proteins and peroxisome proliferator-activated receptors in regulating transcription. *Molecular and cellular biology*, 22, 5114-5127.
- TANAKA, T., YAMAMOTO, J., IWASAKI, S., ASABA, H., HAMURA, H., IKEDA, Y., WATANABE, M., MAGOORI, K., IOKA, R. X. & TACHIBANA, K. 2003. Activation of peroxisome proliferator-activated receptor δ induces fatty acid β -oxidation in skeletal muscle and attenuates metabolic syndrome. *Proceedings of the National Academy of Sciences*, 100, 15924-15929.
- TANG, X., YAN, K., WANG, Y., WANG, Y., CHEN, H., XU, J., LU, Y., WANG, X., LIANG, J. & ZHANG, X. 2020. Activation of PPAR- β/δ attenuates brain injury by suppressing inflammation and apoptosis in a collagenase-induced intracerebral hemorrhage mouse model. *Neurochemical Research*, 45, 837-850.
- TEWARI, M., MICHALSKI, S. & EGAN, T. M. 2024. Modulation of Microglial Function by ATP-Gated P2X7 Receptors: Studies in Rat, Mice and Human. *Cells*, 13, 161.
- THEKA, I., CAIAZZO, M., DVORETSKOVA, E., LEO, D., UNGARO, F., CURRELI, S., MANAGÒ, F., DELL'ANNO, M. T., PEZZOLI, G. & GAINETDINOV, R. R. 2013. Rapid generation of functional dopaminergic neurons from human induced pluripotent stem cells through a single-step procedure using cell lineage transcription factors. *Stem cells translational medicine*, 2, 473-479.
- TREUTER, E. & VENTECLEF, N. 2011. Transcriptional control of metabolic and inflammatory pathways by nuclear receptor SUMOylation. *Biochimica et Biophysica Acta (BBA)-Molecular Basis of Disease*, 1812, 909-918.
- TRITSCH, N. X. & SABATINI, B. L. 2012. Dopaminergic modulation of synaptic transmission in cortex and striatum. *Neuron*, 76, 33-50.
- UENO, M., FUJITA, Y., TANAKA, T., NAKAMURA, Y., KIKUTA, J., ISHII, M. & YAMASHITA, T. 2013. Layer V cortical neurons require microglial support for survival during postnatal development. *Nature neuroscience*, 16, 543-551.
- ULLAND, T. K., SONG, W. M., HUANG, S. C.-C., ULRICH, J. D., SERGUSHICHEV, A., BEATTY, W. L., LOBODA, A. A., ZHOU, Y.,

- CAIRNS, N. J. & KAMBAL, A. 2017. TREM2 maintains microglial metabolic fitness in Alzheimer's disease. *Cell*, 170, 649-663. e13.
- VAN HORSSSEN, J., VOS, C., ADMIRAAL, L., VAN HAASTERT, E., MONTAGNE, L., VAN DER VALK, P. & DE VRIES, H. 2006. Matrix metalloproteinase-19 is highly expressed in active multiple sclerosis lesions. *Neuropathology and applied neurobiology*, 32, 585-593.
- VENEGAS, C. & HENEKA, M. T. 2017. Danger-associated molecular patterns in Alzheimer's disease. *Journal of Leucocyte Biology*, 101, 87-98.
- VILLAPOL, S. 2018. Roles of peroxisome proliferator-activated receptor gamma on brain and peripheral inflammation. *Cellular and molecular neurobiology*, 38, 121-132.
- VIVIANI, B., BARTESAGHI, S., GARDONI, F., VEZZANI, A., BEHRENS, M., BARTFAI, T., BINAGLIA, M., CORSINI, E., DI LUCA, M. & GALLI, C. 2003. Interleukin-1 β enhances NMDA receptor-mediated intracellular calcium increase through activation of the Src family of kinases. *Journal of Neuroscience*, 23, 8692-8700.
- WAKE, H., MOORHOUSE, A. J., JINNO, S., KOHSAKA, S. & NABEKURA, J. 2009. Resting microglia directly monitor the functional state of synapses in vivo and determine the fate of ischemic terminals. *Journal of Neuroscience*, 29, 3974-3980.
- WANG, Y.-X., LEE, C.-H., TIEP, S., RUTH, T. Y., HAM, J., KANG, H. & EVANS, R. M. 2003. Peroxisome-proliferator-activated receptor δ activates fat metabolism to prevent obesity. *Cell*, 113, 159-170.
- WANG, Y.-X., ZHANG, C.-L., YU, R. T., CHO, H. K., NELSON, M. C., BAYUGA-OCAMPO, C. R., HAM, J., KANG, H. & EVANS, R. M. 2004. Regulation of muscle fiber type and running endurance by PPAR δ . *PLoS biology*, 2, e294.
- WANG, Y., NAKAJIMA, T., GONZALEZ, F. J. & TANAKA, N. 2020. PPARs as metabolic regulators in the liver: lessons from liver-specific PPAR-null mice. *International journal of molecular sciences*, 21, 2061.
- WANG, Y., SZRETTER, K. J., VERMI, W., GILFILLAN, S., ROSSINI, C., CELLA, M., BARROW, A. D., DIAMOND, M. S. & COLONNA, M. 2012. IL-34 is a tissue-restricted ligand of CSF1R required for the development of Langerhans cells and microglia. *Nature immunology*, 13, 753-760.
- WARDEN, A., TRUITT, J., MERRIMAN, M., PONOMAREVA, O., JAMESON, K., FERGUSON, L. B., MAYFIELD, R. D. & HARRIS, R. A. 2016a. Localization of PPAR isotypes in the adult mouse and human brain. *Scientific reports*, 6, 1-15.
- WARDEN, A., TRUITT, J., MERRIMAN, M., PONOMAREVA, O., JAMESON, K., FERGUSON, L. B., MAYFIELD, R. D. & HARRIS, R. A. 2016b.

Localization of PPAR isotypes in the adult mouse and human brain. *Scientific reports*, 6, 27618.

- WEISS, J., SAUER, A., HERZOG, M., BÖGER, R. H., HAEFELI, W. E. & BENNDORF, R. A. 2009. Interaction of thiazolidinediones (glitazones) with the ATP-binding cassette transporters P-glycoprotein and breast cancer resistance protein. *Pharmacology*, 84, 264-270.
- WELCH, J. S., RICOTE, M., AKIYAMA, T. E., GONZALEZ, F. J. & GLASS, C. K. 2003. PPAR γ and PPAR δ negatively regulate specific subsets of lipopolysaccharide and IFN- γ target genes in macrophages. *Proceedings of the National Academy of Sciences*, 100, 6712-6717.
- WIELAND, G. D., NEHMANN, N., MÜLLER, D., EIBEL, H., SIEBENLIST, U., SÜHNEL, J. R., ZIPFEL, P. F. & SKERKA, C. 2005. Early growth response proteins EGR-4 and EGR-3 interact with immune inflammatory mediators NF- κ B p50 and p65. *Journal of cell science*, 118, 3203-3212.
- WOLFES, A. C. & DEAN, C. 2020. The diversity of synaptotagmin isoforms. *Current opinion in neurobiology*, 63, 198-209.
- XIAO, Y., XU, J., WANG, S., MAO, C., JIN, M., NING, G., XU, J. & ZHANG, Y. 2010. Genetic ablation of steroid receptor coactivator-3 promotes PPAR- β -mediated alternative activation of microglia in experimental autoimmune encephalomyelitis. *Glia*, 58, 932-942.
- XU, H. E., LAMBERT, M. H., MONTANA, V. G., PARKS, D. J., BLANCHARD, S. G., BROWN, P. J., STERNBACH, D. D., LEHMANN, J. M., WISELY, G. B. & WILLSON, T. M. 1999. Molecular recognition of fatty acids by peroxisome proliferator-activated receptors. *Molecular cell*, 3, 397-403.
- XU, H. E., LAMBERT, M. H., MONTANA, V. G., PLUNKET, K. D., MOORE, L. B., COLLINS, J. L., OPLINGER, J. A., KLIEWER, S. A., GAMPE JR, R. T. & MCKEE, D. D. 2001. Structural determinants of ligand binding selectivity between the peroxisome proliferator-activated receptors. *Proceedings of the National Academy of Sciences*, 98, 13919-13924.
- XU, J., CHAVIS, J. A., RACKE, M. K. & DREW, P. D. 2006. Peroxisome proliferator-activated receptor- α and retinoid X receptor agonists inhibit inflammatory responses of astrocytes. *Journal of neuroimmunology*, 176, 95-105.
- XU, J., STORER, P. D., CHAVIS, J. A., RACKE, M. K. & DREW, P. D. 2005. Agonists for the peroxisome proliferator-activated receptor- α and the retinoid X receptor inhibit inflammatory responses of microglia. *Journal of neuroscience research*, 81, 403-411.
- YAMAMOTO, T., YAMAMOTO, A., WATANABE, M., MATSUO, T., YAMAZAKI, N., KATAOKA, M., TERADA, H. & SHINOHARA, Y. 2009.

Classification of FABP isoforms and tissues based on quantitative evaluation of transcript levels of these isoforms in various rat tissues. *Biotechnology letters*, 31, 1695-1701.

- YANGUAS-CASÁS, N., CRESPO-CASTRILLO, A., AREVALO, M. A. & GARCIA-SEGURA, L. M. 2020. Aging and sex: Impact on microglia phagocytosis. *Aging Cell*, 19, e13182.
- YE, S.-M. & JOHNSON, R. W. 2002. An age-related decline in interleukin-10 may contribute to the increased expression of interleukin-6 in brain of aged mice. *Neuroimmunomodulation*, 9, 183-192.
- YIP, P. K., KAAAN, T. K., FENESAN, D. & MALCANGIO, M. 2009. Rapid isolation and culture of primary microglia from adult mouse spinal cord. *Journal of neuroscience methods*, 183, 223-237.
- YU, S., LEVI, L., SIEGEL, R. & NOY, N. 2012. Retinoic acid induces neurogenesis by activating both retinoic acid receptors (RARs) and peroxisome proliferator-activated receptor β/δ (PPAR β/δ). *Journal of Biological Chemistry*, 287, 42195-42205.
- ZAMANIAN, J. L., XU, L., FOO, L. C., NOURI, N., ZHOU, L., GIFFARD, R. G. & BARRES, B. A. 2012. Genomic analysis of reactive astrogliosis. *Journal of neuroscience*, 32, 6391-6410.
- ZENKER, J., STETTNER, M., RUSKAMO, S., DOMÈNECH-ESTÉVEZ, E., BALOUI, H., MÉDARD, J. J., VERHEIJEN, M. H., BROUWERS, J. F., KURSULA, P. & KIESEIER, B. C. 2014. A role of peripheral myelin protein 2 in lipid homeostasis of myelinating Schwann cells. *Glia*, 62, 1502-1512.
- ZHANG, S., HULVER, M. W., MCMILLAN, R. P., CLINE, M. A. & GILBERT, E. R. 2014. The pivotal role of pyruvate dehydrogenase kinases in metabolic flexibility. *Nutrition & metabolism*, 11, 1-9.
- ZHOU, Y., SONG, W. M., ANDHEY, P. S., SWAIN, A., LEVY, T., MILLER, K. R., POLIANI, P. L., COMINELLI, M., GROVER, S. & GILFILLAN, S. 2020. Human and mouse single-nucleus transcriptomics reveal TREM2-dependent and TREM2-independent cellular responses in Alzheimer's disease. *Nature medicine*, 26, 131-142.
- ZOETE, V., GROSDIDIER, A. & MICHIELIN, O. 2007. Peroxisome proliferator-activated receptor structures: ligand specificity, molecular switch and interactions with regulators. *Biochimica et Biophysica Acta (BBA)-Molecular and Cell Biology of Lipids*, 1771, 915-925.
- ZOLEZZI, J. M., SANTOS, M. J., BASTÍAS-CANDIA, S., PINTO, C., GODOY, J. A. & INESTROSA, N. C. 2017. PPARs in the central nervous system: roles in neurodegeneration and neuroinflammation. *Biological Reviews*, 92, 2046-2069.